ISSN 0257 - 3660

ACTA MINERALOGICA PAKISTANICA

Volume 2 1986

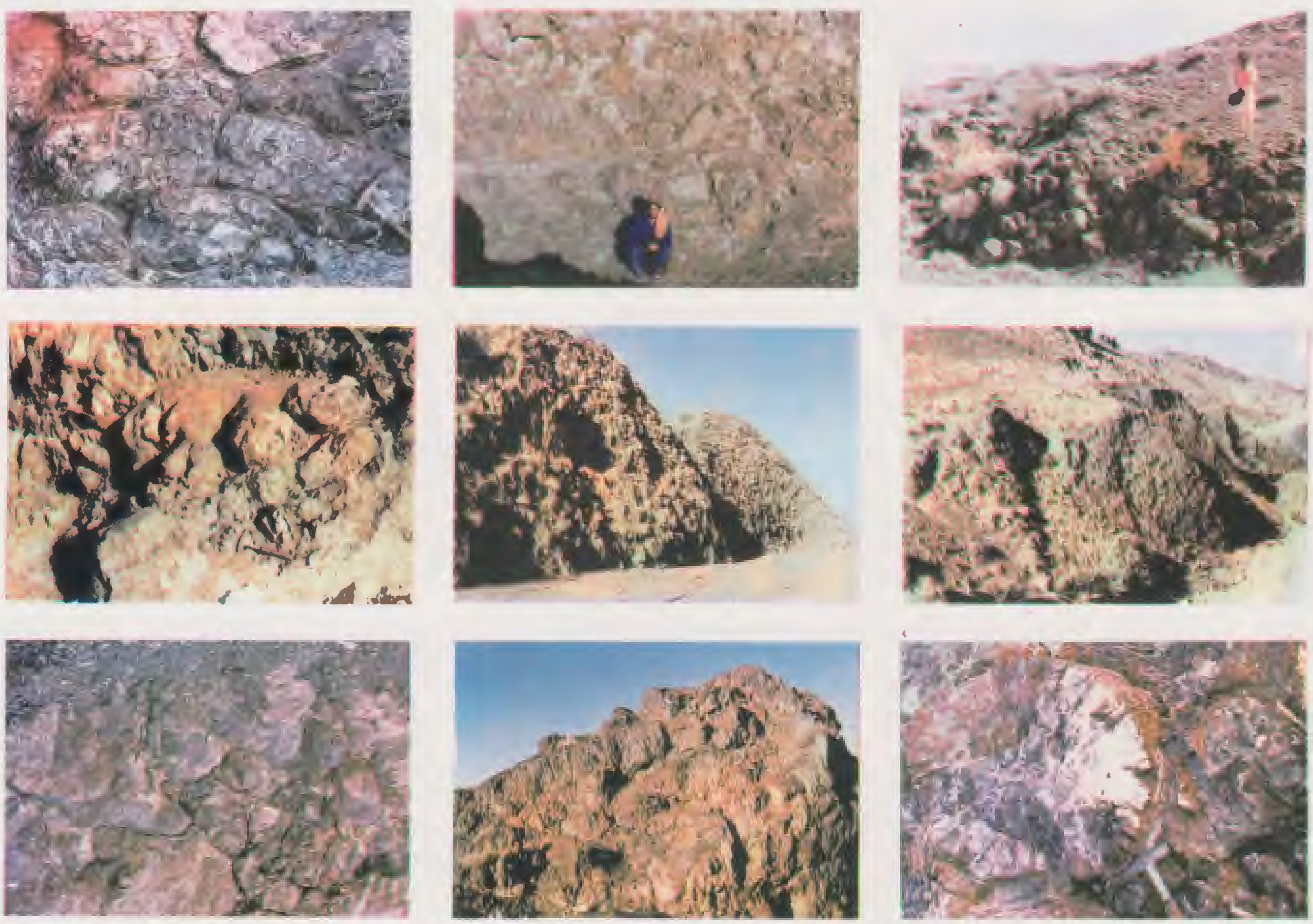

NATIONAL CENTRE OF EXCELLENCE IN MINERALOGY
(UNIVERSITY OF BALUCHISTAN), QUETTA, PAKISTAN

ACTA MINERALOGICA PAKISTANICA

VOLUME 2-1986

CHIEF EDITOR : ZULFIQAR AHMED

ASSISTANT EDITORS : JAWED AHMED & MOHAMMAD MUNIR

ISSN-0257-3660

PRICE

PAKISTANI RUPEES 60.00 OR U.S. $ 8.00 OR U.K. £ 5.00

(includes surface mail postage and handling charges)

Published in December each year.
Printed at KASHMIR OFFSET PRESS, SIRKI ROAD, QUETTA, PAKISTAN.

ACTA MINERALOGICA PAKISTANICA VOLUME 2, 1986.

CONTENTS

ON THE COVER :

Field photographs showing various views of the basaltic pillow lava lobes formed by the undersea eruption of the volcanic sequence of the Bela Ophiolite. The Bela Ophiolite is the largest ophiolite of Pakistan and has the largest pillow lava section amongst the country's ophiolites.

MAP OF PAKISTAN SHOWING LOCATIONS OF AREAS DEALT WITH IN THE PAPERS OF THIS ISSUE.

ROMAN NUMERALS CORRESPOND TO THE SERIAL NUMBER OF EACH ARTICLE ACCORDING TO THE TABLE OF CONTENTS. MAJOR CITIES ARE SHOWN BY SOLID CIRCLES.

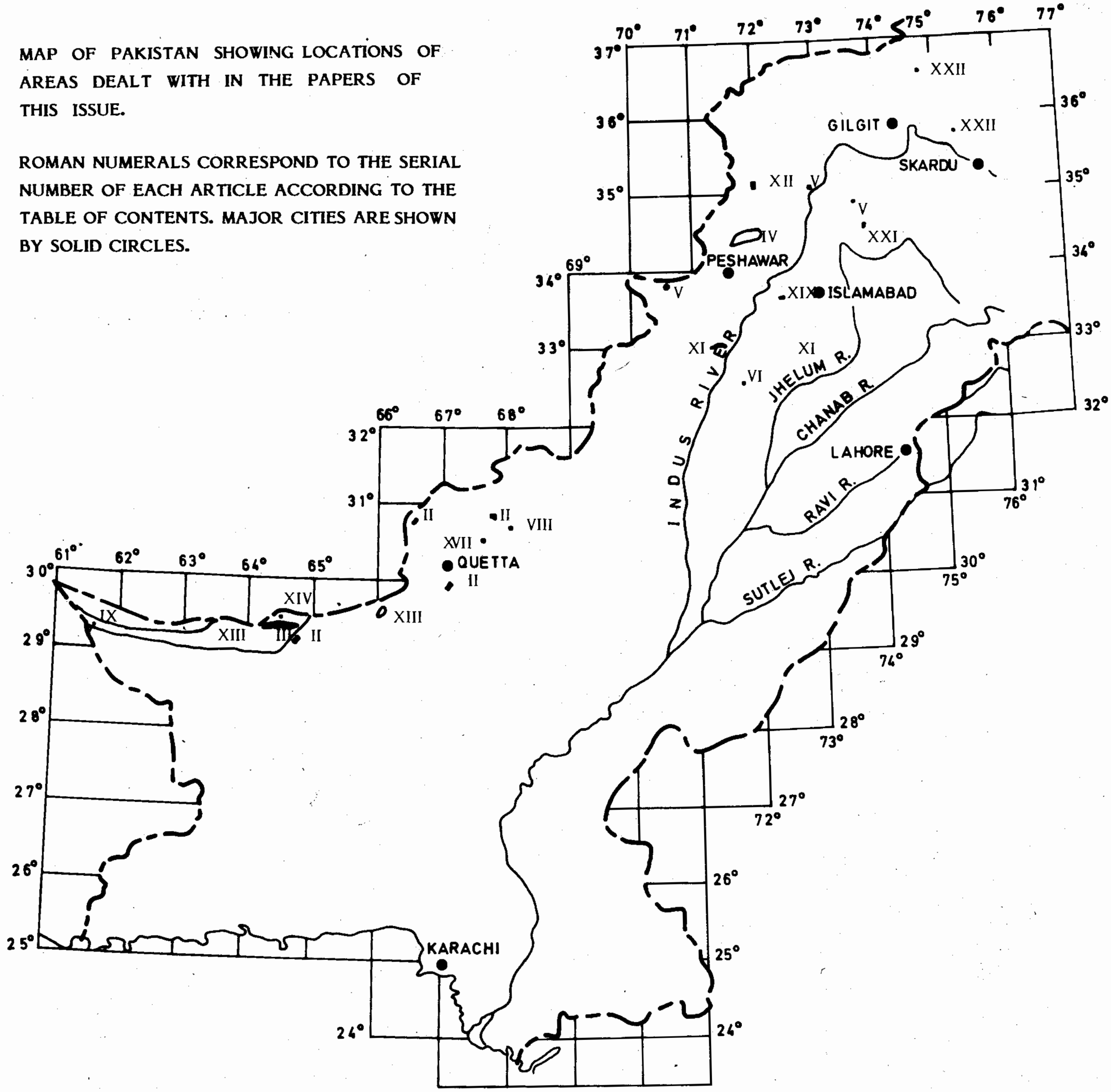

ACTA MINERALOGICA PAKISTANICA
VOLUME 2 (1986) pp. 4 - 11

INTENSITY OF RADIOACTIVITY AND GROUND WATER EXPLORATION IN BALUCHISTAN, PAKISTAN.

ABUL FARAH

National Institute of Oceanography, 37–K, Block 6, PECHS, Karachi–29, Pakistan, & Geological Survey of Pakistan, Quetta, Pakistan.

ABSTRACT: A new technique, using a helicopter-borne gamma ray emission recording device, has been developed in Japan. It has successfully been applied in the delineation of subsurface fractures, faults and fissures in different types of rocks in certain areas of Japan. The fractured, faulted and fissured zones in hard rocks are of high permeability and prove very productive aquifers. The cross-points of faults and fractures in the subsurface delineated by the aerial gamma ray survey are of particular significance in selecting sites for developing high-yield tube wells. The theoretical principles and the practical application of the technique are sound and satisfactory. The technique can be gainfully applied in Baluchistan for the delineation of fault/fracture/fissure zones of high permeability at shallow depths.

INTRODUCTION

A technique for delineating subsurface faults, fractures and fissures in rocks based on detection of variations in gamma ray emission intensity has been developed in Japan (Ochiai, 1972). Under favourable hydrogeological settings the faulted/fractured/fissured rock zones of high permeability prove to be prolific aquifers. As such, the gamma ray intensity detection technique of Dr. Ochiai can indirectly be used in the search of groundwater resources. In various parts of Japan this technique has been tried, and has proven extremely effective in finding large ground water resources in faulted/fractured/fissured buried rocks (200 m deep). The writer, in 1984, was given an opportunity through the efforts of S.R. Poonigar, the then Additional Chief Secretary, Govt. of Baluchistan to study this technique in Japan and discuss the scope of its application in Pakistan with Dr. T. Ochiai and other scientists and officials in Japan. This report is based on these study and disussions.

THE TECHNIQUE

Principles and Instrumentation

The newly developed Japanese technique of surveying subsurface geological features by helicopter-borne gamma ray intensity recording instruments falls in the realm of remote sensing techniques. In such techniques, objective or phenomenal information is collected by a remotely located sensor and analyzed through sensitive and complex computer programming. The technique developed by Dr. T. Ochiai and his associates has been successfully used in delineating subsurface faults, fractures and fissures. The pivotal principles of this technique stem from the concept of Ambronn (1928), who found that the intensity of natural radioctivity – Rn^{222} increases above faults or "tectonic lines". As such, gamma ray emission (electromagnetic radiation) arising in transition from excited states to lower energy states of nucleus has a denser flux over the zones of faults, fractures and fissures. It has been noted that the concentration of natural isotopes of radioactive elements in fractured rocks at depth is several times denser than that recorded from the surface layers. Dr. Ochiai has developed a very sophisticated technique of measuring gamma ray intensity with the help of a helicopter-borne detection and analysis device. He has convincingly demonstrated that the gamma ray intensity in "fracture zones" is 1.3 to 2.0 times higher than that recorded over non-fractured zones. In his helicopter-borne device, measurement is made by counting the ratio of the photo-peak of thallium-208, bismuth–214 and potassium–40, detected by a sodium idodide (NaI) scintillation detector. Although the intensity of radiation of these isotopes is extremely weak compared with gamma ray intensities of uranium ore, yet the variation in intensity over fractured and non-fractured zones is of sufficient quantum.

The device is extremly sensitive and responds positively to the weak variation in gamma ray intensity. There is a built-in device to monitor background radiation and to eliminate it. There is a video camera and a vertical camera to record and confirm positions. Also, the helioopter is equipped with a radar altimeter to compensate gamma ray radiation counts as the altitude changes. After the high-grade compensation the measured values are fed into the mini-computer for control and data analysis. The recording and analysis system is very complex. The entire instrumentation assembly is registered under a Japanese patent.

Method of Survey

A surveying helicopter flies at a constant ground speed of 70-90 km/hr with a ground clearance of 100 metres. In any area of investigation test flights are first made in order to determine the compensation parameters and set the measuring conditions in order to ensure optimum and dependable instrumental sensitivity. During the survey the intensity of gamma rays is continuously measured and analysed. When the helicopter flies over a buried fracture zone the corresponding gamma ray intensity is detected by the automatic analyzer in the sensing device; the fractured zone is automatically recognized and a particular symbol appears on the video screen. Also, the scale of the fractured zone is evaluated on a print-out in one of the four ranks from A to D. The helicopter is usually flown on a grid pattern of 500 metres. Depending on circumstances, however, the spacing may be altered.

Demonstration Area

The area shown to the writer is in Katano city near Osaka, where the helicopter-borne gamma ray intensity survey has helped in delineating buried fractures in granite rocks. The fracture zones of high permeability have been proven to be highly productive aquifers; from one well alone about 2,880 m^3 of water per day is being pumped. The cross-point of fracture lines is the most promising site for development of ground water. Some of the fracture zones delineated by Dr. Ochiai's remote sensing device have been confirmed by geological mapping. In other cases no correlation with surface lineament could be established.

Dr. Ochiai has made a very important remark "Earth layers having large width fractured aquifers belong to volcanic areas and the mean is 240 m. (240 m is the average width of the fractured zone in volcanic rocks). Those of narrow width are attributable to sandstone areas, having about 60 m width. Those of intermediate width between these are in metamorphic rock and granite area." This statement probably holds true in particular geodynamic setting of Japan and may not be applicable in general terms. In my opinion, in Baluchistan, the fractures in limestone and ultramafic rocks (tectonites) may be comparatively larger in width.

Advantages of the Technique

Like any airborne remote sensing technique (geophysical) the helicopter-gamma ray technique bears the premium of expediency. It is extremely sensitive and responds to very small variations in the gamma ray intensity and cosmic radiations are accounted for with great

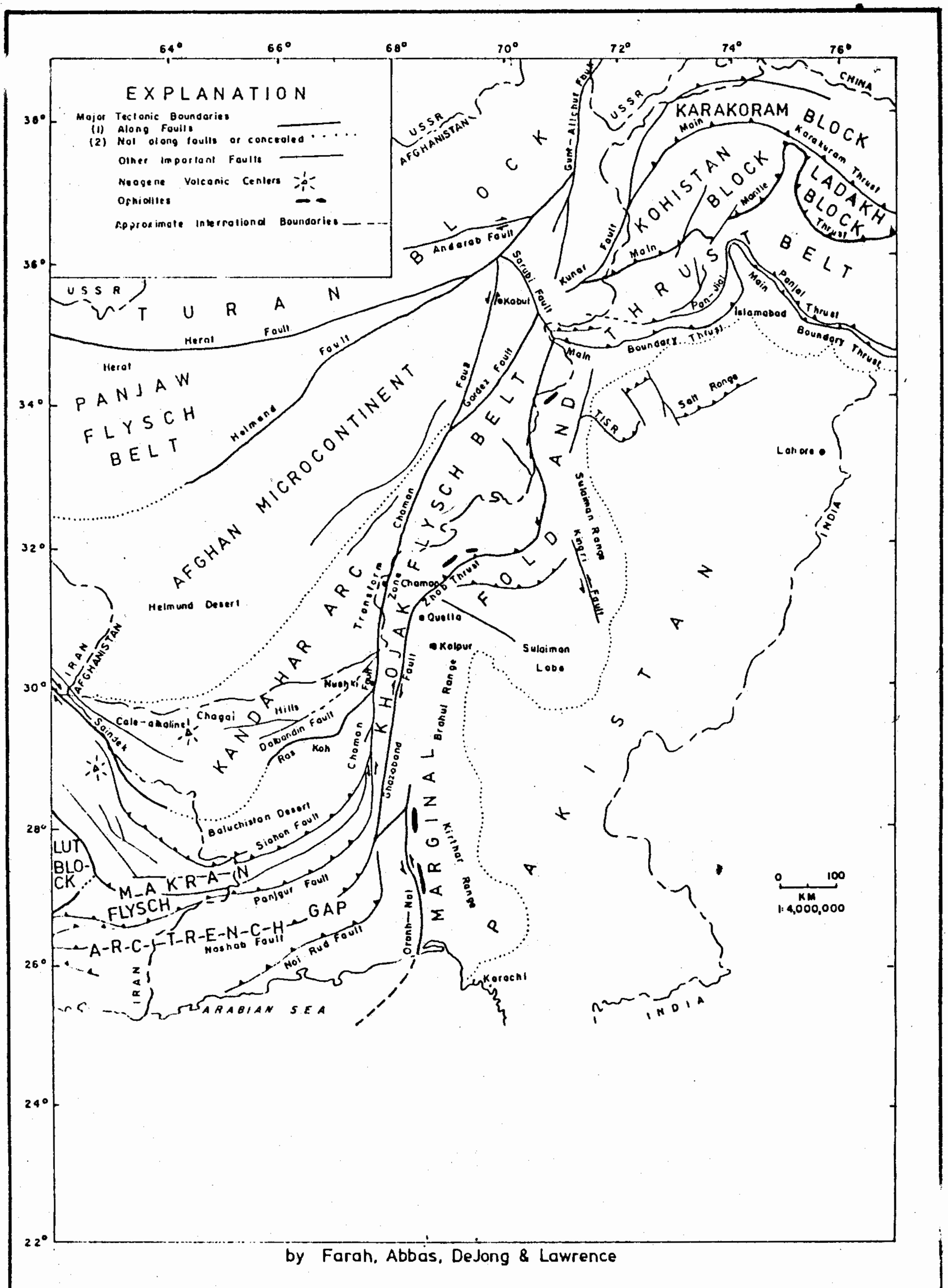

FIG. I. THE TECTONIC BOUNDARIES IN PAKISTAN

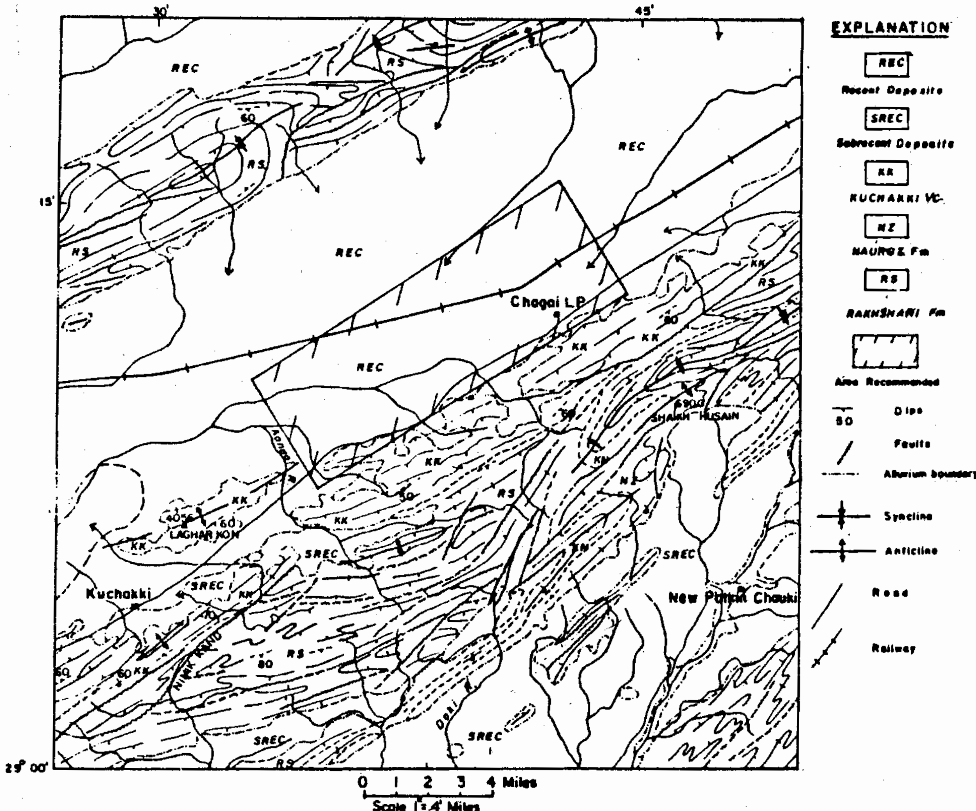

Fig. No. 2 Area Recommended for Heli—Ray Survey near Kuchakki

After Reconnaissance Geology of
Part of Pakistan. Canadian Sheet No, 23 (Hunting Survey Corporation, 1960).

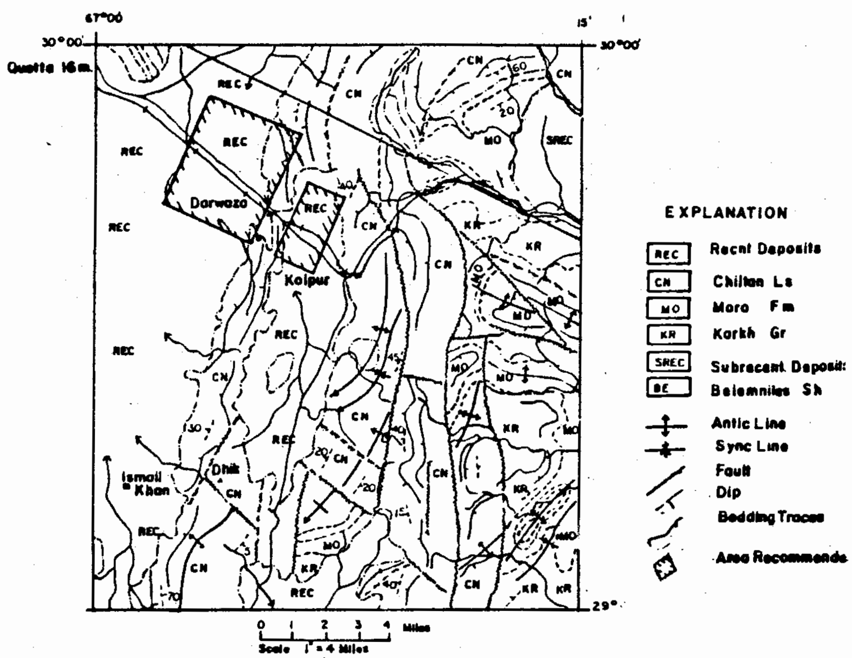

Fig: Area Recommended for Heli—Gamma Ray Surv., Near Kolpur

After Reconnaissance Geology of Part of
Pakistan. Canadian sheet No, 24 (Hunting Survey Corporation, 1960).

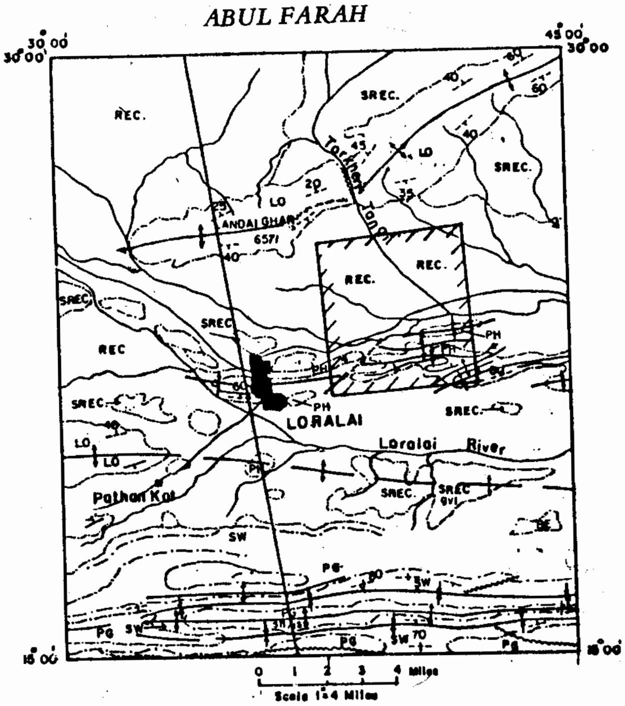

Fig. No.4 Area Recommended for Heli_Gamma Ray Survey Near Loralai.
After Reconnaissance Geology of
Pakistan.Canadian Sheet No.24 (Hunting Survey Corporation, 1960).

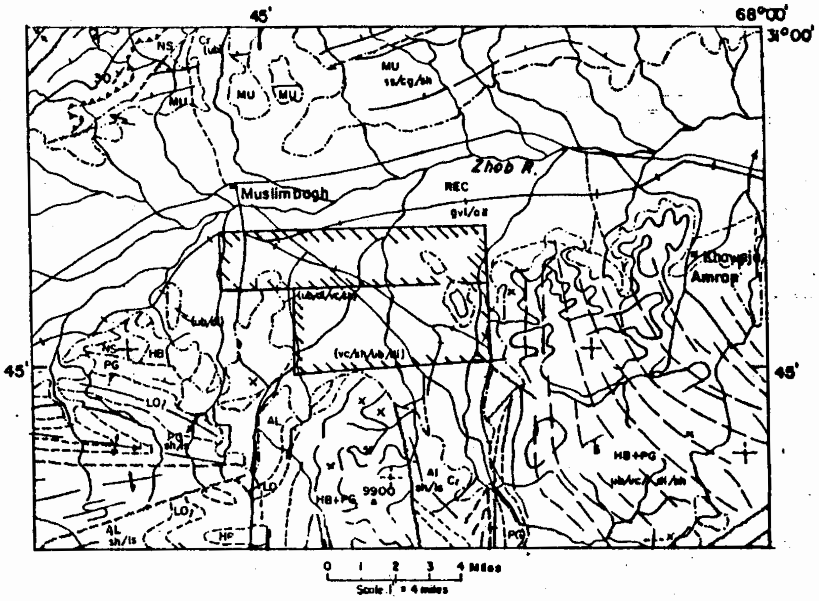

Fig. NO. 5 Area Recommended for Heli-Gamma Ray Survey Near Muslimbagh.

EXPLANATION
MU Multana Cg (MU)
REC Recent Deposits (REC)
Porali intrusions (PO) late Paleocene to early Eocene
PG/HB Hindubagh intrusions (HB) late Cretaceous or early Paleocene
NS Nisai Gr (NS)
AL Alozai Gr (AL)
LO Loralai Ls (LO)
Anticline
Syncline
Fault
Thrust Fault
Dip
Bedding traces
Area recomended

After Reconnoissance Geology of Part of Pakistan.Canadian Sheet NO. 26 (Hunting Survey Corporation, 1960).

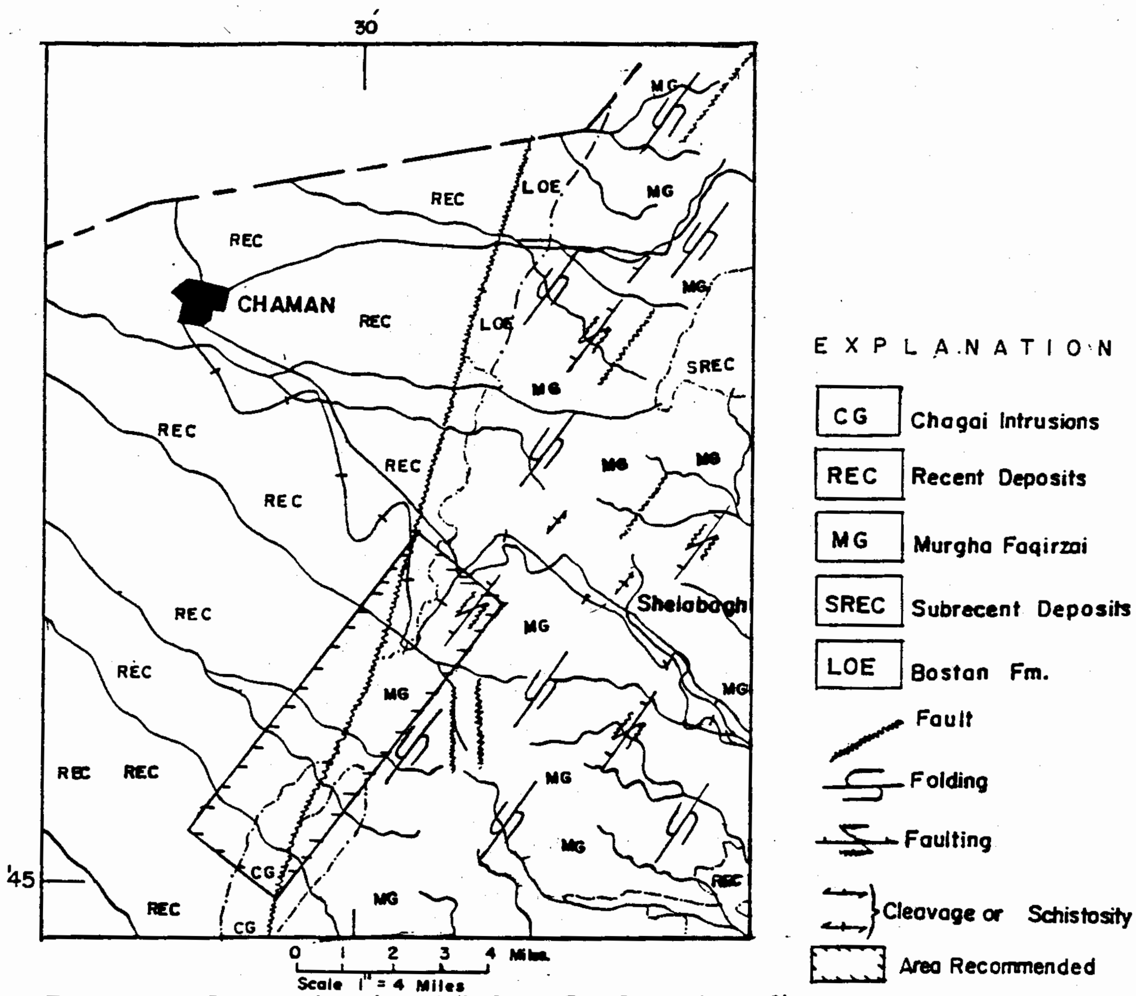

Fig-No.6 Area Recommended for Heli-Gama Ray Survey Near Chaman.
After Reconnaissance Geolog of part of Pakistan Canadian Sheet No.26
(Hunting Survey Corporation, 1960)

precision. The gamma ray intensity is expected to be higher in a fracture zone of a rock body than in the massive, non-cleaved part of the same body. As such, the heli-gamma ray technique is effective in delineating linear narrow fracture zones in a buried rock body. Normally the application of other geophysical techniques in determining such structures is constrained by the limited dimensions of the structure. This has been verified by geological mapping and drilling in several areas in Japan. The example demonstrated to the writer in Katano city is convincing. In fact, the technique appears to be effective in detecting a point source. Therefore, when there is sufficient rainfall in an area of particularly high relief energy the fracture zones (point sources) in massive rocks (granite, limestone, volcanic and ultramafic) prove to be highly productive aquifers and the heli-gamma ray survey in an indirect way proves a very useful device for the detection and development of ground water resources.

Limitations of the Technique

The use of an airborne geophysical technique, based on the detection of variations in gamma ray intensity, in the geological investigation for minerals other than radioactive minerals is still considered experimental, and the scientific credibility of its use as a prospecting tool is yet to be established. In United States a private agency claims to have achieved diagnostic results in oil prospecting by applying the gamma ray intensity detection technique. However, at this stage it has hardly any rating. As for its application in detecting buried fracture/fault zones in hard rocks, the technique has received attention in Japan and good aquifers have been found there in fracture/fault/fissure zones.

Detection capability of the device is reduced if the fractured rock is overlain by a thick sequence of compact clay layers. The areas in which the device has been tried in Japan, however, are not characterized by this geological constraint. Dr. Ochiai (1972) has stated: "In the case of closed faults, however, the rising of the natural radioactive elements is hindered, and no increase in natural radioactivity was detected even where fractured zones are recognized at the outcrop." These important geological factors must be taken into consideration when evaluation of the application of the technique is made in a particular area.

APPLICATION IN BALUCHISTAN

In Pakistan, ground geophysical techniques (electrical resistivity, seismic refraction and gravity) have been applied in ground water surveys in various parts of the country. The gravity method is used for delineating the buried configuration of the basement which controls the shape of the basin. Electrical resistivity and seismic refraction methods are used for mapping the subsurface saturated zones. In Baluchistan, the electrical resistivity method has been proven to be effective in delineating subsurface saturated zones of limited thickness at depths of 20–200 meters. This method, which depends on expanding electrodes separation, is not helpful in detecting a point source of ground water, i.e., saturated faulted, fractured, and fissured zones in solid rocks. The gamma ray survey technique can detect a buried point source: fractures, faults, fissures of limited width. On the basis of the study, discussions and the demonstration of the application of this technique in Japan, it is felt with a certain degree of confidence that the technique patented in Japan can effectively and profitably be used in different areas of Baluchistan where megashears have been mapped (fig. 1).

The following five areas are selected for the pilot project of the heli-gamma ray survey in Baluchistan. The selection is made bearing two factors in mind :–

(i) Areas underlain by different types of rocks – volcanic, ultramafic, intrusive, limestone and shale,

(ii) Areas where there is an acute urgency for the development of ground water resources.

1. Area of about 50 sq. miles (128 sq. km) between Chagai levy post and Kuchakki village about 50 miles (80 km). southwest of Nushki, underlain by volcanic rocks (fig. 2).

2. Area of about 20 sq. miles (51 sq. km) near Kolpur underlain by limestone (fig. 3).

3. Area of about 20 sq. miles (51 sq. km) near Loralai underlain by limestone (fig. 4).

4. Area of about 45 sq. miles (115 sq. km), south of Muslim Bagh, underlain by ultramafic rocks (tectonites) (fig. 5).

5. Area of about 20 sq. miles (51 sq. km) southeast of Chaman, underlain by intrusive rocks and shales (fig. 6).

The areas may be covered on a grid pattern of 500-1000 metres. Sizeable fracture zones are believed to exist in the subsurface at shallow depths in the above areas.

REFERENCES

AMBRONN, R. (1928) ELEMENTS OF GEOPHYSICS, AS APPLIED TO EXPLORATION FOR MINERAL, OIL AND GAS, McGraw Hill Book Co., Chicago, p. 372.

DAVIS, F.J. (1957) Scintillation Counters. *In:* Faul, H. (ed.) Nuclear Geology–A Symposium on Nuclear Phenomena in the Earth Sciences; John Wiley & Sons, Inc., New York, pp. 31-48.

EVANS, R.D.(1957) Fundamental Considerations, Instruments, and Techniques of Detection and Measurements. In Faul, H. (ed.) Nuclear Geology–A symposium on Nuclear Phenomena in the Earth Sciences; John Wiley & Sons, Inc; New York, pp. 7-27.

FARAH, A., ABBAS, G., DEJONG, K.A. & LAWRENCE, R.D. (1984) Evolution of the lithosphere in Pakistan. Tectonophys. 105, pp. 207-27.

HUNTING SURVEY CORPORATION (1960) RECONNAISSANCE GEOLOGY OF PART OF WEST PAKISTAN. Toronto, Canada, pp. 330-400.

JAPAN FAO ASSOCIATION (1983) Recent Agricultural Technology in Japan, pp. 78-80.

KIMURA, S. & KOMAE, T. (Undated) Application of environmental radon^{222} to some cases of water circulation. *In:* Natural Radiation Environment III Vol. 1, DOE Symp. Ser. 51, Tech. Inf. Cent. U.S. Deptt. Energy, pp. 581-99.

OCHIAI, T. (1972) Prospecting of undergound water by the measurement of natural radioactivity. Internat. Assoc. Hydrogeologists, Memoires, 9, pp. 159-63.

———————. (undated) Remote sensing for underground water by the use of Helicopter Gamma Ray Surveys Internal Report, pp. 1-7.

WHITE, H.E. (1964) INTRODUCTION TO ATOMIC AND NUCLEAR PHYSICS. Van Nostrand Reinhold Company; New York, pp. 338-350.

Manuscript received 13.9.1986
Accepted for publication 30.12.1986

ACTA MINERALOGICA PAKISTANICA
VOLUME 2 (1986) pp. 12-23

PETROLOGICAL AND PETROCHEMICAL STUDIES OF NORTH CENTRAL CHAGAI BELT AND ITS TECTONIC IMPLICATIONS

REHANUL HAQ SIDDIQUI, WAZIR KHAN AND MUNIR–UL–HAQUE

Geological Survey of Pakistan, Sariab Road, Quetta.

ABSTRACT:– The present petrological and petrochemical studies of various rock suites from north-central part of Chagai belt lead to the interpretation that the Chagai belt may represent a tholeiitic island arc, which has been constructed on an oceanic crust rather than a continental margin as earlier postulated by Sillitoe (1972) and Stoneley (1974). Southern thrust contact of Chagai belt and fault-bounded ophiolites in the northern flanks of Raskoh range suggest that Chagai island arc is partially obducted onto the Raskoh range, which has been recently interpreted as a welded mass of basaltic oceanic islands. Slivers of ophiolite between Chagai and Raskoh belts may represent the fragments of oceanic crust on which Chagai island arc was constructed.

INTRODUCTION

Chagai magmatic belt of northwestern Baluchistan exhibits excellent and spectacular field exposures of volcanic and plutonic rock suites. This volcano-plutonic area of Baluchistan is structurally and tectonically less disturbed and shows least metamorphic effects.

The present paper interprets tectonic environment with the petrological and petrochemical studies of north-central Chagai belt. The studied area is situated about 25 km north-east of Chagai village of Chagai District, Baluchistan. The area is covered in toposheet nos. 34 C/6 and C/10 and bounded by the latitudes 29° 30′ to 29° 35′ N and longitudes 64° 15′ to 64° 45′ E.

Fourteen representative and least altered rock samples were chemically analyzed for their major element contents in the geochemical laboratories of the Geological Survey of Pakistan at Quetta and Karachi. Five samples out of the fourteen were analyzed in the Geology Department of Budapest University, Hungary.

REGIONAL GEOLOGY

Chagai magmatic belt is situated in the eruptive zone of northwestern Baluchistan. It is about 500 km in length and 150 km in width and trends in an eastwest direction (fig. 1).. This belt is terminated by the Chaman tranform fault zone in the east, bounded by a thrust fault in the south and is convex towards south. (Specter & Associates Ltd., 1981: Farah et al., 1983).

The oldest rock unit of the belt is the late Cretaceous Sinjrani Volcanic Group composed mainly of submarine stratified intercalations of andesitic flows and pyroclastic rocks including agglomerate, volcanic breccia, volcanic conglomerate and tuffs with subordinate amount of basalt limestone, shale and sandstone. Total thickness of the group is about 1000 m and its base is not exposed (Hunting Survey Corporation, 1960), but according to Arthurton et al., (1979), the thickness is about 10,000 m and its age is Senonian assigned on the basis of Maastrichtian fauna present in the overlying Humai Formation.

Sinjrani Volcanic Group is invaded by Chagi intrusions of pre-late Cretaceous to post-Paleocene represented by two intrusive phases, the first phase of granitic to granodioritic rocks with some charnokites(?) is middle to late Cretaceous in age. The second phase with more alkaline granitic suites has a late Paleocene, early Eocene or later age (Hunting Survey Corporation, 1960).

Nigell (1975) described the Chagai intrusions as ranging from granite to gabbro. Dykstra (1978) also divided the Chagai intrusions into two distinct phases, a main phase ranging in composition from quartz diorite to granodiorite and a later phase of granitic composition. Britzman's (1979) radiometric study, has given an Oligocene to Miocene age to the Chagai intrusions and also documented two distinct pulses of intrusive activity at approximately 35 and 20 million years ago, respectively. Rocks of both phases range in composition from tonalite to granite. The present study suggests a higher proportion of mafic rocks in both the Sinjrani Volcanic Group and the Chagai Intrusions, than that described earlier.

Chagai magmatic belt, also known as Chagai calcalkaline magmatic belt (Sillitoe, 1974; Dykstra, 1978) has been postulated to be formed due to northward subduction of an oceanic lithosphere below southern edge of Afghan micro-continent (Stoneley, 1974; Arthurton, et al., 1979). It was therefore considered as n Andean type plate boundry (Sillitoe, 1972; Stoneley, 1974). The above hypotheses was, however, not based on petrochemical or geochemical data.

LOCAL GEOLOGY

More than half of the investigated area is covered by Sinjrani Volcanic Group including basaltic, andesitic and dacitic flows and pyroclastics including agglomerate, volcanic breccias and tuffs. The above volcanic and volcanoclastic sequence is intruded by numerous stocks and batholiths of gabbro, diorite, tonalite, granodiorite and adamellite belonging to the Chagai intrusions. The country rocks around batholiths and stocks are generally baked, hardened and in places slightly metamorphosed to low-grade hornfelses.

Basaltic lava flows are restricted to the east-central side of the investigated area and are exhibited by two different and distinct cycles of eruptions. One, in lower horizon, is dark green porphyritic and displays inclined columnar jointing. Basalt of the upper horizon is greenish-black, microporphyritic and exhibits vertical columnar joints.

Andesite and dacite occur as indistinguishable flows in the west-central side of studied area. Both are dark green, porphyritic and show vertical columnar joints.

Plutonic rocks are represented by two large batholiths of adamellite and granodiorite, in south-central and western side of the area. Gabbro and diorite occur as composite stock in the north-central part and tonalite occurs as small stock intruding the above gabbro-diorite stock. Occurrence of frequent roofpendents within the intrusive rocks and development of relatively thin (30 to 200 cm thick) sheeted joints suggest that still the top of these batholiths and stock are exposed. Their irregular, sharp and generally sinuous contacts with intense shear joints indicate a forcefull injection of magma.

From field observation, three cycles of eruption including two basaltic (earlier and middle) and one undifferentiated andesitic to dacitic (late) are identified. Three phases of intrusive activity including, an earlier phase of composite gabbro-diorite stocks, a middle phase of large batholiths of adamellite and granodiorite, and a late phase of small tonalite intrusion are identified.

PETROGRAPHY

Basalt

The basalt samples (nos. 1 & 2, table 1) are melanocratic, merocrystalline, fine grained and porphyritic to microporphyritic. Euhedral

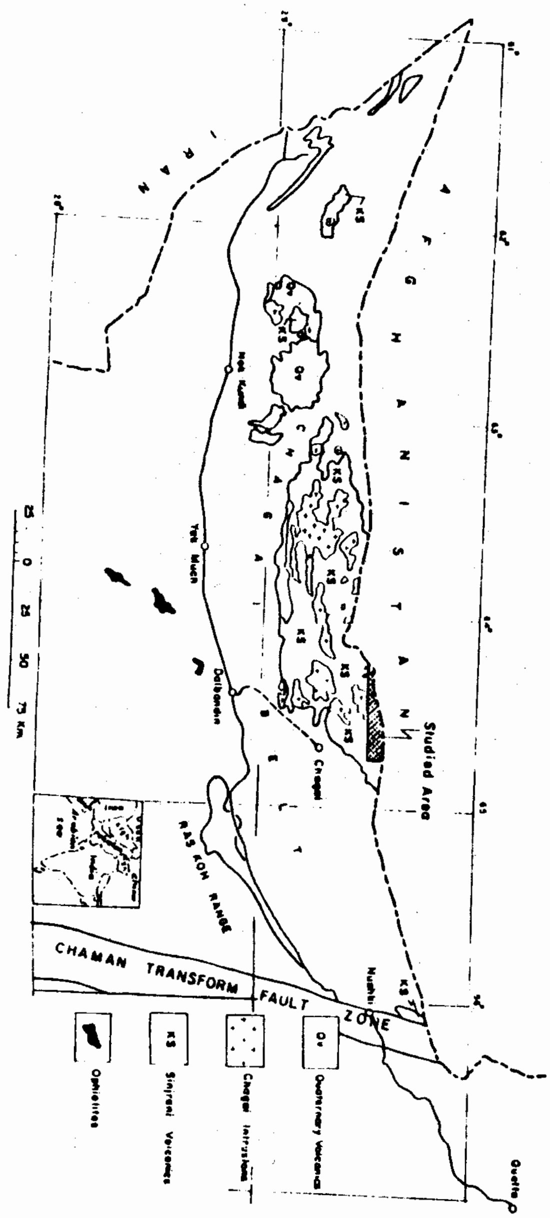

FIG. 1. CHAGAI MAGMATIC BELT BALUCHISTAN, PAKISTAN
(After Bakr and Jackson, 1964)

to subhedral, tabular crystals of plagioclase (An_{49-58}) are embedded in a cryptocrystalline groundmass of mainly plagioclase and ferro-magnesian minerals with minor quartz. Lamp-robolite, pigeonite and augite are suspected in the groundmass. Plagioclase is often dusted with argillization and in places partly epidotized. Ferromagnesian minerals are partly chloritized. Small prismatic grains of rutile and apatite generally occur as inclusions in plagioclase. Anhedral grains of ilmenite and magnetite are scattered throughout the rock.

Andesite and Dacite

Andesite (sample no. 3) is mesocratic holo- to mero-crystalline, fine grained and prophyritic in texture.

Large tabular phenocrysts of plagioclase (An_{28-40}) and subhedral prismatic grains of hypersthene are embedded in a microcrystalline groundmass of plagioclase, hypersthene and quartz. Apatite occurs as small acicular inclusions in plagioclase.

Dacite (sample no. 4) is similar in texture and is characterised by more quartz and lesser ferromagnesian minerals than in andesite.

Gabbro

Gabbros (sample nos. 5,6 and 9 of table 1) are melanocratic, holocrystalline, medium to coarse grained and are subpoikilitic in texture.

Euhedral to subhedral plagioclase (An_{52-68}) laths are interlocked with subhedral to anhedral, columnar grains of hornblende with minor prismatic grains of hypersthene and uralite. Ferromagnesian minerals are also found in the interstices between the plagioclase grains and are partly chloritized. Among accessories, apatite occurs as small prismatic crystals in plagioclase. Anhedral grains of ilmenite and magnetite are generally associated with ferromagnesian minerals. Petrographically the gabbros in the area are termed as "hornblende gabbro".

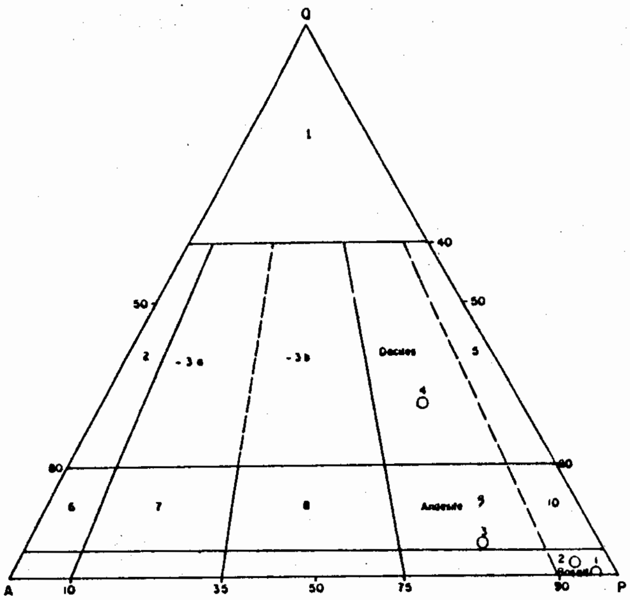

Fig. 2. Ternary plot of normative Q–A–P for volcanic rock suites of north central Chagai Belt (After Streckeisen, 1979).

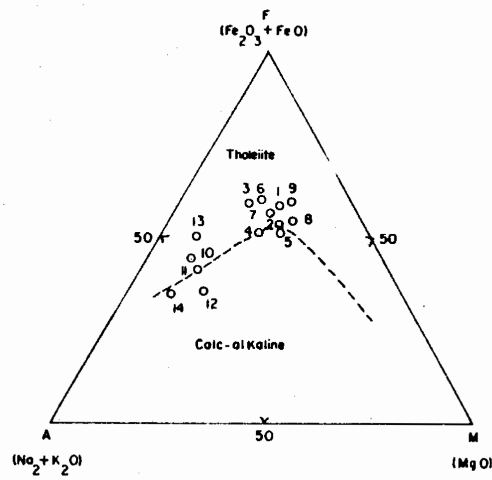

Fig. 4. FAM diagram for the magmatic rock suites of north central Chaghai Belt (After Irvine and Baragar, 1974).

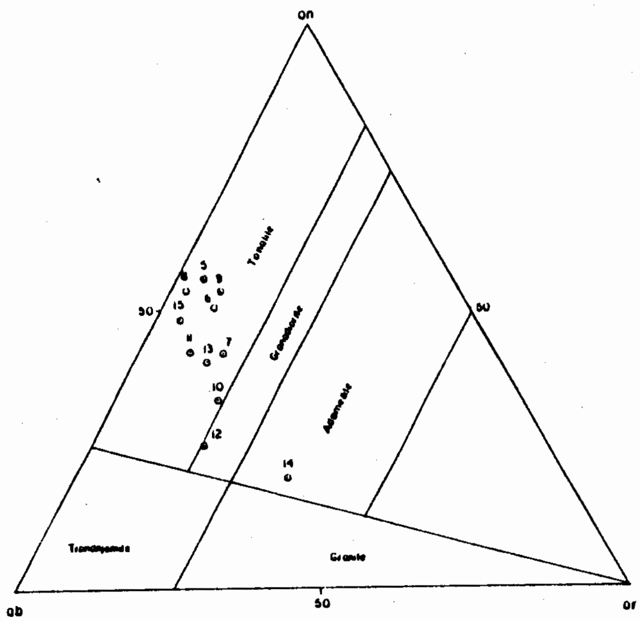

Fig. 3. Ternary plot of normative an–ab–or for plutonic rock suites of north central chagai belt. Compositional boundries are after O'Connor (1965)

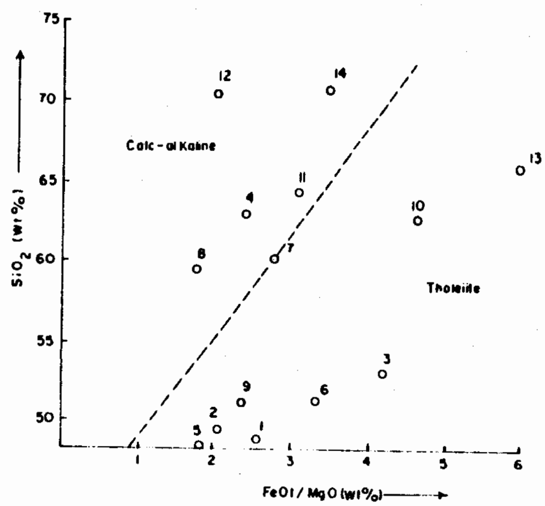

Fig. 5. SiO_2 versus FeOt/MgO plot for the magmatic rock suites of north Centeral Chagai Belt (After Miyashiro, 1974).

Microgabbro is also observed which is similar in mineralogy but characterized by a subpoikilitic to subporphyritic texture and with relatively a lower anorthite content of plagioclase (An_{43-55}).

Diorite

Diorite (sample nos. 7 and 8) is holocrystalline, medium- to coarse-grained, subpoikilitic and hypidiomorphic.

Tabular and lathlike crystals of plagioclase (An_{35-45}) and subhedral columnar grains of hornblende are interlocked. The later is also found in interstices between the plagioclase, which is slightly dusted with argillization. Hornblende is usually twinned and often partly chloritized. Apatite and zircon occur as small inclusions in plagioclase and hornblende. Anhedral magnetite is generally associated with hornblende.

Tonalite

Tonalite (sample no. 10, table 1) is holocrystalline, phaneritic, medium- to coarse-grained, porphyritic and hypidiomorphic granular. Large phenocrysts of biotite laths, tabular and zoned plagioclase (An_{35-43}), large prismatic grains of hornblende and subhedral to anhedral, equant grains of quartz are embedded in a medium grained groundmass of the same minerals. Small euhedral and generally prismatic grains of apatite and rutile are usually found as inclusions in plagioclase and biotite.

Granodiorite

Granodiorite (sample nos. 11 and 12, table 1) is holocrystalline, medium to coarse grained subpoikilitic and hypidiomornhic in texture. Subhedral and tabular crystals of plagioclase (An_{4-32}), anhedral quartz and long prismatic and columnar grains of hornblende occur in subpoikilitic manner. Hornblende and biotite also occur in interstices between plagioclase. Plagioclase grains are often zoned and exhibit polysynthetic pericline twinning. Small prismatic grains of apatite and rutile occur as inclusions in plagioclase and quartz. Magnetite is generally associated with hornblende and biotite. Towards the margin, rock becomes more mafic (sample no. 11).

Adamellite

Adamellite (sample nos. 13 & 14, table 1) is holocrystalline, subpoikilitic and hypidiomorphic granular in texture. Subhedral perthitic orthoclase and tabular plagioclase (An_{4-18}), anhedral quartz, lath-like biotite and prismatic hornblende are arranged in subpoikilitic manner. Hornblende and biotite are also found in interstices between feldspars which are often dusted with argillization. Hornblende is generally biotitized and chloritized. Apatite, zircon, magnetite and rutile occur as accessories. Towards the margin rock becomes porphyritic in textuure and grades into more mafic differentiates (sample no. 13). At places however, adamellite is in direct contact with country rocks.

PETROCHEMISTRY

The chemical analyses and CIPW Norms of magmatic rock suites of Chagai belt are presented in tables 1 and 2. Basalt, andesite and dacite plot in respective fields in the normative Q–A–P plot after Streckeisen (1979) in fig. 2. Gabbro, diorite, granodiorite and adamellite plot in the tonalite field of the or-ab-an plot after O' Connor (1965) given in fig. 3. However, the samples from central zones of granodiorite and adamellite plot in their respective fields in this diagram.

Basalts show 48.07 to 49.51% SiO_2 and are peraluminous. High Al_2O_3 is due to the presence of lamprobolite (basaltic hornblende) in the groundmass. Basalt norms contain 0.5 – 1.6% quartz, 10 – 15.21% hypersthene and 0.2 – 8.08% diposide.

Andesite contains 53.60% SiO_2, and is peraluminous. Its norm contains 4.51% quartz, 16.54% hypersthene and 2% diopside.

Table 1. Chemical composition of magmatic rock suites of north central Chagai belt.

Sample No.	**1**	**2**	**3**	**4**	**5**	**6**	**7**	**8**	**9**	**10**	**11**	**12**	**13**	**14**
SiO_2	48.07	49.51	53.60	63.30	47.40	51.26	60.50	59.45	51.50	63.03	64.44	70.35	66.03	70.90
TiO_2	0.25	0.46	0.60	0.83	0.27	0.80	1.25	1.08	0.50	0.30	0.40	0.22	0.16	0.33
Al_2O_3	21.50	20.41	17.36	13.40	19.32	18.67	14.43	15.60	16.78	18.71	19.84	14.00	16.63	13.30
Fe_2O_3	5.38	6.07	5.44	4.80	5.49	3.51	4.50	4.77	6.87	3.81	1.78	2.65	3.13	3.30
FeO	5.11	4.89	8.03	3.92	5.07	7.60	6.20	4.34	6.02	2.31	2.55	1.71	2.39	1.06
MnO	0.03	0.06	0.12	0.16	–	0.045	0.19	0.06	0.10	–	–	0.06	0.03	0.09
MgO	3.99	5.19	3.22	3.60	5.61	3.22	3.90	4.80	5.24	1.31	1.41	2.08	0.83	1.20
CaO	11.12	7.79	5.60	3.85	11.46	9.53	4.50	5.70	8.41	5.81	5.61	2.75	5.23	2.50
Na_2O	2.80	3.33	3.37	2.77	3.75	3.24	2.77	2.77	2.70	4.32	3.78	3.72	3.50	3.15
K_2O	0.45	0.82	2.34	2.07	0.45	0.92	1.25	0.20	0.78	2.16	0.90	1.92	1.25	3.45
P_2O_5	0.94	0.05	1.27	0.01	1.02	0.17	0.01	–	0.16	0.07	0.07	0.01	0.66	–
SO_3	–	1.20	–	–	–	0.41	–	–	–	0.22	–	–	–	–
CuO	0.01	0.01	0.01	–	0.02	0.01	–	–	–	0.01	–	–	–	–
H_2O^+	0.13	0.15	0.19	1.34	0.10	0.24	0.66	0.94	0.95	0.35	0.20	0.38	0.10	0.67
H_2O^-	0.22	0.04	0.07	0.20	0.11	0.07	0.05	0.18	0.13	0.12	0.02	0.07	0.08	0.13
Total	100.00	99.98	100.84	100.25	100.02	99.69	100.21	99.86	100.14	100.02	100.96	99.92	99.99	100.08
Solidification Index.	22.50	25.57	14.37	20.98	27.54	17.41	20.95	28.44	24.33	9.42	13.33	17.22	7.48	9.87
FeOt	9.95	10.35	12.12	8.24	10.01	10.76	10.25	8.63	12.20	5.74	4.152	4.10	5.21	4.03
K_2O/Na_2O	0.16	0.25	0.69	0.75	0.13	0.28	0.45	0.07	0.29	0.50	0.24	0.52	0.36	1.09
FeOt/MgO	2.49	1.99	3.76	2.79	1.78	3.34	2.63	1.80	2.33	4.38	2.94	1.97	6.28	3.36

FeOt = Total iron oxide expressed as FeO.

Table 2. C.I.P.W. norms of magmatic rock suites of north central Chagai Belt.

Sample No.		**1**	**2**	**3**	**4**	**5**	**6**	**7**	**8**	**9**	**10**	**11**	**12**	**13**	**14**
	Q	0.51	1.60	4.51	24.93	–	2.20	21.44	22.12	7.08	16.21	23.75	32.09	27.91	32.35
	C	–	–	–	–	–	–	0.32	0.44	–	–	2.44	0.79	0.13	–
	or	2.78	4.85	13.85	12.26	2.67	5.54	7.39	1.18	4.62	12.55	5.33	11.36	7.40	20.42
	ab	23.68	28.17	28.50	23.42	24.83	27.41	23.42	23.43	22.84	35.86	31.97	31.46	29.60	26.64
	an	44.68	38.30	25.31	17.99	34.54	33.61	22.35	28.31	31.34	24.78	27.83	13.65	25.59	11.93
	ne	–	–	–	–	3.37	–	–	–	–	–	–	–	–	–
di	en	5.76	0.25	0.99	0.74	13.58	5.52	–	–	6.35	0.29	–	–	–	–
	fs	2.32	0.04	1.01	0.15	3.65	–	–	1.94	0.03	–	–	–	–	–
															wo=0.20
hy	en	7.32	12.90	7.64	8.70	–	5.52	9.73	12.04	10.29	3.09	3.52	5.21	2.07	3.01
	fs	3.38	2.31	8.90	2.02	–	6.70	6.02	2.36	3.59	0.40	2.60	0.68	1.60	–
ol	fo	–	–	–	–	5.44	–	–	–	–	–	–	–	–	–
	fa	–	–	–	–	1.85	–	–	–	–	–	–	–	–	–
	mt	7.78	8.78	7.87	6.95	7.94	5.08	6.51	6.90	9.94	5.43	2.52	3.83	4.53	2.60
	il	0.46	0.87	1.14	1.57	0.51	1.51	2.37	2.04	0.95	0.55	0.76	0.45	0.30	0.62
	hm	–	–	–	–	–	–	–	–	–	–	–	–	–	1.38
	pr	–	0.90	–	–	–	–	–	–	–	0.17	–	–	–	–
	ap	2.35	0.12	0.38	0.02	2.41	0.40	0.02	–	0.38	0.17	0.16	0.02	1.56	–
	DI	26.97	34.62	46.86	60.61	30.87	35.06	52.25	46.73	34.52	64.62	61.05	74.91	64.91	79.41
	An	65	58	47	43	58	55	49	55	58	41	47	30	46	31

DI = Differentiation Index.
An = Anorthite contents of normative plagioclase.

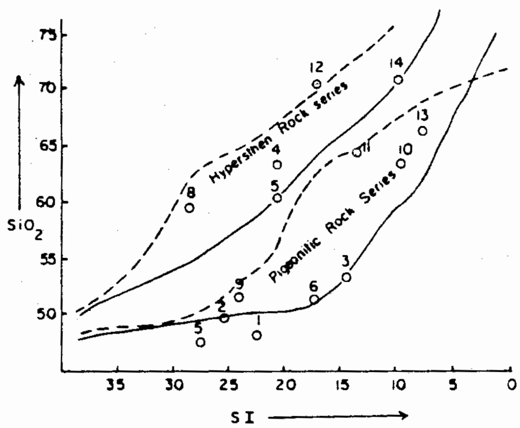

Fig. 6. Solidification Index vesus SiO_2 plot for the magmatic rock suite of north central Chagai Belt (After Kuno, 1968).

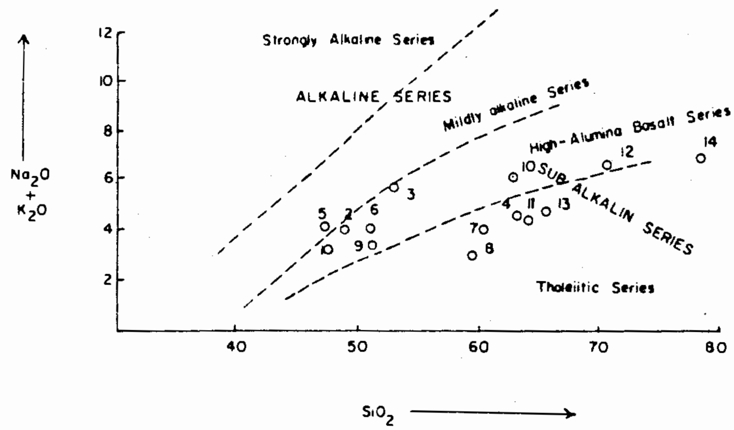

Fig. 8. Alkali versus SiO_2 diagram for the magmatic rock suites of north central Chagai belt (After Schwarzer and Rogers, 1974).

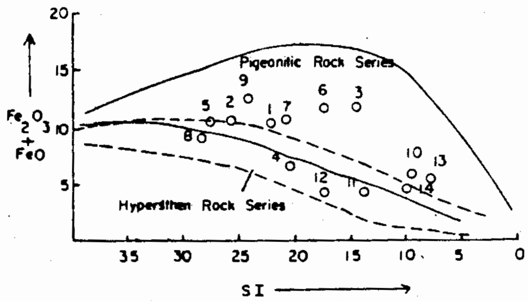

Fig. 7. Solidification Index versus Fe_2O_3+FeO plot for the magmatic rock suites of north central Chagai Belt (After Kuno, 1968).

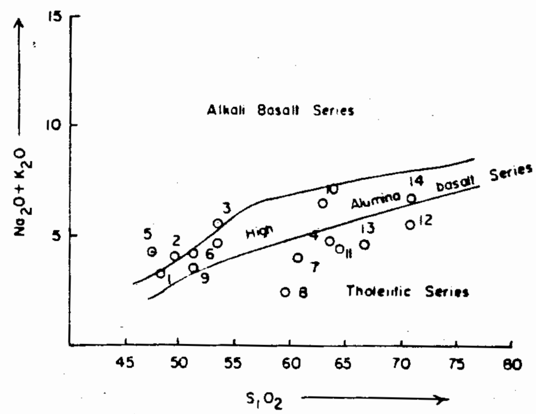

Fig. 9. Alkali versus SiO_2 plot for the magmatic rock suites of north central Chagai belt (After Kuno, 1966).

Dacite is characterised by 63.30% SiO_2 and 13.40% Al_2O_3. It contains 24.93% normative quartz 10.72% normative hypersthene and 0.89% normative diopside.

Gabbro has SiO_2 content from 47.40 to 51.50%. One sample has 7.29% olivine and 3.73% nepheline in the norm. Rest of the samples are quartz normative and contain normative hypersthene and diopside.

Diorite contains 59.45 to 60.50% SiO_2. These are quartz normative and also have normative diopside and hypersthene.

Granodiorite sample from central zone of granodiorite batholith, contains 70.35% SiO_2 while sample from marginal zone contains 64.44% SiO_2. Both the samples have 32.09% and 23.75% normative quartz, respectively.

Adamellite contains 70.90 to 66.03% SiO_2 in samples from central and marginal zones of adamellite batholith, respectively. Normative quartz in both samples ranges from 32.35 to 27.91%. Samples of central zone of batholith also contain 0.20% normative wollastonite.

The above reveals that all the mafic rock suites including basalts and gabbros are quartz normative and contain normative hypersthene, except one gabbro sample which is olivine normative. Therefore, according to the classification of Yoder and Tilley (1962) and Carmichael et al. (1974) majority of the mafic rock suites belong to the quartz tholeiite series and only one appears to be related to the olivine tholeiite series. Tholeiitic nature of these rock suites is also evident from FAM diagram (fig. 4) after Irvine and Barager (1974) and SiO_2 versus FeO_t/MgO plot (fig. 5) after Miyashiro (1974). Only a few rock suites, mainly belonging to felsic members, plot in the range of calc-alkaline series. The felsic members, according to Hyndman (1972), are less important for distinguishing basalt, andesite, rhyolite associations.

Solidification index versus SiO_2 and Fe_2O_3 + FeO plots (Kuno, 1968) in figs. 6 and 7 also confirm the tholeiitic parentage of these rock associations and further suggest that these rocks belong to moderate iron concentration type of tholeiitic or pigeonitic rock series.

Plots of silica versus alkalies in fig. 8 and 9 show a distribution of sample points in all three series (i.e., tholeiitic, high alumina and alkaline) and hence partially contradict the above study but this can be attributed by localized variation in Na_2O contents because of an exchange with sea water as already proposed by Melson et al., (1968), Fyfe (1976) and Shah and Majid (1985).

Fractionation Trends

Major oxides versus solidification index (S.I. = 100 x Mg/(MgO + Fe_2O_3 + FeO + Na_2O + K_2O)) (fig. 10) exhibits a progressive and smooth increase in Na_2O + K_2O and a similar decrease in MgO throughout fractionation with a little drop arround SI=20. Total iron remains almost constant upto SI=20 and then marks a sharp decrease and remains so upto the end of fractionation. TiO_2 and CaO show an uneven progressive increase throughout fractionation. SiO_2 exhibits a scattered increase and P_2O_5 makes a complete scatter and uneven distribution during differentiation.

Fig. 10 (S.I. vs Fe_2O_3 + FeO) also exhibits a maximum iron enrichment in the middle stage of differentiation which is characteristic of tholeiitic association.

A comparison of average (FeO + Fe_2O_3)/MgO ratio of tholeiitic basalt of studied area (Table 1) with average tholeiitic basalt of Allai Kohistan island arc (Shah and Majid, 1985) average island arc tholeiite and average island arc calc-alkaline basalt (Halberg and Villiam, 1972) in the following table shows close affinities with Kohistan island arc tholeiitic basalt and island arc tholeiitic rather than calc alkaline basalt.

Average (Fe_2O_3 + FeO)/MgO

Studied area	Kohistan Island arc	island arc tholeiite	Calc-alkaline basalt
2.37	2.06	1.41	0.93

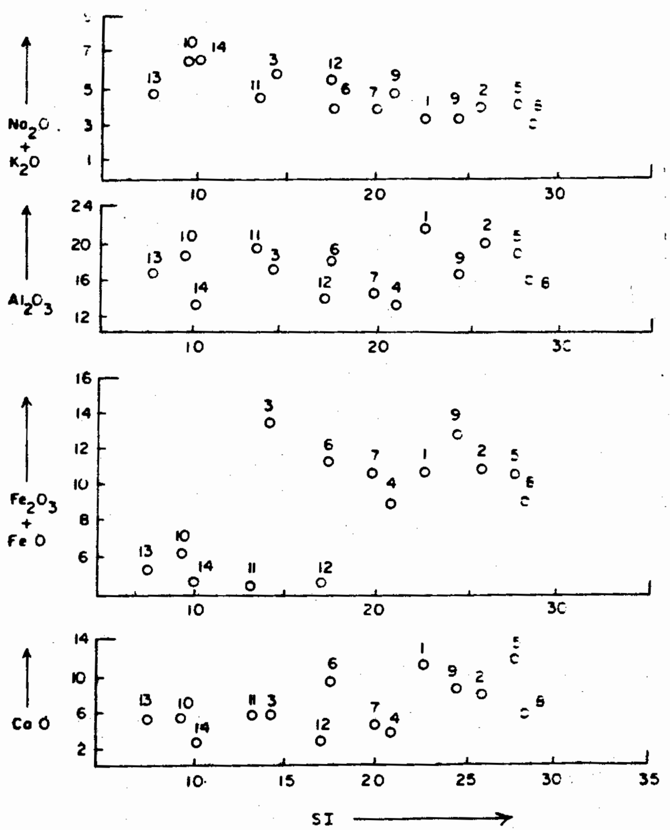

Fig. 10. Major oxides versus solidification index (SI) plot for magmatic rock suites of north central Chagai Belt.

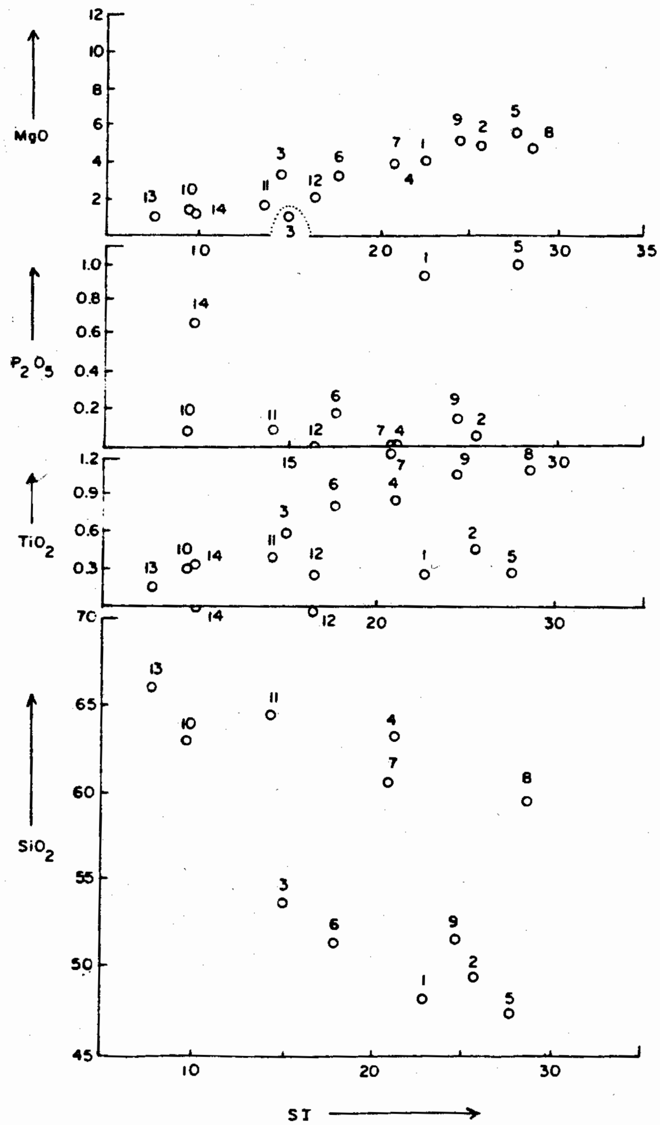

Fig: 10 Continued

Again a comparison of average K_2O/Na_2O ratio of the area (table 1) with Andean type continental margin and island arc (Jakes and White, 1972) in the following table reveals that the magmatic rock association of north central Chagai belt was developed in an island arc environment.

Average K_2O/Na_2O

Studied area	Island arc	Continental Margin
0.41	Less than 0.8	0.60 to 1.1

DISCUSSION

Petrological and petrochemical data given above suggests that magmatic rock suites of north-central Chagai belt represent the tholeiitic rock association and further that these rock suites have been developed in an island arc environment.

The presence of an ancient island arc between Indian plate and Afghan and Iran micro-plate have already been postulated by Powell (1979). This island arc was developed in Late Cretaceous due to an intraoceanic convergence along Zagros-Chitral convergence zone (or ancestral Oman-Makran trench-arc system of Jacob and Quittmeyer (1979) in the southern Tethys. This ancient island arc was disrupted due to continued northward movement of the Indo-Pakistani plate, and its eastern part was shifted towards north.

Tholeiitic nature and island arc character of the Kohistan belt (Majid, et al., 1978 and Shah and Majid, 1985) and Chagai belt (present study), suggest that Chagai and Kohistan island arcs may represent the disrupted parts of a single island arc which was displaced due to northward movement of Indian plate, the northern faulted contact of Chagai belt (Shareq et al., 1977) may perhaps represent the collisional (or convergence) boundry between Afghan-microplate and Chagai island arc. The southern thrusted contact of Chagai belt and fault bounded ophiolites in the northern flanks of Raskoh belt suggest that the Chagai belt is partially overthrusted upon the Raskoh belt (Farah et al., 1983), which has recently been interpreted as a collisional mass of oceanic basaltic-islands (McCormick, 1985). The fault bounded ophiolite sheets between Chagai and Raskoh range may perhaps represent the slivers of oceanic crust on which Chagai island arc was constructed.

CONCLUSION

This paper documents that the Chagai magmatic belt perhaps represents a tholeiitic sequence of an island arc, which has been constructed on an oceanic crust rather than an Andean type continental margin as previously considered. Chagai, and Kohistan magmatic belts may perhaps represent the disrupted parts of an island arc. The southern thrusted contact of Chagai belt and fault bounded ophiolites on northern flank of Raskoh belt suggest the partial obduction of Chagai belt over the Raskoh range.

ACKNOWLEDGEMENTS

The author gratefully acknowledges to Mr. Waheeduddin Ahmed, Director General, Geological Survey of Pakistan and Mr. Mahmood-uddin Ahmed, Director of the same department, for providing field and laboratory facilities. Dr. George Buda, UNDP consultant mineralogist, is extremly thanked for arranging to perform the chemical analyses of some samples in Hungarian University. Messrs Azher Khan, Muhammad Anwar (Senior Chemist), and Messrs Haider Kamal, Zaheer Ali Khan, Muhammad Saleem, Ghulam Muhammad and Tasadduq Hussain Shah (Chemists) of Geological Survey of Pakistan are greatly acknowledged for carrying out the chemical analyses of various rock samples.

Thanks and gratitudes are also due to Mr. Ghazanfar Abbas, Deputy Director, Geological Survey of Pakistan for critically reviewing the manuscript and offering useful suggestions.

REFERENCES

ANDRIEUSE, J. & BRUNEL, M. (1977) Evolution des Chain, Occidentals du Pakistan, Mem. H.S.Soc. Geol, France, 8, pp. 189-208.

ARTHURTON, R.S., ALAM, G.S., AHMAD S.A., & IQBAL S. (1979) Geological history of the Alam red Mashkichah area, Chagai District Baluchistan. *In:* Farah, A. & DeJong, K.A. (eds.) GEODYNAMICS OF PAKISTAN. Geol. Surv. Pakistan Quetta, pp. 325-31.

BAKAR, M.A. & JACKSON, R.D. (1964) Geological map of Pakistan. Geol. Surv. Pak., Scale 1 : 2,000,000.

BRITZMAN, L. (1979) Fission track ages of intrusives of Chagai District, Baluchistan, Pakistan. M.A. thesis Darmouth College, Hanover, New Hampshire, U.S.A. (Unpublished).

CARMICHAEL, I.S.E., TURNER, F.J., & VERHOOGEN, J. (1974) "IGNEOUS PETROLOGY" McGraw Hill Book Company New York.

DYKSTRA, J.D. (1978) A geological study of the Chagai hills, Baluchistan, Pakistan. Using LANDSAT digital data. Unpublished Ph.D thesis, Dartmouth College, Hanover, N.H., 147p.

__________ & BIRNIE, W. (1973) Segmentation of the Quaternary subduction zone under the Baluchistan region of Pakistan and Iran *In:* Farah, A. & DeJong, K.A. (eds.) GEODYNAMICS OF PAKISTAN (op. cit.) pp. 319-23.

FARAH, A., ABBAS, G. DEJONG, K.A. & LAWRENCE, R.D. (1984) Evolution of the Lithosphere in Pakistan. Tectonophysics, 105, pp. 207-227.

FYFE, W.S. (1976) Hydrosphere and continental crust growing or shrinking? Geosco-Can, 3, pp. 82-83.

HALLBERG, J.A. & VILLIAM (1972) Archean mafic and ultramafic rock association in the eastern Goldfield region, western Australia. Earth Planet. Sci. Letters. 15, pp. 191-250.

HUNTING SURVEY CORPORATION LIMITED. (1960) RECONNAISSANCE GEOLOGY OF PART OF WEST PAKISTAN Colombo Plan Cooperative Project, Government of Canada, Toronto, Canada.

HYNDMAN, D.W. (1972) "PETROLOGY OF IGNEOUS AND METAMORPHIC ROCKS" McGraw Hill Company New York 531p.

IRVINE, T.N. & BARAGAR, W.R.A. (1971) A guide to the classification of the common volcanic rocks. Can. Jour. Earth. Sci. 8, pp. 523-549.

JACOB, K.H. & QUITTMEYER, R.C. (1979) The Makran region of Pakistan and Iran: trench-arc system with active plate subduction. *In:* Farah, A. & DeJong, K.A. (eds.) GEODYNAMICS OF PAKISTAN. (op. cit.) pp. 305-17.

JAKES, P. & WHITE, A.J.R. (1972) Major and trace elements abundances in Volcanic rocks of Orogenic areas.

KUNO, H. (1966) Lateral variation of basaltic magma type across continental margins and island arcs. Bull. Volcanol. 29, pp. 195-222.

__________ (1968) Differentiation of basaltic magmas *In:* Hess, H.H. & Poldervaart, A. (eds.) BASALTS. Johm Wiley and Sons New York pp. 623-688.

MAJID, M., SHAH, M.T., LATIF, A., AURANGAZEB, & KAMAL. (1981) Major elements abundance in the Kalam lavas. Geol. Bull. Univ. Peshawar, 14, pp. 45-62.

MELSON, W.T., THOMPOSON, G., & VAN ANDEL, T.H. (1968) Volcanism and metamorphism in the mid-Atlantic ridge 22 degree N Latitude. Jour. Geophys. Res. 73, pp. 5925-41.

McCORMICK, G.R. (1985) Preliminary study of the volcanic rocks of the South Tethyan suture in Baluchistan, Pakistan. Acta Mineralogica Pakistanica 1, pp. 2-9.

MIYASHIRO, A. (1974) Volcanic rock series in Island arcs and continental margin. Am. Jour. Sci. 274, pp. 321-55.

NIGELL, R.H. (1975) Reconnaissance of the geology and ore mineralization in part of the Chagai District, Baluchistan, Pakistan: Proj. Report (I.R), PK-27, U.S. Geological Surv. open file report, pp. 75-550.

O'CONNOR, J.T. (1965) A classification of quartz-rich igneous rocks based on feldspar ratio. U.S. Geol. Surv. Prof. Paper 525-B, pp. B79-B84.

POWELL, C.Mc.A. (1979) A speculative tetonic history of Pakistan and surroundings: some constraints from the Indian ocean. *In:* Farah, A. & DeJong, K.A. (eds.) GEODYNAMICS OF PAKISTAN (op. cit), pp. 5-24.

SCHWARZER, R.R. & ROGER, J.J.W. (1974) A world wide comparison of alkali-olivine basalts and their differentiation trades: Earth Plan. Sci. letters 23, pp. 286-96.

SHAH, M.T. & MAJID, M. (1985) Major and trace elements variations in the lavas of Shergarh Sar area and their significance with respect to the Kohistan tectonic anomaly: Geol. Bull. Univ. Peshawar 18, pp. 163-88.

SHAREQ, A., CHMYRIV, V. M., STAZHILE–ALEKSEEV, K.E., GANNON P.J., LUBEMOVE, B.K., KAFARASKIY, A.K.H., & MALYAROVE, E.P. (1977) MINERAL RESOURCES OF AFGHANISTAN 2nd ed. 419 p (A joint project of Afg/UNDP under Ministry of Mines and Industries Afghan Geol. and Mines Surv.).

SILLITOE, R.H. (1972) A plate tectonic model for the origin of prophyry copper deposits. Econ. Geol. 67, pp. 189-97.

__________ (1974) Metallogenic evolution of a collisional mountain belt of Pakistan. Geol. Surv. of Pak. Rec. 34, 16p.

SPECTER, A. & ASSOCIATES LTD. (1981) Report on interpretation of aeromagnetic survey data, Baluchistan Province, Pakistan: Project Report J 223. A specter & Associates Ltd. 107p.

STONELEY, R. (1974) Evolution of the continental margin bounding a former southern Tethvs. in Burke. C.A. and Drake, C.L., (eds.) THE GEOLOGY OF CONTINENTAL MARGINS. Springer. New York, pp. 889-903.

STRECKEISEN, A. (1979) Classification and nomenclature of volcanic rocks, lamprophyres, carbonatite and melitic rocks. Recommendation and suggestion of IUGS sub-commission on the systematics of Igneous rocks. Geol. 7, pp. 331-5.

YODER, H.S., & TILLEY, C.E. (1962) Origin of basalt magmas: an experimental study of natural and synthetic rock systems: Jour. petrology 3, pp. 342.

Manuscript received 31.12.1986

ACTA MINERALOGICA PAKISTANICA
VOLUME 2 (1986) pp. 24-46.

MINERALOGY OF PROTEROZOIC METAMORPHITES OF SOUTHERN MALAKAND AGENCY, PAKISTAN.

ZULFIQAR AHMED

Centre of Excellence in Mineralogy, University of Baluchistan, Sariab Road, Quetta, Pakistan.

ABSTRACT:— Mineral assemblages of a variety of lithological samples of the greenschist facies metamorphic rocks that occur widespread in southern Malakand Agency and adjacent areas, have been investigated and chemically analyzed by microprobe. Mineral chemical data is presented in respect of chloritoid, chlorite, muscovite, fuschsite, talc, biotite, spessartine, Mn-bearing garnet, apatite, sphene, ilmenite, monazite and rutile. Data on fuchsite is supplemented by its lattice parameters. Chlorite zone is extensively developed with regional metamorphic chloritoid found in a portion. The chloritoid has low Mg, Mn and inferred Fe^{3+}. It equilibrated with chlorite at a temperature higher than that of the comparable rocks from Turkey. The celadonite and Ti contents in muscovite show progressive increase with metamorphic grade. From under the base of an ophiolite an even higher grade spessartine-bearing rock is found affected more by higher pressure than by higher temperature. Its chlorite has relatively high MnO and CaO contents. At or near the contact of ophiolitic rocks, evidence of metasomatic and hydrothermal activity is noticed.

INTRODUCTION

There occur widespread outcrops of greenschist facies metamorphites in the southern Malakand Agency and adjacent areas of Pakistan. They represent the Proterozoic continental crust of this region. For the present study, rock samples covering a variety of rock types were collected from locations on hills west of Dargai town towards Harichand. The whole-rock chemistry including major elements, trace elements and REE contents is given elsewhere (Ahmed, 1986, 1987). The present work comprises an extension of the same work and describes the results of electron probe microanalyses of the mineral constituents performed in order to present their first – time characterization and to discuss their implications on regional metamorphism and other phenomena.

PETROGRAPHIC FEATURES

The samples generally contain abundant quartz and a variety of less abundant minerals. The assemblages in some individual rock samples and localities are tabulated in table 1.

Chlorite is an abundant mineral of the schists and dominates in many samples. It may co-occur with chloritoid. Chlorite of one rock-type, represented by sample Z387, is different from the general lot of chlorite in the schists; has a deeper green colour, and is chemically different as described in the following section on mineral chemistry. Chloritoid is found as scattered small laths in the samples Z329 and Z401, both of which are of chlorite grade, and do not contain biotite.

Table 1. Description of rock samples. Grid-references are from 1:50,000 scale topographic sheets 38 N/11 and 38 N/15 of the Survey of Pakistan.

Sample No.	Grid-Reference	Description
Z267 ZA267 ZB267	4150-8332	Spessartine-quartz-chlorite-muscovite rock with accessory sphene and magnetite. It is green coloured, weakly schistose, fine-grained rock developed locally near the lower (southern) contact of ultramafic rocks.
Z329	4610-8310	Greenish grey coloured schist with chloritoid, quartz, muscovite, chlorite, graphitic patches and some limonite after pyrite.
Z332	4595-8340	Hematitic quartz-muscovite schist. Chlorite and graphite are also present.
Z353	4605-8650	Talc schist with ferritchromite grains commonly present; probably a metamorphosed ultramafic rock.
Z355	4610-8650	Greenish white chlorite schist with quartzite bands. It contains quartz, chlorite, muscovite, dark mica (biotite), apatite, sphene and Mn-ilmenite.
Z385	4500-7560	Phyllite with graphite, quartz, chlorite muscovite, albite, Ti-oxide and dark mica (biotite).
Z387	4630-8650	Chlorite schist; host rock for soapstone deposit. It contains talc, chlorite, monazite, rutile, apatite.
Z389	4630-8650	Brown coloured; spotted schistose quartzite with quartz, muscovite, biotite, hematite, limonite and siderite.
Z391	4625-8655	Schist sample from near fuchsite outcrop, contains quartz, muscovite, dark mica, ilmenite, chlorite, albite, pyrite and veins of calcite.
Z392	4605-8655	Coarse grained brown and white schist rich in fuchsite layers sampled from near contact of gabbro and schists. It contains fuchsite, quartz, muscovite, chlorite, magnetite calcite and hematite.
Z398	4630-8650	Quartz mica schist with quartz, muscovite, dark mica, apatite, and about 2% calcite.
Z401	4605-8310	Chloritoid-quartz-muscovite schist. Chlorite and hematite are also present. Secondary magnetite present as specks.

Muscovite is a common phase all over the metamorphic sequence of this region. It is present in all the samples analyzed for this study. It is much more abundant than biotite and occurs as the usual flakes delineating the foliation of the schists.

The emerald green fuchsite occurs as less than 1 cm to a few metres thick interbeds in a schist outcrop near Musa Mena village. Fuchsite layers parallel schistosity of the rock. The host rock of fuchsite is partly calcareous and as the contact of ultramafic – mafic rock complex,

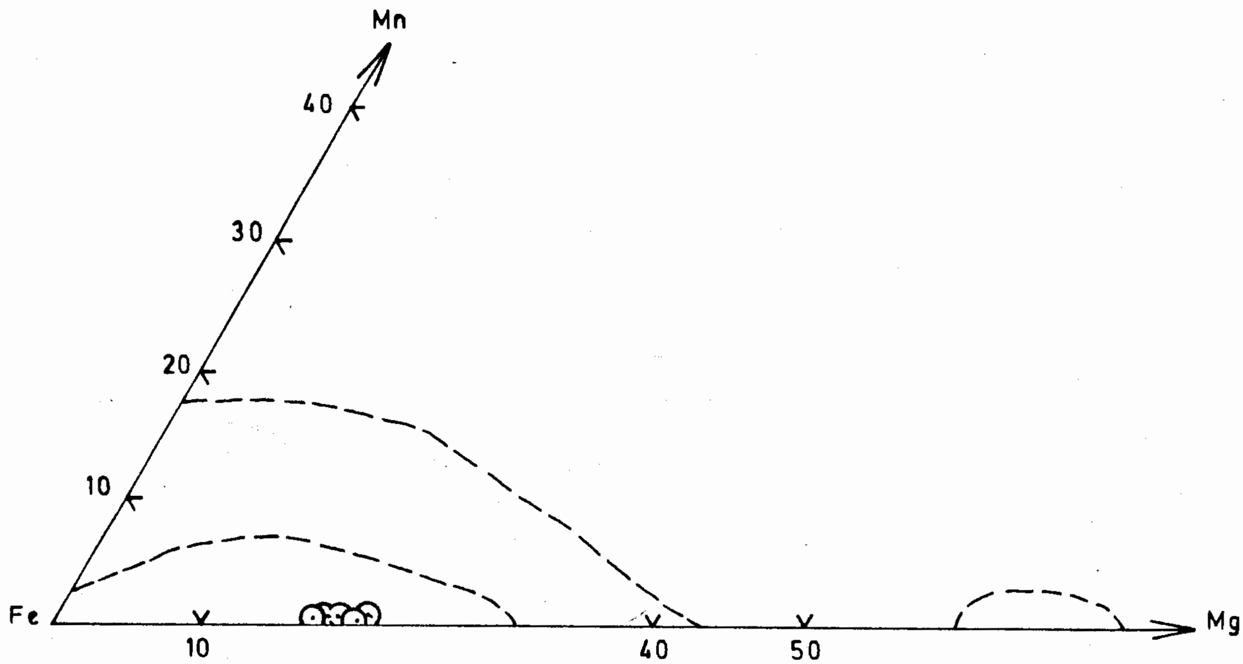

Fig.1. Chloritoid compositions detailed in table 1 showing the variation of Fe^{2+}, Mg, and Mn. Broken lines enclose chloritoid compositions in Halferdahl's (1961) compilation.

the Sakhakot – Qila ophiolite, is very close; the fuchsite may be genetically related to it. From Sierra Nevada, Spain, a mariposite has been described (Martin-Ramos & Rodriguez–Gallego, 1982) similar in occurrence to the Dargai area fuchsite. Biotite is much less abundant than muscovite. Some rocks e.g., Z355, Z385, Z391 and Z398, contain other "dark micas" that are different from biotite or any other mica chemically as described in the section on mineral chemistry. All the samples with biotite or other dark micas contain muscovite as well. Sphene, ilmenite and rutile occur disseminated, forming euhedral to subhedral crystals. Rutile occurs as needle-like, long prisms in the monazite-bearing rock sample (Z387) and is rare in other metamorphic rocks. Further details of the whole rock petrography and chemistry are given in Ahmed (1987).

The polished thin sections of rock samples were analyzed employing the electron probe microanalytical unit set up at the University College, University of London, UK. The results are tabulated separately for each mineral species in tables 2 through 13. The microprobe was operated with 15 kV accelerating potential, 100 live seconds counting time, Si(Li) detector, an on-live computer for ZAF corrections, and a cobalt internal standard. The mineral identifications were confirmed by the powder method X-ray diffraction. The lattice parameters for fuchsite were obtained from diffractograms on Philips X-ray diffractometer with Cu $K\alpha$ radiation and nickel filter. The sample was mixed with powdered glass to avoid alignment of micaceous flakes and was mounted on aluminium holder. Pure silicon standard was run under identical conditions.

CHLORITOID

In table 2, five chloritoid analyses are reported. There is no significant departure from the ideal chloritoid formula given by Deer et al. (1962). Crystals are unzoned. The chloritoid is low in MgO and MnO and characteristic high Al_2O_3 and FeO contents are present. Replacement of

Table 2. Chloritoid analyses.
Total iron oxide is expressed as FeO.

Anal. No.	1	2	3	4	5
Sp. No.	**Z329**	**Z401**	**Z401**	**Z401**	**Z401**
Oxides weight percent :					
SiO_2	24.97	24.96	25.31	24.07	24.46
TiO_2	0.04	0.07	0.57	0.42	0.00
Al_2O_3	40.51	40.99	40.49	39.98	40.57
Cr_2O_3	0.01	n.d.	n.d.	0.04	0.00
V_2O_3	0.12	n.d.	n.d.	0.07	0.22
FeO	23.13	23.85	23.67	25.22	23.89
MnO	0.20	0.23	0.21	0.15	0.16
MgO	3.42	3.12	2.97	2.92	3.41
NiO	0.08	n.d.	n.d.	0.02	0.11
CaO	0.01	0.00	0.00	0.00	0.05
Na_2O	0.05	0.00	0.00	0.36	0.48
K_2O	0.00	0.02	0.00	0.00	0.00
Total	92.54	93.24	93.22	93.25	93.35
Cations based on 12 oxygens (anhydrous) :					
Si	2.045	2.033	2.060	1.985	2.001
Al^{iv}	3.000	3.000	3.000	3.000	3.000
Al^{vi}	0.911	0.936	0.884	0.886	0.911
Ti	0.003	0.004	0.035	0.026	0.000
Cr	0.001	n.d.	n.d.	0.003	0.000
V	0.008	n.d.	n.d.	0.005	0.014
Fe	1.584	1.625	1.611	1.739	1.634
Mn	0.014	0.016	0.014	0.011	0.011
Mg	0.418	0.379	0.360	0.359	0.416
Ni	0.005	n.d.	n.d.	0.001	0.007
Ca	0.001	0.000	0.000	0.000	0.004
Na	0.008	0.000	0.000	0.058	0.076
K	0.000	0.002	0.000	0.000	0.000
Fe/(Fe+Mg)	0.791	0.811	0.817	0.829	0.797
Atom. %					
Fe	78.571	80.446	81.159	82.456	79.282
Mg	20.734	18.762	18.136	17.022	20.184
Mn	0.695	0.792	0.705	0.522	0.534

Fe^{2+} by Mg is upto 20.8 atom % and by Mn is upto 0.8 atom %. In its structural formula, the tetrahedral site is occupied by Si;3 Al atoms are in the corundum-type octahedral sites; whereas the remaining Al, Fe, Mg, Mn and Ni with a sum very close to 3, occupy the brucite-type octahedral site. All analyses of table 2, except the analysis no. 3, show Fe+Mg+Mn in excess of 2.00 per 12 oxygens, coupled with slight deficiencies in Al for the brucite – type octahedral sites. As primary haematite in accessory amounts is present in these rocks, probably some of the total Fe substitutes as Fe^{3+} for Al^{3+} in the mineral (Holdaway, 1978).sThe Fe^{2+}/Fe^{2+}+Mg) ratio of chloritoid varies from 0.791 to 0.829. Its MnO content varies between 0.15 and 0.23%. The Fe–Mn–Mg triangular plot is drawn in fig. 1. The analyses cluster at a point well within the field compiled by Halferdahl (1961).

The chloritoid-bearing rock samples chemically fall within the limitations listed by Halferdahl (1961) for such rocks. Their whole–rock Al_2O_3 content varies from 17.86% to 19.10%, SiO_2 varies from 66.72% to 69.07% and their Fe^{2+}/Mg ratio is rather high (Ahmed, 1987, table 1). Al_2O_3 is quite in excess of total mafic oxides (i.e., Fe_2O_3 + FeO + MnO + MgO) whose contents vary from 7.96% to 8.57%. Σ Fe + Mn in all the samples is more than either MgO or Fe_2O_3. The chloritoid-bearing samples possess (2 Fe_2O_3 x 100)/(2Fe_2O_3 + FeO) ratios from 42.14 to 49.12. The distribution coefficient K_D, between coexisting chlorite and chloritoid, calculated after the method given by Ashworth and Evirgen (1984) for average chloritoid (analysis 3 in table 2) is plotted in fig. 2 and shows a temperature relatively higher than those of the chlorite grade rocks of the Lycian Nappes, Turkey; and are similar to the other chloritoid-bearing pelites from literature. The K_D values should move towards unity with increased temperature of equilibration (Ashworth & Evirgen, 1984). The high Al content of chloritoid (table 2) implies low Fe^{3+}. This indicates decrease in the degree of oxidation of the rock as noted above.

Analyses of chlorite associated with chloritoid (e.g., sample Z401, table 3) shows 0.06% MnO as against 0.15 to 0.23% MnO in the chloritoid. Chlorite has Fe/Fe + Mg) ratio of 0.537 which coexists with chloritoid with Fe/Fe + Mg) ratio of 0.797 to 0.829.

Table 3. Representative microprobe analyses of chlorite from schists. All iron oxide is reported as FeO.

Anal. No.	1	2	3	4	5	6	7	8	9	10	11	12
Sp. No.	Z267	Z355	Z355	Z385	Z385	Z391	Z387	Z387	Z387	Z392	Z392	Z401
SiO_2	29.85	28.64	24.99	25.67	30.75	24.97	28.74	28.66	28.89	25.53	26.02	25.87
TiO_2	0.11	0.23	0.24	0.12	0.27	0.30	0.09	0.00	0.01	0.17	0.17	0.37
Al_2O_3	22.01	23.52	21.45	20.30	22.89	20.89	20.01	20.41	20.23	21.06	22.00	24.18
Cr_2O_3	0.02	0.00	0.04	0.17	0.13	0.02	0.01	0.00	0.05	0.27	0.03	n.d.
FeO	25.97	23.30	26.03	24.28	19.73	29.75	11.43	11.44	11.39	21.39	21.84	24.91
MnO	1.93	0.67	0.93	0.16	0.28	0.04	0.27	0.22	0.18	0.19	0.18	0.06
MgO	12.76	11.44	13.01	15.23	12.46	11.36	25.78	25.53	25.50	16.08	16.88	12.06
NiO	0.30	0.00	0.00	0.09	0.09	0.06	0.00	0.14	0.01	0.08	0.07	n.d.
CaO	1.27	0.07	0.08	0.03	0.04	0.23	0.02	0.00	0.01	0.40	0.15	0.14
Na_2O	0.74	0.17	0.00	0.22	0.00	0.39	0.67	0.51	0.24	0.00	0.00	0.39
K_2O	0.21	1.01	0.12	0.04	1.98	0.04	0.00	0.02	0.01	0.00	0.04	0.12
Total	95.17	89.05	86.89	86.31	88.62	88.05	87.02	86.93	86.52	85.17	87.38	88.10
Cations based on 28 oxygens (anhydrous) :												
Si	5.819	5.845	5.364	5.482	6.185	5.382	5.672	5.657	5.711	5.440	5.394	5.386
Al^{iv}	2.181	2.155	2.636	2.518	1.815	2.618	2.328	2.343	2.289	2.560	2.606	2.614
Al^{vi}	2.877	3.503	2.792	2.593	3.612	2.690	2.326	2.406	2.426	2.731	2.771	3.918
Ti	0.016	0.035	0.039	0.019	0.040	0.048	0.014	0.000	0.001	0.028	0.027	0.058
Cr	0.003	0.000	0.007	0.029	0.020	0.003	0.002	0.000	0.008	0.045	0.004	n.d.
Fe	4.234	3.977	4.674	4.338	3.319	3.652	1.886	1.890	1.882	3.812	3.787	4.336
Mn	0.319	0.116	0.169	0.028	0.047	0.007	0.045	0.036	0.031	0.035	0.032	0.010
Mg	3.707	3.480	4.164	4.849	3.736	3.652	7.582	7.514	7.513	5.109	5.218	3.741
Ni	0.047	0.000	0.000	0.015	0.014	0.009	0.000	0. 22	0.001	0.014	0.012	n.d.
Ca	0.265	0.015	0.018	0.008	0.009	0.054	0.004	0.000	0.003	0.091	0.033	0.031
Na	0.280	0.067	0.000	0.090	0.000	0.163	0.255	0.196	0.093	0.000	0.000	0.159
K	0.052	0.263	0.033	0.011	0.507	0.012	0.000	0.004	0.003	0.000	0.010	0.032
100X $Fe^{2+}/(Fe^{2+}+Mg)$	53.318	53.332	52.885	47.219	47.045	59.490	19.920	20.098	20.032	42.731	42.054	53.683

Chlorite

Twelve chlorite analyses are set out in table 3, representing variations between and within different rock types. Overall. they are quite variable with FeO ranging from 11.4 to 29.8%, MgO from 11.4 to 25.8%, Al_2O_3 from 20.0 to 24.2 and SiO_2 from 25.0 to 30.8%. MnO and CaO are normally low, but are conspicuously higher in the spessartine-bearing schist (sp. Z267). The monazite and rutile-bearing schist (anal. 7-9) shows conspicuously lower FeO, lower TiO_2 and Al_2O_3 and higher MgO than the rest of the samples. This rock is deeper green in colour compared to most other chlorite schists, whose chlorite is generally ripidolite although brunsvigite and pycnochlorite compositions are also encountered. The within sample variations in these schists are large. For example, sample Z355 contains brunsvigite and ripidolite; sample Z385 contains ripidolite and pycnochlorite. The $Fe^{2+}/(Fe^{2+}+Mg)$ for monazite-bearing sample is very low, from 0.199 to 0.201; but for rest of the samples it varies from 0.421 to 0.595. Assuming decrease in Fe^{2+}/Mg indicating higher metamorphic temperature (Miyashiro, 1973), sample Z391 indicates lowest and Z392 indicates higher temperature of metamorphism.

Muscovite

The chemical analyses of muscovite are

Table 4. Muscovite analyses from schists. All iron oxide is expressed as FeO. The sample standard deviation is given under 's'. $\bar{X}$ is the mean of the number of analyses parenthesized.

Sp. No.	Z267		Z355	Z385		Z389	Z398		Z329	Z332	Z392	Z401
No. Anal.	$\bar{X}$(10)	s	$\bar{X}$(2)	$\bar{X}$(10)	s	$\bar{X}$(2)	$\bar{X}$(14)	s	(1)	(1)	(1)	$\bar{X}$(2)
SiO_2	46.72	(1.39)	46.67	49.01	(1.26)	47.60	47.39	(0.81)	46.89	47.65	44.82	47.62
TiO_2	0.63	(0.18)	0.49	0.50	(0.34)	0.54	0.50	(0.42)	0.29	0.17	0.33	0.24
Al_2O_3	28.01	(0.42)	31.32	28.11	(0.77)	27.55	32.84	(1.34)	36.69	35.65	33.05	34.60
Cr_2O_3	b.d.		0.01	0.06	(0.05)	0.00	b.d.		0.09	0.03	0.08	n.d.
FeO	5.82	(0.52)	3.21	3.64	(1.23)	3.44	2.82	(1.69)	0.48	0.61	2.87	0.85
MnO	0.21	(0.09)	0.10	b.d.		0.06	0.06	(0.05)	0.00	0.00	0.00	0.05
MgO	2.05	(0.42)	2.41	3.09	(0.68)	2.06	2.42	(0.89)	0.96	0.59	1.90	0.70
NiO	b.d.		0.00	0.04	(0.04)	0.07	0.04	(0.03)	0.00	0.00	0.03	n.d.
CaO	n.d.		0.05	0.07	(0.06)	0.21	b.d.		0.00	0.00	0.19	0.02
Na_2O	0.61	(0.11)	0.44	0.07	(0.07)	0.26	0.88	(0.23)	1.50	0.76	0.30	0.92
K_2O	10.67	(0.35)	9.45	9.86	(0.61)	10.02	8.38	(0.72)	8.02	8.52	9.63	8.13
Total	94.72		94.15	94.45		91.81	95.33		94.92	93.98	93.20	93.13
Cations on the basis of 22 oxygens :												
Si	6.444		6.324	6.621		6.643	6.284		6.155	6.308	6.141	6.362
Al^{iv}	1.556		1.676	1.379		1.357	1.716		1.845	1.692	1.859	1.638
Al^{vi}	2.998		3.327	3.097		3.175	3.417		3.832	3.871	3.479	3.811
Ti	0.065		0.050	0.051		0.057	0.050		0.029	0.017	0.034	0.024
Cr	b.d.		0.002	0.006		0.000	0.002		0.009	0.003	0.008	n.d.
Fe	0.671		0.365	0.411		0.401	0.313		0.053	0.068	0.328	0.095
Mn	0.025		0.012	0.025		0.007	0.007		0.000	0.000	0.000	0.006
Mg	0.421		0.489	0.622		0.429	0.478		0.188	0.117	0.388	0.139
Ni	b.d.		0.000	0.004		0.008	0.004		0.000	0.000	0.004	n.d.
Ca	b.d.		0.007	0.010		0.031	0.001		0.000	0.000	0.028	0.003
Na	0.163		0.117	0.018		0.071	0.226		0.382	0.195	0.079	0.238
K	1.878		1.634	1.700		1.784	1.418		1.343	1.439	1.683	1.386

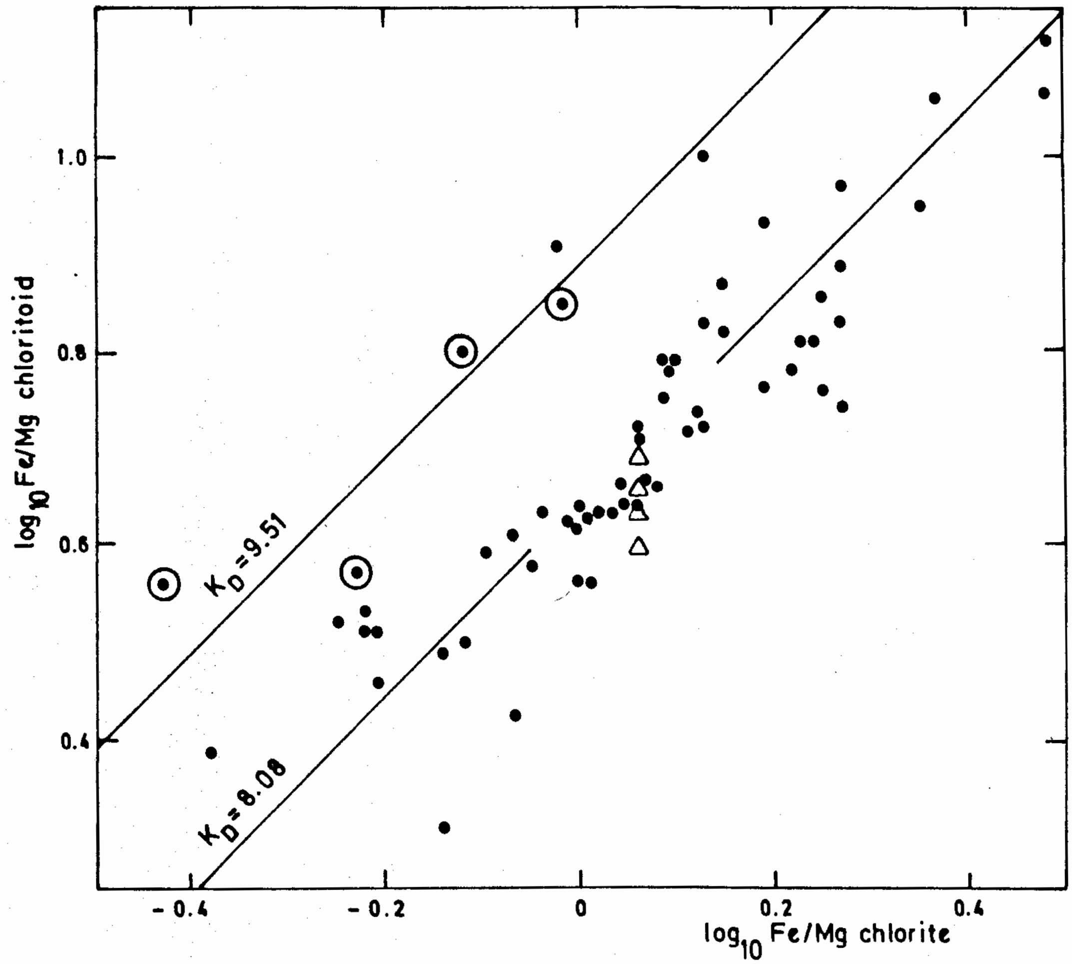

Fig. 2. Fe/Mg partition between chloritoid and chlorite in the study area (triangle) compared with other areas in the literature (average logarithmic ratio indicating K_D= 8.08). Key to literature sources is given in Ashworth & Evirgen (1984). Encircled points are from chlorite-grade rocks, others are of higher grade.

reported in table 4. Compared to ideal stoichiometry, muscovite is slightly deficient in K_2O, whose overall variation ranges from 7.29% to 11.13%. Moreover, the Al_2O_3 values are lower than the muscovite ideal composition; whereas Si is in excess. The number of samples analyzed in the present study is too low to make the pattern of variation compare well with the generally recognized variations in muscovite composition in pelitic rocks with the metamorphic grade, such as those mentioned by Ruiz et al. (1980). Some muscovites indicate unsually higher (O,OH,F), because of their low totals. The higher 's' values for the sample Z398 in table 4 reflect its bimodal Ti and Fe. The highest Al_2O_3 and Na_2O and lowest FeO in the sample Z329 may indicate higher metamorphic temperatures if considered similar to some other known instances (e.g. Miyashiro, 1973). However, its Ti is not higher. Ti is relatively high in sample Z267 which is a spessartine – bearing rock of relatively higher metamorphic grade. Ti in all the analyses of table 4 is below 0.065 atoms/22 oxygens, except two values of 0.08 and 0.112 respectively, from the sample Z267. Thus, the muscovites

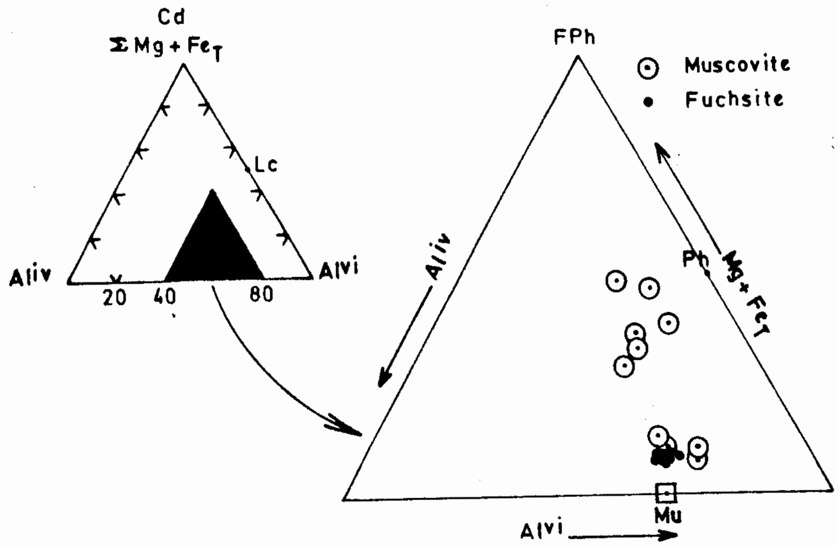

Fig.3. Plot of the K-white micas in terms of amount of Al^{iv}, Al^{vi} and $\Sigma(Mg + Fe_T)$. Mu = muscovite; Cd = celadonite; FPh = ferriphengite; Lc = leucophyllite; Ph = phengite.

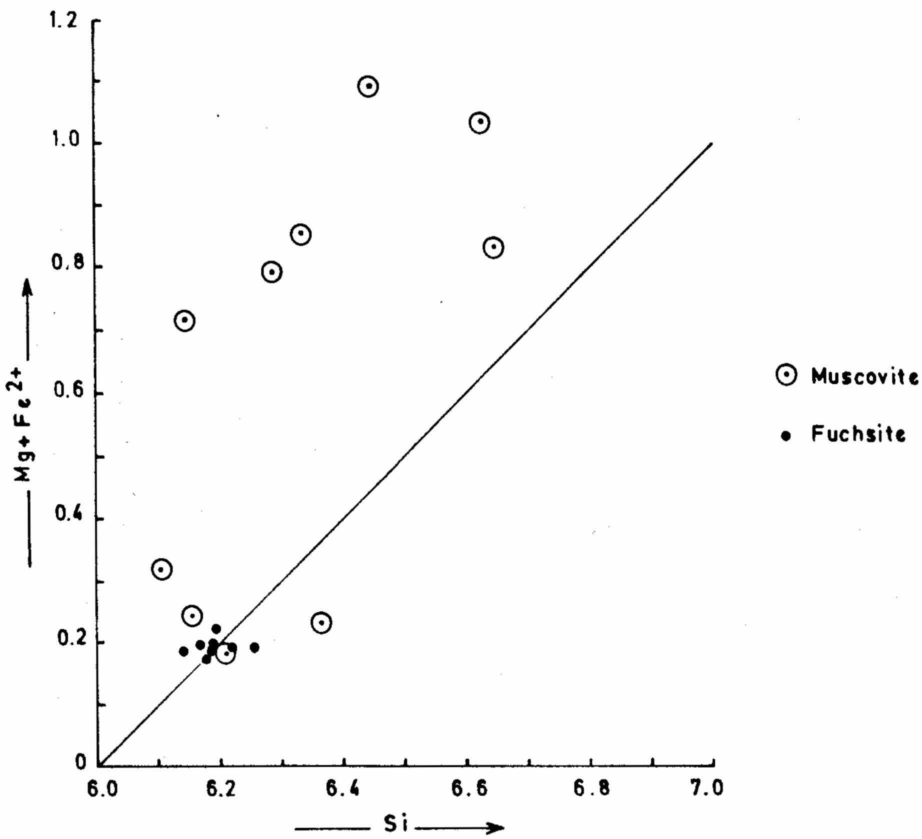

Fig.4. Plot of Si versus $\Sigma(Mg + Fe^{2+})$ with respect to the line for ideal Tschermak substitution, drawn after Guidotti (1984). If all the $(Mg + Fe^{2+})$ were charge-balanced by Si replacing Al^{iv}, the points should cluster along the ideal Tschermak substitution line.

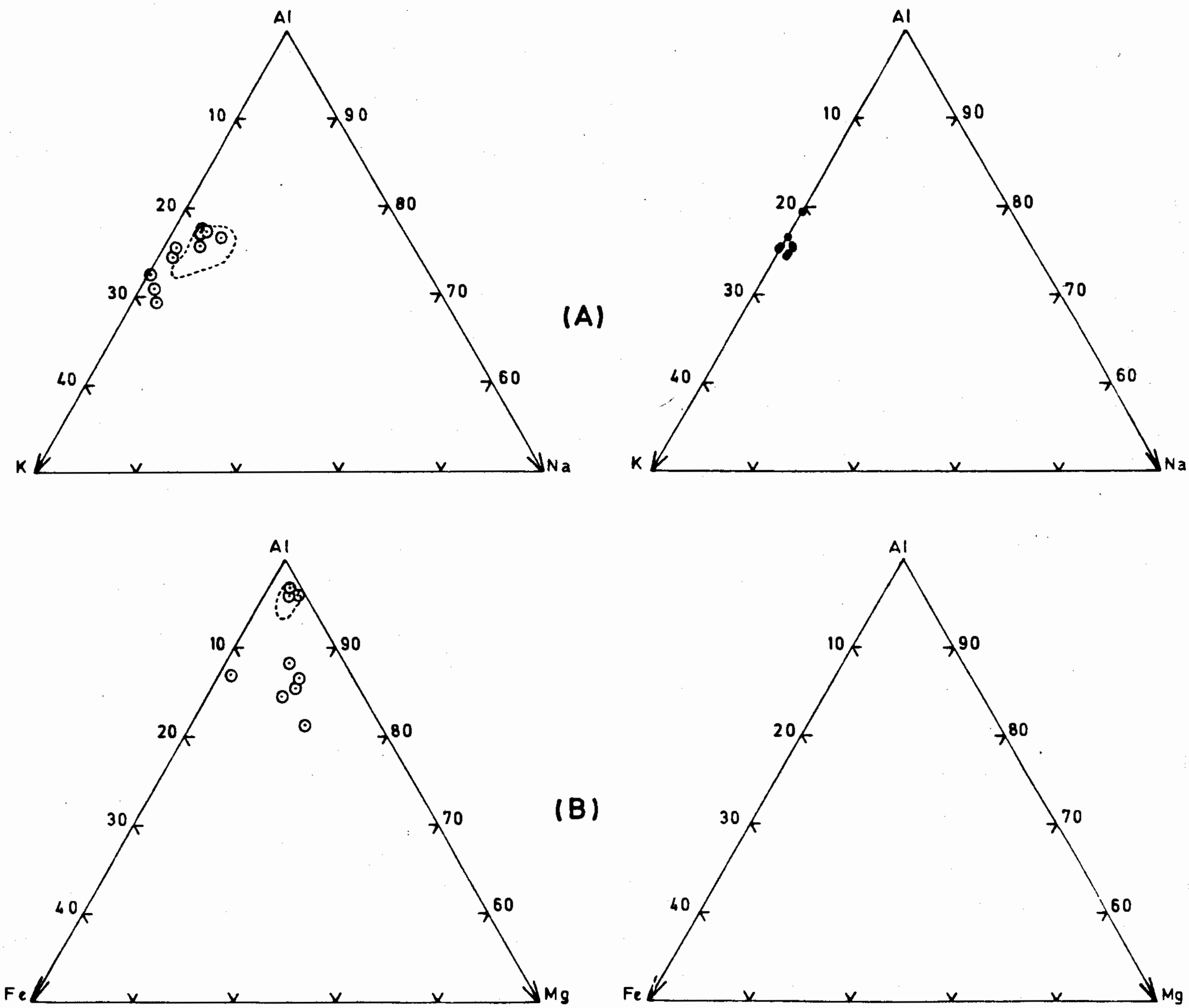

Fig. 5. Projection of the muscovite (circles) and fuchsite (dots) analyses from the metamorphites included in the present study in the triangles Al-K-Na (A) and Al-Fe-Mg (B). Compositional field of muscovites from the Sierra de Guadarrama area, Spain (Ruiz et al., 1980) and Ardnamurchan area, Scotland (Butler, 1967) is shown enclosed by dashed line.

resemble the vast bulk of published analyses which contain Ti values < 0.10 per 4 octahedral sites (Guidotti, 1984). Also, the muscovites of table 4 show clearly an increased Ti content with increasing metamorphic grade and celadonite content. The garnet zone sample (Z267) has Ti mean at 0.065, the biotite-bearing samples (Z355, Z385, Z389, Z398) have Ti means from 0.050 to 0.057 while the lower grade samples contain 0.017 to 0.029 Ti ions per 22 oxygens.

Ratio of Al^{vi} to the total of sixfold coordinated cations is lowest (71.722) in the garnet-bearing sample, it is intermediate in biotite – bearing samples, varying from 73.458 to 80.005; and increases in lower grade samples from 82.033 to 94.971. Thus, celadonite increases with metamorphic grade. This higher metamorphic grade with celadonite indicates, in comparison with the data of Guidotti (1984) that probably higher pressure was more active than increase in T for the higher grade metamorphism especially of sample Z267.

The sum of cations assigned to the 12 – coordinated sites is less than 2 atoms per 22 oxygens and drops to as low as 1.624 in sample Z401. In fuchsite, it is usually ≅ 1.7, but one analysis shows it at 1.425. The garnetiferous sample (Z267) is an exception. It shows mean of 2.041 12-coordinated atoms. Ca is usually below the background levels. Its maximum amount is 0.21% by weight. The Mn content is small. Most muscovites have upto 0.10 Mn ions per 22 oxygens. In table 4, higher Mn for Z267 and Z385 is the mean for a wide range of Mn in analyses from each sample.

The chloritoid-bearing samples (e.g. Z329, Z401), being Al_2O_3 richer, contain muscovites with the lowest celadonite content and the highest Na/(Na + K) ratios. The biotite – bearing samples (e.g. Z355, Z389,, Z385, Z398) show higher celadonite content.

The atomic percent Al among octahedral cations ranges from 94.971 to 71.722; the latter number being for the sample Z267, which plots on the join phengite – ferrimuscovite in fig. 3. The solid solution of muscovite with leucophyllite as well as ferriphengite is likely as these metamorphic rocks commonly contain graphite, hematite and magnetite as mentioned in table 1.

Fig. 3 plots the muscovites and fuchsites of present study to observe the Tschermack exchange and deviations from the ideal muscovite. The Si in muscovites is ⩽ 6.729, and only sometimes exceeds 6.5 atoms per formula unit. Thus, all muscovites are within the 6.8 Si limit for the muscovite – type structure postulated by Radoslovich (1963). No analyses plot close to the muscovite – ferrimuscovite join.

Fig. 4 plots Si versus Σ ($Mg+Fe^{2+}$) displaying little variation of fuchsite analyses but larger variation of muscovite analyses in two groups. One group plots closer to the fuchsite points; the other group plots higher up where the best fit line may slope 45°. Thus the ($Mg + Fe^{2+}$) substitution may be related to charge balance necessitated by the substitution of Si by Al^{iv}, and other substitutions as well.

For most of the muscovite and fuchsite analyses, total octahedral sites exceed the ideal of 4 by small amounts. This may be due to the deviation of these muscovites from being purely dioctahedral towards some trioctahedral mica (Guidotti, 1984). This may be the cause for deficiencies in the 12-coordinated sites.

Fuchsite

The fuchsite structure determined from its X-ray powder diffractograms, shows it to be of $2M_1$ type with the following unit cell parameters: a = 5.213 Å, b = 9.00 Å, c = 20.095 Å and β = 95° 34′. $2M_1$ type polymorph is considered as the most common K-white mica in pelitic schists (Guidotti, 1984). The b value of 9.00 Å of the fuchsite shows its crystallization at very low P, when compared with the b values of ≅ 8.990 Å for the lowest P ranges of greenschist facies metapelites and to ≅ 9.055 Å for the glaucophane schist facies, as given by Sassi & Scolari (1974).

Table 5. Analyses of fuchsite from sample no. Z392. All iron oxide is given as FeO.

Anal. No.	1	2	3	4	5	6	7	8
SiO_2	46.92	44.47	44.70	44.54	44.69	45.57	46.15	45.34
TiO_2	0.23	0.12	0.18	0.22	0.21	0.13	0.17	0.23
Al_2O_3	35.09	33.86	33.87	33.69	33.49	34.08	34.32	34.87
Cr_2O_3	1.75	1.28	1.20	1.70	1.70	1.51	1.83	1.80
FeO	1.12	0.79	0.97	1.27	1.26	1.24	1.03	1.22
MgO	0.34	0.38	0.38	0.24	0.25	0.42	0.36	0.24
Na_2O	0.00	0.31	0.39	0.00	0.00	0.33	0.34	0.00
K_2O	8.38	10.08	9.72	10.15	10.16	10.27	9.77	9.82
Total	93.83	91.29	91.41	91.81	91.76	93.55	93.97	93.52

Cations on the basis of 22 oxygens :

Si	6.253	6.174	6.188	6.167	6.190	6.192	6.215	6.140
Al^{iv}	1.747	1.826	1.812	1.833	1.810	1.808	1.785	1.860
Al^{vi}	3.765	3.715	3.714	3.666	3.658	3.650	3.663	3.706
Ti	0.023	0.013	0.019	0.023	0.022	0.013	0.017	0.023
Cr	0.185	0.141	0.131	0.186	0.186	0.162	0.195	0.193
Fe	0.125	0.092	0.112	0.147	0.146	0.141	0.116	0.138
Mg	0.068	0.079	0.078	0.050	0.052	0.085	0.072	0.049
Na	0.000	0.083	0.105	0.000	0.000	0.087	0.089	0.000
K	1.425	1.786	1.717	1.793	1.796	1.780	1.679	1.697

XRD powder pattern of $2M_1$ fuchsite from Dargai area is as follows :

hkl	I	d Å
002	70	9.990
004	45	4.980
110	22	4.456
021	12	4.400
111	11	4.255
022	5	4.093
11$\bar{3}$	11	3.866
023	16	3.726
11$\bar{4}$	20	3.482
024	78	3.338
006	100	3.326
114	22	3.196
025	22	2.983
115	17	2.855
11$\bar{6}$	14	2.788
20$\bar{2}$	21	2.562
132	8	2.491
20$\bar{4}$	8	2.387
133	8	2.381
043, 135	16	2.133
00.10	34	1.996
312	12	1.644
060, 33$\bar{1}$	37	1.500

The chemical analyses of this fuchsite from sample No. Z392 are reported in table 5. It contains lesser MgO then the muscovites from different metapelitic lithotypes. TiO_2 and Na_2O are also rather low. The Cr_2O_3 content is not high and remains below 2% in this sample; although the fuchsites are known to contain upto 6% Cr_2O_3 (Deer et al., 1962). However, minimum Cr_2O_3 content of 1.2% qualifies it to be called fuchsite rather than Cr-muscovite (Deer et al., 1962). Analyses of non-chromiferous muscovite from the same sample (Z392) are reported in table 4, and show higher FeO, MgO and TiO_2 in muscovite than in fuchsite. The

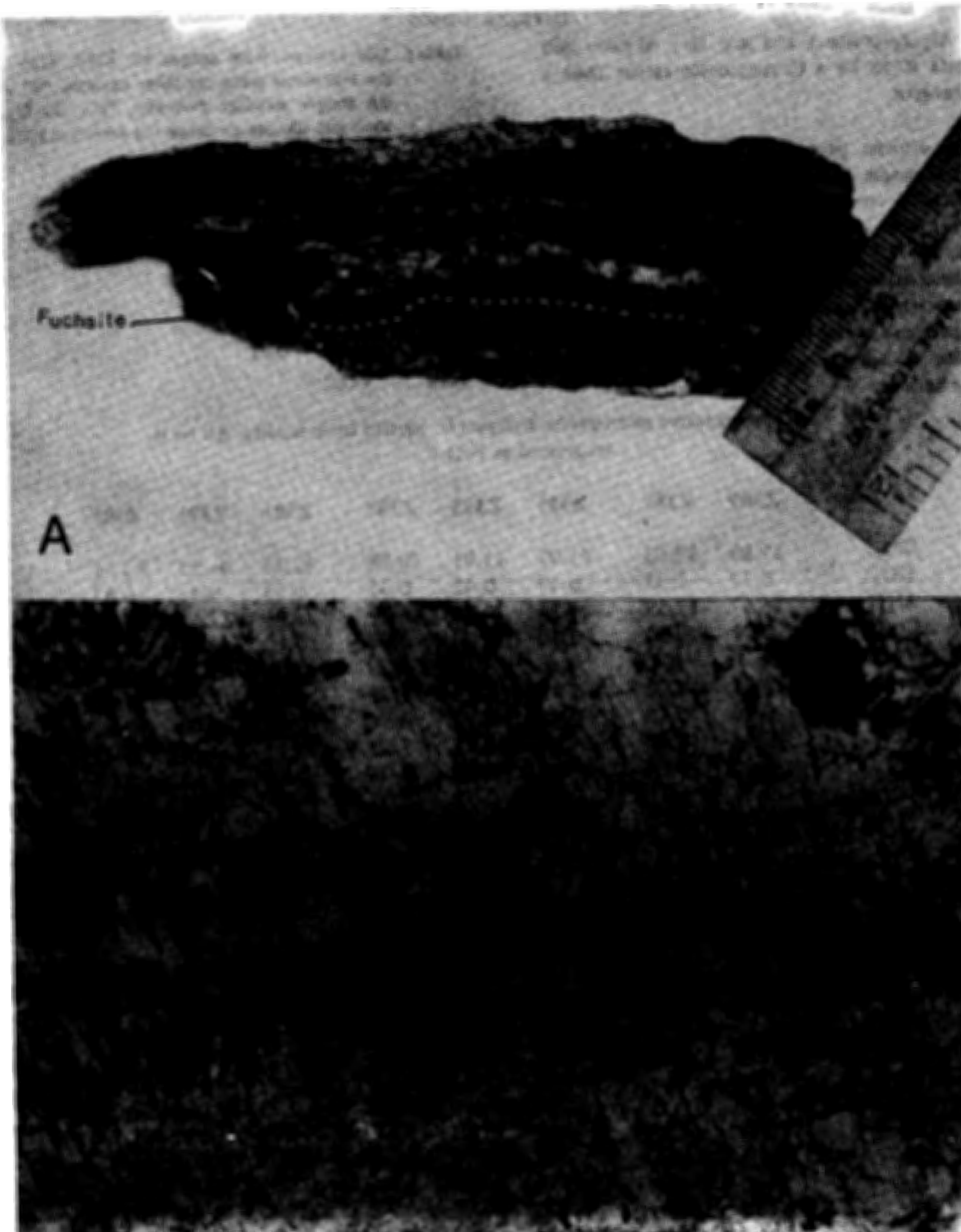

Fig.6 (A) Hand specimen of fuchsite-bearing schistose rock (from sp.no. Z392). White, quartz rich band in the middle defines the schistosity direction. The fuchsite layer runs parallel to it. (B) Transmitted light (X-nicols) photomicrograph showing the flaky aggregates of fuchsite developed perpendicular to the fuchsite layer attitude, and carrying a median parting, probably indicating its post schistosity development

high Al_2O_3 content and low Si : Al ratio also suggests it to be a Cr-muscovite rather than a Cr-phengite.

The atomic precent Al among octahedral cations ranges from 90.010 to 91.613 and indicates a composition nearer the muscovite end-member in the muscovite – celadonite series. In fig. 5 also, the fuchsites plot nearer the muscovite end member, whereas the majority of associated muscovites plot farther towards phengitic end member. The muscovite from the fuchsite – bearing sample (Z392) also shows this behaviour.

Table 6. Talc analyses from sample no. Z353. X(3) is the arithmetic mean for three analyses. "s" is the sample standard deviation. TiO_2, Al_2O_3, MnO and alkalies are below the detection limit.

	$\bar{X}(3)$	s
SiO_2	61.70	0.79
Cr_2O_3	0.11	0.05
FeO	4.60	0.05
MgO	27.19	0.42
NiO	0.39	0.17
CaO	0.03	0.01
Total	94.02	

Table 7. Representative microprobe analyses of biotite from schists. All Fe is expressed as FeO.

Sp. No.	Z389	Z389	Z355	Z355	Z385	Z391	Z391	Z398
SiO_2	37.80	37.63	41.97	41.91	40.98	42.33	41.55	43.05
TiO_2	0.37	2.33	0.47	0.42	0.35	0.53	0.47	0.83
Al_2O_3	16.67	17.39	28.34	29.25	26.79	26.95	27.52	27.70
Cr_2O_3	0.02	0.00	0.00	0.00	0.03	0.12	0.00	0.03
V_2O_3	b.d.	b.d.	n.d.	n.d.	n.d.	n.d.	n.d.	0.03
FeO	18.75	18.20	9.99	8.38	11.38	10.38	11.01	11.50
MnO	0.20	0.13	0.44	0.22	0.16	0.04	0.02	0.02
MgO	10.45	10.86	4.94	4.25	7.52	4.52	4.24	6.17
NiO	0.03	0.00	0.00	0.00	0.04	0.00	0.00	0.06
CaO	0.30	0.310.13	0.13	0.02	0.00		0.00	0.10
Na_2O	0.00	0.52	0.14	0.07	0.00	0.49	0.27	0.67
K_2O	7.41	6.80	5.93	6.54	6.87	7.57	7.64	4.84
Total	94.00	94.17	91.85	91.06	94.12	93.06	92.72	95.17
Cations on the basis of 22 oxygens :								
Si	5.729	5.662	5.961	5.989	5.810	6.042	5.968	5.952
Al^{iv}	2.271	2.338	2.039	2.011	2.190	1.958	2.032	2.048
Al^{vi}	0.707	0.746	2.705	2.916	2.287	2.576	2.628	2.466
Ti	0.270	0.264	0.050	0.045	0.037	0.057	0.050	0.086
Cr	0.002	0.000	0.000	0.000	0.003	0.13	0.000	0.003
Fe	2.377	2.290	1.187	1.001	1.349	1.239	1.323	1.330
Mn	0.026	0.017	0.053	0.027	0.019	0.005	0.003	0.002
Mg	2.360	2.436	1.046	0.905	1.589	0.961	0.908	1.271
Ni	0.004	0.000	0.000	0.000	0.005	0.000	0.000	0.007
Ca	0.049	0.050	0.020	0.003	0.000	0.020	0.000	0.015
N	0.000	0.152	0.039	0.019	0.000	0.134	0.076	0.180
K	1.433	1.306	1.075	1.192	1.243	1.378	1.401	0.854
100Mg/ (Mg+Fe)	46.843	47.482	54.084	49.821	51.545	43.682	40.699	48.866

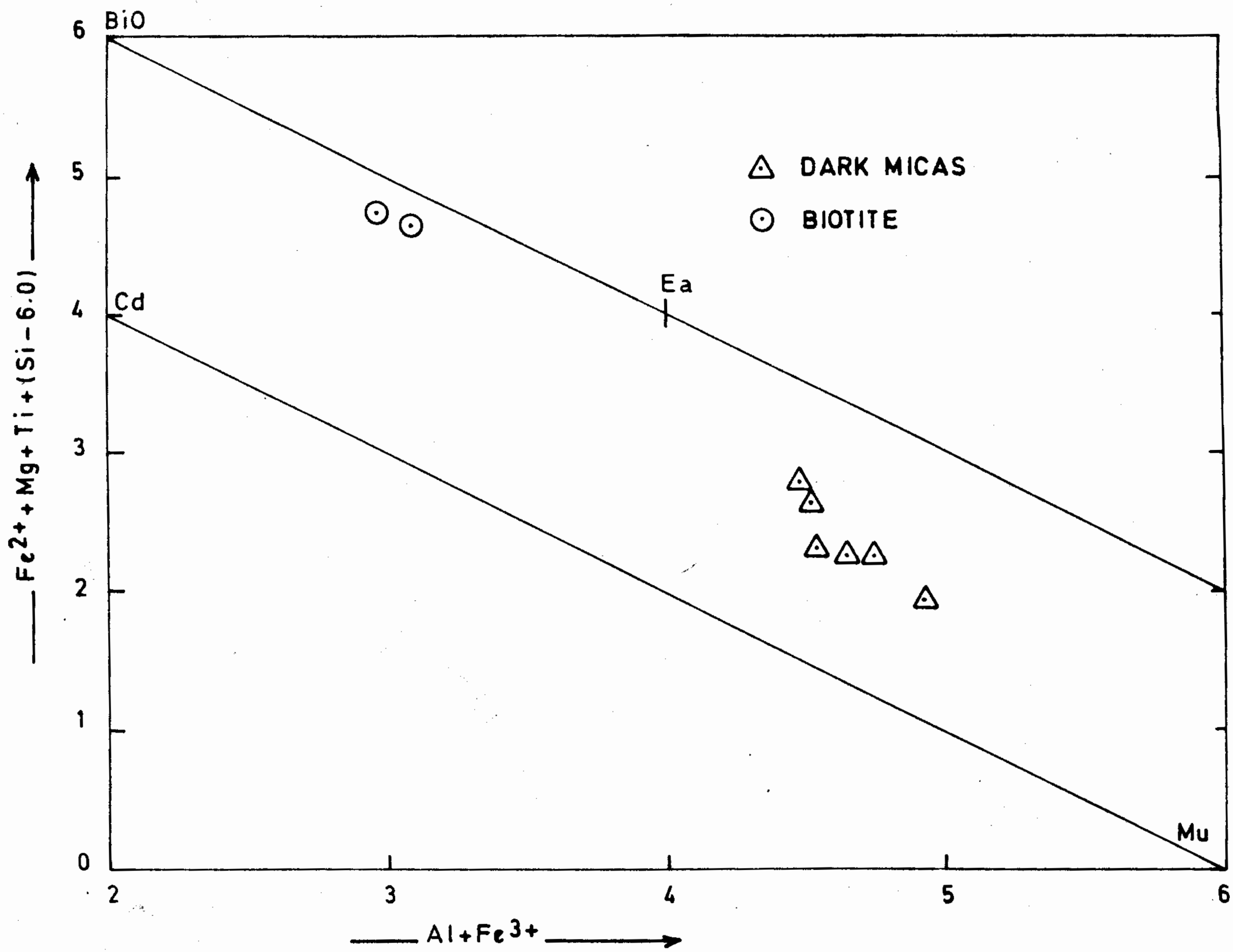

Fig.7. Plot of total ($Al+Fe^{3+}$) versus $Fe^{2+}+Mg+Ti+(Si-6)$ to illustrate the ideal dioctahedral and trioctahedral substitutions in muscovite and biotite, drawn after Guidotti (1984, fig. 12). BiO = Biotite, Cd = Celadonite, Ea = Eastonite, Mu = Muscovite.

Talc

Talc analyses mean values with standard deviations for the talc schist sample no. Z353 are given in table 6, and show presence of Cr_2O_3 and NiO in addition to slightly lower MgO and higher FeO contents. The presence of accessory "ferritchromit" grains in the same rock suggests its origin by hydrothermal activity on serpentinite and thus the rock does not belong to the metasedimentary schists. In this talc, TiO_2, Al_2O_3, MnO and alkalies are below the detection limit and their values are not reported. The SiO_2 ranges from 60.91 to 62.48%, FeO_T from 4.56 to 4.66%, MgO from 26.79 to 27.62%. These values indicate very small variations. The talc schist forms a mineable deposit which is being mined.

Biotite and Other Dark Micas

Table 7 gives two analyses of biotite from sample no. Z389 alongwith the other dark micas analyzed from sample nos. Z355, Z385, Z391 and Z398. All samples contain muscovite as well. All analyses are alkali-deficient and have

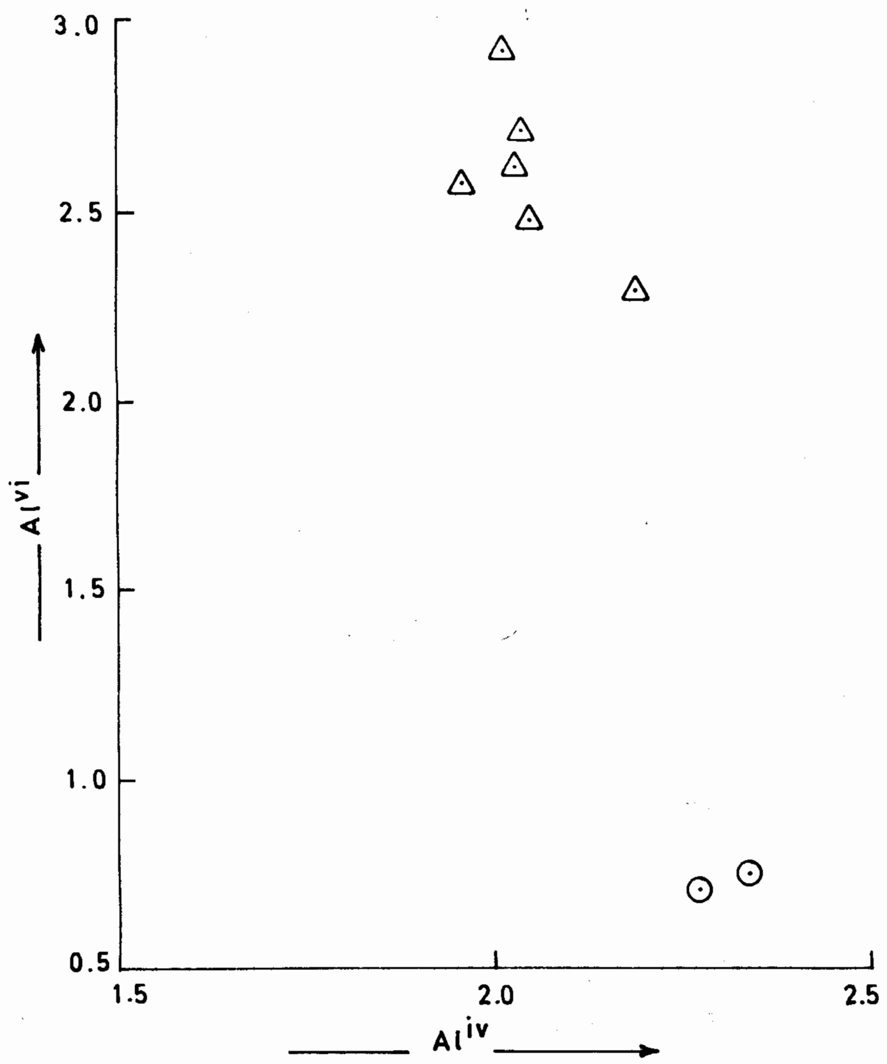

Fig. 8. Formula proportions of Al^{vi} & Al^{iv} in biotite (circles) and other dark micas (triangles) based on 22 oxygens.

upto 0.44% MnO and upto 0.67% Na_2O. MgO is generally low.

The biotite of sample Z389 has TiO_2 content of 2.33 to 2.37% and a Ti-saturated phase was not detected in this sample. The Mg/(Mg + Fe^{2+}) ratio of biotite plots it somewhat midway between the biotite and phlogopite end-members (Guidotti, 1984). The biotite differs from other analyses in table 7 by possessing lower Al_2O_3, SiO_2 and higher TiO_2, FeO and MgO. The rest six analyses in table 7, from sample nos. Z355, Z385, Z391 & Z398 are problematic. The analyses do not match either biotite or any other simple mica, because their K is too low. According to Guidotti (personal communication), these analyses may be of a very fine scale, mixed layer silicate such as biotite-vermiculite or biotite – chlorite, etc., formed by weathering. Another view is that these analyses are probably of a biotite that probably deviates from being trioctahedral. Its Al^{vi} is much higher than that for the normal biotites whose Al at the octahedral sites is generally upto 1.0, and increases to 2.0 in the siderophyllite or eastonite. The manner and extent of this deviation is shown in fig. 7. The trend along the line from biotite to aluminous biotite and

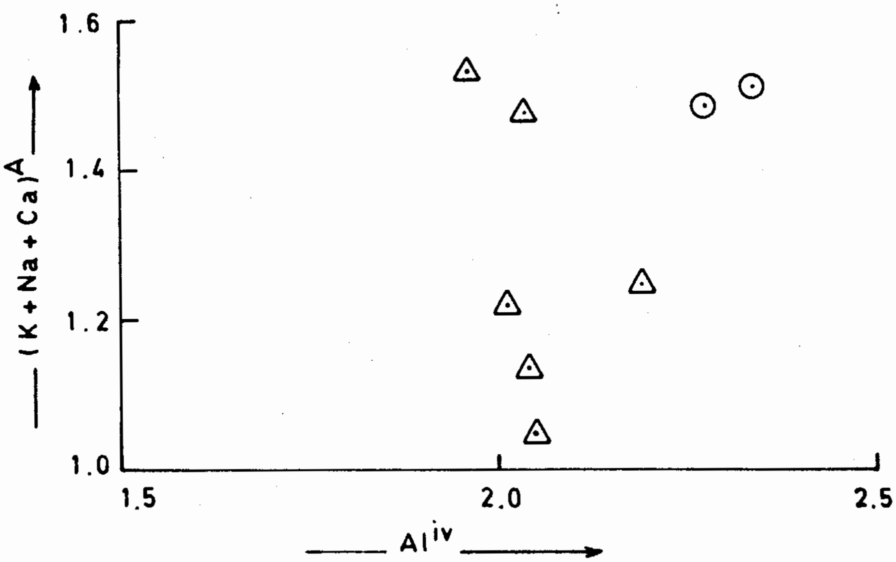

Fig. 9. Part of the K^A – Al^{iv} diagram after Dymek (1983, fig. 8a) showing A-site occupancy versus Al^{iv} in the biotite (circles) and dark micas (triangles).

eastonite, is not followed due to certain substitutions (Guidotti, 1984) leading to deviation towards a dioctahedral mica, resulting in points plotting between the two lines shown in fig. 7. Arbitrary assigment of total Fe to Fe^{2+} also deflects the points off the biotite line towards the muscovite – celadonite line. It is already known (Dymek, 1983) that such dioctahedral substitution is maximized in biotites coexisting with muscovite. All the schist samples of table 7 contain muscovite. Samples Z355 and Z391 contain ilmenite and sample Z385 contains a Ti-oxide phase. However, Ti in biotites of these samples is very low (cf. Dymek, 1983).

The biotite of sample Z389 may indicate its higher metamorphic grade than the rest of the samples with abnormal dark nice, because certain chemical parameters suggested by other studies are consistent with this interpretation. Such parameters are a higher TiO_2 content and lower Fe^{2+}/Mg (Miyashiro, 1973); high Ti and lower Al^{vi} (Schreurs, 1985); and higher A-site occupancy (Holdaway, 1980).

The dark mica compositions are illustrated in fig. 8, in terms of Al^{iv} and Al^{vi}. Compared to similar diagram of Dymek (1983), an excess Al^{vi} is indicated except for the normal biotites of sample Z389. The K contents of all dark micas range from 0.854 to 1.433, and Na from zero to 0.18 cations per formula based on 22 oxygens. The A-site occupancies are plotted in fig. 9. All points show values lower than those for higher grade rocks of Dymek (1983). Normal biotites possess higher values than the other dark micas.

Garnet

Garnet analyses are give in table 8. The spessartine in sample Z267 shows very small unzoned crystals (fig. 6). The spot analyses from various parts of crystals (anal. 1-4, table 8) indicate homogeneity which could be explained by increased diffusion rates within garnet at elevated temperatures (Atherton, 1968; Dietvorst, 1982; Woodsworth, 1977). This also indicates its development as a contact metamorphic mineral at the basal contact of ophiolite, and not as a regional metamorphic product. The finer grain size of the rock and poor schistosity also point towards contact effects. The sample does not contain biotite. Formation of zoned garnets is normally expected at lower meta-

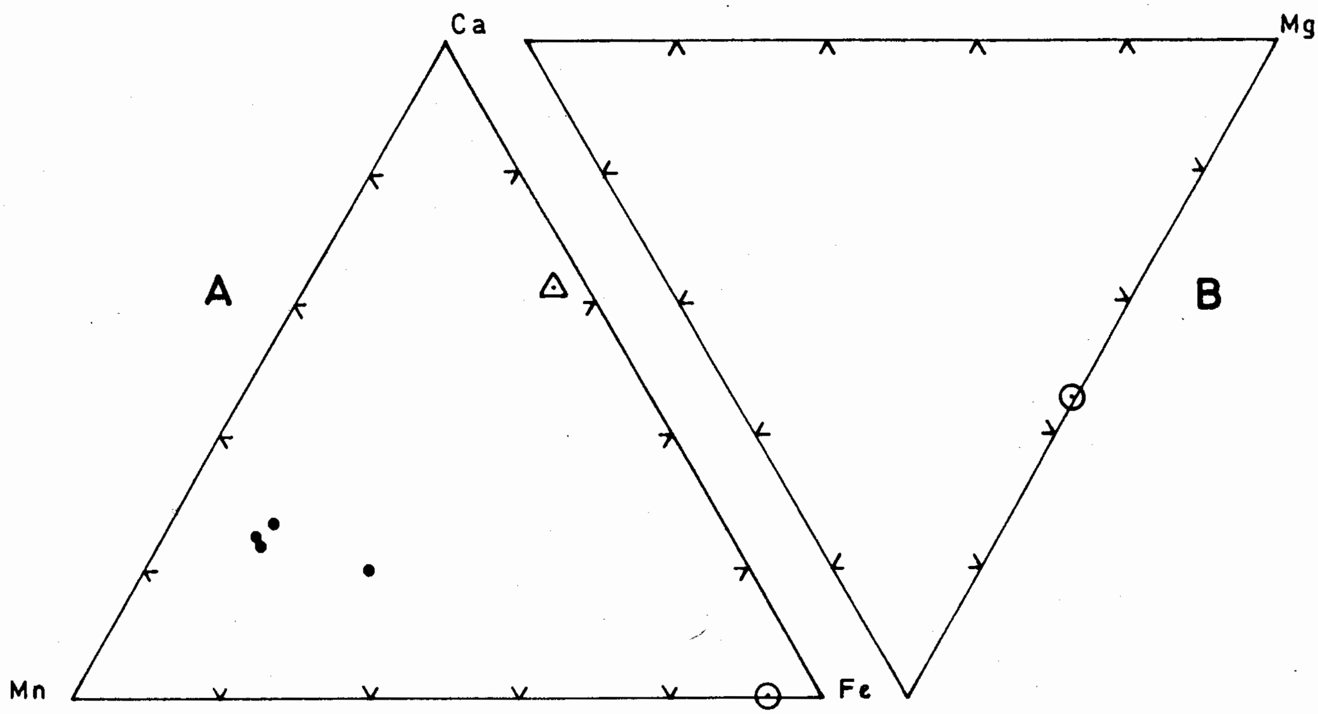

Fig.10. (A) Ca-Mn-Fe ternary diagram for garnets from metapelites. (B) Ca-Fe-Mg ternary diagram for one almandine garnet. Sample no. Z267 (dots), ZA267 (triangle) & ZB267 (circles).

morphic grades (Dietvorst, 1982). The spessartine garnets are relatively Ti-richer than other garnets. From other samples at the same locality, garnets with about 2% MnO (analyses 5 & 6) are analyzed, one Mg-rich and the other Ca-rich (table 8). Na content is very low in all garnets but the almandine has relatively higher Na.

Apatite

The apatite analyses in table 9 show fairly constant composition and totals close to 100%. The Mn and Cl contents are below detection limit of the microprobe used. The apatite was not analyzed for F, OH and CO_2. High CaO values show its negligible substitution by the other elements observed commonly in apatites (Deer et al., 1962). Maximum amount of MnO is 0.06% in sample Z387, although Mn: Ca ratio of 1:8 is not uncommon in apatites (Deer et al., 1962). Presence of Sr and rare-earth elements was not detected in the energy-dispersive spectrum.

Sphene

The energy-dispersive X-ray spectra of sphenes did not display peaks for Zr, Nb, Ta, B, REE, V, or Sn. The analytical data of sphene from two rocks are reported in table 10. Sample Z267 is garnetiferous and probably of higher metamorphic grade than sample Z355. In the Y (octahedral) sites, Al predominates over Fe^{3+}. All Al and Fe has been assigned to the octahedral site, and tetrahedral sites are assumed to be filled by Si alone (Higgins & Ribbe, 1976). There is negligible or extremely small substitution of Na, Mg or Mn for Ca, but Fe^{3+} and Al do show slight substitution for Ti. Sphene in the higher metamorphic grade sample (Z267) possesses higher TiO_2 but lower CaO and SiO_2 than the sample from lower metamorphic grade (Z355) where sphene coxists with Mn-ilmenite. Al_2O_3 and Fe_2O_3 are also somewhat higher in the former case.

Table 8. Analyses of spessartine (1 – 4) and Mn-bearing garnet (5–6) from the southern contact schists. Total Fe is expresses as FeO.

Anal. No.	**1**	**2**	**3**	**4**	**5**	**6**
Sp. No.	**Z267**	**Z267**	**Z267**	**Z267**	**Z267**	**ZB267**
SiO_2	38.29	36.60	32.63	35.05	39.29	37.51
TiO_2	0.32	0.26	0.48	0.21	0.02	0.02
Al_2O_3	19.32	18.78	16.01	17.02	20.65	19.94
Cr_2O_3	0.11	0.06	0.12	0.00	0.03	0.01
V_2O_3	0.08	0.00	n.d.	n.d.	0.08	0.10
FeO	5.86	5.91	16.00	6.64	14.71	25.78
MnO	24.85	30.00	26.72	30.63	1.98	2.08
MgO	0.76	0.39	0.32	0.13	0.13	2.11
NiO	0.03	0.00	0.00	0.00	0.00	0.00
CaO	8.57	9.05	8.17	8.63	21.35	0.07
Na_2O	0.49	0.23	0.44	0.04	0.13	0.84
K_2O	n.d.	0.03	0.04	0.04	0.00	0.07
Total	98.68	101.31	100.93	98.39	98.37	98.75
Cations to 24 oxygens :						
Si	6.200	5.946	5.589	5.944	6.186	5.887
Al^{iv}	0.000	0.054	0.411	0.056	0.000	0.113
Al^{vi}	3.688	3.542	2.821	3.347	3.832	3.576
Ti	0.039	0.032	0.062	0.027	0.002	0.002
Cr	0.014	0.008	0.016	0.000	0.004	0.001
V	0.010	0.000	n.d.	n.d.	0.010	0.013
Fe	0.794	0.803	2.292	0.942	1.937	3.384
Mn	3.409	4.128	3.876	4.401	0.264	0.277
Mg	0.183	0.094	0.082	0.033	0.031	2.833
Ni	0.004	0.000	0.000	0.000	0.000	0.028
Ca	1.487	1.575	1.499	1.568	3.602	0.012
Na	0.154	0.072	0.146	0.013	0.040	0.256
K	n.d.	0.006	0.009	0.009	0.000	0.014

Table 9. Apatite analyses. b.d. = Below the detection level.

Sp. No.	**Z387**	**Z387**	**Z398**	**Z398**	**Z398**	**Z398**
FeO	0.46	0.30	0.00	0.18	0.19	0.33
MnO	0.00	0.06	b.d.	b.d.	b.d.	b.d.
MgO	0.22	0.08	b.d.	b.d.	b.d.	b.d.
CaO	55.50	55.60	55.72	54.75	55.67	55.64
Na_2O	0.05	0.06	0.35	0.29	0.15	0.07
K_2O	0.03	0.00	0.00	0.00	0.09	0.06
P_2O_5	42.35	42.30	43.49	44.84	43.00	42.86
Total	89.61	98.40	99.56	100.06	99.10	98.96

Table 10. Microprobe analyses of sphene. EOCR is effective octahedral cation radius.

Anal No.	1	2		1	2
Sample No.	Z267	Z355	Number of ions on the basis of 4Si:		
SiO_2	30.90	32.80	Si	4.000	4.000
TiO_2	40.22	38.44	Al	0.214	0.184
Al_2O_3	1.40	1.28	Fe^{3+}	0.090	0.028
Cr_2O_3	0.06	0.11	Ti	3.915	3.525
V_2O_3	0.18	n.d.	V	0.012	n.d.
Fe_2O_3	0.92	0.30	Cr	0.006	0.011
MnO	0.16	0.05	Mn	0.018	0.005
MgO	0.00	0.10	Mg	0.000	0.018
NiO	0.03	0.00	Ni	0.003	0.000
CaO	26.51	28.32	Ca	3.676	3.700
Na_2O	b.d.	0.00	Na	b.d.	0.000
K_2O	0.00	0.07	K	0.000	0.011
Total	100.38	101.47	O	20.009	19.112
			(EOCR)	0.602	0.602

Ilmenite

Ilmenite analyses are reported in table 11. Sample Z355 has manganese ilmenite (Deer et al., 1962) in which MnO varies from 9.56 to 14.5% conforming to 0.4 to 0.606 Mn cations per formula unit based on 6 oxygens. Sample Z391 has ilmenite with MnO decreased to 0.65% and compensated by reciprocal increase in FeO_T. Its TiO_2 is also slightly lower than that of manganese ilmenite. The impurities in ilmenite are not large: SiO_2 is below 0.49% and Al_2O_3 hardly discernible in the manganese ilmenite, is upto 0.59% in the non-maganese ilmenite. Higher TiO_2 and low FeO and Al_2O_3 of analyses from sample Z355 is probably not due to the presence of alteration phases such as pseudorutile (cf. Frost et al., 1983) because the spots analyzed were of homogeneous, single-phase unaltered ilmenite. However, the possibility that the alteration phases may be present intergrown on a very fine irresolvable scale cannot be ruled out.

Table 11. Microprobe analyses of ilmenite.

Anal. No.	1	2	3	4	5
Sp. No.	Z355	Z355	Z355	Z355	Z391
SiO_2	0.47	0.40	0.42	0.49	0.29
TiO_2	54.09	54.03	54.26	54.09	52.65
Al_2O_3	0.04	0.10	0.02	0.27	0.59
Cr_2O_3	0.06	0.05	0.09	0.12	0.13
FeO	31.57	32.08	31.87	36.40	43.79
MnO	14.19	12.82	14.50	9.56	0.65
MgO	0.03	0.22	0.00	0.03	0.31
NiO	0.00	0.03	0.00	0.09	0.00
CaO	0.21	0.14	0.00	0.00	0.00
Total	100.61	99.87	101.16	101.05	98.41
Number of cations on the basis of 6 oxygens:					
Si	0.023	0.020	0.021	0.024	0.015
Al	0.002	0.006	0.001	0.016	0.035
Cr	0.002	0.002	0.003	0.004	0.005
Ti	2.015	2.023	2.015	2.007	2.003
Mg	0.002	0.016	0.000	0.002	0.023
Fe^{2+}	1.308	1.336	1.316	1.502	1.853
Mn	0.595	0.541	0.606	0.400	0.028
Ni	0.000	0.001	0.000	0.004	0.000
Ca	0.011	0.007	0.000	0.000	0.000
Parameters :					
Ti/(Ti+Fe)	0.606	0.602	0.605	0.572	0.519
Fe/Ti	0.649	0.660	0.653	0.748	0.925

Table 12. Microprobe analyses of rutile from sample no. Z387.

Anal.No.	1	2		1	2
Sp. No.			Cations to 2 oxygens:		
TiO_2	98.73	95.24	Ti	0.989	0.966
SiO_2	0.30	0.99	Si	0.004	0.013
Cr_2O_3	0.06	0.04	Cr	0.001	<0.001
Al_2O_3	0.00	0.52	Al	0.000	0.008
FeO	1.05	1.25	Fe	0.012	0.014
MnO	0.00	0.04	Mn	0.000	<0.001
MgO	0.00	0.68	Mg	0.000	0.014
CaO	0.05	0.00	Ca	0.001	0.000
NiO	0.00	0.00	Ni	0.000	0.000
Na_2O	0.00	0.00	Na	0.000	0.000
K_2O	0.00	0.05	K	0.000	0.001
Σ	100.19	98.81			

b.d. = below detection level.
n.d. = not determined.

Table 13. Monazite analyses.

Anal. No.	1	2	3	4	5	6	7
Core/rim	core	rim	core	rim	core		
P_2O_5	29.86	29.56	30.38	30.32	29.56	29.94	30.15
La_2O_3	20.05	18.83	17.38	18.25	19.93	19.62	19.71
Ce_2O_3	31.07	29.61	29.93	28.82	30.95	31.18	31.25
Pr_2O_3	1.92	2.34	2.50	1.88	1.92	3.43	3.40
Nd_2O_3	12.24	10.98	14.84	11.01	12.18	12.37	12.45
Sm_2O_3	1.93	1.15	1.36	0.36	1.93	0.71	0.65
Gd_2O_3	0.32	0.28	0.51	0.41	0.32	0.28	0.27
Dy_2O_3	0.20	0.07	n.d.	n.d.	0.20	n.d.	n.d.
ThO_2	1.44	2.83	1.91	2.48	1.44	2.11	2.12
U_3O_8	Present	Present	Present	Present	Present	Present	Present
CaO	0.48	0.60	0.58	0.59	0.00	0.60	0.50
Y_2O_3	0.00	b.d.	b.d.	b.d.	b.d.	b.d.	0.00
Total:	99.51	96.25	99.39	94.14	98.43	100.24	100.50

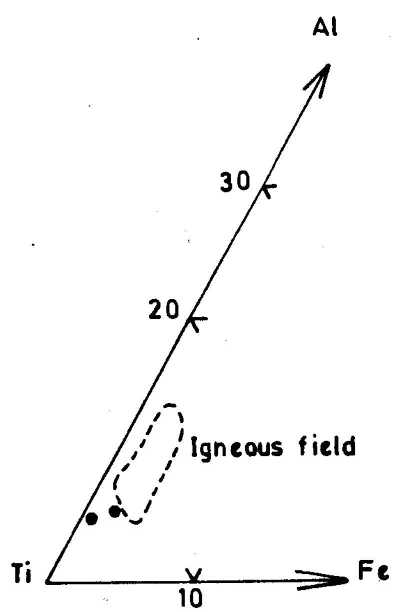

Fig.11. Composition of sphene in samples Z 267 and Z 355 plotted as proportions of Al, Ti, Fe^{3+} after Tulloch, 1979.

Rutile

Rutile analyses from sample Z387 are given in table 12. If forms euhedral long prismatic crystals. Total iron as FeO ranges from 1 to 1.25%. Niobium and tantalum are not displayed in its energy-dispersive spectrum.

Monazite

A review of the monazite paragenesis by Deer et al., (1962) does not mention its occurrence in chloritic schists. From analyses given in table 13, monazite appears to be zoned with Ce and Nd being higher in the cores and Th higher in the rims. Prominent uranium peaks were observed, but not analyzed quantitatively. Details of monazite have already been published (Ahmed, 1985).

DISCUSSION

The rock outcrops of the region are dominated by the Proterozoic metasedimentary schists represented by the samples Z329, Z332, Z353, Z355, Z385, Z389, Z391, Z398 and Z401. Protolith compositions are dominantly pelitic; arenaceous rocks come next. Ferruginous, and graphitic lithologies as well as distinct marble beds are well–exposed east of Dargai town. The metamorphism is of low grade; garnet grade occurs northwards, biotite zone is thinner than the chlorite grade. Sample Z389 represents the biotite grade. Chloritoid has developed by the regional metamorphism in the samples Z329 and Z401; both of which are compositionally suited to chloritoid formation as they are high in Al_2O_3 and Fe/(Fe+Mg) and low in alkalies (Manby, 1983). The logarithmic plot of Fe/Mg in chlorite versus chloritoid (fig. 2) depicts a lower range of $K_D^{Fe/Mg}$ chloritoid-chlorite as compared to the reported chlorite zone chloritoid from Turkey (Ashworth & Evirgen, 1984). This comparison indicates a higher temperature of equilibration for the Dargai chloritoid within the chlorite zone.

Guidotti (1978) found systematic muscovite compositional trends with increasing metamorphic grade from lower garnet zone to upper sillimanite zone of the metapelites from northwestern Maine. The trends from lower garnet to upper staurolite zone include: decrease in Si^{4+}, (Mg + Fe) and increase in Al^{iv}, Na/Na + K), Mg/Fe and Ti. The present study includes metapelites of lower metamorphic grade and the same muscovite trends may not hold. Amongst table 4 analyses, sample Z329 has the highest Na/(Na + K), Mg/Fe, and very low (Mg + Fe), and Si^{iv} values, showing its high metamorphic grade but its lower Ti content does not support it. Z385 has the lowest Na/(Na+K), quite low Mg/Fe, very high (Mg + Fe) and Si values, which may indicate lower metamorphic grade, but its low-Ti does not agree with it. Sample Z267 has highest Ti, (Mg+Fe) values and lowest Mg/Fe, Al^{vi}, Fe, Mn and K values which indicate its higher grade of metamorphism further supported by the presence of spessartine in the same sample.

The chlorite composition indicates higher metamorphic temperature for Z392 than Z391 and other metasedimentary schists.

Closer to the contact of ophiolitic rocks, these metamorphic rocks are affected either by the tectonics only; or they may show variations in their mineral assemblages. In the present study, samples Z267, Z392 and Z387 contain minerals which probably reflect some effects of the nearby ophiolitic rocks. Z267 is a sample with spessartine development due to higher pressure and probably temperature at the basal contact of the ophiolite. Its higher metamorphic grade than all other samples is noticed in the chemistry of all its minerals. Its muscovite has higher TiO_2 and other features of higher metamorphic grade. Its sphene has higher TiO_2 and lower CaO.

Sample Z392 is typically metasedimentary but has layers of fuchsite whose Cr content is probably ophiolitic. The co-occurrence of muscovite with and without Cr in the same rock, reflects the role of two processes. The non-chromiferous muscovite was probably formed by the regional metamorphism alongwith all the other minerals like chlorite, whereas the Cr-muscovite crystallized afterwards with the addition of Cr. Chlorite composition indicates stronger metamorphic conditions but fuchsite, from *b*—values for example, indicates weaker pressure conditions, for the same rock sample. The fuchsite shows a hydrothermal growth (fig. 6) as it occurs in veined fashion with sharp contacts, forming large books in an otherwise Cr-poor schist. Thus, the fuchsite seems much younger than its enclosing Proterozoic schist. Other occurrences with a similar paragenesis have also been reported (Max et al., 1983). Sample Z387 also has minerals formed from ophiolitic source materials. Magnesian minerals include not only talc but also chlorite whose composition is drastically different from the chlorite of the rest of schist samples. It is a sample unique in containing monazite and rutile.

CONCLUSIONS

Regional metamorphic rocks occur widespread in the southern Malakand Agency, and cover a broad spectrum ranging from lower chlorite zone to garnet zone rocks. They also reflect variations in mineral chemistry due to protolith variations. The effects of ophiolitic rocks are noticeable in the mineral chemistry of schists at immediate contact only. Muscovites of the chloritoid-bearing sample contain the lowest celadonite content and the highest Na/(Na+K) ratio.

The chlorite in the monazite- and rutile-bearing talcose schist developed near the ophiolitic rock contact (sample Z387) has a distinct composition indentified by higher MgO, and lower FeO, TiO_2 and Al_2O_3 than the rest of the samples with typical metasedimentary minerals. Ripidolite is the most abundant type of chlorite in these schists, although sometimes brunsvigite and pycnochlorite also occur. Sample Z389 shows increased metamorphic grade, in terms of biotite chemistry compared to the rest of the samples below the garnet grade.

ACKNOWLEDGEMENTS

Generous use of the electron microprobe analytical facilities at the University College, London, and of the Philips X-ray diffractometer unit formerly at the King's College, London, UK; are very gratefully acknowledged. Dr. A. Hall of Royal Holloway & Bedford New College, University of London, UK, was frequently consulted during the XRD work.

REFERENCES

AHMED, Z. (1985) A new occurrence of uranium – bearing thorian monazite, northwestern Pakistan. Acta Mineralogica Pakistanica, 1, pp. 27-33.

AHMED, Z. (1987) Geochemical characterization of Proterozoic upper crustal metamorphic terrain of southern Malakand Agency, Pakistan. Geol. Bull. Punjab Univ. special issue, (in prep).

ASHWORTH, J.R. & EVIRGEN, M.M. (1984) Mineral chemistry of regional chloritoid assemblages in the Chlorite Zone, Lycian Nappes, South – west Turkey. Min. Mag. 48 (347), pp. 159-65.

ATHERTON, M.P. (1968) The variation in garnet, biotite and chlorite composition in medium grade pelitic rocks from the Dalradian, Scotland, with particular reference to the zonation in garnet. Cont. Min. Pet. 18, pp. 347-71.

BUTLER, B.C.M. (1967) Chemical study of minerals from the Moine schists of the Ardnamurchan area, Argyllshire, Scotland. Jour. Petrology 8, pp. 233-67.

DEER, W.A., HOWIE, R.A. & ZUSSMAN, J. (1962) ROCK FORMING MINERALS Volumes 1 to 5, Longmans Group Ltd. London.

———— (1982) ROCK FORMING MINERALS: Volume 1A, Orthosilicates. Second Edition. Longman Group Ltd. London, p. 919.

DIETVORST, E.J.L. (1982) Retrograde garnet zoning at low water pressure in metapelitic rocks from Kemiö, SW Finland. Contrib. Min. Pet. 79, pp. 37-45.

DYMEK, R.F. (1983) Titanium, aluminium and interlayer cation substitutions in biotite from high grade gneisses, West Greenland. Amer. Mineral. 68, pp. 880-99.

FORST, M.T., GREY, I.E., HARROWFIELD, I.R. & MASON, K. (1983) The dependence of alumina and silica contents on the extent of alteration of weathered ilmenites from Western Australia. Min. Mag. 47, (2) 343, pp. 201-8.

GUIDOTTI, C.V. (1978) Compositional variation of muscovite in medium – to high – grade metapelites of northwestern Maine. Amer. Mineral. 63, pp. 878-84.

GUIDOTTI, C.V. (1984) Micas in metamorphic rocks. In: Bailey, S.W. (ed.) MICAS. Reviews in Mineralogy 13, Min. Soc. America. pp. 357-456.

HALFERDAHL, L.B. (1961) Chloritoid: its composition, X-ray and optical properties, stability and occurrence. Jour. Petrology 2, pp. 49-135.

HIGGINS, J.B. & RIBBE, P.H. (1976) The crystal chemistry and space groups of natural and synthetic titanites. Amer. Mineral. 61 (9-10), pp. 878-88.

HOLDAWAY, M.J. (1978) Significance of chloritoide – bearing rocks in the Picuris Range, New Mexico. Geol. Soc. America Bull. 89, pp. 1404-14.

———— (1980) Chemical formulae and activity models for biotite, muscovite, and chlorite applicable to pelitic metamorphic rocks. Amer. Mineral. 65, pp. 711-9.

MANBY, G.M. (1983) A reappraisal of chloritoid-bearing phyllites in the Forland Complex rocks of Prins Karls Forland, Spitsbergen. Min. Mag. 47 (344), pp. 311-8.

MARTIN—RAMOS, J.D. & RODRIGUEZ — GALLEGO, M. (1982) Chromian mica from Sierra Nevada, Spain. Min. Mag. 46, pp. 269-72.

MAX, M.D., TRELOAR, P.J., WINCHESTER, J.A. & OPPENHEIM, M.J. (1983) Cr mica from the Precambrian Erris Complex, Nw Mayo, Ireland. Min. Mag. 47 (3)344, pp. 359-64.

MIYASHIRO, A. (1973) METAMORPHISM AND METAMORPHIC BELTS. George Allen & Unwin, London, 492 p.

RADOSLOVICH, E.W. (1963) The cell dimensions and symmetry of layer-lattice silicates. V. Composition limits. Amer. Mineral. 48, pp. 599-616.

RUIZ, J.L., APARICIO, A. & CACHO, L.G. (1980) Chemical variations of muscovites from the Sierra de Guadarrama metamorphic area, Sistema Central, Spain. Geol. Rundshau 69, pp. 94-106.

SASSI, F.P. & SCOLARI, A. (1974) The *b* value of the potassic white micas as barometric indicator in low-grade metamorphism of pelitic schist. Contrib. Min. Pet. 45, pp. 143-52.

SCHREURS, J. (1985) Prograde metamorphism of metapelites, garnet – biotite thermometry and prograde changes of biotite chemistry in high grade-rocks of West Uusimaa, southwest Finland. Lithos 18, pp. 69-80.

WOODSWORTH, G.J. (1977) Homogeneization of zoned garnets from pelitic schists. Canad. Mineral. 15, pp. 230-42.

Manuscript received 9.10.1986
Accepted for publication 9.10.1986

ACTA MINERALOGICA PAKISTANICA
VOLUME 2 (1986) pp. 47 - 52 .

UNIT CELL DIMENSIONS OF URANINITES FROM VARIOUS GEOLOGICAL ENVIRONMENTS IN PAKISTAN

KHURSHID ALAM BUTT[1] & KHALID MAHMOOD[2]

1. Hardrock Division, P.O.Box 734 (University) Peshawar.
2. Mineralogy Division, AEMC, P.O. Box 658, Lahore.

ABSTRACT:— Uraninite has been identified from various geological environments in Pakistan. These include detrital grains of uraninite in the sands of river Indus and its tributaries, Miocene to Pleistocene sandstones of Siwalik Formation, Cambrian pegmatites of Mansehra complex and Kaghan Valley, migmatitic pegmatoids in Parachinar and veins associated with migmatites in Thakot and Dobair.

This paper presents an X-ray diffraction study of these uraninites from various geological settings. It is demonstrated that the geologcal environment of formation of uraninite, i.e., sedimentary, hydrothermal or orthomagmatic, is reflected in its unit cell size. The implications of this relationship of uranium exploration strategy are discussed.

INTRODUCTION

Uraninite or pitchblende from hydrothermal veins have a smaller cell size than uraninites from pegmatites (Berman 1955). Conversion of U^{+4} to U^{+6}, and substitution of thorium and rare earth ions in uraninite structure are considered to be the main cause of increase in unit cell size of the minerals. The cell size can also vary with the amount of radiogenic lead. Pitchblende from sedimentary environments is generally very low in thorium and rare earths whereas that formed in pegmatitic paragenesis contains large amounts of thorium and rare earths in its structure. Vein type pitchblendes should theoretically represent an intermediate situation between the sedimentary and pegmatitic types. This paper presents unit cell size data on uraninite from various localities in Pakistan and an interpretation of certain genetic aspects of these occurrences.

Uraninite occurrences have been reported from various geological environments in Pakistan. These environments include recent alluvial sands of river Indus and its tributaries, fluviatile deposits of Siwalik sandstones of Miocene to Pleistocene age, pegmatites associated with Cambrian granitic rocks of Mansehra and Kaghan, disseminations in Precambrian migmatites of Parachinar and vein fillings in Precambrian, pegmatoid-metasedimentary complex in Thakot.

X-ray diffraction data on uraninite from these geological environments is presented and unit cell dimensions calculated thereof suggest a variability in cell size as a function of their geological environments. High temperature uraninites from pegmatites and migmatized terrains tend to have a larger cell edge, hydrothermal joint fillings show intermediate cell size whereas the sedimentary uraninite shows the smallest cell edge.

URANINITE OCCURRENCES IN PAKISTAN

Uraninite from Indus Rivers and its Tributaries

Present day river sand in Shyoke, Hunza and Indus rivers is known to contain uraninite. Other heavy minerals include gold, magnetite, ilmenite and garnet. In addition to these recent sands, similar heavy mineral assemblages containing gold have been reported from Quaternary river terraces in parts of Chitral, Hunza, Gilgit and Skardu. However, uraninite occurrence in these terrains was not investigated.

Uraninite from Siwalik Sandstone, D.G. Khan

The Siwaliks are a thick sequence of clastic material deposited in a foredeep in front of the rising Himalayas during Miocene to Pleistocene times. Uranium mineralization occurs in the sandstones of Middle Siwalik formation of upper Miocene age. The sandstones are grey, fine to medium grained with quartz, oligoclase, microcline, biotite, muscovite and hornblende and minor tourmaline, epidote, chlorite, garnet, magnetite and ilmenite.

Matrix in these sandstones is either argillaceous material or calcite or both. These sandstones have been classified as impure arkoses (Rahman, 1972). Both oxidized and unoxidized uranium minerals have been reported from these sandstones. The primary minerals include pitchblende and coffinite (Besham & Rice, 1974).

Secondary minerals such as tyuyamunite, carnotite and uranophane have been reported from various localities. These are considered to be the oxidation products of uraninite - coffinite assemblage deposited by ground water (Besham & Rice, 1974). Most of the Siwalik Formation lies in a tectonically unstable zone. The tectonic instability causes great fluctuation in groundwater regimes and thereby uranium concentrations which are a product of precipitation from groundwaters. Sinking of the ground water table causes exposure of such uranium minerals to oxidizing environments and a variety of oxidized minerals are formed. Primary pitchblende may give rise to secondary uranium or uranium-vanadium minerals which may in turn get further destroyed to yield tertiary uranium mineral species. Such an extreme form of oxidation has been observed from Siwalik sandstones in Bhimber area where further oxidation of uranium/vanadium minerals has resulted in a complete removal of highly mobile uranium resulting in extreme enrichment of vanadium to cause precipitation of vanadium minerals (Butt & Mahmood, 1983).

Uraninite from Pegmatites in Mansehra & Kaghan Vaelley

A pitch black, radioactive mineral has been reported from pegmatites at Bagrian and Naran (District Mansehra). This mineral has been tentatively identified as samarskite (Ashraf, 1974). However, our investigation (Butt, in preparation) suggests that there are two types of radioactive minerals in the pegmatites :–

1. Metamict samarskite (?)
2. Metamict uranium oxide (?)

Since both species are metamict, their cell size cannot be calculated without heat treatment and that again will not be useful in this study as it will reflect the laboratory condition of reconstitution of the minerals.

Uranium from Migmatites of Parachinar

The geology of the Parachinar area is not very well defined except the sedimentary cover which consists of a sequence of Jurassic limestone, Patala Shale, Chichali Shale and Murree Formation, of Palaeocene to Miocene. These sediments are in faulted contact with a metasedimentry sequence of quartzites which this author proposes to correlate with Tanawal Formation of possible Precambrian age which at places has been migmatitized. These migmatites are separated by high angle thrust faults.

Uraninite in this area occurs as evenly disseminated grains in medium grained, granitic as well as pegmatitic parts of the migmatized rocks of possible Precambrian age. Uraninite also occurs as inclusions in biotite. In addition to uraninite, other radioactive minerals reported from the area are limonite, allanite and epidote (Rahman & Jaseem ud-din, 1978).

Table 1. Cell dimensions of uraninites from various localities in Pakistan.

Locality	No of reflection used.	Average cell size a (Å) $\overline{X}$	Standard deviation a (Å) S
Pegmatite Uraninite Parachinar.	13	5.4599	0.0173
Vein Uraninite Dobair.	12	5.4370	0.0109
Vein Uraninite Thakot 1	14	5.4407	0.0187
Thakot 2	14	5.4460	0.0122
Thakot 3	12	5.438	0.0143
(Pegmatite Uraninite)			
Thakot 4	13	5.4589	0.0075
Thakot 5	14	5.4448	0.0129
Sedimentary Uraninite D. G. Khan.	3	5.3520	0.0162

Vein Type Hydrothermal Uraninite from Thakot & Dobair

In Thakot area uraninite mineralization was identified to be vein type by Butt et al. (1978). These veins occur in a migmatitic terrain which has been variously described as higher grade parts of the Salkhala Formation (Gansser, 1964), Thakot metasediments (Ashraf et al. 1980) and Swat Buner Schistose Group (Martin et al. 1962). Butt (1983) described the detailed geology of the area and assigned a Precambrian age to this migmatite zone including the so called Lahor granite on the basis that these metasediments are intruded by Mansehra granite gneiss dated to be Cambrian (Le Fort et al., 1980).

Uraninite veins occur in both pegmatoids as well as associated schistose rocks following two sets of joints. These veins contain distinct alteration halos (Butt et al., 1978). The mineral assemblage in these veins has been described to be of uraninite – base metal type possibly related to the main phase of anatectic activity (Butt, 1983).

EXPERIMENTAL TECHNIQUE

Uraninites from various localities were separated initially by heavy liquid separation and subsequently by hand picking under a binocular microscope. The powder diffraction data were obtained on film with Cu–Kα radiation and a Ni filter on a Siefert–4000 XRD unit. The

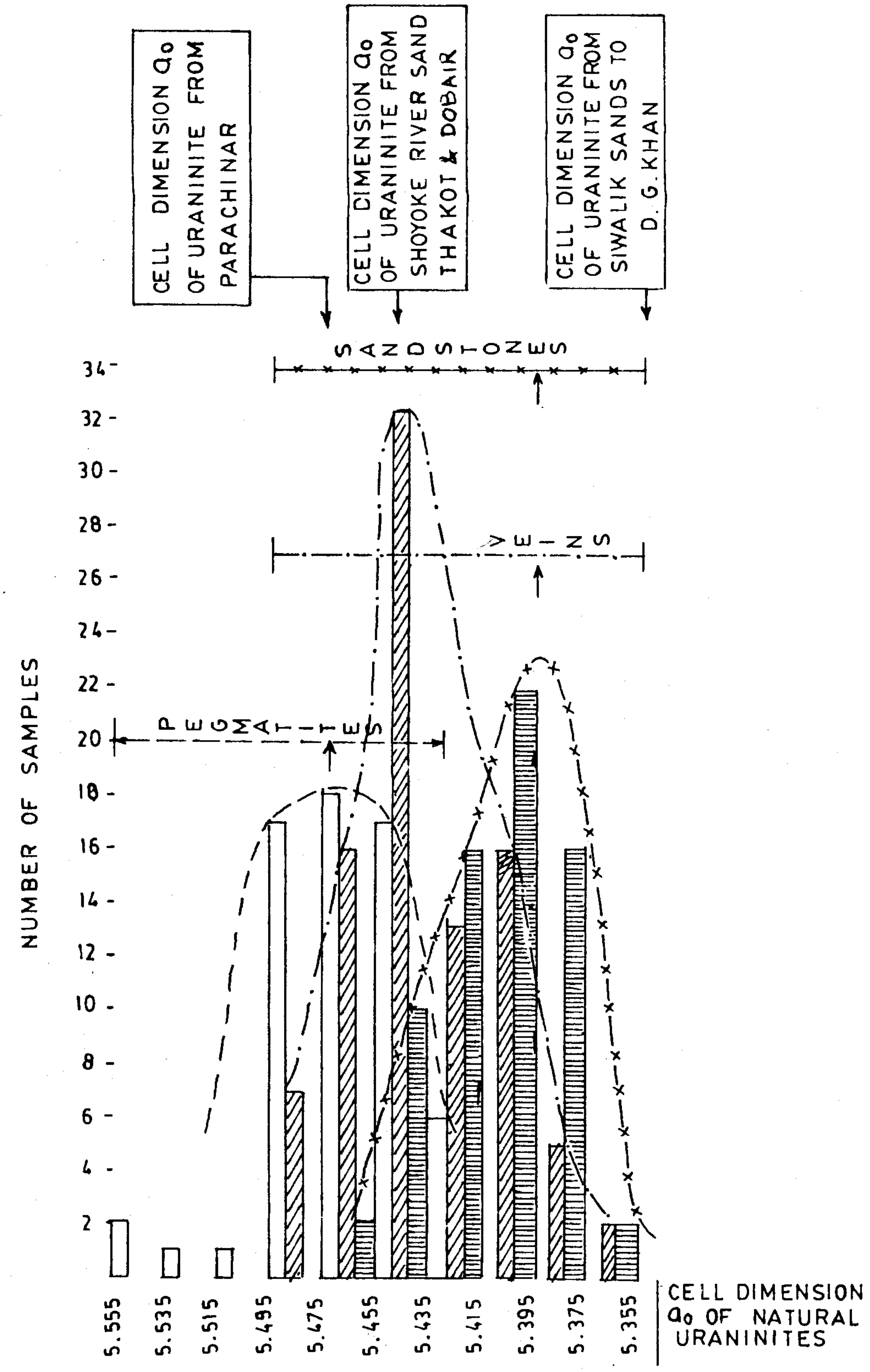

Fig. 1. Histogram of 230 cell dimensions determination on uraninites listed in Frondel (1953).

unit cell dimensions were calculated for a number of reflections for each sample by a method given in Klug & Alexander (1974).

THE DATA

Unit cell dimensions of eight uraninites from four different localities are presented in table 1. A histogram of unit cell dimensions a (Å) of 230 uraninites (Frondel, 1956) is shown in figure 1.

DISCUSSION

The observed wide variation in d-spacing is due principally to the varying extent of oxidation of U^{+4} to U^{+6}, i.e., the cell size decreases with increasing oxidation (Frondel, 1956). Additional factors for variations in cell size are the amount of radiogenic lead, Th, rare earths or other elements in substitution for U, the amount of O or OH present interstitially in valence compensation for U^{+6}, and the amount of structural damage by internal α – particle bombardment. Croft (1964) has demonstrated that in natural uraninites the oxidation of U^{+4} to U^{+6} is accompanied by line broadening due to decrease in particle size. Brooken and Naffield (1952) suggested that a mixture of materials of varying cell size due to varying degree of oxidation is responsible for line broadening in uraninite. In spite of these complicating factors it was observed by Benman (1955) that in a general way, the uraninite of pegmatites has a relatively larger cell size than that of hydrothermal veins and sandstone type deposits. This is also reflected in fig. 1 where data of 230 cell dimensions are plotted on a histogram. The maximas for uraninite cell size from pegmatites, hydrothermal veins and sandstones attest to the fact that there is a higher probability for a larger cell size to belong to pegmatitic or orthomagmatic source whereas a smaller size may owe its crystallization in sedimentary environments. Hydrothermal veins probably represent a transition from the above two extremes.

Data on pegmatitic uraninite from migmatites of Parachinar and Thakot gave the highest cell dimensions (table 1) where those from uraninite from Siwalik sandstone in D.G. Khan were the lowest. Hydrothermal fracture fillings in Thakot and Dobair yielded uraninites with intermediate cell values.

After having demonstrated a general validity of this concept of Berman (1955) in uraninites from Pakistan, the following conclusion can be drawn for detrital uraninites in sands of Indus river and its tributaries.

CONCLUSIONS

A close correspondence between the cell size of detrital uraninite from Indus river and its tributaries with fracture filling type uraninite from Dobair and Thakot suggest that the source area is dominated by vein type uranium mineralization. Orthomagmatic uraninite has rarely yielded good size uranium deposits whereas vein type occurrences are producing maximum uranium from magmatic and metamorphic environments. In view of the above, the exploration strategy on the Asian Plate of Northern Pakistan should consider a vein type source for detrital uraninite in Indus River system indicating the possibility of large scale concentration rather than disseminated type from granites and pegmatites.

REFERENCES

ASHRAF, M. (1974) Personal communication.

CHAUDHRY, M.N. & HUSSAIN, S.S., (1980) General geology and economic significance of Lahor granite and rocks of southern ophilite belt in Allai Kohistan area. Geol. Bull. Peshawar Univ. 13, pp. 207-13.

BASHAM, I.R. & RICE, C.M. (1974) Uranium mineralization in Siwalik Sandstone from Pakistan. Proc. Symp. IAEA, Vienna pp. 405-17.

BERMAN, E (1955) Unit cell dimensions of Uraninite. Amer. Mineral., 40, pp. 925-7.

BUTT, K.A. & MAHMOOD, K. (1983) Munirite, naturally occurring sodium vanadium oxide hydrate, a new mineral. Min. Mag. 47, pp. 391-2.

BUTT, K.A. (1983) Petrology and geochemical evaluation of Lahor pegmatoid/granite complex, Northern Pakistan and genesis of associated Pb-Zn-Mo and Uranium mineralization. *In:* Shams, F.A. (ed.) GRANITES OF THE HIMALAYA, KARAKORUM AND HINDUKUSH. Univ. Punjab, Lahore, pp. 309-36.

BUTT, K.A., ARIF, M. & QAMAR, H.A. (1978) Evaluation of Uranium mineralization in pegmatoid rocks in Thakot and radiometric prospecting in adjoining area. Unpublished report No. AEMC/Ev-2, AEMC, Lahore.

BROOKER, E.J. & NAFFIELD, E.W. (1952) Studies of radioactive compounds; IV, Pitchblende from Lake Athabaska, Canada. Amer, Mineral. 37, pp. 363- 85.

CROFT, W.J. (1954) An X-ray line study of Uraninite in Annual report for June 30, 1953 and April 1, 1954 Part 2; U.S. AEC. RME-3096 (Part 2), P. 7-71 issued by U.S.A.E.C. Tech. Inf. Service extension Oak ridge Tenn; Also New York Acad. of Sci. Annals, 1956, Vol. 62, (20), pp. 449-502.

FRONDEL, C. (1958) Mineralogy of Uranium and Thorium, USGSB Bull 1064.

GANSSER, A. (1964) GEOLOGY OF THE HIMALAYAS, Interscience Publication, London, 298 p.

KLUG, H.P. & ALEXANDER, L. (1974) X-ray diffraction procedures. Wiley – Interscience publication 2nd edn.

LEFORT, P., DEBON, F. &SONCT, J. (1980) The "Lesser Himalayan" cordierite granite belt; topology and age of the pluton of Mansehra (Pakistan), Geol. Bull. Peshawar Univ. 13, pp. 51-61.

MARTIN, N.R., SIDDIQUI, S.F.A. & KING, B.H. (1962) A geological reconnaissance of the region between the lower Swat and Indus rivers of Pakistan. Geol. Bull. Punjab Univ. Lahore 2, pp. 1-15.

RAHMAN, M.A. (1972) Sedimentary tyuyamunite deposits in D.G. Khan District, West Pakistan, The Nucleus, 9, pp. 33-8.

__________ & JASEEM-UD-DIN, M. (1978) Nature of Uranium-Thorium mineralization in Parachinar area, NWFP, Pakistan. Report AEMC/Geo. 13, AEMC Lahore, 39 p.

Manuscript received 17.11.1986
Accepted for publication 22.12.1986

ACTA MINERALOGICA PAKISTANICA
VOLUME 2 (1986) pp. 53-59 .

DISAPPEARANCE AND REAPPEARANCE OF SOME MESOZOIC UNITS IN LALUMI SECTION, WESTERN SALT RANGE–A STRATIGRAPHIC RIDDLE.

ALI NASIR FATMI[2] & IQBAL HUSSAIN HAYDRI[1]

1. Geological Survey of Pakistan, 22, Ali Block New Garden Town, Lahore, Pakistan.

2. Geological Survey of Pakistan, Sariab Road, Quetta, Pakistan

ABSTRACT: Stratigraphy of Lalumi area, about 10 km east of Chhidru or 9 km WSW of Sakesar (38 P/14) is described with particular reference to the reappearance of Chichali Formation below the Early Tertiary Hangu Formation. The Chichali Formation in Lalumi area is disconformably underlain by a thin lower unit (20 m) of Shinawari Formation and both these stratigraphic units disappear east, west and northwest of this section where Paleocene rocks disconformably overlie the Datta Formation.

An overstepping relationship of Datta Formation with the disconformably underlying Triassic rocks is also reported for the first time from Lalumi area. Datta Formation oversteps Kingriali Formation in the west to Mianwali Formation in the east.

INTRODUCTION

Geological Map of Western Salt Range by Dr. E.R. Gee (Sheet No. 2, 38 P/14, 1980) has disclosed "ghost" out crops of Chichali Formation and Samana Suk Formation (regarded here as Basal Shinawari Formation) overlying Datta Formation in Lalumi area, 2 kms north west of Sarai Village (38 P/14). The Chichali Formation and "Samana Suk Formation" (Shinawari Formation), however, disappear further north west (in Nammal, Buri Khel area) and southeast in Sarai sections of Western Salt Range where the Early Paleocene rocks (Makerwal group) directly overlie the Datta Formation disconformably.

Further northwest in Chitta Wahn-Khairabad sections the normal Early Cretaceous-Jurassic sequence similar to the trans–Indus Surghar Range appears. The disappearance of Lumshiwal, Chichali, Samana Suk Formation and most of the Shinawari Formation from Buri Khel-Nammal Chhidru Sections, the reappearance of Chichali and Shinawari Formations (20 meters approx. each) in Lalumi section and again its disappearance for good further east in Salt Range is the subject of this paper. It was further noted that in Lalumi area the relationship of Datta Formation with the underlying Triassic Sequence is not a normal disconformity over the Kingriali Formation but an overstepping relationship in which Datta Formation is sitting disconformably on Kingriali Formation in western Lalumi section, on Tredian Formation in Central Section and resting on Mianwali Formation in Eastern Lalumi Section, near Sarai (fig. 1, 2). Lateritization of Kingriali dolomite with a considerable reduction in thickness below the Datta Formation is well seen in Central Lalumi area.

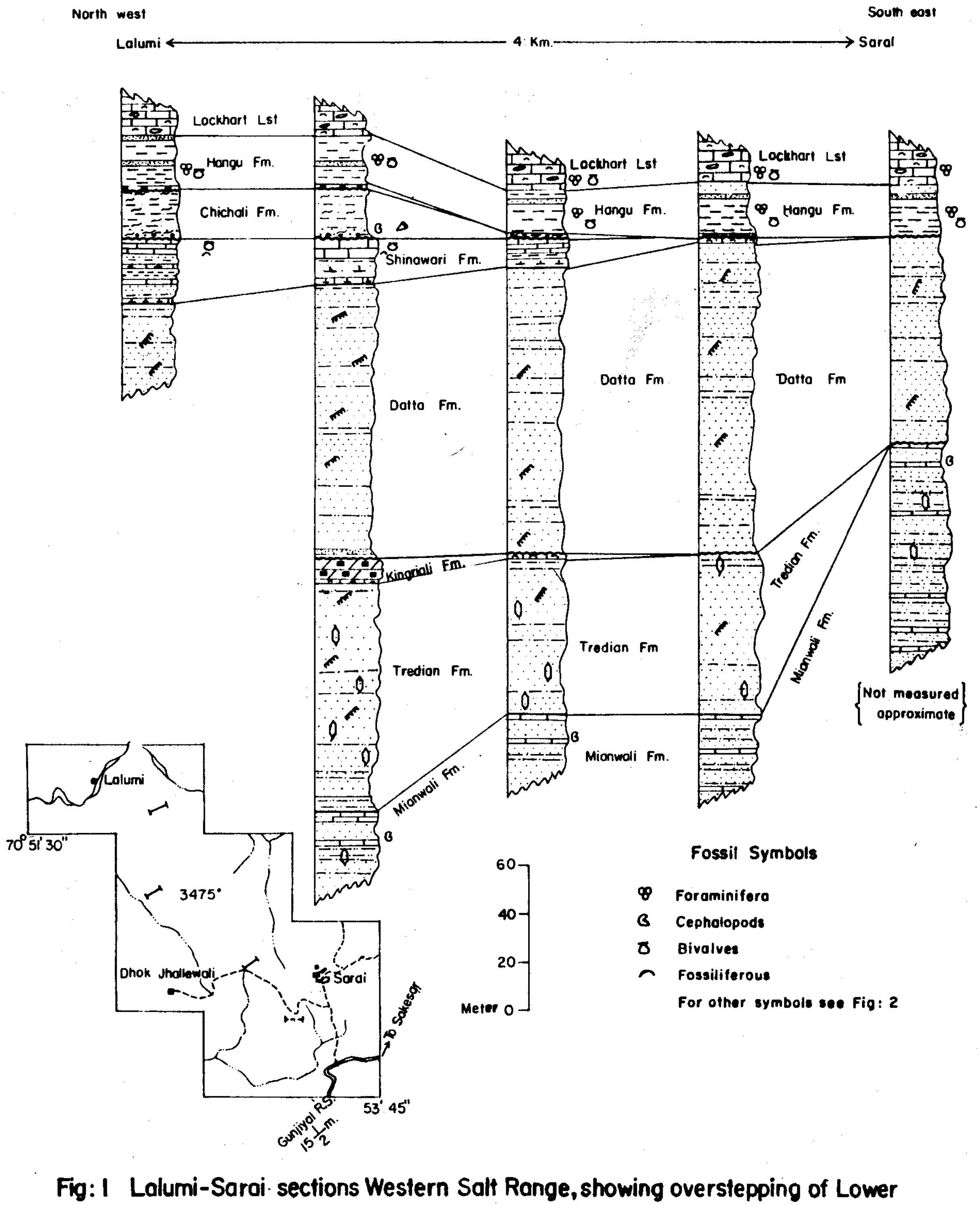

Fig: 1 Lalumi-Sarai sections Western Salt Range, showing overstepping of Lower Jurassic Datta Fm. on Triassic and of Paleocene Hangu Fm. on Chichali, Shinawari and Datta Formations.

Drafted by: Sultan malik

Fatmi / Hydri

The authors are indebted to Dr. E.R. Gee for pointing out this stratigraphic riddle which he very correctly recorded excepting that what Dr. Gee thought as Samana Suk Formation is considered here as the remnants of Lower Jurassic Shinawari Formation which is transitional to the underlying Datta Formation.

The best approach to Lalumi is from Warcha Salt Mines Rest House on the newly constructed Gunjial-Sakesar Road upto the Sarai Village and than walking 2 to 3 kms to the Lalumi Section.

STRATIGRAPHIC SUMMARY

In the extreme north western end of Salt Range (Gee, 1980, Sheet No. 1) near Khairabad a typical Early Cretaceous-Jurassic Sequence is developed overlying unconformably the Triassic Kingriali Formation and underlying unconformably the Paleocene rocks of Makerwal group (Hangu Formation). The stratigraphic relationship, however changes near Buri Khel-Nammal, Lalumi and Sarai Sections to the southeast (see fig. 1,2,3 and Dr. Gee's Geological Map, 1980, Sheet No. 1,2).

INTERPRETATION OF MESOZOIC SEQUENCE OF LALUMI SECTION, WESTERN SALT RANGE.

On the eastern end of Lalumi section close to Gunjiyal-Sarai-Sakesar Road (1 km south of Sarai village) Early Jurassic Datta Formation is directly underlain, with a disconformity by the Early Triassic Mianwali Formation and overlain disconformably by Early Paleocene rocks (Hangu Formation). Moving north-westward into Lalumi Section; the Datta Formation overlies first Tredian Formation (Middle Triassic) and than the Kingriali Formation (Late Triassic) close to Lalumi village.

The relationship with the overlying Tertiary rocks in the Central Lalumi Section is also very interesting. The Early Paleocene Rocks disconformably overlie first on a basal eroded beds of Shinawari Formation which appear in Central Lalumi and within short distance toward north west, it disconformably overlies Chichali Formation consisting of glauconitic soft sandstone and sandy shale yielding belemnites and Late Jurassic ammonites ***(Perisphinctes, Mayites, Belemnopsis, Hibolithes)*** in lower part. The Early Paleocene rocks thus in Central and Western Lalumi Sections have a disconformable relationship with the Chichali Formation instead of Datta Formation as in the extreme north eastern section south of Sarai (see figs. 1,2).

The Chichali Formation itself has a peculiar unconformable relationship with the lower carbonate beds of Shinawari Formation instead of Samana Suk Formation as is the case in extreme north west section of Khairabad and across Indus in Surghar Range.

The strange relationship of Jurassic and Tertiary rocks within a short 3 to 4 kms strike distance in Lalumi area can be explained if we trace back the geological history to the Pre-Jurassic uplift which is recognized in Salt Range, Trans-Indus Ranges, Kalachitta and even Hazara and to the events that followed during Jurassic-Early Cretaceous times before the Paleocene transgression in the Salt Range and other areas of Potwar and Kohat.

Our explanation to this riddle may be summarized as follows.

1. Uplift followed by erosion near the close of Triassic involving gentle west and south westerly tilting of Salt Range (fig. 2) in which Upper and Middle Triassic units were subjected to greater erosion (in Eastern half of Lalumi Section) before the deposition of Early Jurassic Datta Formation in a shore line continental environment. This Pre-Jurassic erosional surface with its westerly tilting could have been influenced by the Chhidru High (see fig. 3b).
2. This westerly tilting and uneven erosion was responsible for the overstepping of Datta Formation on Kingriali Formation in the western and Mianwali Formation in the eastern sections of Lalumi. The Datta-Mianwali Formations unconformable contact has also been mapped by Gee (1980) from section

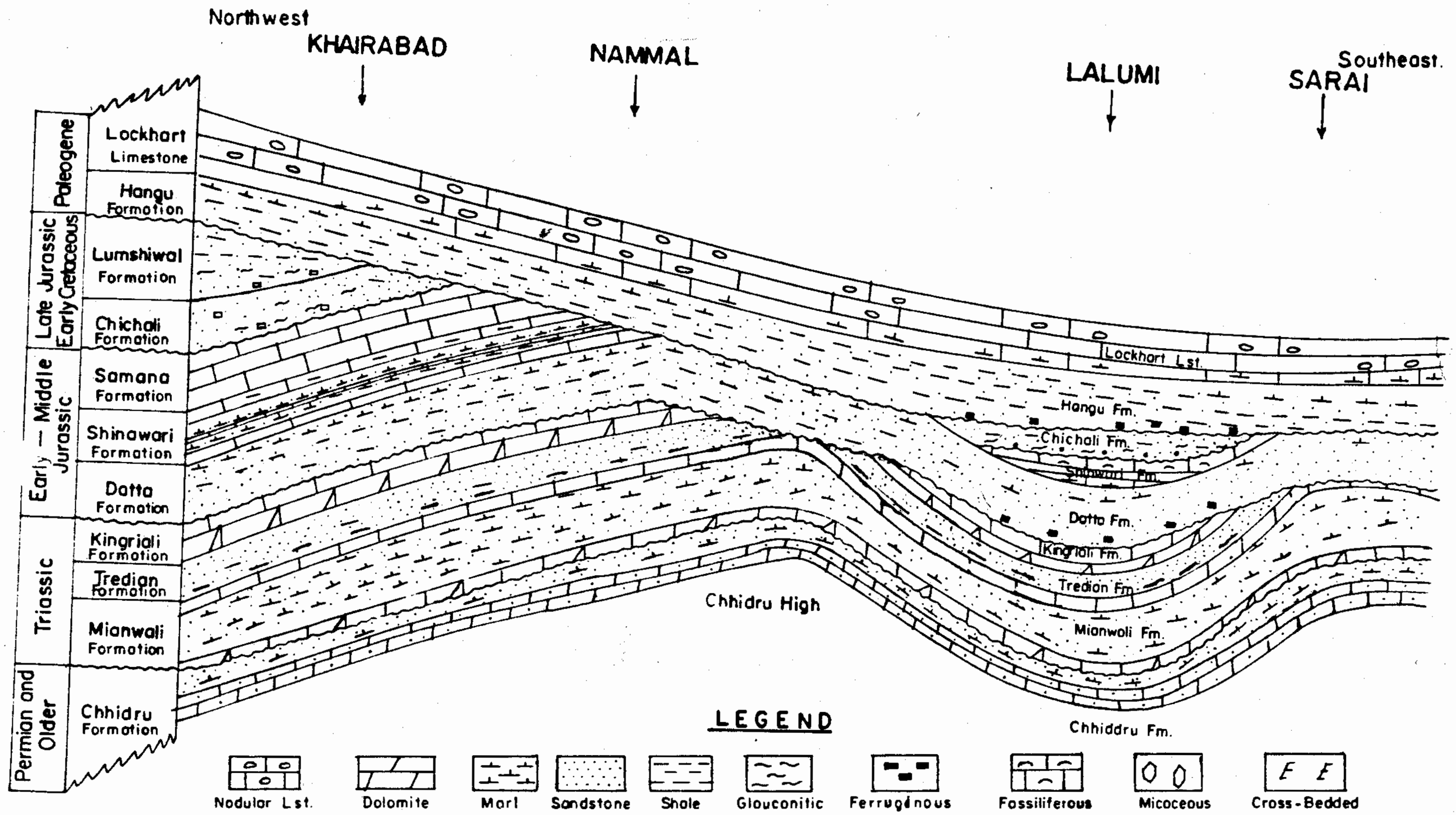

FIGURE 2.—SCHEMATIC STRATIGRAPHIC SECTION OF WESTERN SALT RANGE SHOWING EFFECTS OF UNCONFORMITIES, WESTERLY TILTING AND CHHIDRU HIGH ON MESOZOIC AND TERTIARY SEDIMENTATION (NOTE THE REMANANT OUTCROPS OF CHICHALI AND SHINAWARI FORMATIONS AND THE OVERSTEPPING OF PALEOCENE ROCKS AND DATTA FORMATION ON OLDER UNITS IN LALUMI AREA. (Parts of Sheet 38P).

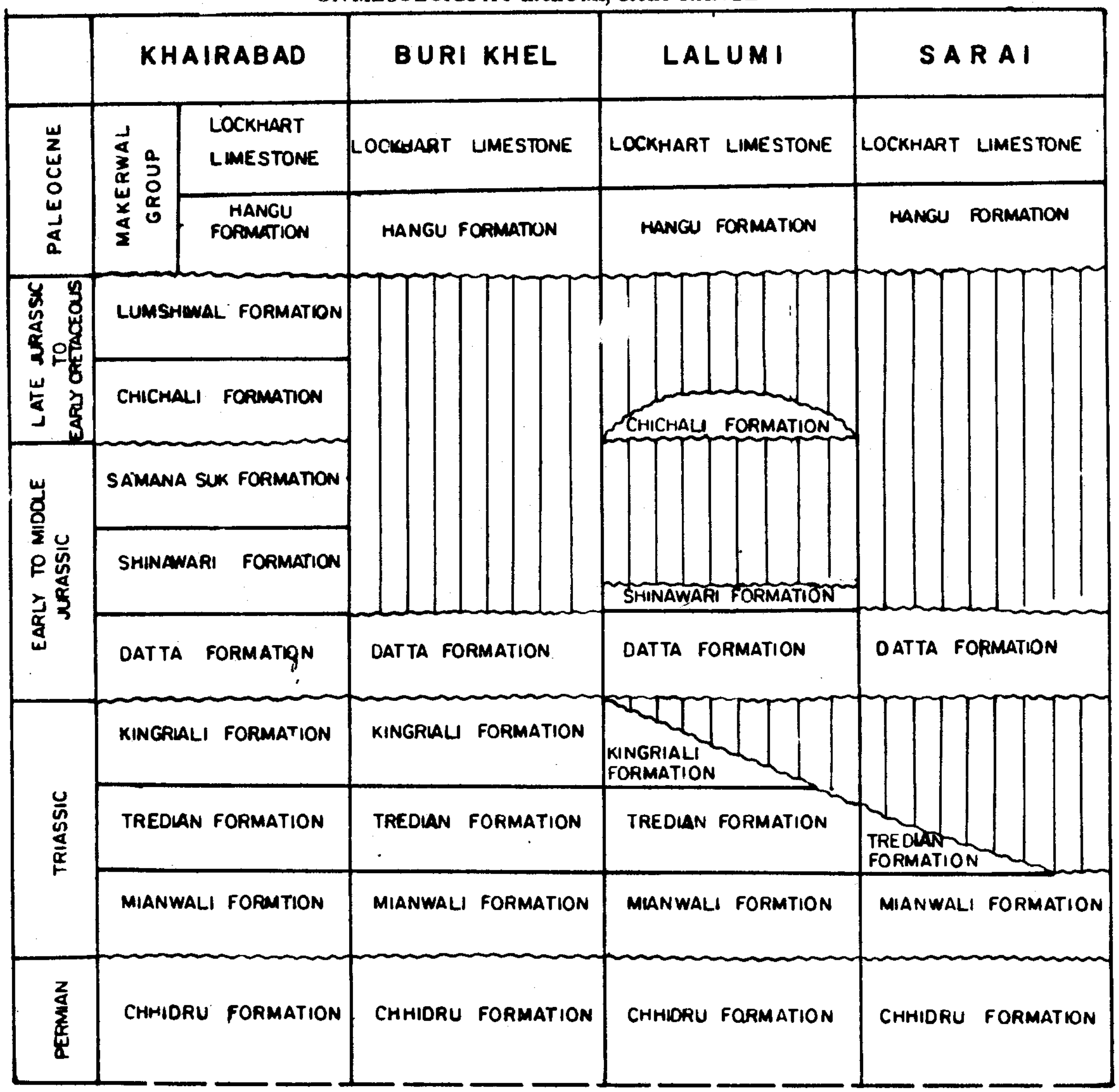

FIG:—3a, STRATIGRAPHIC RELATIONSHIP OF MESOZOIC ROCKS IN WESTERN SALT RANGE'

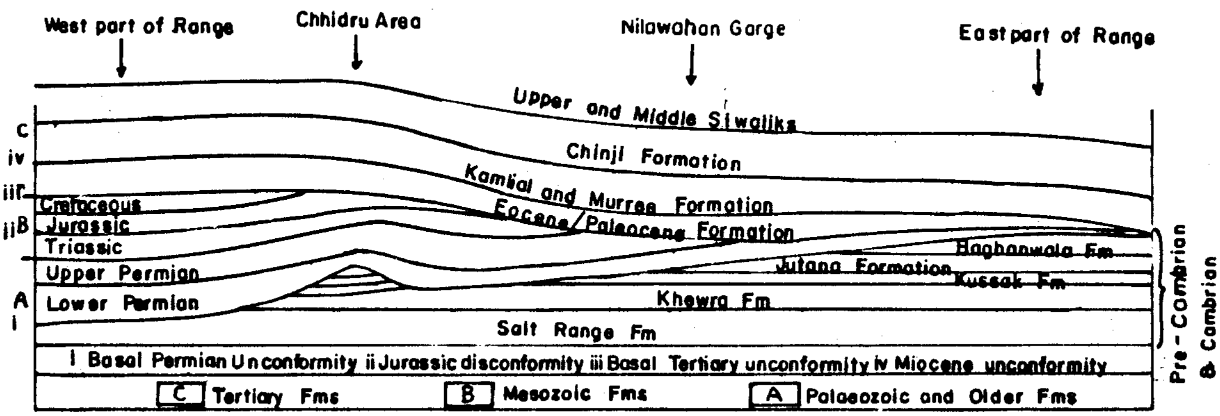

FIG—3b, REPRODUCED AFTER E. R. GEE GEOLOGICAL MAP 1980.

east-north-east of Chhidru village but a normal Datta-Kingriali Formations unconformity is present like western Lalumi section in Nammal and further north west in Khairabad.

3. Shallow marine transgression in the latter part of Early Jurassic (Toarcian) in which the mixed clastic and carbonate rocks of Shinawari Formation (with molluscan and other fauna) were deposited followed by dominant carbonate sedimentation during Middle Jurassic (Samana Suk Formation).

4. Uplift and erosion in Pre-Upper Oxfordian (Late Jurassic time) probably was influenced by similar west and south-westerly tilting of Salt Range in which Samana Suk Formation and part or whole of Shinawari Formation were eroded from parts of Western salt Range (absence of these rocks in Buri Khel-Nammal, Chhidru-Lalumi Sections).

5. Subsidence and shallow marine transgression in Late Jurassic depositing the sandy and silty glauconitic shale and soft sandstone of Chichali Formation. It is very likely that Chhidru-Nammal Axis may have remained a high during Late Jurassic (Chichali Formation) times but Lalumi was a low subsiding narrow basin connected with the shallow marine sea of the Late Jurassic of Trans Indus Ranges from north west as an arm of the sea.

6. Regression during Aptian-Albian with deposition of Lumshiwal Formation continental beds in the north-western end of Salt Range and Surghar Range accompanied by earlier uplift of rest of the Salt Range.

7. Erosion and non-deposition during Late Cretaceous times subjecting the west and south-westerly tilted Salt Range basin to greater erosion in the east than in the west with lateritization of the erosional surface bauxite and laterite development at the base of Tertiary in Central Salt Range).

8. Subsidence and marine transgression during Early Tertiary starting with a shore line environment depositing clastic rocks with the development of coal followed by more shallow open marine environment higher up in the Paleocene with deposition of carbonate rocks.

9. The Paleocene transgression and overstepping on older rocks ranging in age from Early Cretaceous (extreme north western end) to Paleozoic in Central and Eastern Salt Range are the cumulative effects of several periods of uplift, tilting, regression and transgressions in which the positive areas (like Chhidru High, Sargodha High) played an important role in the erosion or none to thin deposition of various Mesozoic units.

10. It may be noted that the Early Permian Tobra Formation shows a reverse tilting of the area as it oversteps rocks of Salt Range Formation (Early Cambrian-Precambrian) in the north western part of Buri Khel-Khairabad to younger Cambrian Bhaganwala Formation (Middle Cambrian) in the Eastern Salt Range.

CONCLUSIONS

The disappearance of Chichali Formation and other Jurassic units like Samana Suk and Shinawari Formations from Buri Khel-Nammal-Chhidru Sections of Western Salt Range and the reappearance of Chichali and Shinawari Formation in Lalumi Section appear to be the cumulative outcome of at least 3 major periods of uplift, erosion, west to south-west tilting and influence of positive structures like Chhidru High. These are related to post Triassic, post Middle Jurassic (Middle Callovian) and post Early Cretaceous movements (mainly epierogenic).

It is further suggested that after the post Early Cretaceous (Post Middle Albian) emergence, southern Potwar and Salt Range remained areas of non-deposition and erosion during Late Cretaceous while north Potwar (Northern Kala

Chitta), Hazara and Kohat were areas of marine sedimentation during the Late Cretaceous connecting Hazara-Northern Kala Chitta-Kohat through Waziristan with Sulaiman-Kirthar provinces of Baluchistan.

The general post-Cretaceous uplift in many parts of Pakistan (except south Baluchistan) was followed by subsidence and Paleocene transgression effecting most of the areas including Salt Range and a thick sequence of Lower Tertiary clastic and carbonate rocks were deposited in subsiding basin. Unlike Northern Potwar, Kohat and Hazara where Paleocene overlies the Late Cretaceous rocks with a disconformity in Southern Potwar and Salt Range, it oversteps rocks from Early Cretaceous to Paleozoic.

ACKNOWLEDGEMENTS

The senior author wishes to record his personal gratitude to Dr. Gee for providing guidance from his 40 to 45 years old field note book from England regarding the approach including the name of Malik of Sarai who is dead and survived by his grandsons. These grandsons recall Dr. Gee's visit to the Sarai, Lalumi through village tales conveyed by their father and grandfather. Thanks are due to Sohail Khan for typing the manuscript.

REFERENCES

FATMI, A.N. (1972) Stratigraphy of the Jurassic and Lower Cretaceous rocks and Jurassic ammonites from northern areas of West Pakistan. Bull Brit. Mus. (Nat. Hist.) **20**, no. 7 London.

———— 1973, Lithostratigraphic units of Kohat Potwar Province, Indus Basin Pakistan Mem. Geol. Surv. Pakistan, **10.**

———— 1984, Stratigraphy and stratigraphic problems of Jurassic rocks of Pakistan. Int. Symp. on Jurassic stratigraphy. Symp. Vol. III Copenhagen.

GEE, E.R. (1980) Pakistan Geological Salt Range Series Maps on 1:50.000 Scale, Directorate of Overseas Surveys, U.K.

Manuscript received 11.12.1986
Accepted for publication 31.12.1986

ACTA MINERALOGICA PAKISTANICA
VOLUME 2 (1986) pp. 60-64.

PLATE TECTONICS AND THE UPPER CRETACEOUS B10 STRATIGRAPHIC SYNTHESIS OF PAKISTAN

AFTAB AHMAD BUTT

Institute of Geology, Punjab University, Lahore–20, Pakistan.

ABSTRACT:– Global marine transgression – expansion of world oceanic environments – is an episode of active plate movement associated with rapid radiation and evolution of marine organisms, whereas global marine regression – shrinking of world oceanic environments– is an episode of slow plate movement associated with extinction of biota. The Upper Cretaceous forminiferal biostratigraphy of the northwestern margin of the Indo-Pakistani Plate is discussed with reference to such geological concepts.

INTRODUCTION

Plate tectonics is a modern version of an earlier geological concept of continental drift. It is based on the concept that the Earth's surface is composed of a mosaic of fragments called plates, which are floating on a more viscous inner mantle. Moreover, periods of active plate movements have alternated with periods of quiescence in the geological past and the margins of the plates have been tectonically more active during collision and, therefore, exhibit conspicuous structural features along their margins.

In this context, global marine transgression has been expressed as an episode of active plate movement drowning the margins and many inland depressions of the world continents with shallow epicontinental seas. This significantly expanded the world oceanic environments associated with rapid radiation and evolution of marine organisms, whereas global marine regression is an episode of slow plate movement causing major lowering of the sea level. It means that the epicontinental seas and much of the continental shelf areas were periodically drained, thereby reducing world oceanic environments considerably, and this being associated with the extinction of biota.

Kauffman (1976), very explicitly presented a synthesis of major evolutionary events influenced by the plate tectonic history by taking an example of the Cretaceous period because "it is known as a time of active plate movement and rapid evolution including 'abrupt' origin and extinction periods". Marine molluscs were chosen by him as test organisms because "they are the most common and widespread megafossils of the period; many species rapidly attained intercontinental to cosmopolitan distribution". Kauffman (1976) summed up by stating that the widespread fluctuations of sea level and marine environments controlled by plate tectonic activity, were major natural selective forces shaping the evolutionary patterns of marine organisms. The Upper Cretaceous (mainly Campanian to Maastrichtian) foraminiferal biostratigraphy of the northwestern margin of the Indo-Pakistani Plate (fig. 1) is discussed in the present contribution as a testimonial to the fluctuations of sea level and marine environments controlled by plate tectonic activity.

STRATIGRAPHIC SYNTHESIS

Since the Cretaceous period is known as the time of active plate movement and rapid evolution including abrupt origin and extinction periods, globotruncanids, among foraminifera, are the most common and widespread biota of the Cretaceous period, preserved in open marine, outer neritic environments (from 100m to 200m). Due to the cosmopolitan nature of several species, world-wide correlation is possible with

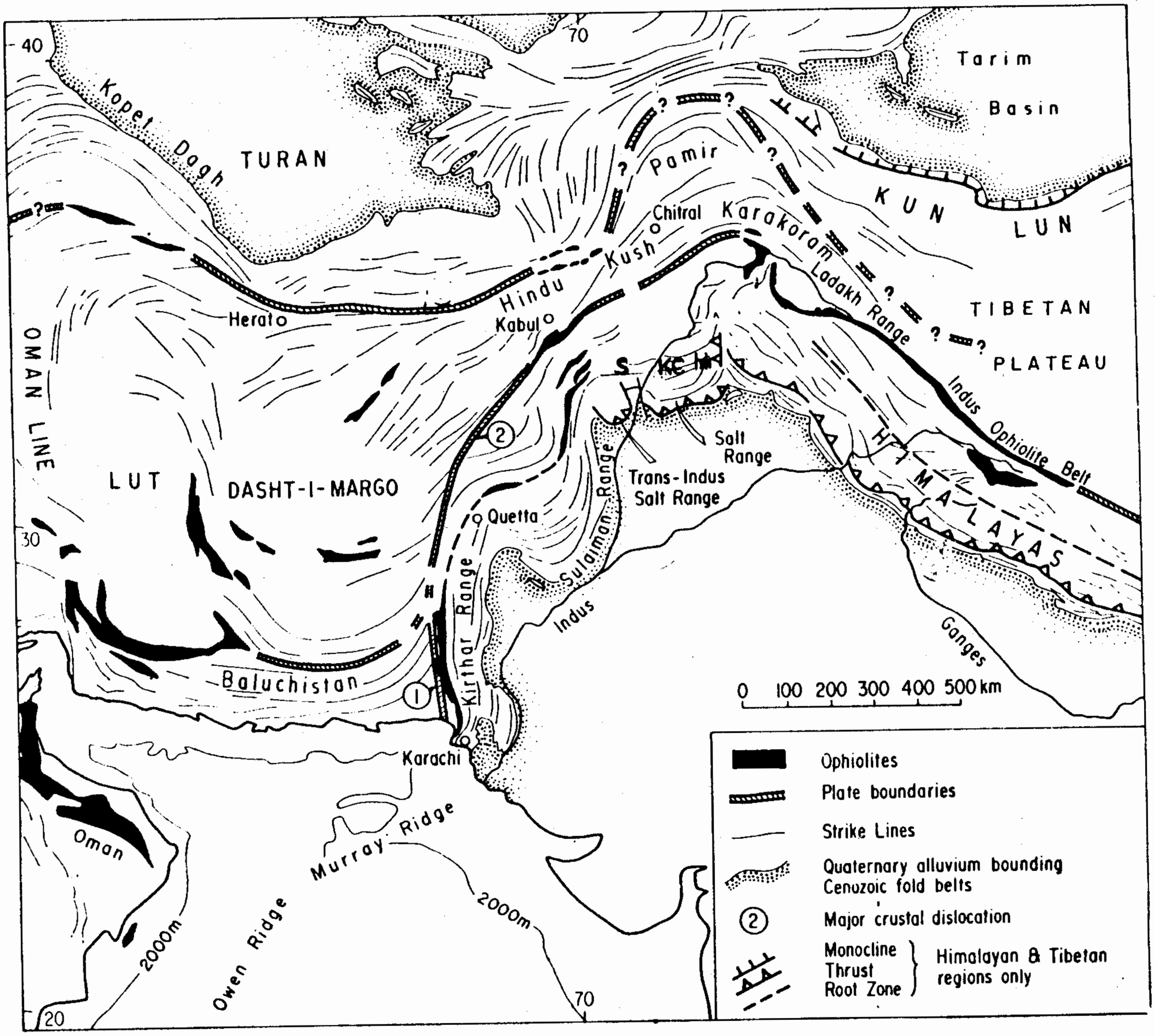

Fig. 1. Northwestern margin of the Indo-Pakistani Plate bounded by ① Ornach-Nal, and ② Chaman, faults culminating further northward into the Main Mantle Thrust. Locations of Hazara (H), Kala Chitta (KC) and Samana (S) ranges are also shown. Diagram after Powell (1979).

great precision. In a similar manner, the shallow-water marine environments (< 50m) are characterised by the presence of stratigraphically important orbitoidal foraminifera of world-wide occurrences.

The Campanian sediments in northern Pakistan (Kohat-Potwar-Hazara province covering Samana, Kala Chitta, Hazara Ranges) are termed the Kawagarh Formation, while these are known as the Parh Limestone in southern Pakistan (i.e., Sulaiman and Kirthar Ranges). Both of these have similar sedimentary facies and environments as well as the microfaunal composition. These micritic sediments are characterised by the *Globotruncana* biofacies (table 1).

Table 1. Upper Cretaceous foraminiferal biostratigraphy of the northwestern margin of the Indo-Pakistani plate.

AGE		NORTHERN PAKISTAN (SAMANA, KALACHITTA, HAZARA RANGES)	SOUTHERN PAKISTAN (KHIRTHAR, PAB RANGES)	NORTHWESTERN PAKISTAN (SULAIMAN RANGE)	
				SOUTHERN	NORTHERN (RAKHI NALA)
UPPER CRETACEOUS	MAASTRICHTIAN	R E G R E S S I V E			
			Lepidorbitoides minor Biofacies PAB SANDSTONE Shallow shelf clastic deposition (< 50 m)	Orbitoides apiculatus Biofacies (Murree-Brewery Gorge, Quetta Syntaxis) Shallow shelf carbonate platform deposition (< 50 m)	Lepidorbitoides minor Biofacies PAB SANDSTONE Shallow shelf clastic deposition (< 50 m)
	CAMPANIAN	T R A N S G R E S S I V E			REGRESSIVE
		G L O B O T R U N C A N A B I O F A C I E S			Orbitoides tissoti Biofacies MUGHALKOT FORMATION Shallow shelf carbonate platform deposition (< 50 m)
		K A W A G A R H F O R M A T I O N	P A R H L I M E S T O N E		
		O U T E R N E R I T I C C A R B O N A T E S H E L F D E P O S I T I O N (100 m – 200 m)			TRANSGRESSIVE
					Globotruncana Biofacies PARH LIMESTONE Outer neritic (100m-200m) Carbonate deposition
		M I C R I T I C F A C I E S			

The paleogeographic setting during the deposition of these sediments draws attention towards a major regional flooding of the northwestern margin of the Indo-Pakistani Plate. In other words, a major transgression took place marking a period of active plate movement during which the expansion of the marine environments all along the plate margin provided congenial conditions for the flourishment of the biota both in number and species, as is manifested by the occurrence of globotruncanids in these sediments. Locally (Rakhi Nala Section, Sulaiman Range), there is observed an upward shallowing trend in the paleobathymetry, thereby resulting in the creation of shallow-water facies, the Mughalkot Formation, which succeeds the Parh Limestone. It is characterised by the Campanian species ***Orbitoides tissoti*** (Marks, 1962).

The Maastrichtian time interval envisages a major episode of draining of the northwestern margin of the Indo-Pakistani Plate – a period of destruction of the marine environments creating limited shallow-water living space. This all amounts to a major regression causing major extinction of biota. The reduced marine environments are manifested by observing the complete absence of the Maastrichtian sediments in northern Pakistan (Samana, Kala Chitta and Hazara Ranges), and the development of a major regressive clastic facies in southern Pakistan, the Pab Sandstone, by virtue of lowering of the sea level. This facies is almost fossil – starved except for the rare occurrence of the age-diagnostic orbitoidal foraminifera ***Lepidorbitoides minor*** (Vrendenburg, 1908).

Around Quetta Syntaxis at the southern end of the Sulaiman Range (Murree-Brewery Gorge Section), the Maastrichtian sediments are outcropping as ***Orbitoides***-bearing calcareous facies reminiscent of the Mughalkot Formation, except for the presence of the Maastrichtian species ***Orbitoides apiculatus*** (Alleman, 1979). This may recall a carbonate platform deposition of the Mughalkot Formation in a narrow belt in the Sulaiman Range from Campanian age comprising ***Orbitoides tissoti*** in the Rakhi Nala in northern Sulaiman Range, to the Maastrichtian towards the southern end of the Sulaiman Range containing ***Orbitoides apiculatus*** in the Murree-Brewery Gorge. The geographical extension of the Sulaiman Range and its structural framework strongly favours this paleogeographic concept suggestive of time-transgressive nature of the Mughalkot Formation.

The Maastrichtian paleogeography would, therefore, point out towards the existence of a restricted carbonate platform among the widely distributed Pab Sandstone along the northwestern margin of the Indo-Pakistani Plate.

CONCLUSION

It is agreed with Kauffman (1976) that massive environmental changes caused by plate tectonics can be visualised as a predominant driving force in the evolutionary history of life on Earth. This has been elucidated by having a perusal of the Upper Cretaceous foraminiferal biostratigraphy along the northwestern margin of the Indo-Pakistani Plate.

REFERENCES

ALLEMAN, F. (1979) Time of emplacement of the Zhob Valley Ophiolites and Bela Ophiolites. *In:* Farah, A. & De Jong, K.A. (eds.) GEODYNAMICS OF PAKISTAN. Geol. Surv. Pakistan, Quetta, pp. 215-24.

BUTT, A.A. (1969) A note on the Cretaceous – Tertiary boundary in Hazara, West Pakistan. Geol. Bull. Punjab Univ. 8, pp. 73-8..

———— (1973) The Kawagarh Formation in Kala Chitta northern Pakistan. Proc. 24th Pakistan Sci. Conf. Islamabad.

FATMI, A.N. (1973) Lithostratigraphic units of the Kohat – Potwar province, Indus Basin, Pakistan (Rept. Strat. Comm. Pakistan). Mem. Geol. Surv. Pakistan, Quetta, 10, pp. 1-80.

GIGON, W.O. (1962) Upper Cretaceous stratigraphy of the well Giandari-1 and its correlation with the Sulaiman and Kirthar Ranges, West Pakistan Second ECAFE Petrol. Symp. Teheran, pp. 1-18.

KAUFFMAN, E.G. (1976) Plate tectonics: major force in evolution. THE SCIENCE TEACHER, 43(3), 5 p.

LATIF, M.A. (1970) Micropaleontology of the Chanali Limestone, Upper Cretaceous of Hazara, West Pakistan. Jahrb. Geol. Bundesanst. 15, pp. 25-62.

MARKS, P. (1962) Variation and evolution in Orbitoides of the Cretaceous of the Rakhi Nala, West Pakistan. Geol. Bull. Punjab University 2, pp. 15-30.

MAGAPPA, Y. (1959) Foraminiferal biostratigraphy of the Cretaceous – Eocene succession in the India-Pakistan-Burma region, Micropaleontology, 5, pp. 145-92.

POWELL, McA.C. (1979) A speculative tectonic history of Pakistan and surroundings: some constraints from the Indian Ocean. *In:* Farah, A. & DeJong, K.A. (eds.) GEODYNAMICS OF PAKISTAN, (op. cit.), pp. 5-24.

SARWAR, G. & DeJONG, K.A. (1979) Arcs, Oroclines, Syntaxes: the curvature of mountain belts in Pakistan. *In:* Farah, A. & DeJong, K.A. (eds.) GEODYNAMICS OF PAKISTAN (op. cit.), pp. 341-349.

SHAH, S.M.I. (1977) Stratigraphy of Pakistan (Rept. Strat. Comm. Pakistan). Mem. Geol. Surv. Pakistan, 12, pp. 1-138.

VRENDENBURG, W. (1908) The Cretaceous Orbitoides from India. Rec. Geol. Surv. India, 36, pp. 171-213.

Manuscript received 12.11.1986
Accepted for publication 21.12.1986

ACTA MINERALOGICA PAKISTANICA
VOLUME 2 (1986) pp. 65-73.

OPHIOLITIC ULTRAMAFIC–MAFIC ROCKS FROM BAGH AREA, ZHOB DISTRICT, PAKISTAN.

ABDUL SALAM[1] & ZULFIQAR AHMED[2]

1. Department of Geology, University of Baluchistan, Quetta,& Centre of Excellence in Mineralogy, Quetta, Pakistan.

2. Centre of Excellence in Mineralogy, University of Baluchistan, Quetta, Pakistan.

ABSTRACT:– A large scale geological map of the area around Bagh (30° 40' N; 68° 6'E) was prepared to plot emphatically the ultramafic-mafic cumulates of the Saplaitorgarh segment of the Muslimbagh–south ophiolite (Ahmed, 1986). The olivine–richer lower portion of the cumulate section has lithotypes repeated in at least five cycles magmatically and not tectonically. The sequence in each of these cycles, when complete, has from bottom upwards: dunite–wehrlite–clinopyroxenite–gabbro. Some cycles lack gabbro, but when present, it shows cm–scale layering. Satellitic dolerite dykes are mainly confined to this lower portion of cumulates. The olivine-poorer upper portion of the cumulates also has a variety of rocks topped by massive gabbro which is overlain by sheeted dykes interspersed with a few gabbroic screens.

INTRODUCTION

The Muslimbagh–south ophiolite is spread over a vast area and has been studied by many workers including Ahmad & Abbas (1979), Ahmed (1974), Ahmed (1986), Ahmed & Chudhry (1969), Bilgrami (1964) Hunting Survey Corporation (1960), Moores et al. (1980), Rossman et al. (1971) Van Vloten (1967) and many others. The ophiolite is now required to be studied by preparing larger scale maps of small parts bringing out local features and variations in detail. In the present study, a geological map of the area near Bagh village (30° 40′ N; 68° 6′ E) is prepared (fig. 1). The area is situated in the southeast corner of the Saplatiorgarh segment. Petrography of the rocks is described alongwith the main features of the cumulate sequence.

GENERAL GEOLOGY

The salient features of the geology of Bagh area are seen in the geological map given in fig. 1. The stratigraphic order is as given in table 1 below:

The Loralai Limestone Member, with moderate westward dips, forms a hillock. The limestone is partly oolitic, thin–to medium–bedded, grey in colour, yellowish brown to reddish brown in weathering colour and is traversed by abundant fractures some of which are filled by recrystallized calcite.

The Parh Group strata outcrop in the southern and southeastern part of the mapped area (fig. 1) and bear a general dip of 55° NW. Its subdivisions are not separately mapped in fig. 1. The Sembar Formation has dark grey to olive green, glauconitic, fissile, thin-bedded shale and grey siltstone. The Goru Formation is composed of greyish and greenish glauconitic, splintry shales; fine-grained, thin bedded, grey to green limestone and olive-grey or maroon, thin-bedded, fractured siltstone. The Parh Limestone has light grey to creamy white colour, conchoidal

Table 1. Stratigraphic sequence of Bagh area

Rock unit	Age	Thickness	Lithology
QUATERNARY DEPOSITS	Recent (Holocene)	Variable	Argillaceous matrixed rock debris and alluvium
OPHIOLITIC ROCKS	Emplaced in Paleocene to Early Eocene.	3000 m to 4000 m.	Ultramafic-mafic rocks, metamorphic rocks and a mélange zone.
PARH GROUP			
Parh Limestone	Late Cretaceous	100 m-150 m.	Lithographic, massive, fine-grained limestone.
Goru Formation	Early Cretaceous	100 m-125 m.	Interbedded shale and siltstone of variegated colours.
Sembar Formation	Late Jurassic to Early Cretaceous	200 m-300 m.	Shale and siltstone. disconformity
SHIRINAB FORMATION			
Loralai Limestone Member	Early Jurassic	400 m-600 m.	Limestone with some interbedded shale.

fracture and is hard, thin-bedded and procellaneous. The ophiolitic mélange is 100 m to 600 m thick and tectonically overlies the Parh Group. Its age is probably early Palaeocene. Tertiary, fossiliferous limestone and shale, belonging to the lower part of the Nisai Formation and called Sra Salwat Formation (Lower Eocene), are exposed outside the mapped area of fig. 1. They unconformably overlie the ophiolitic rocks. At places, near the lower contact of ophiolitic rocks, metamorphic rocks, only a few tens of metres in thickness, outcrop. Their rock-types include amphibolite, schist, marble and phyllite.

The ophiolitic rocks generally trend NE. They belong to the Muslimbagh-south ophiolite (Ahmed, 1986) and are divisible into four units: cumulates, sheeted dykes, isolated dykes and pillow lavas. The cumulates are about 4.5 km thick and are divisible into a lower cumulate zone and an upper one. The lower zone lithologies display cyclic variation and include dunite, wehrlite, diopsidite and gabbro. Adcumulates are abundant. The rocks show serpentinization which is more advanced in dark green serpentinites developed along shear zones. Dolerite dykes are present in the lower zone and are absent in the upper zone. The upper zone contains gabbro which is generally massive and non-layered. It may bear some accessory olivine or orthopyroxene, but lacks cyclic repetitions. It may contain accessory Fe-Ti oxides. Adcumulates are not present. Some massive gabbro is also present in the lower cumulate zone. The ophiolitic rocks contain small portions of diorite, anorthosite and plagiogranite which may form irregular, vein-like areas in the massive gabbro. Being more resistant to erosion, massive gabbro occurs in upper reaches of the hillocks.

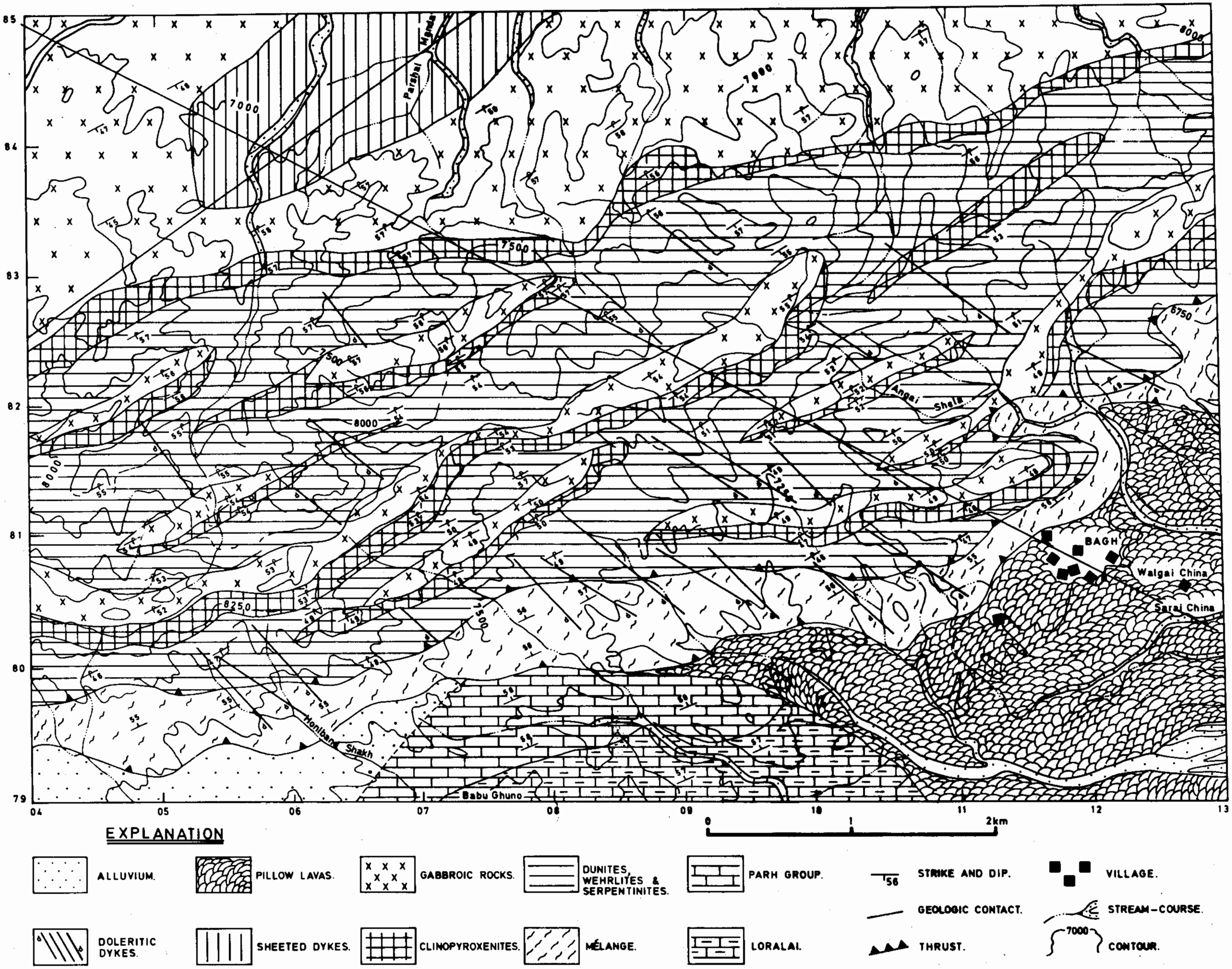

Fig. 1. GEOLOGICAL MAP OF BAGH AREA.

Table 2. Modal analyses of the Bagh area serpentinites (1–7), dunites (8–15), wehrlites (16–19), pyroxenites (20–36), anorthosite (37), gabbro (38–52), diorite (53–54), plagiogranite (55–57), normal dolerites (58–78), quartz dolerites (79–81), dolerites with green hornblende (82–89) and dolerites with brown hornblende (90–92). Mineral symbols are after Kretz (1983). Anal. No. = Analysis number. Sp. No. = Sample number. – = Not detected.

Anal. No.	**1**	**2**	**3**	**4**	**5**	**6**	**7**	**8**	**9**	**10**	**11**
Sp. No.	**303**	**312**	**328**	**355**	**360**	**372**	**378**	**304**	**305**	**331**	**343**
Ol	2.3	2.0	18.2	0.3	0.8	–	1.0	82.0	48.6	83.4	40.2
Opx	–	–	4.2	–	–	6.0	1.9	9.5	–	–	–
Cpx	–	–	–	–	–	–	–	–	–	0.8	–
Srp	91.5	95.5	75.4	93.6	94.0	93.7	93.0	7.2	50.4	13.3	57.6
Opaques	6.2	2.5	2.2	6.1	5.2	0.3	5.1	1.2	1.0	2.5	2.2

Anal. No.	**12**	**13**	**14**	**15**	**16**	**17**	**18**	**19**	**20**	**21**	**22**
Sp. No.	**345**	**383**	**404**	**406**	**338**	**358**	**398**	**407**	**325**	**329**	**330**
Ol	54.8	60.9	72.3	67.7	56.2	54.4	72.0	69.2	24.0	–	15.9
Opx	4.0	4.1	2.5	3.5	2.2	2.9	1.3	2.5	–	1.5	5.3
Cpx	–	–	–	1.2	17.3	36.5	14.0	11.2	63.8	96.7	71.7
Srp	39.1	33.1	23.0	25.7	21.1	2.7	10.2	14.0	9.3	1.0	2.8
Hbl	–	–	–	–	–	1.5	–	–	–	–	–
Opaques	2.1	1.9	2.2	1.9	3.2	2.0	2.5	3.1	2.9	0.8	4.3

Anal. No.	**23**	**24**	**25**	**26**	**27**	**28**	**29**	**30**	**31**	**32**	**33**
Sp. No.	**332**	**333**	**335**	**336**	**342**	**354**	**356**	**357**	**362**	**382**	**387**
Ol	18.4	–	0.8	16.4	12.1	8.5	10.3	6.0	7.2	–	–
Opx	9.4	2.8	1.4	4.3	10.0	4.2	3.5	8.3	4.0	3.4	1.9
Cpx	71.0	93.9	97.1	71.3	74.1	86.0	83.0	84.2	86.5	95.2	97.5
Srp	–	1.9	–	3.9	2.7	0.7	0.9	–	–	–	0.5
Hbl	–	–	–	–	–	–	1.0	–	–	–	–
Opaques	1.2	1.4	0.7	4.1	1.1	0.6	1.3	1.3	2.3	1.4	0.1

Anal. No.	**34**	**35**	**36**	**37**	**38**	**39**	**40**	**41**	**42**	**43**	**44**
Sp. No.	**392**	**403**	**405**	**413**	**301**	**313**	**314**	**318**	**320**	**311**	**326**
Ol	5.3	14.5	11.2	–	–	–	–	–	–	4.1	5.0
Opx	1.9	2.0	1.3	–	8.1	15.0	34.0	14.7	–	5.1	8.5
Cpx	90.4	78.0	82.0	1.4	11.4	6.0	6.6	13.1	1.1	23.1	42.0
Srp	1.2	3.5	2.3	–	–	–	–	–	–	0.5	1.0
Hbl	–	–	–	5.1	13.2	5.4	2.0	0.7	37.0	7.0	–
Pl	–	–	–	91.8	62.2	66.0	52.8	69.4	61.0	60.0	42.0
Qtz	–	–	–	–	4.9	5.8	2.0	–	–	–	–
Opaques	1.2	2.0	3.2	1.7	0.2	1.8	2.6	2.1	0.9	0.2	1.5

Anal. No.	**45**	**46**	**47**	**48**	**49**	**50**	**51**	**52**	**53**	**54**	**55**
Sp. No.	**337**	**339**	**368**	**370**	**402**	**400**	**412**	**414**	**415**	**416**	**417**
Ol	2.0	–	–	–	–	–	–	–	–	–	–
Opx	9.0	21.9	7.0	9.3	2.0	1.9	21.1	28.4	–	–	–
Cpx	18.5	12.7	14.0	3.0	10.1	9.2	17.8	7.3	–	–	–
Srp	2.3	–	–	–	–	–	–	–	–	–	–
Hbl	3.8	13.3	13.1	29.2	48.1	51.2	1.8	8.1	51.8	53.0	24.3
Pl	63.4	48.0	57.0	52.3	34.0	36.4	52.0	50.8	42.1	41.0	43.1
Qtz	–	1.9	4.0	4.7	1.9	1.3	2.2	3.4	5.1	5.8	29.0
Opaques	1.0	2.2	4.9	1.5	3.9	–	5.1	2.0	1.0	0.2	3.6

Anal. No.	**56**	**57**	**58**	**59**	**60**	**61**	**62**	**63**	**64**	**65**	**66**
Sp. No.	**367**	**369**	**315**	**322**	**323**	**324**	**327**	**334**	**349**	**350**	**418**
Cpx	1.8	2.6	18.9	24.8	20.2	21.5	22.0	23.3	20.2	19.4	23.8
Srp	–	–	–	–	–	–	–	–	–	–	–
Hbl	8.3	13.0	4.1	2.7	1.0	0.4	6.1	5.1	2.3	5.6	1.0
Pl	52.5	55.1	65.2	60.3	64.2	65.4	64.9	61.0	65.9	67.8	63.1
Qtz	32.5	24.0	–	–	0.9	0.6	–	–	2.6	0.3	–
Chl	4.9	5.1	6.2	6.8	7.0	5.0	2.0	2.6	5.0	3.9	7.9
Opaques	–	2.0	5.6	5.4	6.7	7.1	5.0	8.0	4.0	3.0	4.2

Anal. No.	**67**	**68**	**69**	**70**	**71**	**72**	**73**	**74**	**75**	**76**	**77**
Sp. No.	**351**	**352**	**357**	**309**	**373**	**395**	**302**	**321**	**346**	**353**	**366**
Cpx	17.7	22.9	29.5	30.0	25.2	31.5	16.2	14.4	10.8	14.2	16.5
Hbl	1.3	2.1	1.6	3.2	2.2	1.4	1.9	2.1	2.4	1.1	3.4
Pl	65.7	62.7	60.0	59.1	61.5	55.3	69.4	76.1	67.0	73.1	68.0
Qtz	1.9	–	–	0.3	–	0.2	1.1	1.8	1.7	0.7	2.3
Chl	8.5	7.3	2.2	2.9	7.2	9.3	8.4	3.7	12.2	6.9	5.3
Opaques	4.9	5.0	5.9	4.5	3.9	1.3	3.0	2.9	5.9	4.0	4.5

Anal. No.	**78**	**79**	**80**	**81**	**82**	**83**	**84**	**85**	**86**	**87**	**88**
Sp. No.	**388**	**316**	**320**	**296**	**307**	**319**	**310**	**340**	**348**	**364**	**365**
Cpx	10.8	15.2	10.4	12.5	12.6	3.4	–	–	2.9	–	5.2
Hbl	6.4	3.3	8.6	4.2	35.8	43.1	48.8	49.1	50.0	49.5	44.0
Pl	62.3	61.8	65.8	64.7	50.2	51.1	49.0	47.2	45.9	48.9	50.3
Qtz	2.5	7.0	5.2	6.3	0.9	1.5	1.2	2.1	0.7	1.6	–
Chl	12.7	8.0	5.6	8.4	–	–	–	–	–	–	–
Opaques	5.3	4.7	4.4	3.9	0.5	0.9	1.0	1.6	0.5	–	0.5

Anal. No.	**89**	**90**	**91**	**92**
Sp. No.	**399**	**344**	**346**	**361**
Cpx	3.8	2.3	1.0	2.9
Hbl	45.6	59.0	49.0	52.1
Pl	49.7	38.0	50.0	45.0
Qtz	–	0.4	–	–
Opaques	0.9	0.3	–	–

The sheeted dyke complex occurs above the gabbro of upper cumulate zone. The dykes dip steeply towards southeast. Individual dykes have a few cms to a few metres width. They also show asymmetric chilled margins, sometimes aphanitic.

Satellitic subvertical dykes of dolerite occur scattered in the lower cumulate zone. Variations recorded include finer grain size, occurrence of quartz, brown hornblende or green hornblende as observed previously in the region (Bilgrami, 1964). Normal dolerities are 2 m to 12 m thick, and dip generally 60° – 80° towards northeast. Dolerite dykes generally occupy tension fractures trending 55°W.

Pillow lavas form small hillocks, have a greyish green colour, are highly fractured with fractures healed by calcite. Some pillow lobes show chilled rims with predominant glass.

An ophiolitic mélange is exposed south of the lower cumulate rocks (fig. 1) forming small hills with rugged toporgraphy. Varied lithologies make up this mélange including serpentinite, ultramafic rocks, metagabbro, metabasalt, white marble, diabase, radiolarian chert, pillow lavas, limestone and clastic sediments. The tectonic blocks vary considerably in size and shape. They may be angular blocks upto 15 m across or small slivers or angular fragments less than 1 m wide. The mélange overlies the Cretaceous Parh Group limestone and shale which were deposited on the margin of the Indo-Pakistani continental plate.

The rocks in the mapped area (fig. 1) show intense tectonic deformation. The cumulates form a nearly isoclinal fold overturned to the northwest with plunge towards northeast. Sheeted dykes occur in the core of a syncline. Two parallel thrust faults with NW dips, occur in the southern part. One of these emplaced the mélange over the Parh Group metasediments and the other emplaced the cumulate section over the mélange. Many small scale folds and reverse faults are seen in the sedimentary rocks and the mélange.

Quaternary terrace deposits are usually 7 to 10 m thick and lie along banks of major streams and lower climbs of hillocks. These contain boulder– to sand–size particles held by calcareous to argillaceous cement. Recent alluvium occurs widespread and conceals the southern border of ophiolitic mélange.

PETROGRAPHY

Ultramafic Rocks

The ultramafic cumulate rocks of the area comprise serpentinite, dunite, wehrlite, clinopyroxenite and anorthosite. The serpentinites have light to dark green colour, fine grain-size, mesh-texture, over 90 percent serpentine minerals and some opaque oxide. Antigorite and fibrous chrysotile are both present. Small amounts of relict grains of olivine and pyroxene are present. Fractures in olivine may be abundant and may contain iron oxide. Anhedral accessory chromite is ubiquitous.

Dunite has olive green to black colour that weathers to yellowish brown. Olivine is abundant, subhedral or anhedral and bears irregular fractures filled with serpentine or magnetite. Serpentine is much less and shows mesh texture. Some thin sections contain a few grains of enstatite or dipside. Accessories include chromite and magnetite.

Wehrlite possesses olivine, 48 to 55%; diopside, 15 to 40%; and accessory amounts of orthopyroxene, chromite, magnetite and serpentine. Sometimes hornblende is produced by alteration of diopside. The rock shows cataclastic features as well.

Clinopyroxenite contains abundant diopside, 80 to 95%, with accessory amounts of orthopyroxene, 2 to 5%, olivine and opaque minerals. Very rarely, by townite plagioclase forms upto 2% of rock.

Anorthosites contain predominant plagioclase and less than 10% ferromagnesian minerals including orthopyroxene, clinopyroxene, hornblende and chlorite. Optically determined composition of plagioclass is An_{75} to An_{80}. Albite twins are common, and grains are moderately altered.

Mafic Rocks

The gabbroic cumulate rocks include olivine gabbro, gabbro, noritic gabbro, norite and hornblende-rich gabbro. In many, the dark minerals form synneusis texture producing dark bands. The minerals of these rocks include plagioclase, 45 to 70%; clinopyroxene, 15 to 30%; orthopyroxene, 10 to 20%; magnetite and ilmenite. Secondary minerals include hornblende, tremolite, chlorite and sericite. Olivine gabbros contain upto 8% olivine, and their plagioclase is more calcic (An_{70-72}). Quartz gabbros contain upto 5% quartz. Hornblende-rich gabbros contain upto 48% hornblende. Plagioclase is mostly labradorite with An_{62-65}, and is moderately sericitized. Pyroxene is usually clinopyroxene which is varyingly uralitized. Hypersthene is faintly coloured and pleochroic from pale green to pale reddish brown. It is often anhedral and rounded, and is outwardly altered to hornblende. Pyroxene and olivine may form tiny crystals enclosed in plagioclase.

Leucocratic Rocks

These include diorite and plagiogranite. Diorites are generally hypidiomorphic granular, but some hornblende is poikilitic enclosing smaller subhedral grains of plagioclase. Diorites are composed of green hornblende, 50-53%; plagioclase, 40-43%; quartz, upto 50% and accessory iron oxide. Hornblende may alter to chlorite along grain margins and its fractures may be filled by magnetite. Plagioclase is oligoclase to andesine, sometimes zoned, strongly altered and usually interstitial to hornblende.

Plagiogranite is mainly composed of plagioclase, 43-54%; hornblende, 8-24%; and quartz 24-32%. Accessories include chlorite and iron oxides. Plagioclase is sodic, mainly albite (An_{16-18}) rarely oligoclase (An_{22}) and some is zoned with more calcic cores. Sericitization is more advanced

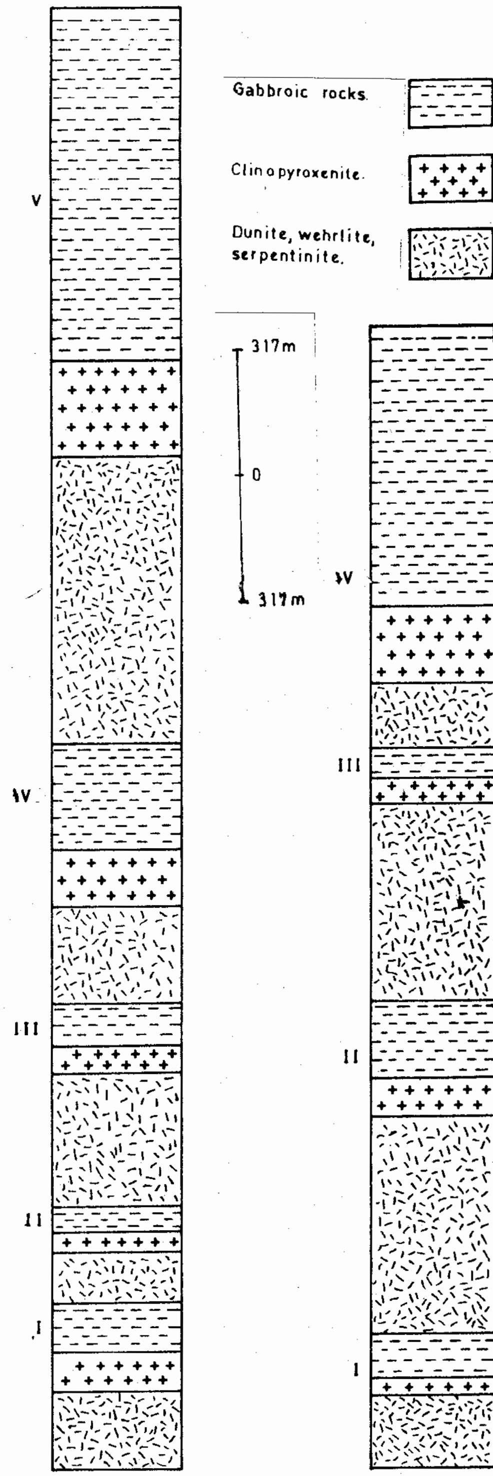

Fig. 2. Cumulate rock sequence from Bagh area showing repititions of cycles and differences in thickness. Gabbros of different levels have following varieties: I = olivine-bearing gabbro; II = gabbroic norite; III = norite; IV = hornblende-bearing hypersthene gabbro, V = hornblende gabbro.

in cores of grains. Green hornblende is usually interstitial to plagioclase. Quartz anhedra occupy interstices between plagioclase and hornblende. They may form veins. Opaque iron oxides form anhedra and skeletal crystals. In addition to magnetite, hematite may be present.

Dolerite Dykes

Dolerites are grey and mottled white and grey in colour and weathered surfaces are brownish black. Typical ophitic texture is frequent. Their minerals include plagioclase, 55 to 75%; pyroxene, 15 to 30%; opaque iron oxide, 2-8%; accessory quartz; and secondary products like hornblende, 4-6%; chlorite, 1-2%, and sericite. Plagioclase is strongly altered and when fresh, it is estimated to be andesine or labradorite with An_{45-55}. Its laths show random orientation. Pyroxene is mainly augite, highly fractured and strained, and alters to hornblende and chlorite. Anhedral quartz is present in interstices between plagioclase laths, and shows wavy extinction and may form micropegmatite. Opaque iron oxide includes ilmenite, magnetite and picotite.

Fine grained dolerites are greyish coloured rocks, sometimes porphyritic with euhedral phenocrysts of plagioclase and pyroxene and aphanitic groundmass. Some are subophitic. Finer material includes plagioclase, pyroxene, green hornblende, chlorite and opaque oxide. Plagioclase is usually lath-shaped and sericitized, and is andesine to labradorite. Groundmass plagioclase is microcrystalline and much altered. Pyroxene is diopside, often euhedral, colourless, zoned and may enclose plagioclase laths completely or partially. Opaque iron oxides include magnetite and ilmenite. The dolerites often display chilled margins and high degree of saussuritization.

Quartz dolerites contain significant anhedral quartz and micropegmatite forming upto 8% in addition to the normal dolerite minerals such as plagioclase, 60-70%, and pyroxene, 15 to 20%. Pyroxene is augite and may be zoned. It alters to chlorite. Skeletal ilmenite is frequent accessory and alters to dense brown isotropic material.

Hornblende–rich dolerites may contain abundant green or brown hornblende. The former type contains about 40 to 45% green hornblende in addition to the plagioclase, 45-55%; pyroxene, 2 to 6%, and opaque iron oxides, upto 2%. Plagioclase laths are highly altered. Pyroxene is mainly augite which is partly altered to hornblende and chlorite. The dolerites with brown hornblende contain 50 to 60% hornblende, 40-50% altered plagioclase and accessory quartz, augite and iron oxide. The plagioclase phenocrysts sometimes resemble augen. Secondary chlorite occurs in large amounts.

Lavas

The volcanic rocks are mainly spilitic and fine grained. Intersertal texture is common with abundant plagioclase laths and augite, minor chlorite and accessory epidote, ilmenite and secondary actinolite. The rocks may contain amygdules filled with calcite and chlorite. They may also be traversed by irregular fractures filled with calcite and/or zeolites.

PETROGENETIC FEATURES

In Bagh area, the lower cumulate part contains more ultramafic rocks than the mafic ones which dominate in the upper cumulate part. The petrographic rock-types in the lower cumulate section are repeated vertically displaying mafic to femic cyclic patterns. Each cycle differs in its thickness of lithologic layers and in their sequential arrangement which may be due to different timing of crystallization of cumulus minerals. Such repetitions of cumulates are quite commonly observed in ophiolites. In Bagh area, at least five cycles are represented. Each cycle has basal dunite whose lower contact is sharp, but upper contact grades into wehrlite which itself grades upwards into clinopyroxenite which, in turn, shows gradation into gabbro, and sometimes locally on a minor scale, into anorthosite. Thus each cycle has a plagioclase-rich cumulate top-layer. Even within the gabbro, a cm to a few metres thick layers are made by the olivine-bearing pyroxene-rich and olivine-lacking plagioclase-rich cumulates. Generally, the thickness of gabbros in individual cycles increases upwards as shown in fig. 2. Thickness of individual cycles varies from 200 to 1000 m. Normally, a complete cycle comprises dunite-wehrlite-clinopyroxenite-gabbro sequence, but some cycles are incomplete and lack gabbro. Gabbros from different cycles may differ in mineralogy as well (fig. 2). The Bagh area cumulate apparently lack websterites. The dolerite dykes represent postcumulus liquid phase but occur in the lower cumulate section only.

CONCLUSIONS

The Bagh area contains a cumulate section of the Muslimbagh-south ophiolite. The petrographic types comprise cycles of dunite-wehrlite-clinopyroxenite-gabbro type formed by multiple intrusions of fresh magma, sometimes even before the crystallization of previous batch of magma is finished. Adcumulate texture is common in ultramafic rocks and indicates their very slow accumulation.

REFERENCES

AHMAD, Z. & ABBAS, S.G. (1979) The Muslim Bagh ophiolites. *In:* Farah, A. & De Jong, K.A. (eds.) GEODYNAMICS OF PAKISTAN. Geol. Surv. Pakistan, Quetta. pp. 243-9.

AHMAD, Z. (1974) Geology and petrochemistry of a part of the Zhob Valley igneous complex (Baluchistan) Pakistan Rec. Geol. Surv. Pakistan. 24, 22p.

AHMED, Z. (1986) Ophiolites and chromite deposits of Pakistan *In:* Petraschek, W.E. et al. (eds.) CHROMITES. Theophrastus Publications, Athens, Greece, pp. 241-62.

———— & CHAUDHRY, M.N. (1969) Geology of Palak Lara Area, Saplaitorgarh, Zhob District, Pakistan. Geol. Bull. Punjab Univ. 8, pp. 61-73.

BILGRAMI, S.A. (1964) Mineralogy and petrology of the Hindubagh igneous Complex, Zhob Valley, Pakistan. Rec. Geol. Surv. Pakistan 10 (2-c), 28p.

HUNTING SURVEY CORPORATION LTD. (1960) RECONNAISSANCE GEOLOGY OF PART OF WEST PAKISTAN. Colombo Plan Cooperative Project Report, Toronto, Canada. 550 p.

KRETZ, R. (1983) Symbols for rock-forming minerals. Amer. Mineral. 68 (1-2), pp. 277-9.

MOORES, E.M., ROEDER, D.H., ABBAS, S.G. & AHMAD, Z. (1980) Geology and emplacement of the Muslim Bagh ophiolite complex. *In:* Panayiotou, A. (ed) OPHIOLITES. Proc. Int. Ophiolite Symp. Cyprus 1979, Geol. Surv. Deptt. Cyprus, pp. 424-9.

ROSSMAN, D.L., AHMAD, Z. & ABBAS, S.G. (1971) Geology and chromite deposits of the Saplaitorgarh Nasai area, Zhob Valley complex, Hindubagh, Quetta Division, West Pakistan. Geol. Surv. Pakistan & U.S. Geol. Surv. Interim Report PK-51, 47p.

VAN VLOTEN, R. (1967) Geology and chromite deposits of chromite in the Nasai area, Hindubagh Mining District, West Pakistan. Geol. Surv. Pakistan pre-publication issue 2, 31p.

Manuscript received 9.10.1986
Accepted for publication 9.10.1986

ACTA MINERALOGICA PAKISTANICA
VOLUME 2 (1986) pp. 74-77

XENOTHERMAL ALTERATION AND TUNGSTEN MINERALIZATION IN SAINDAK AREA, BALUCHISTAN, PAKISTAN.

REHANUL HAQ SIDDIQUI, ZAFARULLAH KHAN & SYED ANWAR HUSSAIN

Geological Survey of Pakistan, Sariab Road, Quetta, Pakistan.

ABSTRACT:— Tungsten mineralization at a new prospect, located towards NE of Amalaf, is mainly associated with a pyroclastic sequence including tuffaceous siltstone, tuff and agglomerate of Eocene age; and with a small quartz porphyry intrusion and a tourmaline breccia pipe. Xenothermal alteration is followed outwardly by argillic and propylitic alterations. Tungsten mineralization is mainly represented by scheelite which occurs as disseminations in xenothermal and argillic alteration zones.

INTRODUCTION

Hypogene tungsten mineralization has recently been discovered in the Chagai District of Baluchistan province (Siddiqui et al., 1986). The prospect occurs about 9 km to the north-east of R.D.C. Colony at Amalaf (fig. 1). Approximate co-ordinates of the prospect are 29° 18′ N and 61° 37′ E which fall in Survey of Pakistan topographic sheet No. 30 G/11. The Present paper deals with a brief description of geology, xenothermal alteration and mineralization in the area.

GEOLOGY OF THE PROSPECT

The present tungsten mineralization occurs in western extremity of Chagai calc-alkaline magmatic belt which is about 500 km long and about 140 km wide and believed to have formed by northward subduction of an oceanic lithosphere under the southern margin of Afghan micro-continent. Therefore it may be considered as an Andean type magmatic arc (Sillitoe, 1972).

Hydrothermal alterations in the area are mainly associated with a stratified pyroclastic sequence belonging to Saindak formation of Eocene age (Hunting Survey Corporation, 1960) which is mainly composed of tuffaceous siltstone, tuff and agglomerate; and with a tourmaline intrusive breccia pipe and a small dyke-like intrusion of quartz porphyry. Both are elongated in NNW direction and are intruded into the tuffaceous pyroclastic sequence (fig. 2).

In southern half portion of the mapped area tuffaceous pyroclastic rocks and a quartz porphyry intrusion have undergone xenothermal alteration which is represented by tourmalinization, silicification and argillization, with minor propylitization and gypsification which is followed outwardly by argillic and propylitic alterations.

The above pyroclastic sequence and quartz porphyry intrusion are transected by a swarm of NW and NS trending post-alteration dykes, mainly dioritic and andesitic in composition and porphyritic in texture. The above rock suites are also traversed by numerous viens of tourmaline, hematite, chlorite, epidote and gypsum.

XENOTHERMAL ALTERATION

Co-existence of tourmalinization, silicification and argillization with abundance of vesicles suggest a high-temprature, low-pressure environment. Although tourmalinization in the area

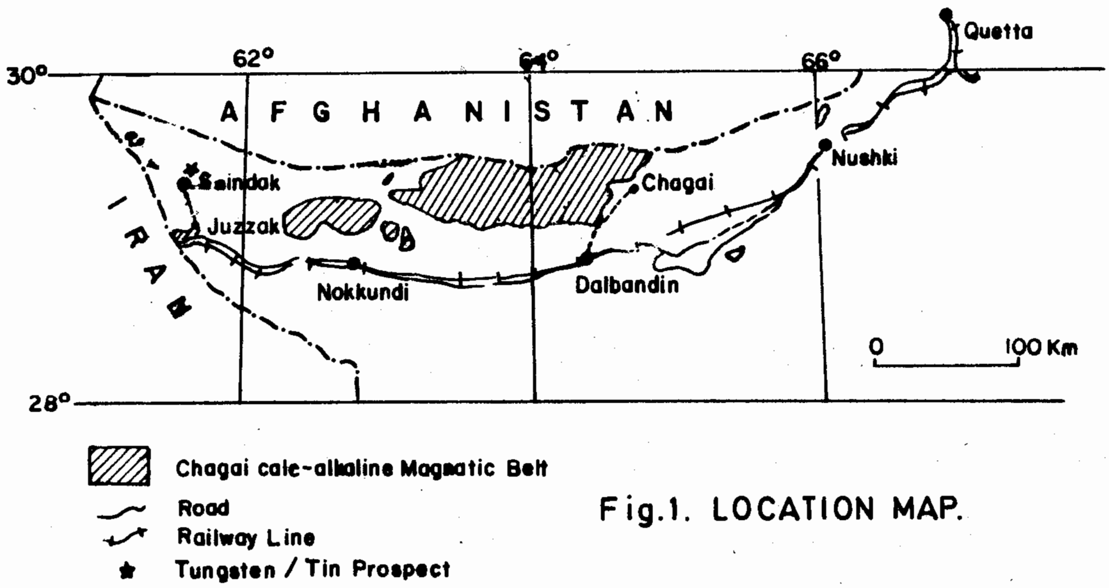

Fig.1. LOCATION MAP.

was previously indicated by many authors (Ahmed et al, 1972; Sillitoe & Khan, 1977), but during persent study it is for the first time recognized as an indication of xenothermal alteration and tungsten mineralization.

Tourmalinization in the area is mainly represented by schorlite variety which is accompanied with fine silicification. It generally occurs in veins and veinlets and also in vugs, cavities and stringers. It has also been developed as replacement of groundmass in the tuff and quartz porphyry intrusion. As replacement it occurs as small prismatic and radial aggregates. At least two generations of tourmaline have been observed: bluish green and yellowish brown under the microscope. Paragenetic study of tourmaline shows that yellowish brown variety is earlier. Tourmalinization in the area is subdivided into low and intense tourmalinized zones during mapping. Argillization is also associated with the xenothermal alteration and appears to be represented by kaolinite.

MINERALIZATION

Surface mineralization in the area is represented by jarositic and goethitic limonite after pyrite, pyrrhotite, chalcopyrite and hematite. Mineralization is also developed as tungstite, scheelite, molybdite and minor cassiterite.

Jarositic and goethitic limonite occurs as staining, on fracture planes and as replacement of gangue minerals. Tungstite occurs as yellow ochrous and resinous masses. Molybdite occurs as yellow molybdic ochre. Pyrite and hematite occur as desseminations and veinlets. Micaceous hematite is also observed occurring as fine flaky aggregates.s Cassiterite is observed only under ore microscope as fine subhedral twinned grains in the intensely tourmalinized zone. Scheelite generally occurs in xenothermal and argillic alteration zone as disseminations ranging in grain size from 1 mm to about 1 cm. Higher concentration of scheelite is generally observed in the intensely tourmalinized zone (fig. 2).

DISCUSSION

Coexistence of two generations of tourmaline and porphyritic texture in the quartz porphyry intrusion suggests that it has gone through two different environments during its course of emplacement. In deeper environments with high T-P conditions, larger crystals of quartz and alkali feldspar were formed and when the partially crystallized magma further rose up and reached to a shallower environment with low T-P conditions, a fine grained groundmass and abundant vesicles developed.

Presence of tourmaline breccia, shows that at the end of magmatic stage when the partially

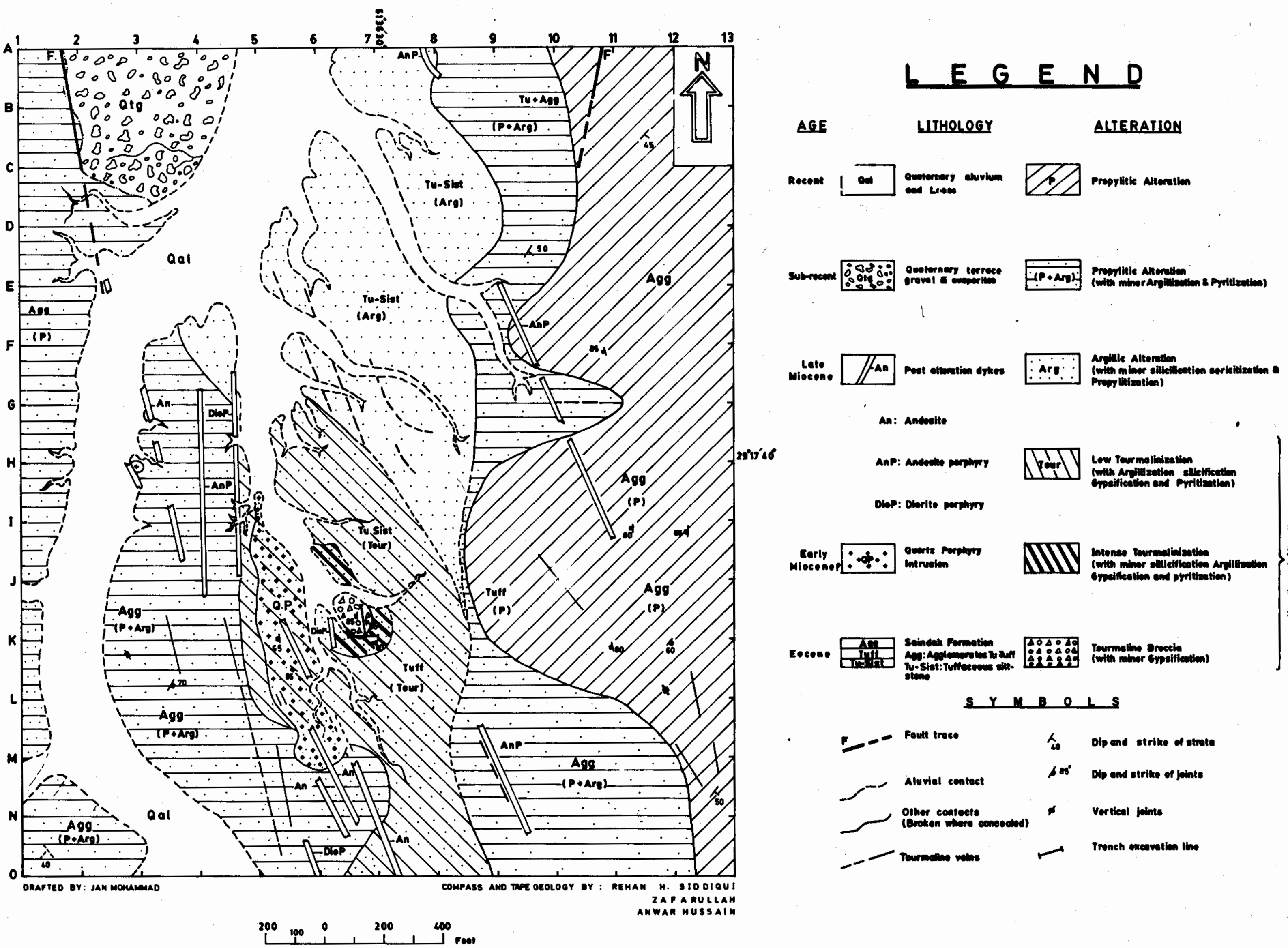

Fig. 2. GEOLOGIC AND ALTERATION MAP OF TUNGSTEN AND TIN PROSPECT OF SAINDAK AREA

crystallized magma reached a shallower environment, due to decrease in confining pressure over the magma a volatile phase, rich in boron fluorides and silica, separated. A further increase in vapour pressure produced hydraulic fracturing and shattering of outer solid shell and the shattered material intruded through weak zones as intrusion breccia (Phillips, 1973). Contemporaneously volatiles were also released from the magma, which were responsible for xenothermal alteration and mineralization in the area.

The authors contradict the idea that the tourmalinization in the area is related to the pneumatolitic stage of tonalite porphyry intrusion of Saindak area. Rather, a near surface acidic intrusion, differentiates of which are exposed as quartz porphyry intrusion, might be responsible for this tourmalinization.

CONCLUSION

Field and laboratory studies made so far indicate a possibility of tungsten potential in the area. The present xenothermal alteration extends several km to the south, and occurs as several isolated patches to the north of the mapped area (Siddiqui et al., 1986), so the prospects for widespread mineralization are encouraging. Therefore, further detailed exploratory and evaluation work is required for the area, provided the chemical assay also confirms anomalous zone.

ACKNOWLEDGEMENT

The authors gratefully acknowledge to Mr. Waheeduddin Ahmed, Director General, Geological Survey of Pakistan for providing field and laboratory facilities. Mr. Shahid Noor Khan, Director of the same department is greatly acknowledged for his able guidance and valuable suggestions. Thanks are also due to Chief Executive, officers and staff of Resource Development Corporation for providing logistics during field work.

REFERENCES

AHMAD, W., KHAN, S.N. & SCHMIDT, R.G. (1972) Geology and Copper mineralization of the Saindak Quadrangle, Chagai District, West Pakistan. Prof. Pap. U.S. Geol. Surv. 716, 21p.

HUNTING SURVEY CORPORATION LTD. (1961) Reconnaissance geology of part of West Pakistan. Colombo Plan Cooperative Project Report, Toronto, Canada, 550p.

PHILLIPS, J.W. (1973) Mechanical effects of retrograded boiling and its probable importance in the formation os some porphyry ore desposits. Trans. Inst. Min. & Metall. Sec. B, pp. B90-B97.

SIDDIQUI, R.H. HUSSAIN, S.A. & KHAN, Z. (1986) Discovery of tungsten/Tin mineralization in Saindak area, Baluchistan. Submitted for publication to Geol. Surv. Pakistan.

SILLITOE, R.H. (1972) A plate tectonic model for the origin of porphyry copper deposits. Econ. Geol. 67, pp. 184-97.

__________ & KHAN, S.N. (1977) Geology of Saindak porphyry copper deposit, Pakistan, Trans. Inst. Min. Metall. Sec. B, pp. B90-B97.

Manuscript received 30-9-1986.
Accepted for publication 30.11.1986.

ACTA MINERALOGICA PAKISTANICA
VOLUME 2 (1986) pp. 78-82

CATHODOLUMINESCENCE STUDY OF VARIOUS ALTERATION STAGES IN PHOSPHATE ROCK SAMPLES FROM CONDA MINE, IDAHO, U.S.A.

NASIR ALI BHATTI[1], KEITH PRISBREY[2] & GEORGE A. WILLIAMS[3]

1. Geological Survey of Pakistan, 14, Canal Park, Gulberg II, Lahore, Pakistan.
2. Department of Metallurgy, University of Idaho, Moscow, ID 83843, USA.
3. Department of Geology, University of Idaho, Moscow, Idaho 83843.

ABSTRACT:– Thin sections of the samples of phosphate rock from Simplot E-2 pit of Conda Mine, southeastern Idaho, USA, representing a range of alteration sequence are petrographically examined in the plain light and under the cathodoluminescene. The study shows that luminescene does not help in tracing the alteration sequence.

The MgO content of the samples corresponds with the phosphate alteration but a distinct phase of discrete dolomite crystals is not seen. Obliteration of the dolomite phase is probably due to the changes subsequent to dolomitization process.

INTRODUCTION

Potentially large resources of the phosphate rock in Idaho, USA, are in the form of unaltered rock which has not undergone the weathering process. The unaltered rock is high in carbonate content and is not amenable to beneficiation. It is, therefore, uneconomical to utilize these resources.

Behaviour of the carbonate gangue minerals in the unaltered ore is similar to the phosphate constituents. In addition, the phosphate pellets are naturally locked in by the carbonate in a manner that their total physical liberation is almost impossible even by fine grinding. Hence, a lack of the economical beneficiation method for upgrading the unaltered phosphate rock is the foremost problem of the Idaho phosphate industry.

As the mining progresses deeper, the naturally altered or weathered phosphate reserves approach depletion, and the problem to utilize unaltered phosphate rock becomes more serious. More recently it has been reported by the geologists of J.R. Simplot Company that resources of altered phosphate ore at the Conda Mine shall be depleted in the next few years (Idahonian, September 22, 1981). This would result in the closure of one of the largest phosphate mining operations in southeastern Idaho.

Some of the companies have adopted means of inducing artificial weathering by creating cracks and fissures and then leaving the fractured phosphate rock exposed for several years. At present, large quantities of the unaltered phosphate ore are either being left in place or are stock-piled.

In view of the above, an understanding of the alteration process and its corresponding relationship with the amenability to beneficiation is ncessary because of its economic importance.

Alteration brings about chemical and mineralogical changes in the composition of the phosphate ore. These changes in composition are directly related to the carbonate/dolomite content. A petrographic study under cathodoluminescence has the advantage of detecting and identifying the sequential stages of rock alteration which are otherwise not discernible (Smith and Stenstorm, 1965, p. 627). Therefore, phosphate rock samples representing a range of totally unaltered to completely altered phosphate ore with a maximum and minimum carbonate content are examined under cathodoluminescence. This report gives the results of the study to determine if cathodoluminescence can be useful in tracing the phosphate alteration sequence. Our experimental procedure is to compare cathodoluminescene analyses of two extremes of the phosphate alteration which is indeed present in the samples included.

CATHODOLUMINESCENE

The process of cathodoluminescence refers to the emission of light during electron bombardment. Energy levels of the light thus emitted are characteristic of the individual material and correspond with textural and chemical compositional changes. These changes reflect variation in the trace elements which act as activators and in turn cause differentiation in the energy level of the luminescence. Therefore, textural and compositional changes within a material itself which are not otherwise discernible, become distinguishable under cathodoluminescence. In the classic study on the usefulness of cathodoluminescence in the geological materials, Smith and Stenstorm (1965) have shown that, particularly in carbonates and phosphates, the distinguishing features of the compositional and textural variation are well-exhibited. Especially visible is the zoning of the dolomite rhombs in the calcitic rock that has undergone dolomitization. Variation in the intensity of the luminescence indicates compositional changes. Different concentrations of magnesium produce different colours and intensities in the phosphate rock.

PROCEDURE

Phosphate ore samples for the study were provided by Bureau of Mines, Albany Research Centre, Oregon, USA. These samples were collected from Simplot EW-2 pit of the Conda Mine north of Soda Springs, southeastern Idaho. The phosphate ore samples are described in table 1.. The samples are mostly greyish black (N2), medium hard to soft, non-calcareous, slightly friable, and highly carbonaceous siltstones. Some are indistinctly granular, some are clayey and vary from dark grey (N3) to black (N1) in clour. In physical appearance they are more or less alike. Dominance of the carbonaceous material and the soft nature of the phosphate ore samples made preparation of the thin sections difficult.

All the thin sections of the phosphate ore samples described in table 1 were petrographically examined in the plain light and under the cathodoluminescene.

Table 1. Lithological description of the phosphate ore samples.

Serial No.	U.S.B.M. Code Number	Description
1	1323	Silty mudstone to clayey siltstone, indistinctly granular, dark grey (N3) to greyish black (N2), friable, non-calcareous weathered surface brownish grey (5 YR 4).
2	1324	Same as above.
3	1325	Clayey siltstone, moderately hard, black (N1), and non-calcareous.
4	1326	Clayey siltstone, black (N1), and non-calcareous.
5	1327	Clayey siltstone, greyish black (N2), non-calcareous.
6	1328	Muddy siltstone, indistinctly granular, friable, greyish black (N2), whitish encrustation on weathered surface.
7	1329	Clayey siltstone, indistinctly granular desk grey (N3).
8	1330	Siltstone, dark grey (N3) to black (N1), whitish encrustation on weathered surface.

Table 2. Reference, thickness, and analysis of the phosphate ore samples.

Sample Number	Simplot Number	U.S.B.M. Number	Unit Referred as	Thickness of the Unit	MgO %	P_2O_5 %
1	39833	ME 1323	Footwall Main Bed	82"	0.13	32.0
2	39834	ME 1324	Cap Rock Foot wall	18"	12.9	17.4
3	39835	ME 1325	Lowermost Shale Footwall	36"	1.25	23.6
4	39836	ME 1326	Limestone Footwall	6"	10.8	11.3
5	39837	ME 1327	Second Lower Seam Shale	18"	2.39	20.9
6	39838	ME 1328	Second Limestone Seam	6"	13.3	7.2
7	39839	ME 1329	Upper Shale Footwall	56"	0.20	27.8
8	39840	ME 1330	False Cap Rock	30"	14.4	11.2

Comparative visual examination of the completely altered, partly altered and mostly unaltered phosphate ore samples separately in the plain light, and then under cathodoluminescence, does not provide any additional diagnostic feature which may be of help in tracing the alteration sequence, other than seen in the plain light. A distinctly differentiable dolomite phase corresponding with the alteration sequence is not seen in the samples. In order to determine that indeed we have unaltered, partially altered, and altered phosphate ore, analysis of the samples with respect to their content of P_2O_5 and MgO along with their pertinent references is given in table 2.

Respective values of MgO and P_2O_5 in the study samples are plotted in figure 1. From this figure it is apparent that P_2O_5 values are inversely proportional to MgO values. With the decrease in MgO there is a corresponding increase in P_2O_5 and vice versa.

It is determined by Campbell (1962) that most of the carbonate in the phosphate rock of the Phosphoria Formation is dolomitized limestone. Therefore, MgO in the phosphate ore samples represents almost the total sum of the carbonate content in the samples which in turn is inversely proportional to the degree of phosphate alteration. The higher the carbonate content, the lesser is the degree of phosphate alteration. Therefore, variation in MgO can rightly be regarded as a measure of the phosphate alteration sequence. Sample serial number 1 (table 2), which contains a minimum MgO of 0.13%, is the most altered phosphate ore, and it contains 32% P_2O_5. Sample serial number 8, containing a maximum of 14.4% Mgo, is the least altered ore which contains only 11.2% P_2O_5 (table 2). The rest of the samples with MgO values represent an alteration sequence within the two end members–sample numbers 1 and 8.

Therefore, in the absence of any other physical criteria, the compositional values of

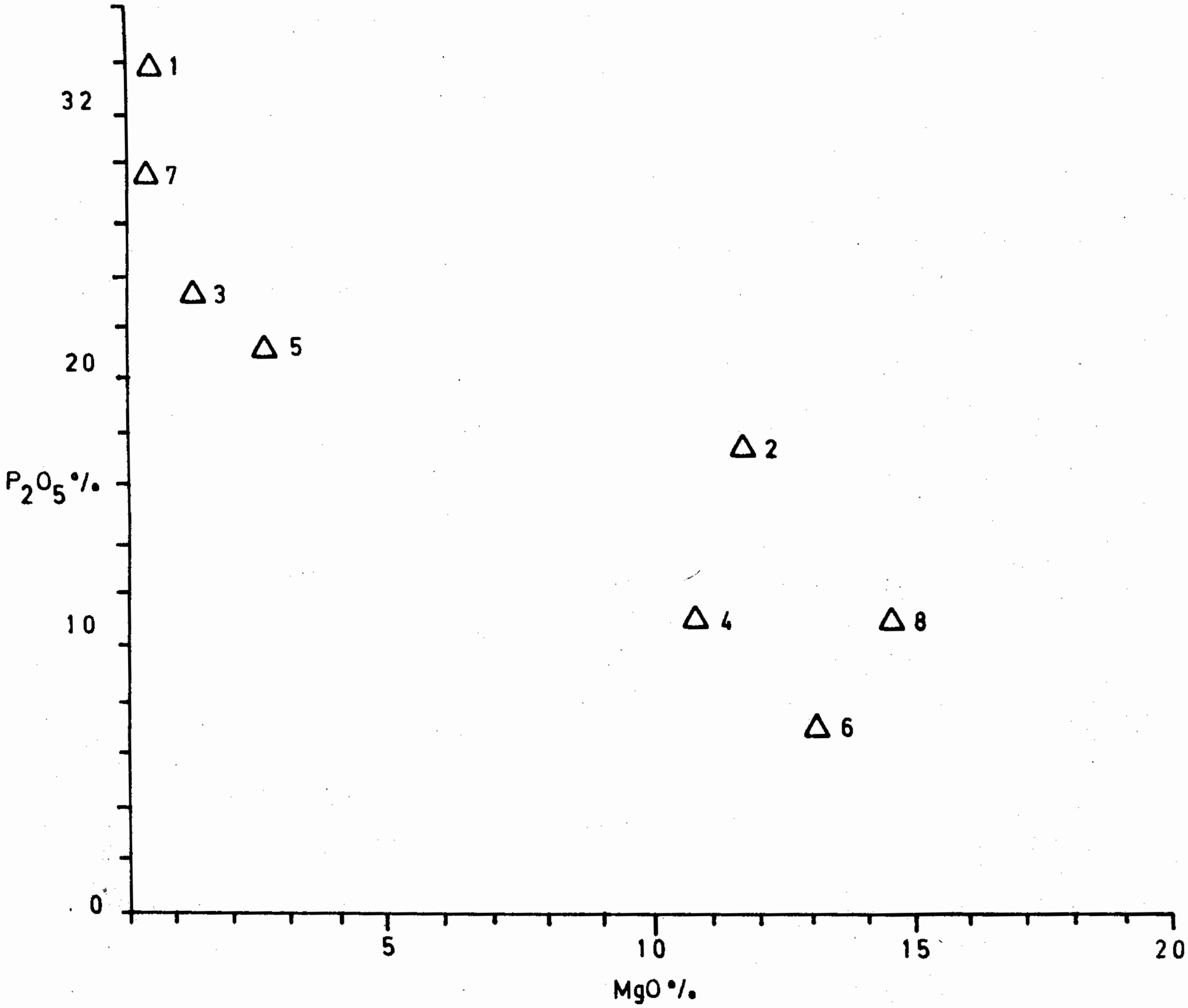

Fig.1. A corresponding inverse relationship between P_2O_5 and MgO. Numbers on triangles refer to serial numbers of the phosphate ore samples as given in table 1.

MgO in the samples provide a measure of phosphate alteration sequence. In addition, the MgO values directly correspond with the intensity of the dolomitization process that the carbonate has undergone. Hence, it is concluded from the above discussion that phosphate alteration, particularly with respect to study samples, is directly comparable with the dolomitization process. Admittedly, the phosphate alteration and dolomitization are altogether two different processes well apart in time and space, but the analytical values obtained for MgO and P_2O_5 in the phosphate ore samples, explicitly show that there is a corresponding relationship between the net results of the two processes.

CONCLUSION

Phosphate alteration is directly dependent on the phosphate-carbonate relationship. This relationship can be traced to an original carbonate environment (Gulbrandsen, 1960, 1965), dolomitization (Campbell, 1962), diagenesis

(Berner, 1980), and the recent weathering effects (McKelvey and Carswell, 1955).

An absence of the dolomite phase in the study samples is attributable to the changes subsequent to the dolomitization process.

As seen from the limited number of samples, cathodoluminescence does not appear to be a viable tool in tracing the alteration sequence in the Idaho phosphate rock.

ACKNOWLEDGEMENTS

Phosphate rock samples for this investigation were provided by U.S. Bureau of Mines, Albany Research Center, Oregon. A.R. Rule of the Research Centre was extremely helpful in making the samples available. Jeff G. Spence, a friend and colleague of the Principal Investigator, assisted in preparing thin sections of the phosphate rock samples. The investigation was funded by a grant from the Idaho Mining and Minerals Resources Research Institute.

REFERENCES

BERNER, R.A. (1980) EARLY DIAGENESIS, Princeton University Press, Princeton, New Jersey.

CAMPBELL, C.V. (1962) Depositional Environment of Phosphoria Formation (Permian) in South Eastern Big Horn Basin, Wyoming, Am. Assoc. Pet. Geo. Bull. 46 (4), pp. 478-502.

GULBRANDSEN, R.A. (1960) Petrology of the Mead Peak Phosphatic Shale Member of the Phosphoria Formation. U.S. Geol. Surv. Bull. 1111-C,D, pp. 98-105.

———— (1965) Chemical Composition of Phosphorite of the Phosphoria Formation. Geochim. Cosmochim. Acta. 30, pp. 769-78.

IDAHONIAN, September 22, (1981) News-Review Publishing Co., Inc., Moscow, Idaho, V. 88, No. 22, p. 8.

McKELVEY, V.E & CARSWELL, L.D. (1955) Uranium in Phosphoria Formation. Proc. Internat. Conf. Peaceful Uses of Atomic Energy, 6, p. 503.

SMITH, J.C. & STENSTORM, R.C. (1965) Electron excited luminescence as a Petrographic Tool. Jour. Geology, 73, pp. 627-35.

Manuscript received 1.12.1986
Accepted for publication 31.12. 1986

ACTA MINERALOGICA PAKISTANICA
VOLUME 2 (1986) pp. 83-92 .

HEAVY MINERAL ANALYSES AND PETROGRAPHY OF CHINJI AND NAGRI FORMATIONS OF SALT RANGE POTWAR AREAS, PUNJAB, PAKISTAN.

GHULAM SARWAR ALAM[1], ALLAH BAKHSH KAUSAR[2] & SHAHID JAWED[1]

1. Geological Survey of Pakistan, 14, Canal Park, Gulberg II, Lahore, Pakistan.
2. Geological Survey of Pakistan, Quetta, Pakistan.

ABSTRACT:– The paper describes the lithology and mineral content of Chinji and Nagri Formations of late Tertiary age, from sections located in the Salt Range and Potwar. Minerals in the heavier than bromoform fractions of sandstone include amphibole, chlorite, tourmaline, garnet, epidote, magnetite and pyrite. The sandstone samples are also chemically analyzed for major and certain trace element contents.

INTRODUCTION

The mountainous area lying north of Jhelum River is known as Salt Range, which extends approximately east-west over 250 km. It is a continuous range of flat topped mountains rising abruptly out of the Punjab plain. The Potwar Plateau is an elevated area bounded on the north by the Kalachitta hills, on the south by the Salt Range, and on the east and west by the Jhelum and Indus Rivers, respectively.

The Salt Range – Potwar Plateau area is underlain by rocks ranging in age from Cambrian to Recent. The record of sediments and geological events is very well preserved and exposed in the area except a major break from Ordovician to Carboniferous. The area has been mapped and studied in considerable detail by many renowned workers like Anderson (1927), Cotter (1933), Fatmi (1973), Gee (1947, 1982), Gill (1952) and Wynne (1878).

The late Tertiary rocks comprising the Rawalpindi and Siwalik Groups were not examined in as much detail as the older rocks. Now some detailed work on different aspects of late Tertiary rocks has been done by workers like Baig (1984), Khan (1984), and Pilbeam et al. (1977).

The Chinji and Nagri Formations have been studied in detail to know the mineralogical composition and heavy mineral distribution in the Salt Range-Potwar area. The formations are exposed throughout the area and have been investigated in the localities shown in fig. 1.

LITHOLOGICAL DESCRIPTION

The lithological description of the formations is based on the study and measurement of different sections in the areas shown in fig. 1. The details of each formation are as follows.

Chinji Formation

Chinji formation is present throughout the Potwar area and parts of the Salt Range. The formation is mainly composed of claystone, mudstone and siltstone of distinctive brick red colour with subordinate grey sandstone. The percentage of sandstone is higher in Khertop and Daudkhel area where it makes up to 30% of the total thickness whereas in Pail, Souj and Dharial areas the percentage ranges from 6.8% to 9.2%. The detailed average lithological composition and thickness in different localities is given in table 1.

The sandstone is fine to medium grained and

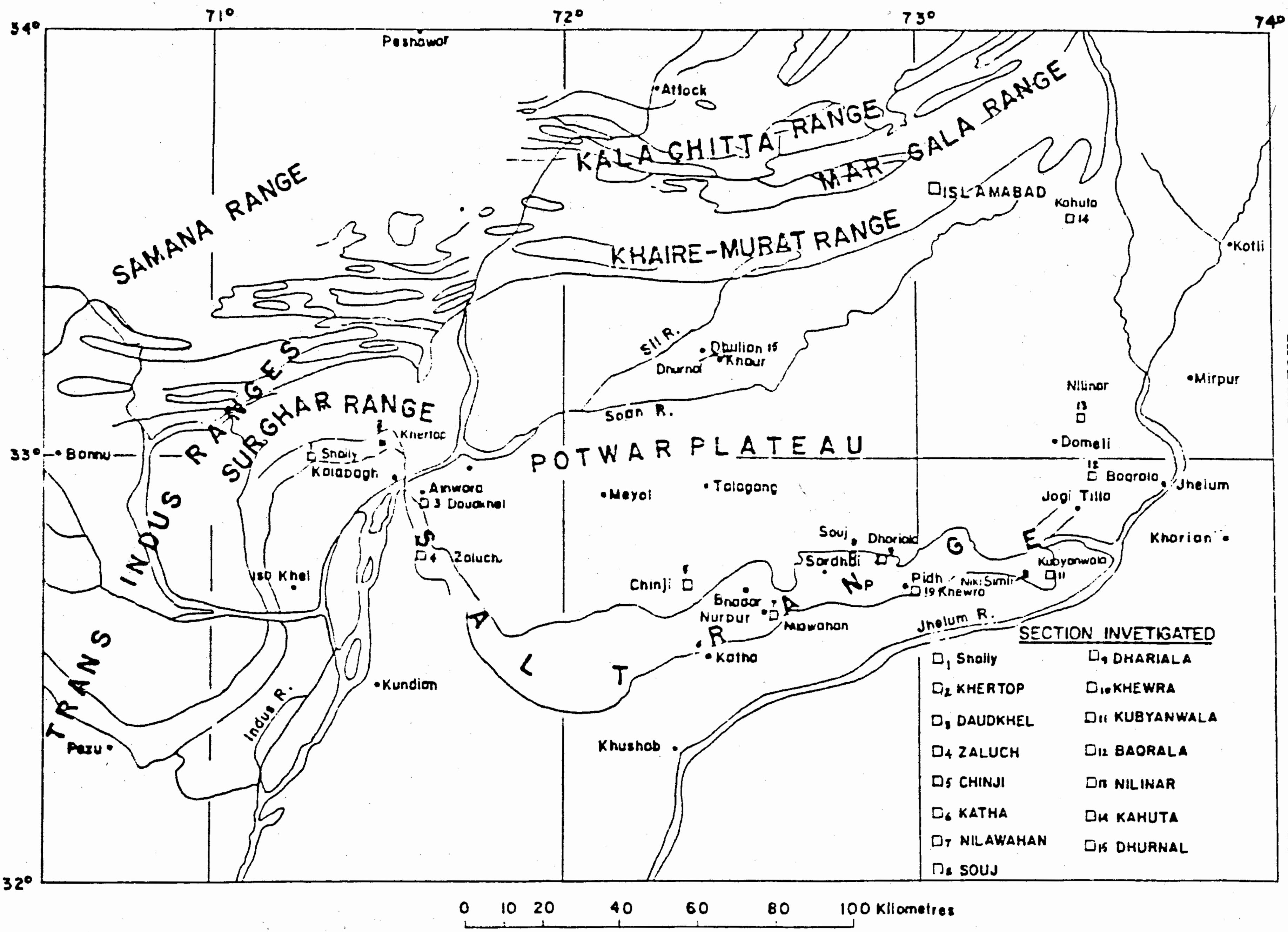

FIG.1 LOCATION MAP OF PLACER SAMPLES IN SALT-RANGE, POTWAR AREA

Table 1. Average lithologial compositions.

Locality	CHINJI FORMATION Thickness (Metres)	CHINJI FORMATION Average Lithological Composition (%)				NAGRI FORMATION Thickness (Metres)	NAGRI FORMATION Average Lithological Composition			
Khertop	726.21	Sandstone	30 &	Claystone plus Siltstone	70	1134.76	Sandstone	93	& Claystone/Silstone	7
D. Khel	1138,27	”	32 &	” ”	68	1195.42	”	54	”	46
Pail	340.60	”	18 &	” ”	82	216.75	”	62	”	38
Souj	227.0	”	7 &	” ”	93	1046.49	”	47	”	53
Dhariala	806.28	”	9 &	” ”	91	413.15	”	59	”	41
Ber Faqir	346.65	”	7 &	” ”	93	332.89	”	51	”	49
Kubyanwala	352.0	”	7 &	” ”	93	791.00	”	45	”	55
Dhurnal	1020.0	”	28 &	Claystone plus Mudstone	72	1032.14	”	60	”	40
Nili Nar	557.61	”	9 &	” plus Slitstone	91	468.91	”	44	”	56
Baqrala	380.00	”	8 &	” plus Mudstone	92	1194.00	”	42	”	58
Ghulman Kas	404.49	”	2 &	” plus Mudstone	77	957.00	”	35	”	65

Table 2. Petrographic composition of the Chinji Formation samples. All figures are percentages.

Locality	Quartz	Calcite	Feldspar	Amphibole	Micas	Chlorite	Epidote	Garnet	Tourmaline	Iron ore	Rutile	Rock–fragments
KHERTOP	23	48	20	–	5.0	0.5	0.5	0.5	–	1.0	0.5	1.0
KHERTOP	23	48	20	–	4.8	0.5	0.5	0.5	–	1.2	0.5	1.0
DAUD KHEL	42	32	18	0.5	3.0	0.5	0.5	0.5	–	2.0	–	1.0
DAUD KHEL	39	35	16	0.5	4.0	1.0	0.5	0.5	–	2.0	–	1.5
CHINJI	40	40	12	–	3.0	1.0	0.5	0.5	0.5	1.0	0.5	1.0
SOUJ	37	38	15	0.5	5.5	0.5	0.5	–	–	2.0	–	1.0
B. FAQIRKAS	32	35	25	–	3.5	1.0	0.5	0.5	–	1.0	0.5	1.0
KOBYANWALA	15	50	23	–	7.0	1.0	0.5	0.5	0.5	1.0	0.5	1.0
NILINAR	30	40	20	1.0	3.0	1.0	1.0	1.0	–	2.0	–	1.0
KAHOTA	31	38	22	1.0	2.0	0.5	1.0	1.0	–	2.0	0.5	1.0

at places gritty. It is thin- to medium-bedded and exhibits cross-bedding. The sandstone is softer and easily erodable, makes very low topographic features except at Khertop area, where it is harder and makes prominent ridges. The sandstone occurs as lenticular bodies extending laterally few hundred metres. At the base of each sandstone bed, pebbly layers of siltstone and claystone, are present. This type of pseudo-conglomerate beds are also present in some of the mudstone units. These disc-shaped, somewhat rounded, claystone pebbles lie parallel with the bedding and generally are 1.5 cm to 3 cm in diameter. Such balls occur selectively along the partings which define the individual sandstone beds indicating a cycle of deposition. Two distinctive types of sandstone have been noticed in the measured sequence. The one is blue-grey sandstone and the other is buff-sandstone. The blue-grey sandstone is characterized by its distinctive colour. It is well-sorted, clean and consists of quartz, feldspar, garnet, muscovite, biotite and schist clasts. The sandstones extend as sheets which laterally merge into siltstone and claystone over long distances. The conglomeratic layers are rare in this type. The buff-sandstone is typically buff- to grey-brown. It is more mature in composition and contains quartz, feldspar, calcite, garnet, fewer mafic minerals and more weathered rock fragments. Two distinct types of sandstones suggest different environments of deposition suggesting two different drainage systems.

The sandstone units grade upward into the much thicker siltstone and claystone beds. This claystone is indistinctly bedded and poorly sorted.

Nagri Formation

Nagri Formation is present throughout the Potwar area. It is composed of roughly 50% sandstone and the rest claystone plus siltstone, except in Khertop area where percentage of sandstone is higher, and makes upto 93 percent. The detailed average lithological composition and thickness in different localities is given in table 1.

The sandstone is light grey to greenish grey, and buff in colour, medium grained, and medium to thick-bedded. Almost all the beds show pronounced graded bedding which is much prominent in thick beds. Cross bedding is also present in almost all the beds. The beds range in thickness from 0.5 m to 4 m.

These sandstones like those of the Chinji Formation are of two types. The blue-grey sandstone consists of quartz, feldspar, garnet, muscovite, biotite and calcite. It extends as sheets which laterally grade into siltstone over distance of several kilometres. Its individual beds range from 7 to 9 m in thickness. In some areas multistoried sandstones are formed by individual sandstone levels laid one upon the other. The buff sandstone is buff to yellow brown, fine to medium grained, and silty at places. It is cross-bedded and contains carbonate nodules. The conglomerate interbeds are also common.

The intraformational pseudo-conglomerates are composed of mud pellets, pebbles of volcanic rocks, pellets and balls of sandstone and clay, all set in a sandy matrix. These are common in the lower and upper parts of the formation. The above conglomerates form distinctive and important deposits in the Nagri Formation. These conglomerates occur as thin-beds, lenses, or stringers. The pellets are greyish-red and irregular in shape, though flattened ellipsoids are common. Some pebbles are spherical especially mud balls; and edges and corners of the most of the pebbles are subrounded. The mud-pellet conglomerates record intraformational pauses in sedimentation, their repeated recurrence and ubiquity, although commonly only as small lenses, represents the break in sedimentation. The clay which is mixed with sand or silt is orange reddish grey, grey and olive-grey at places. The claystone is red, reddish grey, orange or brown and weathers into subrounded to angular irregular blocks.

Table 3. Petrographic composition of Nagri Formation samples. All figures are percentages.

Locality	Quartz	Calcite	Feldspar	Amphibole	Mica	Chlorite	Epidote	Garnet	Tourmaline	Iron–ore	Rutile	Zircon	Rock–fragments
KHERTOP	15	45	30		4	1	0.7	0.5		1.0	0.5	0.8	1.5
KHERTOP	21	45	25	—	4	1	0.5	0.5	0.5	1.0	0.5	—	1.0
DAUD KHEL	36	35	20	0.5	3	1	0.5	0.5	—	1.5	0.5	—	1.5
CHINJI	30	33	26	0.5	4	1	1.0	1.0	—	1.8	0.5	0.2	1.0
SOUJ	41	35	15	0.5	3	1	1.0	0.5	—	1.5	0.5	—	1.0
SOUJ	30	35	25	0.5	4	1	0.5	0.5	0.5	1.5	0.5	—	1.0
B. FAQIRKAS	32	38	22	—	3	1	0.5	0.5	0.5	1.0	0.5	—	1.0
KOBYANWALA	22	40	30	0.5	3	1	0.5	0.5	0.5	1.0	0.5	—	0.5
KOBYANWALA	26	35	30	0.5	4	1	0.5	0.5	—	1.0	0.5	—	1.0
NILINAR	30	28	30	1.0	6	1	0.5	—	1.0	1.0	0.5	—	1.5

MINERAL CONTENTS

Chinji Formation

The sandstones of Chinji Formation are generally fine grained, moderately sorted with subangular to subrounded grains. The sizing analyses of selected sandstone samples from different localities have been undertaken using standard sieves. The results have been plotted in the form of frequency distribution curves (fig. 2). The curves indicate that more than 50% grains lie between 125 to 250 microns and on this basis the sandstones have been classified as fine grained (fig. 2). The mineral contents are given in table 2.

Quartz content in sandstone from different places varies between 15 and 42% (table 2). in Khertop samples quartz grains are widely separated in a field of carbonate showing floating texture. Such sandstones have been interpreted as being composed of an original matrix of clastic quartz and limestone grains, where later on limestone has been recrystallized and now shows no trace of its clastic origin ***(Pettijohn,*** 1974). Generally the grains are subangular but variation from subangular to angular is also present. The outer margins are corroded by surrounding calcitic material and the pore-spaces are filled by calcitic cement.

Feldspar constitutes about 12 to 25% of the sandstones. It includes microcline, microperthite, orthoclase and oligoclase. The grains are generally subrounded and are sericitized and kaolinized. Some grains are partially replaced by calcite.

Biotite is found almost in all the samples. The flakes show moderate pleochroism from light brown to yellow brown, and are randomly distributed. Some grains are altered to chlorite and form small flakes and long laths, which are sometimes bent in between other equidimensional mineral grains due to pressure of compaction. ***Chlorite*** occurs as small individual flakes or as irregular structureless patches. Inclusions of feldspar, epidote and biotite are frequent. Some grains are pseudomorphous after biotite.

Carnet grains are colourless to light pink.

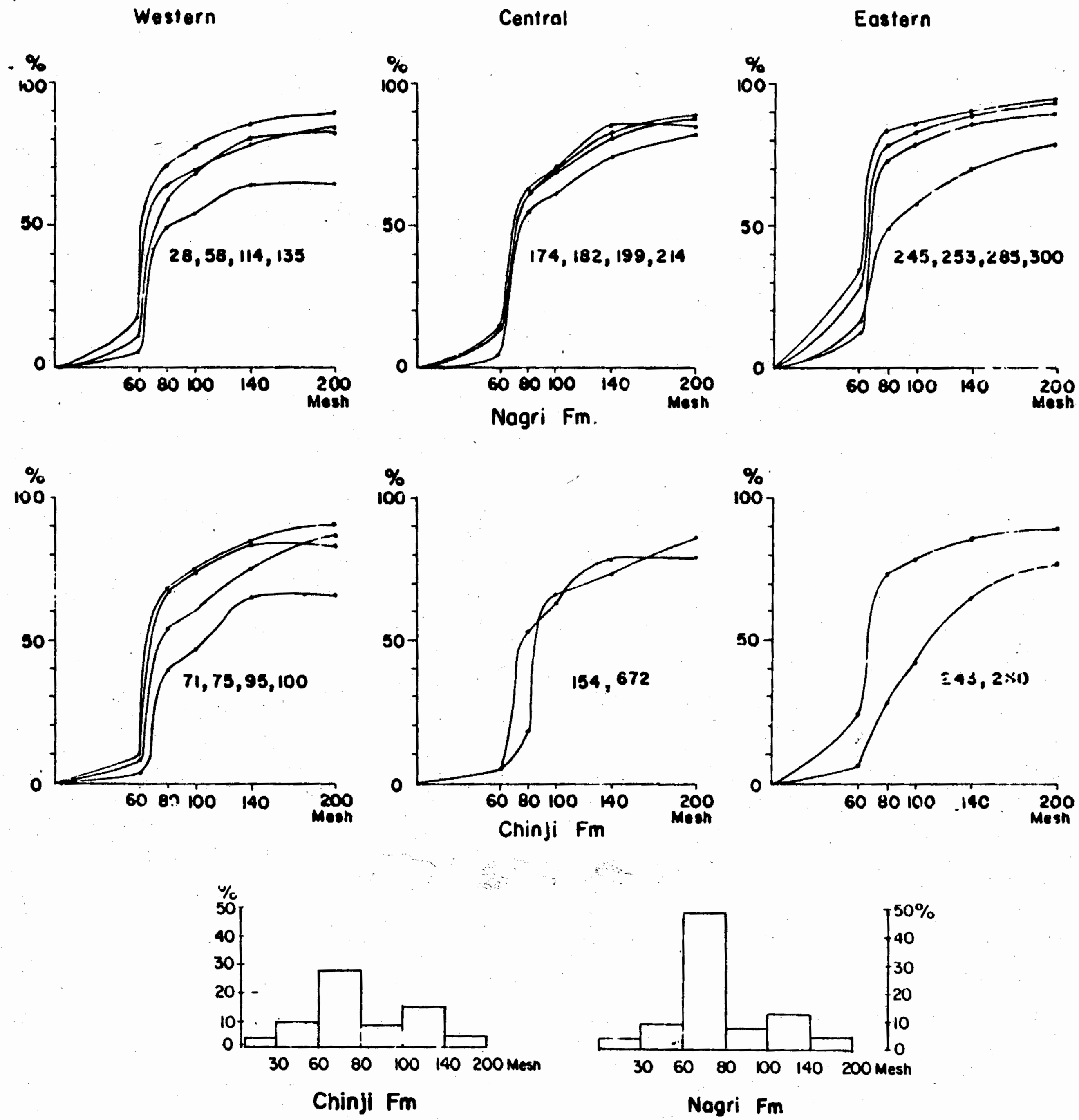

FIG. 2. CUMULATIVE CURVES, SHOWING GRAIN SIZE DISTRIBUTION IN CHINJI & NAGRI SANDSTONES

Tourmaline grains are randomly distributed and show pleochroism from brownish-green to dark greenish brown.

Magnetite and hematite occur as small individual grains, randomly distributed. Both minerals are intimately associated and often, occur as stains, thin streaks as well as in the cement.

Calcite occurs mostly as precipitated matter but clastic carbonate grains are also present. These grains enclose quartz and feldspar poikilitically. Rock fragments are dominantly of volcanic rocks which are mostly andesite in composition and show signs of abrasion. The chert fragments have also been noticed. The carbonaceous matter occurs as amorphous-looking tiny aggregates. All the quartz and feldspar grains are cemented together by carbonates.

Nagri Formation

The sandstones of Nagri Formation are generally fine grained, moderately sorted with subangular to subrounded grains. The sizing analyses of selected samples from different localities have been undertaken using standard sieves. The results have been plotted in the form of frequency distribution curves. The curves indicate that more than 70% grains lie in the range of 125 to 250 microns. On this basis the sandstones, have been classified as fine grained (fig. 2). The mineral contents are given in table 3 and the mineral descriptions are as follows :

Quartz grains showing floating texture are widely separated in the field of carbonate cement in the Khertop area. The grains are angular to subangular, composite grains are also visible in few thin sections. About 5 to 10% of the grains show undulose extinction. In several cases the grains appear to have suffered marginal corrosion by reaction with calcitic material.

Feldspar constitutes about 10 to 25% of the sandstones. The plagioclase is oligoclase to albite. Most of the plagioclase grains are completely altered to sericite and kaolinite while some are slightly clouded. The potash feldspar is orthoclase and microcline. They are mostly medium grained and associated with quartz and moderately altered to sericite and kaolin.

Biotite shows slight pleochroism and iron-staining.

White mica occurs as finely divided grains and elongated tabular, curved, flakes between quartz grains.

Chlorite occurs as individual flakes or as small irregular aggregates and is randomly distributed.

Amphibole occasionally occurs as fine anhedral grains.

Epidote occurs as anhedral grains. It is light green in colour.

Garnet is subangular and colourless to light pink.

Tourmaline shows moderate pleochroism from brownish green to dark green. It is mostly fine grained.

Magnetite and hematite occur as small individual grains and are randomly distributed. Hematite occurs as thin streaks and grains.

Calcite is fine to medium grained, & subangular to subrounded. It is very difficult to distinguish between detrital and cementing calcite because cementing calcite has also developed somewhat crystalline form. Polycrystalline calcite is also noticed, sometimes it encloses the quartz and feldspar grains.

In addition, volcanic rock fragments have also been noticed and these seem to be andesitic. In few thin sections the carbonaceous matter occurs as amorphous-looking tiny aggregates. All the quartz and feldspar grains are cemented together by carbonates which have completely filled the pore-space between different grains.

Table 4. Heavy mineral fraction percentage (P) calculated from the weight of heavy minerals fraction (W) in 10 gms of each sample, after bromoform separation.

CHINJI FORMATION

Sample No.	Location	W	P
PKS–73–82	588737	0.1191	1.191
PKS–95–82	714593	0.3276	3.276
PKS–153–82	43 D/6 298489	0.0418	0.418

NAGRI FORMATION

Sample No.	Location	W	P
PKS–123–82	757636	0.320	3.20
PKS–181–82	442374	0.420	4.20
PKS–209–82	870473	0.446	4.46
PKS–245–82	43 H/6	0.235	2.35
	458403	0.235	2.35
PKS–291–82	534456	0.145	1.45
PKS–334–82	43H/9 698718	0.847	8.47
PKS–350–84	43 C/7	0.229	2.29
PKS–374–82	43 C/7	0.273	2.73

HEAVY MINERALS

The selected samples from Chinji and Nagri formations were subjected to bromoform separation for heavy minerals. The heavy minerals were studied under binocular microscope and estimates of various heavy minerals were made by visual counts.

Chinji Formation

The percentage of heavy minerals varies from 0.4 to 3.3. The minerals identified include amphibole, chlorite, tourmaline, garnet, epidote, magnetite and pyrite (table 5). Traces of metamict zircon have also been identified using an ultraviolet lamp. The percentage of heavy mineral fraction is given in table 6.

Nagri Formation

The study indicates the percentage of heavy minerals varying from 1.54 to 8.47%.

The mineralogical study of the heavy fraction shows the minerals suite of amphibole, chlorite, tourmaline, garnet, epidote, magnetite and pyrite. The results of the study are given in table 6.

The mineralogical study with the help of ultraviolet lamp for zircon and scheelite minerals indicates the presence of zircon in few samples in minor armounts.

CHEMISTRY

Chinji Sandstone: Two sandstone samples from Chinji Formation were analyzed. They gave SiO_2 from 39.36 to 49.43%; Al_2O_3 from 10.82 to 13.56%; Fe_2O_3 from 5.58% to 5.98% and CaO from 11.78 to 19.63%. The variation of other elements is given in tables 7 and 8.

Nagri Sandstone: Two samples from Nagri Formation were analysed and gave SiO_2 from 28.68 to 35.13%, Al_2O_3 from 9.01 to 10.68%, Fe_2O_3 from 3.19 to 4.29% and CaO from 24.11 to 30.84%. The detailed analyses are given in table 7. Selected samples were spectrographically analysed and they contain 20 ppm Co, 20 to 300 ppm Cr, 2000 to 5000 ppm Mn, 20 to 250 ppm Ni, 50 to 350 ppm Pb, 7000 to 10,000 ppm Ti, 150 to 700 ppm V, 50 to 500 ppm Zr, 30 ppm Y, 100 ppm Zn (table 8).

CONCLUSION

The study has shown that the sandstones of Chinji and Nagri Formations are fine grained and the particle size of most of the grains lies from 150 to 250 microns. The sandstones of both the formations show almost similar degree of sorting and are poor to well-sorted.

The petrographic studies have shown that the sandstones are calc sub feldspathic arenites and

Table 5. Heavy minerals in the Nagri Formation.

Sample No.	Toposheet No. & Grid Reference	Light Minerals Fraction %	Heavy Minerals Fraction %	Quartz	Feldspar	Amphibole	Tourmaline	Ilmenite & others	Muscovite & biotite	Magnetite	Pyrite	Garnet	Chlorite	Epidote	Rutile	Zircon	Scheelite
PKS–45–82	38 0/12 046746	88.4	11.6	25.0	16.0	7.0	3.0	20.0	1.0	10.0	2.0	5.0	6.0	4.0	1.0	–	–
PKS–123–82	757636	96.8	3.2	34.0	10.0	3.0	1.0	12.0	2.0	12.0	2.0	4.0	10.0	8.0	2.0	–	–
PKS–181–82	442374	95.8	4.2	35.0	18.0	4.0	–	20.0	–	10.0	–	2.0	7.0	4.0	–	Tr	–
PKS–209–82	870473	95.54	4.46	31.0	16.0	5.0	–	18.0	1.0	6.0	1.0	2.0	12.0	7.0	1.0	Tr	–
PKS–245–82	43 11/6 458403	97.65	2.35	14.0	6.0	8.0	4.0	20.0	1.0	7.0	2.0	9.0	14.0	12.0	2.0	1.0	–
PKS–291–82	534450	98.55	1.45	30.0	12.0	6.0	2.0	20.0	–	4.0	2.0	1.0	13.0	10.0	–	Tr	–
PKS–334–82	43 11/9 698718	91.53	8.47	31.0	10.0	5.0	2.0	20.0	2.0	3.0	2.0	5.0	10.0	8.0	2.0	Tr	–
PKS–350–82	43 C/7	97.71	2.29	42.0	15.0	5.0	2.0	20.0	1.0	5.0	–	1.0	5.0	4.0	–	–	–
PKS–374–82	–do–	97.27	2.73	19.0	8.0	8.0	4.0	17.0	8.0	20.0	1.0	3.0	9.0	7.0	1.0	1.0	–

Table 6. Chemical composition of sandstone samples of the Chinji and Nagri Formations of the Salt Range. LOI stands for loss on ignition.

Sample No.	Locality	LOI	SiO_2	Fe_2O_3	Al_2O_3	TiO_2	P_2O_5	CaO	MgO	MnO	Na_2O	K_2O	Total
CHINJI FORMATION													
PKS–64–82	Khertop	14.21	49.43	5.58	13.56	0.60	0.10	11.78	4.03	0.11	0.34	0.18	99.93
PKS–90–82	Daudkhel	20.47	39.36	5.98	10.82	0.25	0.05	19.63	2.82	0.25	0.17	0.09	99.87
NAGRI FORMATION													
PKS–23–82	Khertop	26.03	28.67	3.19	9.01	0.25	0.03	30.84	1.21	0.22	Tr	0.21	99.62
PKS–174–82	Pail	22.47	35.13	4.29	10.68	0.30	0.03	24.11	2.82	0.15	0.17	0.06	100.21

Table 7. Emission spectrographic analyses of sandstone of the Nagri Formation, Salt Range.

SAMPLE NO.	LOCATION	Co	Cr	Mn	Ni	Pb	Ti	V	Zr
	43 C/15								
PMP–80–74	862,235	Nil	300	> 5000	20	350	> 10000	250	100
PMP–80–76	865,232	10	90	> 5000	20	300	> 10000	500	50
	43 C/11								
PMP–80–86	658,044	20	200	2000	90	50	10000	300	150
PMP–80–93	663,024	20	200	5000	30	50	> 10000	300	500
PMP–80–94	662,020	20	200	> 5000	250	80	> 1000	700	200
PMP–80–96	663,018	20	70	5000	70	70	9000	350	100
	43 C/7								
PMP–80–103	553,048	10	50	> 5000	20	150	> 10000	400	150
PMP–80–106	553,048	20	50	5000	50	70	8000	150	200
	43 C/8								
PMP–80–127	448,910	20	150	5000	150	80	10000	300	400
PMP–80–132	446,902	Nil	20	> 5000	20	100	> 10000	20	50

contain quartz, feldspar and calcite as essential minerals. Some of the sandstones show pronounced floating texture developed due to scattered quartz grains enclosed in carbonate field.

The percentage of heavy minerals varies from 0.418 to 3.276 in Chinji Formation and from 1.45 to 8.47% in Nagri Formation. The heavy minerals include amphibole, chlorite, tourmaline, garnet, epidote, magnetite and pyrite. The provenance of heavy minerals suite indicates that the source rocks include granodiorite and diorite. The sandstones from Chinji and Nagri Formations show 20 to 300 ppm Cr, 20 to 200 ppm Ni, 50 to 400 ppm V indicating basic source rocks and 50 to 500 ppm Zr showing that the materials have also been derived from acidic to intermediate rocks. The presence of alkali feldspars in the sandstones also indicats acidic igneous source rocks.

REFERENCES

ANDRESON, R.V. (1927) Tertiary stratigraphy and orogeny of the Northern Punjab. Bull. Geol. Soc. America 38.

BAIG, M.A.S. (1984) Some observations about change of fluvial pattern in cis- and trans-indus exposures of Dhok Pathan Formation. Volume of Abstracts First Pakistan Geol. Con. pp. 46-7.

COTTER G.de. P. (1933) The geology of the part of the Attock District west of longitude 72° 45′ E: Mem. Geol. Surv. India, 55.

FATMI, A.N. (1973) Lithostratigraphic units of the Kohat Potwar province, Indus Basin, Pakistan: Mem. Geol. Surv. Pakistan 10.

GEE E.R. (1947) Further note on the age of the saline series of the Punjab and of Kohat. Mem. Geol. Surv. Pakistan, B—V (16).

——————— (1982) Geological map of Salt-Range (Scale 1 : 50,000), Geol. Surv. Pakistan, Quetta.

GILL, W.D. (1952) Facies and fauna in the Bhadrar Beds of the Punjab Salt Range, Pakistan. Jour. Palaent, 27, (6).

KHAN M.J. (1984) Sedimentation and tectonics of the Tran-Indus Siwalik Group, by paleomagnetic method. Volume of Abstracts First Pakistan Geol. Congress, pp. 11-12.

PETTIJOHN, F.J. (1974) SEDIMENTARY PETROLOGY, 3rd Edition. Harper & Row, New York, pp. 195-250.

PILBEAM, D., BARRY, J., ET AL. (1977) Geology and Palaeontology of Neogene strata of Pakistan. Nature 270, (5639), pp. 684-9.

WYNNE, A.B. (1978) On the geology of the Salt-Range in the Punjab. Mem. Geol. Surv. India 14, p. 313

Manuscript received 7.12.1986
Accepted for publication 31.12.1986.

ACTA MINERALOGICA PAKISTANICA
VOLUME 2 (1986) pp. 93-99 .

PETROGRAPHY AND GEOLOGY OF THE JOGABUNJ–SADIQABANDA AREA, DIR DISTRICT, PAKISTAN.

AFTAB MAHMOOD & SYED ALIM AHMAD

Institute of Geology, University of the Punjab, New Campus, Lahore-20, Pakistan.

ABSTRACT:– A geological map covering about 66 square miles of the Jogabunj-Sadiqa banda area on the scale of 1" = 0.789 miles is presented. The area is mainly composed of metasedimentary complexes; the units are amphibolite, granodiorite, pegmatite and hornblendite. The amphibolites are the oldest rocks. After their formation, an acidic magma intruded the amphibolites, resulting in the formation of granodiorite: the contact between them is sharp. Dykes are present both in granodiorite and amphibolite, showing the late residual composition of the granodioritic magma; quartzo-feldspathic and pegmatite veins are present in the whole area. Garnet-bearing quartzofeldspathic rocks are intrusive.

Modal analyses and petrography of 32 selected samples are presented and mineralogical statistical variation diagrams are plotted. The petrogenesis of the amphibolite and granodiorite is briefly discussed.

INTRODUCTION

The investigated area lies between 35° 4' 44" to 35° 9' 13" N and 72° 0' to 72° 6' 22" E on toposheet No. 43 A/4 issued by the Survey of Pakistan on the scale 1" = 0.789 miles.

Tectonically the area is a part of Kohistan island arc (Tahirkheli, 1979) which is sandwiched between the subducting Indian Shield and the obducting Eurasian Shield. It forms part of a group of metasediments and metaigneous rocks which are intruded by acidic and intermediate igneous rocks of various ages.

A number of geologists have worked in Dir District. H.H. Hayden (1981) was the first geologist to describe its geology and his observations were based merely upon a reconnaissance survey of Dir and Chitral. Bakr and Jackson (1964) showed the geology of Dir as consisting of granite gneiss, schist and metasedimentary rocks of Precambrian to early Tertiary age; they regarded the rocks as an extension of Laddakh range.

Detailed mapping and investigations were carried out by Chaudhry & Chaudhry, (1974); Chaudhry et al. (1974 a,b,c), Tahirkheli (1979), Alim et al. (1985) and Mahmood & Alim (1985).

The investigated area has been divided into amphiboiite, granodiorite, pegmatite and hornblendite rock units. Amphibolite covers more than 86% of the area. The rest of the rocks are intruded into the amphibolite, intersecting it at various angles. The contacts of the amphibolites with the rest of the rocks are sharp showing chilled margins occassionally.

In the present contribution the petrography and modal compositions of the rocks are described and statistical diagrams are plotted on Streckeisen's (1967) triangle.

PETROGRAPHY

Amphibolite

Amphibolite forms the major rock unit, covering 75% of the area investigated. It is the

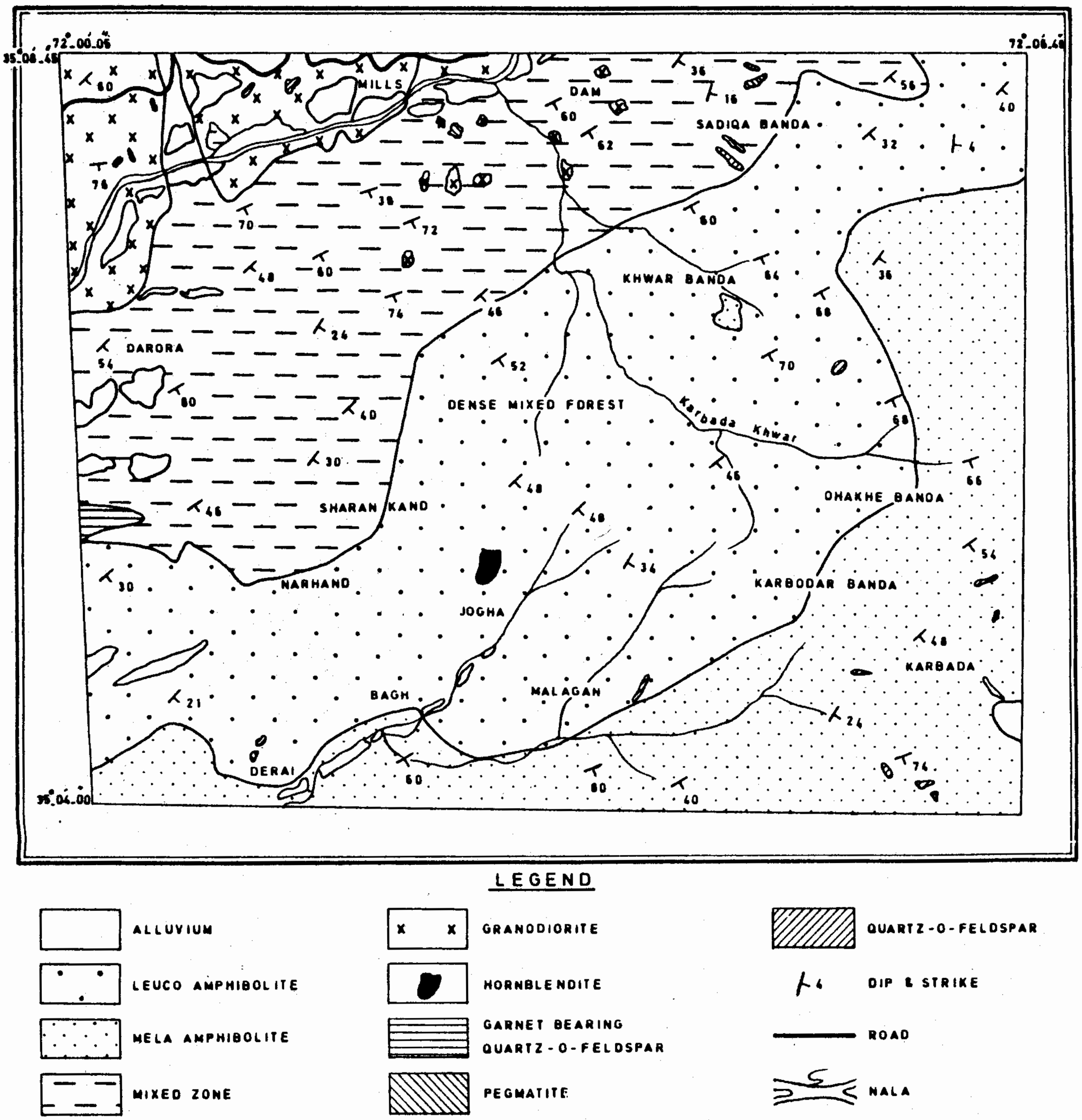

FIG.1. GEOLOGICAL MAP OF JOGA BUNJ-SADIQA BANDA AREA, DIR.

host rock for the other rocks, striking NE–SW and dipping towards SE, with a colour index up to 80%, and is massive, banded and occassionally foliated. In the banded amphibolites, bands which range from 1 to 4 mm are developed due to segregation of dark and light minerals in alternate positions and boudinage structures developed during this process. In the dark bands the essential mineral is hornblende while in the white bands feldspar and quartz are the essential minerals. Milky whitish veins of quartzofeldspar, green veins of epidote, patches of hornblendite and dykes of pegmatite are present occasionally. Structurally the amphibolite can be classified into layered and non-layered types. The layered variety can be further subdivided into hornblende-layered amphibolite, epidote-layered amphibolite, and epidote-rich quartzofeldspathic-layered amphibolite.

The rock is medium to coarse grained, porphyroblastic and poikilitic texture is common. Hornblende is highly pleochroic from light green to dark green, altering into chlorite and muscovite along the cleavage planes. Inclusions of anhedral quartz are present forming sieve-like structure. The subordinate inclusions of iron ore are also present in the hornblende.

Plagioclase is the second essential mineral which is euhedral with albite and pericline twinning, albite is usually sericitized. Mostly plagioclase and quartz are segregated into thin bands. Usually plagioclase is kaolinized to some extent. The composition of plagioclase ranges from oligoclase to andesine.

Quartz is anhedral to subhedral, medium to coarse grained, gives strained extinction. Occasionally grains are fractured.

Chlorite is present as a flaky secondary mineral, pleochroic from light green to light inkly blue, with weak birefringence. Epidote is fine to medium-grained, prismatic, columnar and granular, with a perfect cleavage in one direction, minute grains of magnetite and hematite are present as inclusions in the epidote.

Minor and accessory minerals are orthoclase, zoisite, calcite, sericite, biotite, apatite, sphene, muscovite and iron ores. More orthoclase occurs in the massive amphibolite than in the banded variety.

Granodiorites

The amphibolite is intruded by medium to coarse-grained granodioritic dykes in various directions. It is massive to poorly foliated, and well jointed. A few joints are filled with quartz and quartz-feldspar intergrowths.

The granodiorite is generally hypidiomorphic and granular, whereas porphyritic and myrmekitic textures are also common.

Quartz is the main mineral, in fine to medium, euhedral to anhedral, fresh grains. It is rarely fractured; graphic and myrmekitic textures are common, with strain extinction occasionally.

Plagioclase is present as euhedral to subhedral, medium to coarse grains, of andesine composition. Apart from alteration products, the plagioclase is usually free from inclusions. Anhedral quartz is present in the outer rims of the plagioclase grains.

The orthoclase is coarse-grained,s subhedral to anhedral, and cloudy, due to incipient alteration, in contrast with thicker quartz.

The accessories include biotite, muscovite, hornblende, epidote and chlorite. The biotite flakes range from 1 to 8 mm in size; the phenocrysts are mostly aligned in a parallel to subparallel manner, well marked occasionally, giving a flow structure. The biotite crystals are well developed and uniformly distributed throughout the rock. Alteration to chlorite is clearly observed locally. Muscovite forms scaly aggregates or shreds. Hornblende occurs as coarse to medium grained, subparallel, prismatic crystals with well-developed cleavages;

Table 1. Modal analyses of granodiorite.

Sample no.	19990	20043	20044	20049	19915	19921	19954	19985	19875	19876	19878	19909
Quartz	38.8	20.3	19.8	18.7	24.5	41.4	27.2	29.5	30.8	40.1	28.0	36.9
Orthoclase	11.6	11.4	11.3	16.9	16.6	12.6	06.5	09.0	15.8	12.0	10.8	14.0
Plagioclase	28.7	44.3	50.6	46.7	44.2	34.0	28.5	45.9	37.7	40.5	52.3	30.0
Biotite	10.2	10.2	07.3	11.0	09.4	05.5	10.8	13.9	00.5	05.4	01.7	14.0
Iron ore	01.3	07.9	00.5	03.1	02.1	00.0	00.5	00.4	01.3	01.6	04.8	05.2
Muscovite	00.3	00.0	10.3	03.6	01.1	03.9	00.0	01.2	13.8	00.4	02.4	00.0
Epidote	01.1	01.5	00.0	00.0	0.10	00.1	02.6	00.0	00.1	00.0	00.0	00.0
Hornblende	00.0	04.5	00.0	00.0	00.0	00.0	20.4	00.0	00.0	00.0	00.0	00.0
Chlorite	00.0	00.0	00.0	00.0	00.0	00.1	00.0	00.0	00.0	00.0	00.0	00.0
Recalculated												
Quartz	49.1	26.7	23.4	22.8	85.3	47.3	43.7	35.0	36.0	43.3	30.7	45.6
Orthoclase	14.7	14.9	14.0	20.5	19.4	14.2	10.5	10.7	18.8	13.0	11.9	17.3
Plagioclase	36.2	58.35	62.54	56.7	51.9	38.5	45.8	54.4	44.7	43.7	57.4	37.1

Table 2. Modal analyses of amphibolite.

Sample no.	20030	20050	19894	19945	20013	20022	20025	20001	20009	20010	20041	19971	20047
Hornblende	46.2	36.8	25.1	20.2	42.3	40.8	27.5	57.1	58.4	60.2	55.9	50.0	47.3
Quartz	22.0	23.0	35.3	39.4	20.3	25.1	18.6	12.0	11.1	06.7	06.3	10.4	17.0
Epidote	02.9	17.7	10.2	02.1	02.1	08.1	13.6	03.5	10.2	10.2	08.3	10.3	12.4
Orthoclase	15.2	00.1	25.0	00.0	00.0	00.5	04.0	00.0	00.0	00.4	00.0	07.6	03.0
Chlorite	00.1	00.0	00.0	00.0	00.0	00.0	04.4	01.6	00.0	02.0	02.1	00.1	02.0
Iron ore	00.4	00.0	00.6	00.0	21.1	00.5	01.6	03.0	01.1	00.0	03.3	00.0	03.0
Plagioclase	11.7	22.0	02.6	19.4	11.2	25.0	28.0	20.6	19.0	20.0	24.0	26.8	12.0
Calcite	00.0	00.0	01.3	00.0	00.0	00.0	00.0	00.9	00.1	00.0	00.0	00.0	02.0
Sericite	00.0	00.0	00.0	01.0	02.1	00.0	00.0	00.9	00.0	00.6	00.0	00.0	00.5
Apatite	00.0	00.0	00.0	00.0	00.0	00.0	00.0	00.3	00.1	00.0	00.0	00.4	00.2
Biotite	00.0	00.0	00.0	00.0	00.0	00.0	00.0	00.2	00.0	00.0	00.0	00.4	00.2
Sphene	00.0	00.0	00.0	00.0	00.0	00.0	00.0	00.0	00.0	00.0	00.1	00.1	00.3

Table 3. Modal analyses of minor dykes and veins.

Sample no.	PEGMATITES 20056	20060	QUARTZOFELDSPATHIC ROCK 19871	19877	19900	HORNBLENDITE 20080	20085
Quartz	61.8	65.2	56.0	37.7	53.9	13.3	14.4
Orthoclase	14.9	06.1	13.3	20.3	16.5	00.7	06.9
Plagioclase	19.5	16.2	07.5	13.2	03.0	03.0	02.2
Muscovite	03.5	10.9	00.0	00.8	05.6	00.0	00.0
Biotite	00.0	00.0	00.0	15.0	00.0	00.3	00.0
Chlorite	00.0	00.0	00.0	00.0	00.0	04.0	03.9
Kaolin	00.0	00.0	00.0	11.1	10.0	00.0	03.8
Haematite	00.0	00.0	06.7	01.5	00.0	00.0	00.0
Limonite	00.0	00.0	06.8	0.00	05.2	0'00	00.0
Magnetite	00.0	00.0	00.0	00.0	00.0	01.4	00.7
Sphene	00.3	01.6	00.0	00.0	00.0	01.9	01.3
Garnet	00.0	00.0	09.7	00.4	05.2	00.0	00.0
Hornblende	00.0	00.0	00.0	00.0	00.0	75.4	55.7
Epidote	00.0	00.0	00.0	00.0	00.0	00.0	11.1

it is euhedral and fresh at the contact zones but at other places is altering to epidote. Inclusions of anhedral quartz are common. Epidote occurs as prismatic grains as an alteration product of hornblende and plagioclase. Chlorite occurs as scaly, pleochroic, hydrothermal alteration product of biotite and hornblende. Fine grained iron ore grains occur occasionally.

Hornblendite

The rocks are fine to coarse grained, euhedral to subhedral and idioblastic to hypidiomorphic textures are common. Hornblende is the main mineral. Chlorite, plagioclase and magnetite are accessory minerals.

Hornblendite occurs as patches, ellipsoidal shapes and dykes. The hornblendite patches are produced from hot emanations from acidic magma. Hornblendite dykes in amphibolite are due to metamorphic segregation.

Minor Dykes and Veins

Pegmatites and garnet-bearing quartzofeldspathic rocks occur as thin dykes, veins and patches. Among the pegmatites, quartz, plagioclase and orthoclase are the essential constituents whereas kaolin, muscovite and sphene are the accessories. The quartzofeldspathic dykes range from 1 to 4 m in width. They are fine to medium grained, with garnet, biotite, muscovite, sphene, kaolin as well as iron ore minerals as accessories.

DISCUSSION

Moorhouse (1959) proposed the main criteria for distinguishing between amphibolites resulting from basic lavas or intrusive rocks and those having a metasedimentary origin. Some workers regard the association, in the field, of amphibolite with marble as proof of a metasedimentary origin, e.g. Heier (1962).

According to Wilcox and Poldervaart (1958) the banded nature of amphibolite is strong evidence in favour of a metasedimentary origin. Many authors have stressed the importance of the chemical differences between the types e.g. Leake (1964) and Leake & Evans (1960). According to Leake higher contents of Ni, Cr, and Ti confirm a metaigneous origin for amphibolite. In the view of Khattak et al. (1985),

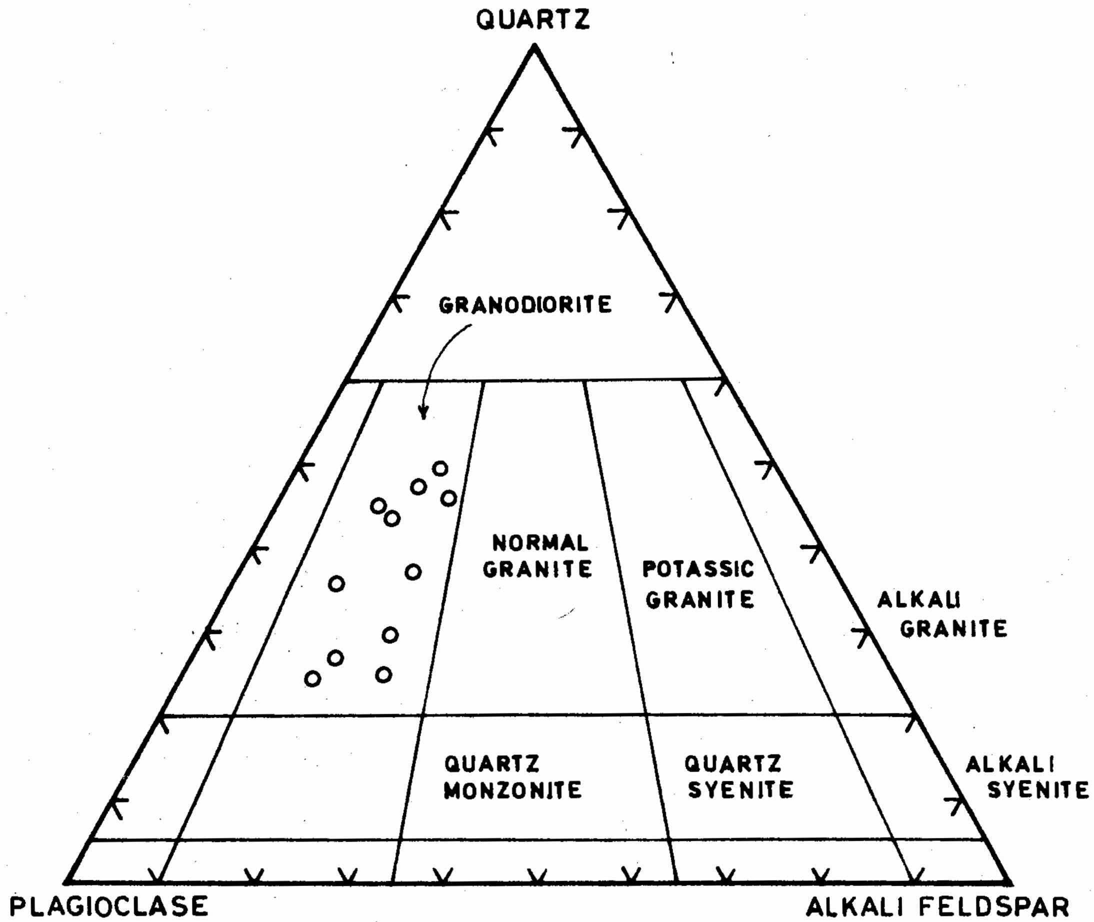

FIG. 2. PLOTS OF MODAL ANALYSIS OF SOME GRANODIORITIC ROCKS FROM 'JOGA BUNG' SADIQA BUNDA AREA (DISTRICT DIR N.W.F.P. PAKISTAN) IN STRECKEISEN'S TRIANGLE (1967)

the banded varieties of amphibolite owe their origin to shearing rather than to the inheritance of sedimentary structures.

The above authors conclude with the opinion that when deciding on the origin of amphibolite it is necessary to consider chemical, mineralogical and petrographic factors. In the case of the present amphibolite, the authors have based their observations on petrographic, mineralogical, field and structural studies in evaluating the origin of amphibolite.

The above criteria suggest that the amphibolite in the mapped area is of metasedimentary origin. In the view of the authors, the following evidence is strongly in favour of such a view;

1. The absence of cummingtonite, which indicates an igneous origin; no traces of cummingtonite are seen in any of the sections.

2. The banded nature of the amphibolite is strong evidence in favour of a metasedimentary origin (Walker et al., 1960).

Petrological and field evidences show the formation of granodiorite, as a result of magma which is dominantly not fully molten; and not as a product of metasomatism in situ, as evidenced by the following facts.

1. The contact of granodiorite with host amphibolite rock is sharp.

2. Occassionally chilling effects are seen at the contact.

3. The granodioritic dykes and apophyses can only be indicated by 'forceful' intrusion of magma. Metasomatism does not explain these facts.

4. The absence of sedimentary structures in granodiorite is also a proof in favour of magmatic origin of granodiorite.

5. The general hypidiomorphic texture which is the most characteristic of granodiorite shows features inherited from magmatic crystallization.

ACKNOWLEDGEMENTS

The authors wish to acknowledge the guidance and encouragement by Professor F.A. Shams, Director, Institute of Geology, Professor Shafeeq Ahmad and M.N. Chaudhry, Institute of Geology, University of the Punjab, Lahore.

REFERENCES

ALIM, S.A., MAHMOOD A. & KHAN A.R. (1985) Geology and petrology of Gulpatobanda Saoni area, District Dir, Pakistan. Acta Mineralogica Pakistanica 1, pp. 90-4.

BAKR, M.A. & JACKSON R.O. (1964) Geological map of Pakistan, (Scale 1:2,000,000), Geol. Surv. Pak. Quetta.

CHAUDHRY, M.N., & CHAUDHRY A.G. (1974) Geology of Khagram area, District Dir, N.W.F.P., Geol. Bull. Punjab Univ. Lahore, **11**, pp. 21-44.

CHAUDHRY, M.N., KAUSAR A.B. & LODHI S.A.K. (1974a) Geology of Timurgara – Lal Qila Area, District Dir, N.W.F.P. Geol. Bull.s Punjab Univ. Lahore, **11**, pp. 53-74.

CHAUDHRY M.N., MAHMOOD A. & CHAUDHRY A.G. (1984b) The orthoamphibolites and the para-amphibolites of District Dir N.W.F.P. Geol. Bull. Punjab Univ. Lahore, **11**, pp. 89-96.

CHAUDHRY, M.N., MAHMOOD A. & SHAFIQ M. (1974c) Geology of Sahibabad-Bibiore area, District Dir N.W.F.P., Geol. Bull. Punjab Univ. Lahore, **10**, pp. 73-90.

HEIER K.S. (1962) The possible origin of amphibolites in an area of high metamorphic grade. Norsk. Geol. Tiddskr. **42**, pp. 452-65.

HAYDEN, H.H. (1981) General report. Geological Survey of India for the year 1916. Rec. Geol. Surv. India. **48**, 12p.

KHATTAK, M.U.K., KHAN M.L., BANGASH, M.I. & JAN, M.Q. (1985) Petrology of hornblendites and associated rocks at Mahak, Upper Swat. Acta Mineralogica Pakistanica, **1**, pp. 78-82.

LEAKE, B.E. (1964) The Chemical distinction between ortho-and para-amphibolites. Jour. Petrol., **5**, pp. 238-254.

———— **& EVANS B.W. (1960)** The composition and origin of striped amphibolites of Connemara, Ireland. Jour. Pet., **1**, pp. 332-363.

MAHMOOD A., ALIM S.A. (1985) Geology of Warai Jogabung area District Dir, Transhimalayan Island Arc. Acta Mineralogica Pakistanica **1**, pp. 83-9.

MOOREHOUSE, W.W. (1959) STUDY OF ROCKS IN THIN SECTIONS. Jah Weatherhill Inc. Tokoyo.

STRECKEISEN , A. (1967) Classification and nomenclature of igneous rocks, Neus. Jb. Miner. Abh. **107**, pp. 144-240.

TAHIRKHELI, R.A.K. (1979) Geology of Kohistan and adjoining Eurasian and Indo-Pakistan continents, Pakistan. Geol. Bull. Univ. Peshawar **11**, pp. 1-30.

WALKERS & POLDERVAART, A. (1949) Karoo dolerite of Union South Africa. Geol. Soc. Amer. Bull. **60**, pp. 591-706.

WILCOX, R.E. & POLDERVAART, A. (1985) Metadolerite dyke swarm in Bakrgille-Roan Mountain area, North Carolina, Geol. Soc. Amer. Bull. **69**, pp. 1327-68.

Manuscript received 4.10.1986
Accepted for publication 30.12.1986

ACTA MINERALOGICA PAKISTANICA
VOLUME 2 (1986) pp. 100-106.

A COMPARISION OF HYDROTHERMAL ALTERATION IN PORPHYRY COPPER MINERALIZATION OF CHAGAI CALC–ALKALINE MAGMATIC BELT, BALUCHISTAN, PAKISTAN

REHANUL HAQ SIDDIQUI[1] & WAZIR KHAN[2]

1. **Geological Survey of Pakistan, Sariab Road, Quetta, Pakistan.**
2. **Geological Survey of Pakistan, Quetta, & Centre of Excellence in Mineralogy, Baluchistan University, Quetta, Pakistan.**

ABSTRACT:– Hydrothermal alterations in porphyry copper occurrences of Chagai belt are mainly associated with tonalite porphyry stocks, except Durbanchah and Humai prospects which are hosted in dacite porphyry stocks, whereas Missi Prospect occurs in a granodiorite batholith. Alteration is generally developed in a concentric zonal pattern as observed elsewhere by Lowell and Guilbert (1970), except that absence of regular argillic and peripheral zones in Chagai belt. In certain occurrences the potassium sillicate alteration zone (K-Zone) occurs usually within the intrusive porphyry, but in Saindak and Koh Dalil areas some of the adjacent wall rock sediments, and in Durbanchah the microdioritic country rock, has also undergone the K-alteration. Quartz sericitic alteration zones are developed in all the Chagai occurrences as continuous or discontinuous haloes around K-zone except in Durbanchah prospect. In Humai prospect an advanced argillic zone is developed around K-Zone. Propylitic alteration has also developed in all of the occurrences and encircles the quartz sericitic alteration.

INTRODUCTION

Several porphyry copper prospects have recently been found in the Chagai calc-alkaline magmatic belt of the Eruptive Zone of Baluchistan ranging in age from Cretaceous to Pleistocene. The Chagai Belt trends east-west and is about 500 km long and 140 km wide. It extends from Siah-koh near Naushki in the east to Chah Muhammad Raza on Pakistan Iran border in the west (fig. 1). At least 10 porphyry copper occurrences have been found in the belt, out of which, 7 are selected for the present comparison, because relatively more geologic work has been done on them. These include well known Saindak porphyry copper deposit and lesser known porphyry copper prospects of Kohe Dalil, Durbanchah, Humai, Missi, Ziarat Pir Sultan and Dasht-e-Kain. The eastern part of the Chagai belt between the Chagai hills and Siah Koh is covered by Recent and Subrecent alluvial deposits and may also be hosting a few hitherto unknown porphyry prospects (Ahmed et al., 1982).

The hydrothermal alteration, developed around all of the prospects, is important in ore mineral association. Three hydrothermally altered zones, namely potassium silicate, quartz sericitic and propylitic, have been identified in almost all of the porphyry copper occurrences in the region. However, the argillic and peripheral zones as described by Lowell & Guilbert (1970) are not developed anywhere. In this paper an attempt has been made to compare the alteration zones in various prospects of the Chagai Belt.

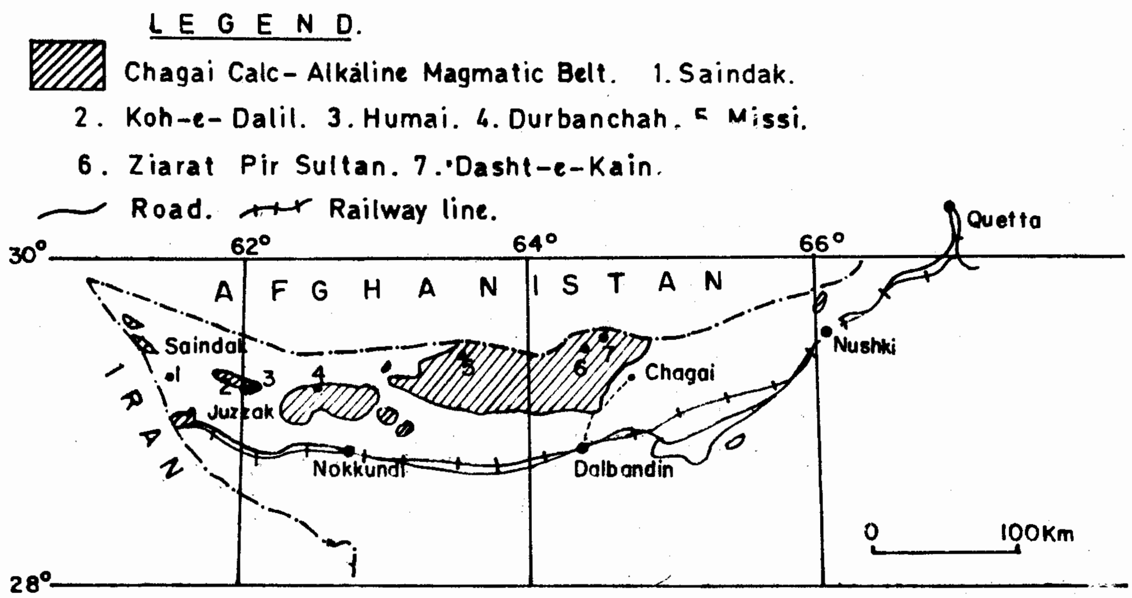

Fig. 1. Map of part of Pakistan showing location of various porphyry copper prospects, Chagai district, Baluchistan.

REGIONAL GEOLOGY

The Chagai Belt is believed to be formed due to northward subduction of an oceanic lithosphere under the southern leading edge of Afghan micro-continental plate and may be considered continental margin of the Andean type (Sillitoe, 1972).

The oldest rock suite developed in the Chagai Belt is a submarine stratified volcanic and volcanoclastic, calc-alkaline suite known as Sinjrani Volcanic Group (Hunting Survey Corporation, 1960) which is late Cretaceous in age and is composed mainly of andesitic flows, agglomerates, volcanic conglomerate, tuffs and subordinate amounts of limestone, shale and sandstone. The total thickness of the Group is about 10,000 m (Arthurton, et al., 1979) and it has been intruded by the Chagai intrusions (Hunting Survey Corporation, 1960) which range in size from cupolas and stocks to batholiths and include granite, quartz-monzonite, granodiorite, monzonite, diorite, quartz diorite and gabbro. These intrusions are as old as pre-Late Cretaceous (Hunting Survey Corporation, 1960) and as young as Lower Miocene (Sillitoe, 1977; and Siddqui, 1984). Multiple episodes continued in pulsatory fashion were responsible for the emplacement of the volcanic and plutonic rocks of the region (Arthurton et al., 1979).

The Chagai Belt is very important for its economic minerals. The magmatic rocks are intimately associated with deposits of copper, and iron including the porphyry copper skarn copper and/or iron, manto-type copper, vein-type copper and volcanogenic sulphur and stratiform iron. In addition, zinc- and silver-rich Kuroko type sulphide deposits have also been reported.

HYDROTHERMAL ALTERATION

Hydrothermal alteration in each of the porphyry copper occurrences is developed concentrically. In each occurrence, the potassium silicate alteration zone (K-zone) occurs in the centre, followed outwards by the quartz sericitic and the propylitic alteration zones, but none of the occurrences has regular argillic and peripheral zones proposed by Lowell and Guilbert (1970). The zones developed are discussed below.

1. **Potassium Silicate Alteration Zone (K-zone):**

This type of alteration zones occur centrally within each intrusive porphyry ore prospect; but at Saindak and Kohe Dalil, some of the adjacent wall rock sediments and, at Durbanchah, microdioritic wall rocks have also undergone such alteration (table 1).

At Saindak, K-alteration is mainly associated with three comagmatic tonalite porphyry stocks, named respectively, north, south and east stocks according to their positions. Potassium silicate alteration at Saindak is characterized by biotite, K-feldspar, quartz anhydrite, epidote, chlorite, tourmaline, pyrite, chalcopyrite, magnetite and minor molybdenite, Biotite occurs disseminated or as replacement of primary hornblende, in veinlets with other minerals and alone on partings. Southern body has quartz-magnetite type of K-alteration in the centre whereas in the eastern ore body, K-alteration is superimposed by retrograded quartz sericitic alteration (Sillitoe et al., 1977).

At Kohe Dalil, potassium silicate alteration is generally associated with five tonalite porphyry stocks, some of the adjacent wall rock sediments have also undergone the same alteration. K-alteration. in this prospect, is characterized by biotite, K-feldspar, quartz, tourmaline, magnetite, pyrite, chalcopyrite and minor molybdenite. The main eastern body is centered by quartz-magnetite type of K-alteration, and retrograded quartz sericitic alteration has developed towards its eastern boundary. At Kohe Dalil prospect, K-zone is generally destroyed by the emplacement of post-mineralization dacite porphyry intrusions (Khan & Ahmed, 1982).

At Humai prospect, potassium silicate alteration is restricted to a dacite porphyry stock and is represented by chlorite after biotite, quartz, magnetite and minor pyrite and chalcopyrite (Sillitoe, 1978).

The largely concealed Durban Chah porphyry copper prospect has a small outcrop of K-alteration, restricted in a marginal part of alluvial depression bordered by andesites of Sinjrani Volcanic Group. Potassium sillicate alteration at this prospect is associated with a dacite porphyry stock and is represented by biotite, K-feldspar, quartz, chlorite, and minor pyrite, chalcopyrite and molybdenite (Khan, 1975; Sillitoe, 1979).

At Ziarat Pir Sultan, alteration is mainly associated with two tonalite porphyry stocks and K-alteration is exhibited by biotite and quartz with minor pyrite, chalcopyrite and molybdenite (Sillitoe, 1979).

At Missi prospect, potassium silicate alteration zone has not been observed on the surface but it is expected to occur below the quartz sericitic zone (Sillitoe, 1978).

At Dashte Kain, alteration is mainly associated with two tonalite porphyry stocks, named eastern and western stocks by position. The later stock is invaded by an intrusive breccia pipe. K-alteration is centered in each stock and is characterized by biotite, K-feldspar, anhydrite, chlorite, carbonate, sericite and kaolinite with minor magnetite, pyrite, chalcopyrite, pyrrhotite, molybdenite, bornite and enargite. A considerable part of the K-zone of western stock has been superimposed by retrograded quartz sericitic alteration (Siddiqui, 1980).

2. **Quartz Sericitic or Phyllic Alteration Zone:**

Quartz sericitic alteration zone has developed as continuous and/or discontinuous halos around potassium silicate alteration zone in all of the porphyry Cu settings of the Chagai belt, except at Durbanchah where it has not been encountered, whereas at Humai an advanced argillic zone has been found around K-zone (table 1).

Quartz sericitic alteration at Saindak ranges from pervasive to veinlet-controlled and comprises quartz, sericite, anhydrite, pyrite and minor chalcopyrite and molybdenite. Pyrite is locally abundant and may attain more

TABLE I. COMPARISON OF VARIOUS PORPHYRY COPPER PROSPECTS OF CHAGAI CALC–ALKALINE MAGMATIC BELT, CHAGAI DISTRICT, BALUCHISTAN, PAKISTAN.

PROSPECT	PREORE HOST ROCKS	AGE	MINERRALIZED ROCK	MINERALIZATION AGE (M.Y.)	HYDROTHERMAL ALTERATION ZONES: POTASSIUM SILICATE ALTERATION MIN. ASSEMB.	QUARTZ SERICITIC ALTERATION MIN. ASSEMB.	PROPYLITIC ALTERATION MIN. ASSEMB.	ALTERED AREA
SAINDAK	Amalaf Fm: Silt stone, shale, sand stone and tuff.	Oligocene	Tonalite porphyry. (Three bodies)	20.3 ± 0.8 [1]	Biotite, anhydrite, k-feldspar and minor, quartz, magnetite and tourmaline.	Quartz, sericite, anhydrite, pyrite, chalcopyrite (minor) and molybdenite.	Chlorite, epidote, albite, calcite (minor), anhydrite and pyrite.	3 Km^2
KOH-E-DALIL	Juzzak Fm: Andesitic, agglomerate, tuff and lava flows.	Paleocene to Miocene.	Tonalite porphyry. (Five bodies)	Not determined	Biotite, k-feldspar, magnetite, pyrite (minor), chalcopyrite and molybdenite.	Quartz, sericite, pyrite and chalcopyrite.	Chlorite, epidote, pyrite and calcite.	18 Km^2
HUMAI	Juzzak Fm: Volcano-sediments, andesite, andesitic agglomerate and tuff.	Late Cretaceous to Miocene.	Dacite to andesite porphyry. (One body)	Not determined	Quartz, magnetite, chlorite, pyrite and chalcopyrite.	Aphenitic silica, alunite Sericite sulphur (native) and pyrite.	Chlorite, epidote and pyrite.	1.1 Km^2
DURBUNCHAH	Chagai Intrusions: Granodiorite and diorite. Sinjrani Volcanics: Andesite.	Late Cretaceous to Miocene.	Dacite porphyry. (One body)	10.9 ± 0.7 [2]	Biotite, k-feldspar, quartz and minor pyrite, chalcopyrite and molybdenite.	Absent	Chlorite, epidote and carbonates.	8.75 Km^2
MISSI	Chagai Intrusions: Granodiorite and diorite. Sinjrani Volcanics: Andesite.	Late Cretaceous to Miocene.	Granodiorite. (One body)	Not determined	Absent	Sericite, quartz, pyrite minor chalcopyrite and molybdenite.	Chlorite, epidote, calcite, tourmaline, quartz, furqoise and delafossite.	1 Km^2
ZIARAT PIR-SULTAN	Chagai Intrusions Granodiorite and diorite. Sinjrani Volcanics: Andesite.	Late Cretaceous to Miocene.	Adamillite and tonalite porphyry. (Two bodies)	21.0 ± 0.7 [2]	Biotite, quartz, pyrite and chalcopyrite.	Quartz, siricite and pyrite.	Chlorite, epidote and pyrite.	2.5 Km^2
DASHT-E-KAIN	Chagai Intrusions: Hornblende diorite, minor gabbro. Sinjrani Volcanics: Andesite, andes andesitic tuff and agglomerate.	Late Cretaceous to Miocene.	Tonalite porphyry. Two bodies	31.6 ± 1.2 [3]	Biotite, k-feldspar, quartz, magnetite, chlorite, pyrite, chalcopyrite, molybdenite, bornite and Enargite	Quartz, sericite, kaolinite and pyrite.	Chlorite, epidote, cabonates and pyrite.	3 Km^2

The age of mineralization is after Sillitoe, 1977[1], Breitzman, 1979[2], and Siddiqui 1984[3].

than 10% by volume of the rock (Sillitoe, et al., 1977).

At Kohe Dalil prospect, quartz sericitic alteration coincides with a partially alluvial plain in the middle of a deeply eroded strato-volcano. The sericitization is also partially superimposed on and surrounded by largely propylitized volcanic rocks. The characteristic mineral assemblages of the prospect are quartz, sericite, pyrite and chlorite (Khan & Ahmed, 1982).

At Humai prospect, an advanced argillic alteration zone is developed around K-zone instead of quartz sericitic alteration, which is represented by alunite, quartz, sulphur and pyrite (Sillitoe, 1978).

There is no quartz sericitic alteration zone at Durbanchah, at least on the surface and

K-alteration is directly surrounded by propylitic zone. At Ziarat Pir Sultan, quartz sericitic alteration occurs as a discontinuous halo around K-zone and is exhibited mainly by sericite, quartz and pyrite (Sillitoe, 1979).

Quartz sericitic alteration at Missi prospect is widely developed and characterized by sericite, quartz and pyrite with minor chalcopyrite and molybdenite.

At Dashte Kain, quartz sericitic alteration zone partly encircles the K-alteration and is represented by quartz, sericite and pyrite. At places this alteration is also superimposed over a hydrothermal intrusion breccia. The northern portion of quartz sericitic alteration at Dashte Kain is alluvium covered.

3. Propylitic Alteration Zone:

The propylitic alteration zone is widely developed in all of the porphyry copper settings so far found in the Chagai belt and generally encircles the quartz sericitic alteration zone (table 1).

At Saindak, the area beyond the quartz sericitic zone represents the propylitic alteration and its outer limits were defined as the outer limits of pervasive pyritization. This alteration at Saindak is typified by chlorite, epidote, albite, calcite, anhydrite and pyrite (Sillitoe et al., 1977).

The Kohe Dalil prospect shows this zone around the quartz sericitic alteration zone, mainly associated with andesitic flows and characterized by the presence of chlorite, epidote and carbonate (Khan & Ahmad, 1982).

At Humai propylitic alteration zone is marked by chlorite, epidote and carbonate (Sillitoe, 1978).

The propylitic alteration at Durbanchah is represented by the extensive development of chlorite, epidote and carbonate. At the contact zone the andesite is completely replaced by epidote and thus is a good indicator of mineralized zone in the vicinity (Khan, 1975).

At Ziarat Pir Sultan, this alteration is characterized by chlorite, epidote and pyrite.

At Missi prospect, the propylitic alteration was identified by the presence of chlorite, epidote and calcite.

Propylitic alteration at Dashte Kain is restricted in the pre-ore dioritic and andesitic rocks and is represented by epidote, chlorite, carbonate and pyrite. Epidote generally occurs in the groundmass replacing the plagioclase and ferromagnesian minerals and chlorite has developed after hornblende and biotite. Calcite generally occurs as open space fillings. At places intense epidotization is observed replacing the whole rock (Siddiqui, 1984).

DISCUSSION

All the porphyry copper prospects of Chagai belt are associated with tonalitic to dacitic porphyritic rocks except Missi prospect, which is associated with granodioritic rocks. Hydrothermal alteration has been developed in concentric zonal patterns. The intensity of alteration is generally decreased from the centre in each case as proposed by Lowell and Guilbert (1970).

The presence of porphyritic texture in the host rocks of all the porphyry Cu settings suggest that they have gone through two different physico-chemical environments during their course of emplacement. In deeper environments and at high P,T conditions, larger crystals formed and when the partially crystallized magma further rose up and reached relatively in the shallower environments having low T,P conditions, smaller crystals of the groundmass were formed and consequently a porphyritic texture was developed contemporaneously due to decrease in confining pressure. Over the magma, a vapour phase was released as hydrothermal solution, which is responsible for hydrothermal alteration in the porphyry systems.

Rose (1970) proposed that hydrothermal alteration is generally controlled by the temperature and HCl/KCl ratio in the brines. The alteration in the porphyry copper system is mainly metasomatic/hydrothermal in nature and is in accordance with the mesothermal zone of Lindgren (1933). The alteration at the central zones might be caused perhaps by primary magmatic, highly saline, Na, K, Ca, Cl, brines at about 500-75°C, while the alteration in the outer zone may be produced by the circulation of less saline meteoric water at about 250°C (Sheppard, 1977; Henlay & McNohby, 1978).

The source of metal of porphyry copper setting of the Chagai belt may be the upper basaltic part of the subducted oceanic lithosphere in which massive copper sulphide mineralization, was emplaced during oceanic spreading along mid-Tethyan ridge and subsequently partial melting of the above basalt along with massive copper sulphides, during subduction under the southern margin of Afghan microcontinent produced calc-alkaline magmatism and associated porphyry copper mineralization in the Chagai belt (Sillitoe, 1972).

Small quantities of both copper and molybdenum might have been derived from the wedge of mantle overlying the Benioff zone (Oxburg & Turcott, 1970; Jensen, 1971).

CONCLUSION

Comparison of hydrothermal alteration in the foregoing pages reveals that almost all the prospects exhibit a similar pattern of hydrothermal alteration which is quite comparable with the model proposed by Lowell and Guilbert (1970).

Brines associated with the late magmatic fluid may be responsible for hydrothermal alteration in the central zones and less saline meteoric water is responsible for the alteration in the outer zone in all the porphyry systems of Chagai belt. Copper and other associated metals might have been derived from the subducted basaltic crust and partially may derive from the wedge of the mantle overlying the Benioff zone of Chagai area.

Out of the above porphyry copper settings, only Saindak deposit and to some extent Dashte Kain have been explored and evaluated so far. At Saindak proved copper ore reserves are about 412 million tons and at Dashte Kain estimated reserves are about 300 million tons. Other porphyry copper prospects of the Chagai belt have the alteration area equivalent to Saindak or even more. Thus, huge reserves of copper ore may be obtained from these prospects.

REFERENCES

AHMED, M.U., CHAUDHARY, M.A. & SIDDIQUI, R.H. (1982) Geochemistry and Hydrothermal Alteration of Dasht-e-Khain Porphyry copper/molybdenum prospect, Chagai District, Baluchistan, Pakistan. Rec. Geol. Surv. Pakistan 55, 17p.

ARTHURTON, R.W., AHMED, S.A. & IQBAL, S. (1979) Geological history of the Alem reg-Mashki Chah area, Chagai District, Baluchistan. *In:* Farah, A. & De Jong, K.A. (eds.) "GEODYNAMICS OF PAKISTAN" Geol. Surv. Pakistan. p. 361.

BRITZMAN, L. (1979) Fission track ages of intrusives of Chagai District Baluchistan Pakistan. M.A. dissertation Dartmouth College, Hanover New Hampshire USA. (Unpublished).

HENLEY, R.W. & McNABBE, A. (1978) Magmatic Vapour plumes and ground water inter action in porphyry copper emplacement. Econ. Geol. 73, pp. 1-20.

HUNTING SURVEY CORPORATION LTD. (1960) RECONNAISSANCE GEOLOGY OF PART OF WEST PAKISTAN. Colombo Plan Cooperative Project, Toronto, Canada.

JENSON, M.L. (1970) Province of Cordilleran intrusives and associated metals. Econ. Geol. 66, pp. 34-42.

KHAN, A.L. (1975) A preliminary report on the discovery of sulphide mineralization in Durbanchah and Mashki Chah areas Chagai District, Baluchistan. Inf. Rel. Geol. Surv. Pakistan 90, 6p.

KHAN, & AHMED, W. (1982) Reconnaissance geology of Kohe Dalil porphyry copper prospect, Chagai District, Baluchistan. Geol. Surv. Pakistan, Unpublished report, 9p.

LINDGREN, W. (1933) MINERAL DEPOSITS. McGraw Hill, New York.

LOWELL, J.D. & GUILBERT, J.M. (1981) Lateral and vertical alteration mineralization zoning in porphyry ore deposits. Econ. Geol. 65, pp. 373-408.

OXBURG, E.R. & TURCOTTE, D.L. (1970) Thermal structure of island areas. Bull. Geol. Soc. Amer. 81, pp. 1665-88.

ROSE, S.W. (1970) Zonal relation of wall rock alteration and sulphide distribution at prophyry copper deposits. Econ. Geol. 65, pp. 920-36.

SHEPPARD, S.M.F. (1981) Identification of the origin of ore-forming solutions by the use of stable isotopes. *In:* Mitchel, A.H.G. & Garson, M.S. (eds.) MINERAL DEPOSITS AND GLOBAL TECTONIC SETTINGS. Academic Press, London. 405p.

SIDDIQUI, R.H. (1984) Petrographic and ore microscopic study of Dashte Kain porphyry copper/molybdenum prospect Chagai District, Baluchistan, Pakistan Inf. Rel. Geol. Surv. Pakistan 213, 26p.

SILLITOE, R.H. (1972) A plate tectonic model for the origin of porphyry copper deposits, Econ. Geol. 67, pp. 189-97.

——————— (1975) Metallogenic evolution of a collisional mountain belt of Pakistan. Rec. Geol. Surv. Pakistan. 34: 16p.

——————— (1978) Evolution of mineral prospect and suggestion for exploration in Baluchistan Pakistan. U.N. Report (unpublished).

——————— & Khan, S.N. (1977) Geology of Saindak porphyry copper deposit, Pakistan. Trans. Inst. Min Metall. Sec. B. 86, pp. 27-42.

Manuscript received 30.9.1986
Accepted for publication 31.12.1986

ACTA MINERALOGICA PAKISTANICA
VOLUME 2 (1986) pp.107 - 114.

PARAGENETIC AND PETROCHEMICAL STUDY OF K-SILICATE ALTERATION AND HYPOGENE MINERALIZATION OF DASHTE KAIN PORPHYRY Cu–Mo PROSPECTS, BALUCHISTAN.

REHANUL HAQ SIDDIQUI, MUSHTAQ AHMED CHAUDHARY & MALIK ABDUL HAFEEZ

Geological Survey of Pakistan, Sariab Road, Quetta, Pakistan.

ABSTRACT:– Potassium silicate alteration and copper and molybdenum mineralization is mainly centered in two tonalite porphyry stocks at Dashte Kain porphyry copper prospect. The following paragenetic sequence is suggested for K-silicate alteration in the western tonalite porphyry stock:

biotite – K-feldspar and quartz (quartz continues to form throughout the course of alteration) – sericite – kaolinite – rutile – chlorite – anhydrite and calcite.

Hypogene mineralization at Dashte Kain starts from a depth of 6.5 m and extends upto 290 m depth. The following paragenetic sequence is suggested for hypogene mineralization:

titanomagnetite – magnetite – pyrrhotite – molybdenite : pyrite – chalcopyrite & pyrite – pyrite.

Petrochemical study of K-altered tonalite porphyry suggests that brines responsible for K-silicate alteration were rich in K, Na, Mg, Fe, Cl, S, Cu and Mo ions and the alteration was mainly controlled by K-metasomatism.

INTRODUCTION

About ten porphyry type copper settings have recently been found in Chagai belt of northwestern Baluchistan. Dashte Kain is one of them, on which preliminary exploration and evaluation work has been completed. The present paper is a brief study of paragenesis and petrochemistry of potassium silicate alteration and hypogene mineralization of the western tonalite porphyry stock.

Dashte Kain prospect is located 35 km northwest of Chagai, as given in Siddiqui & Khan (1986). Approximate co-ordinates of the prospect are 29° 33′ N and 64°E′ on the topographic sheets nos. 34 C/6 and 34 C/10.

GEOLOGICAL SETTING

Dashte Kain porphyry copper prospect occurs in the northeastern part of the Chagai calc-alkaline magmatic belt of eruptive zone of Baluchistan. This belt is about 500 km in length and about 140 m in width, and has been constructed on a convergent plate margin formed by the northward subduction of oceanic lithosphere below the southern leading margin of Afghan microcontinent. Therefore, it may be considered a continental margin of Andean type (Sillitoe, 1972).

The oldest rock unit in the Chagai belt is a submarine volcanic and volcanoclastic, calcalkaline suite, known as Sinjrani Volcanic

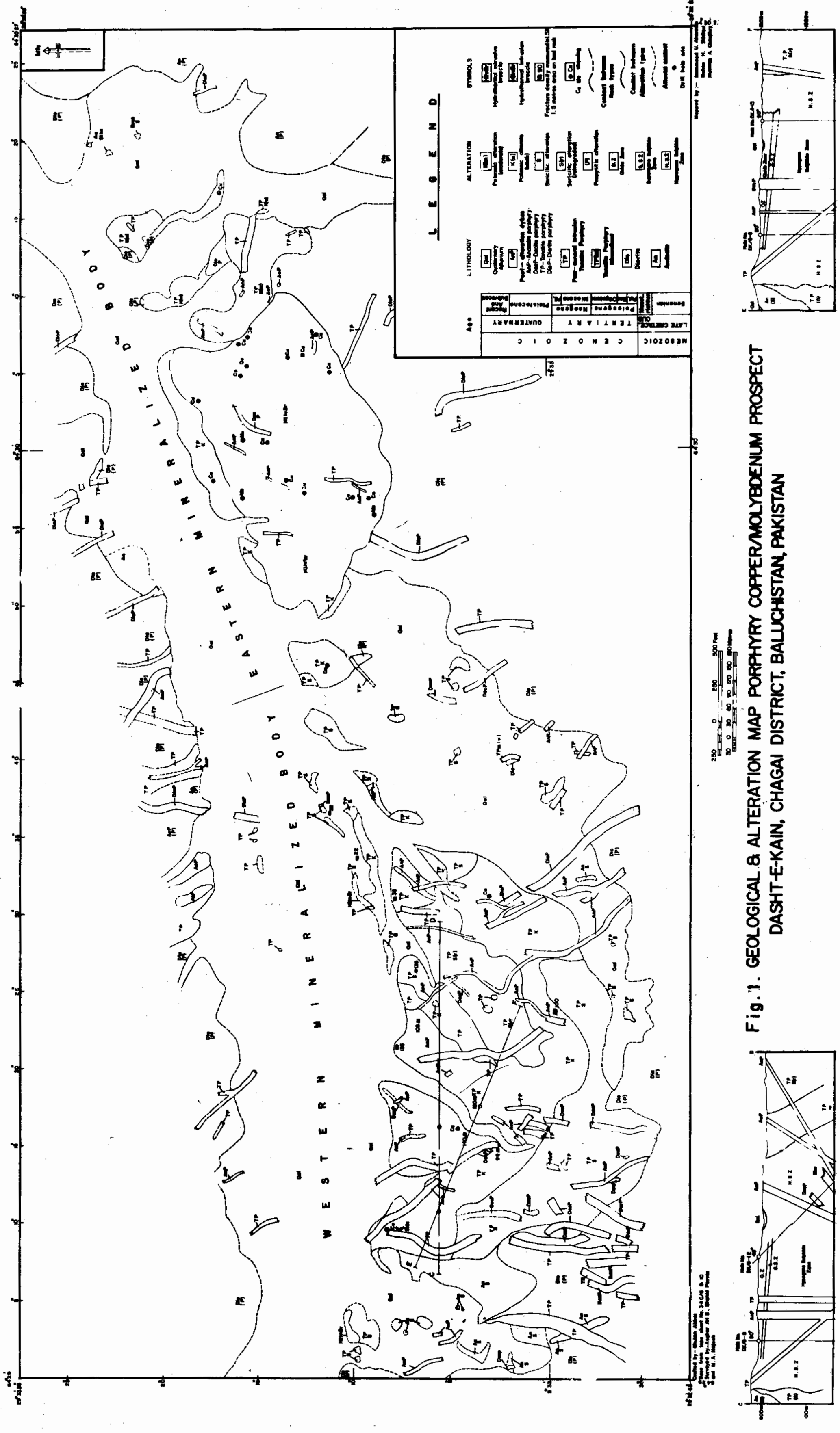

Fig. 1. GEOLOGICAL & ALTERATION MAP PORPHYRY COPPER/MOLYBDENUM PROSPECT DASHT-E-KAIN, CHAGAI DISTRICT, BALLUCHISTAN, PAKISTAN

Group (Hunting Survey Corporation, 1960), which is late Cretaceous in age and composed mainly of stratified intercalation of andesitic flows and pyroclastic rocks including tuff, agglomerate, volcanic conglomerate with subordinate amount of basalt, limestone, shale and sandstone. The Sinjrani Volcanic Group is intruded by the Chagai Intrusions (Hunting Survey Corporation, 1960) during late Cretaceous to Miocene, representing many phases of intrusions including granite, quartz monzonite, granodiorite, quartz diorite, tonalite, monzonite, diorite and gabbro.

GEOLOGY OF THE PROSPECT

At Dashte Kain, hydrothermal alteration is mainly associated with two tonalite porphyry stocks elongated in ENE direction and named as eastern and western stocks geographically (Ahmed et al., 1985). These stocks are intruded into the diorite cupola, related to a composite parent batholith magmatically differentiated into quartz monzonite, monzonite and diorite (Siddiqui, 1984). This composite batholith itself is intruded into the Sinjrani Volcanic Group. The eastern tonalite porphyry stock is invaded by an eastwest trending intrusive breccia pipe and both the stocks are also transected by a swarm of NW and NE trending post-mineralization dykes, which are tonalitic, dacitic, dioritic and andesitic in composition and porphyritic in texture.

POTASSIUM SILICATE ALTERATION

In the western tonalite porphyry stock of Dashte Kain prospect, potassium silicate alteration zone stretches over an east-west elongated area, about 900m x 400m, which has been surrounded by quartz sericitic alteration towards its western and southern side whereas its eastern and northern side is largely alluvium covered. K-silicate zone towards the eastern side is partly superimposed by retrograded quartz sericitic alteration. K-alteration is also destroyed by a swarm of NW– and NE– trending, post-alteration dykes. The central north portion of the K-zone is also invaded by an unaltered and north-easterly elongated tonalite porphyry intrusion.

Potassium silicate alteration in the western stock is mainly represented by secondary biotite, K-feldspar, quartz and minor sericite, kaolinite, chlorite, calcite, anhydrite and rutile.

The secondary biotite may occur as books, biotite pseudomorphs after hornblende (fig. 2) and partly altered hornblende. Biotite also occurs as fine grained disseminations and patches, as irregular shreds and stringers (fig. 2). At places it is partially or completely chloritized. K-feldspar occurs as microperthite and accompanied with quartz in veins. It is also found as replacement of plagioclase in groundmass. Quartz occurs as equant grains in veins upto 15 cms thick and also in veinlets and microveinlets. Sericite and kaolinite occur in groundmass as replacement of plagioclase and rarely in veinlets and on fracture planes. Calcite, anhydrite and chlorite occur in veinlets and on fracture planes and in groundmass. Rutile occurs as anhedral to subhedral disseminations in groundmass and as blades and acicular crystals within chloritized biotite.

PARAGENESIS IN POTASSIUM SILICATE ALTERATION ZONE

Detailed megascopic and petropraphic study of the surface and core samples revealed that the paragenetic sequence has been developed in potassium silicate alteration zone as follows:

Secondary biotite appears as the earliest mineral formed by alteration in the K-zone which replaces the plagioclase & hornblende but does not replace any of the other alteration minerals. It is followed by K-feldspar veinlets which transect the groundmass having secondary biotite. Quartz comes contemporaneously with K-feldspar since it is found interlocked with K-feldspars in veins and veinlets. But it appears to be continuous throughout the course of alteration. K-feldspar is followed by sericite which occurs on fracture planes and sparsely in groundmass replacing the earlier formed

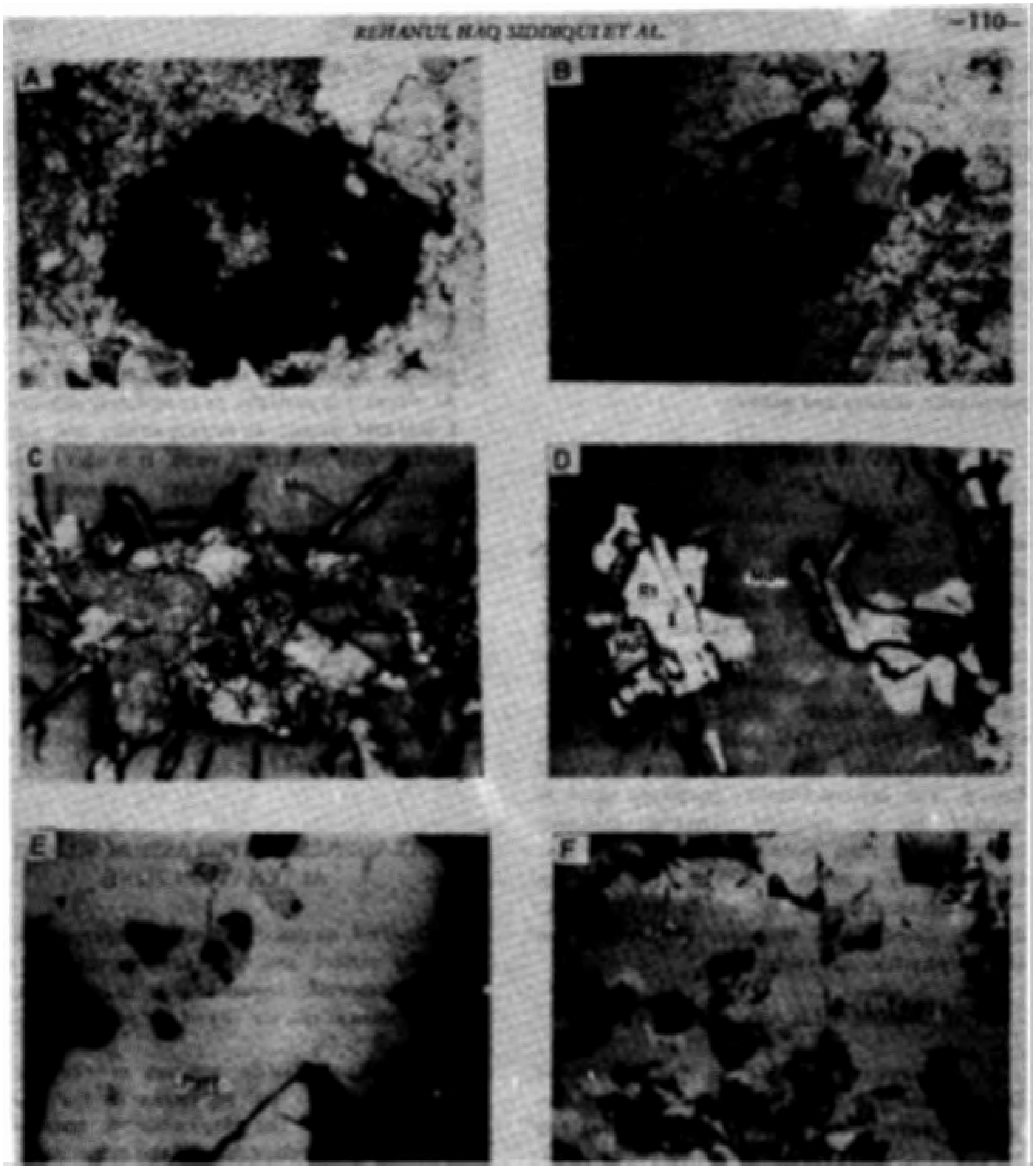

Fig. 2. Photomicrographs displaying features of Dashte Kain rocks. (A) Biotite pseudomorph after hornblende in K-Altered Tonalite porphyry (PPL-X25). (B) Phenocryst of partly biotitized hornblende (Hbn) in K-Altered Tonalite porphyry (PPL-X25). (C) Prismatic grains of molybdenite (Mo) within quartz gangue (PPL-X160). (D) Molybdenite (Mo) replacing rutile (Rt) (PPL-X160). (E) Pyrrhotite enclosing blebs of Chalcopyrite (PPL-X160). (F) Titanomagnetite exhibiting martitization (PPL-X40).

minerals. Kaolinite appeared after sericite because it replaces all the alteration minerals except quartz. Chlorite appeared later because its veinlets transect the groundmass having its predecessor minerals, but before chlorite, rutile might have appeared as it occurs as blades and acicular crystals within the chloritized biotite. Chlorite is followed by anhydrite and calcite which usually occur in veins, veinlets and microveinlets transecting the groundmass having earlier alteration minerals. Both the minerals do not show any textural relationship with each other, and they might be synchronous. Accordingly following paragenetic sequence is suggested for K-silicate alteration:

Biotite – K-feldspar and quartz (quartz continues throughout the course of alteration) – sericite – kaolinite – rutile – chlorite – anhydrite & rutile.

PETROCHEMISTRY

A comparative study of geochemical analysis of fresh and potassium silicate altered tonalite prophyries of Dashte Kain prospect showed a drastic increase in K_2O, MgO, FeO and SO_3 contents in the potassium silicate altered rock, and MnO, CuO and P_2O_5 contents in the same rock have also been slightly increased (table 1). Na_2O, CaO, FeO and TiO_2 contents are found to be considerably decreased in the K-altered rock. Although SiO_2 contents show a minor decrease in the K-altered rock, but normative quartz in the same rock shows a slight increase.

Norms of fresh and K-altered tonalite prophyry exhibit differences (table 1). Normative orthoclase and femic minerals in the K-altered rock are drastically, increased and quartz, apatite, pyrite and other sulphides are also slightly increased. Normative hypersthene and diopside appear as enstatite in the potassium silicate altered rock. Normative magnetite and ilmenite are replaced by hematite and rutile in the K-altered rock. Normative corundum is also introduced.

Table 1. Chemical analysis and CIPW norms of fresh (A) and K–altered (B) tonalite porphyry.

	A	B			A	B
SiO_2	61.85	60.16		Q	16.21	16.65
TiO_2	0.29	0.10		C	–	0.35
Al_2O_3	18.36	13.08		or	12.55	21.99
Fe_2O_3	3.75	5.12		ab	35.86	25.80
FeO	2.27	1.14		an	24.78	10.05
MnO	tr	0.02	di	en	0.29	–
MgO	1.29	4.83		fs	0.03	–
CaO	5.08	2.24	hy	en	3.09	12.12
Na_2O	4.24	3.05		fs	0.40	–
K_2O	2.12	3.62		mt	5.43	–
P_2O_5	0.07	1.84		hm	–	5.11
SO_3	0.22	4.52		pr	0.17	1.92
CuO	0.01	0.03		il	0.55	–
H_2O^+	0.35	0.38		ap	0.16	4.36
H_2O^-	0.12	0.23		rt	–	0.10
Total	100.02	100.36				

HYPOGENE MINERALIZATION

At Dashte Kain hypogene mineralization generally starts from a depth of 6.5m and extends upto 290m depth and this zone is marked by the appearance of pyrite, chalcopyrite, magnetite, titanomagnetite, molybdenite and minor pyrrhotite, enargite and bornite.

Pyrite and chalcopyrite occur as subhedral to anhedral disseminated grains and also as shreds replacing the gangue minerals generally biotite. Chalcopyrite also occurs as blades within chloritized biotite and as blebs within the larger grains of pyrite, pyrrhotite and magnetite (fig. 2). Molybdenite occurs as anhedral to subhedral elongated aggregates, and as disseminations in groundmass. It also occurs in microveinlets and occasionally in veinlets upto 1 cm thick. Enargite occurs as inclusions within the blebs of chalcopyrite. Chalcopyrite occurs within the larger grains of pyrite, pyrrhotite and magnetite. Pyrrhotite, occurs as anhedral disseminations and also in veinlets and microveinlets. Magnetite and titanomagnetite occur as subhedral to anhedral disseminations, veinlets and microveinlets. Both are martitized along their outer boundaries.

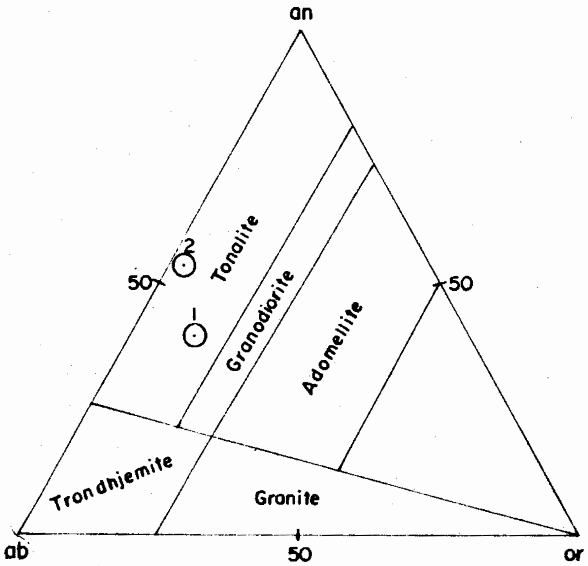

Fig. 3 Ternary plot of normative an-ab-or for tonalite porphyry (1) and diorite (2) of Dasht-e-Kain porphyry Cu-Mo prospect. The compositional boundaries are after O' Connor (1965).

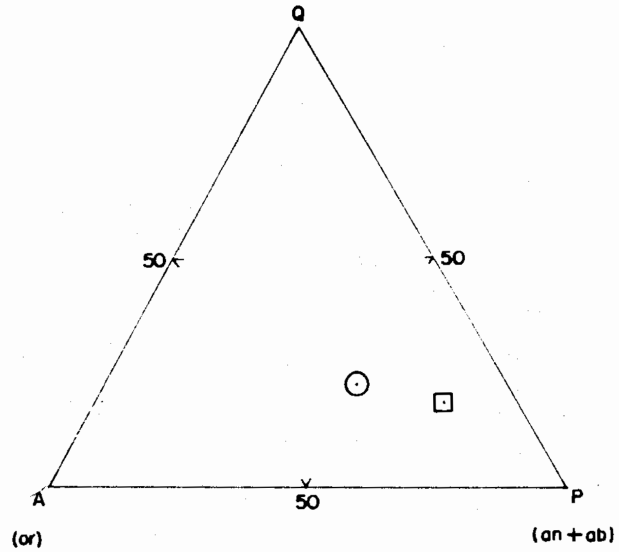

Fig. 5. Ternary plot of normative Q-A-P for fresh (⊡) and K-altered (⊙) tonalite porphyries of Dasht-e-Kain porphyry Cu/Mo prospect.

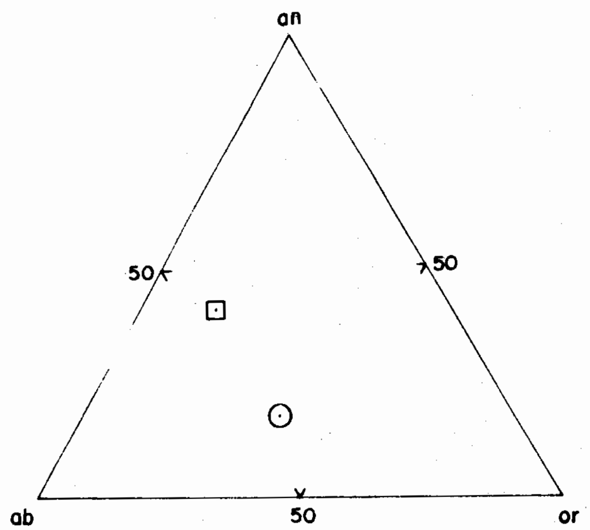

Fig. 4. Ternary plot of normative an-ab-or for fresh (⊡) and K-altered (⊙) tonalite porphyries of Dasht-e-Kain porphyry Cu/Mo prospect.

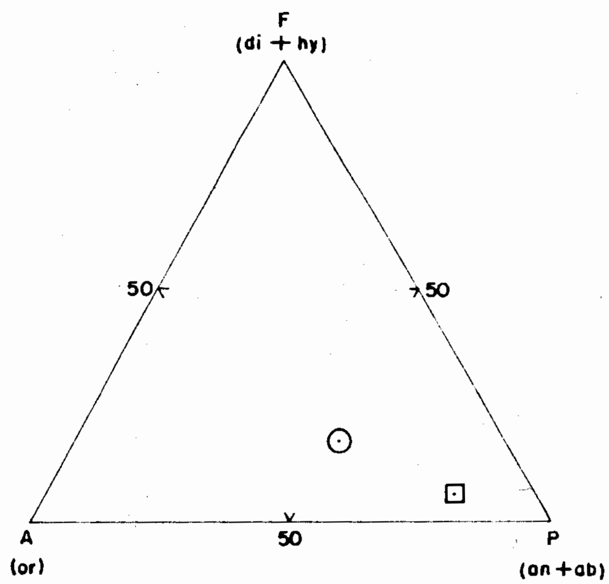

Fig. 6. Ternary plot of normative F-A-P for fresh (⊡) and K-altered (⊙) tonalite porphyries of Dash-e-Kain porphyry Cu/Mo prospect.

PARAGENESIS IN HYPOGENE MINERALIZATION

Detailed megascopic and ore microscopic study of core samples obtained from the three bore holes drilled in the K-zone indicated the following paragenetic sequence for hypogene mineralization. Bornite and enargite are very scarcely developed and appear to be deuteric in origin.

Titanomagnetite and magnetite appears to be the earliest formed minerals in the K-Zone, which have been replaced by pyrrhotite, pyrite and chalcopyrite but does not replace any of the latter. Magnetite was followed by pyrrhotite which was the earliest formed mineral among sulphides. Pyrrhotite has been replaced by pyrite and chalcopyrite but it does not replace them. Molybdenite appeared afterward since it occurs as inclusions in pyrite; and chalcopyrite is also found to be replacing the molybdenite. Subsequently appeared pyrite, which has been replaced by chalcopyrite but at places the later itself has been replaced by pyrite, suggested that pyrite continued to form after chalcopyrite. This suggests the following paragenesis:

Titanomagnetite – magnetite – pyrrhotite – molybdenite – pyrite – chalcopyrite – pyrite.

DISCUSSION

The alteration in the porphyry copper system is mainly metasomatic hydrothermal in nature and is in accordance with the mesothermal zone of Lindgren (1933). The alteration at K-silicate zone might be caused perhaps by primary magmatic highly saline Na, K, Ca, Cl brines at about 500-750°C (Sheppard 1977), Henley and McNabbe (1978).

Petrochemical study of fresh and K-altered tonalite porphyries of Dashte Kain area indicates a slight to marked increase in K_2O, MgO, SO_3 and CuO contents in the K-silicate zone, which is also reflected by a drastic increase in normative orthoclase and femic minerals (table 1) and as secondary biotite and K-feldspar in K-altered tonalite porphyry.

The above study and petrographic, ore microscopic study of K-silicate alteration and hypogene mineralization in the foregoing suggest that brines responsible for K-silicate alteration at Dashte Kain prospect were not only rich in Na, K, Ca, Cl as already mentioned, but also were rich in Mg, Fe, S, Cu, and Mo ions.

The introduction of secondary biotite and K-feldspar as replacement of primary mineral in the groundmass of K-altered tonalite porphyry suggest that potash metasomatism is mainly involved in the process of K-silicate alteration in the area.

CONCLUSION

The following paragenetic sequence is developed in the K-silicate zone at Dashte Kain:

Biotite–K-feldspar and quartz (quartz continues throughout the course of alteration)–Sericite–Kaolinite–Rutile–Chlorite –Anhydrite and calcite.

Study of subsurface drill core samples indicates the following paragenetic sequence for hypogene mineralization in the potassium sillicate alteration zone :–

Titanomagnetite – Magnetite –Pyrrhotite–Molybdenite–Pyrite–Chalcopyrite–Pyrite.

Petrochemical study of fresh and K-altered tonalite porphyry indicates a slight to marked increase in K_2O, MgO, CuO and SO_3 contents in the K-silicate zone. Normative orthoclase and femic minerals are also considerably increased in the same zone, which suggests that brines responsible for K-alteration were rich in Na, K, Mg, Fe, S, Cu and Mo ions and the potash metasomatism was mainly involved in the process of K-silicate alteration.

REFERENCES

AHMED, M.U., SIDDIQUI, R.H. & CHAUDHARY, M.A. (1985) Geological and geochemical exploration and preliminary evaluation of Dashte Kain porphyry copper–molybdenum prospect, Chagai District, Baluchistan. Rec. Geol. Surv. Pakistan 72 (in press).

HENLEY, R.W. & McNABBE, A. (1978) Magmatic vapour plumes and groundwater interaction in porphyry copper replacement. Econ. Geol. 73, pp. 1-20.

HUNTING SURVEY CORPORATION LTD. (1960) RECONNAISSANCE GEOLOGY OF PART OF WEST PAKISTAN. Colombo Plan Cooperative Project, Toronto, Canada.

LINDGREN, W. (1933) MIINERAL DEPOSITS. Mc Graw-Hill, New York.

SHEPPARD, S.M.F. (1977) Identification of the origin of ore forming solutions by the use of stable isotopes. *In:* Mitchell, A.H.G. & Garson M.S. (eds.) MINERAL DEPOSITS AND GLOBAL TECTONIC SETTING. Academic Press, London.

SIDDIQUI, R.H. (1984) Petrographic and ore Microscopic study of Dashte Kain Porphyry Copper/Molybdenum prospect, Chagai District Baluchistan, Pakistan. Inf. Rel. Geol. Surv. Pakistan 213, 26p.

———— & KHAN, W. (1986) A comparison of hydrothermal alteration in porphyry copper mineralization of Chagai calc-alkaline magmatic belt, Baluchistan, Pakistan. This Volume.

SILLITOE, R.H. (1972) A plate tectonic model for the origin of porphyry copper deposits. Econ. Geol. 67, pp. 184-97.

Manuscript received 30.9.1986
Accepted for publication 31.12.1986

ACTA MINERALOGICA PAKISTANICA
VOLUME 2 (1986) pp. 115-118.

REMARKS ON THE UPPER CRETACEOUS BIOSTRATIGRAPHY OF LIBYA

AFTAB AHMAD BUTT

Institute of Geology, University of the Punjab, New Campus, Lahore, Pakistan.

ABSTRACT:— The marine Upper Cretaceous strata are present in northern Libya in the structural units of the Ghadames Basin, the Sirte Basin, the Cyrenaica Platform and the Jabal Al Akhdar. In each structural entity, the stratigraphic terminology is unique.

The Jabal Al Akhdar, north of Cyrenaica Platform, contains the most valuable, though of limited geographical extent Upper Cretaceous marine sequence, where the standard planktonic biostratigraphy can be used from Albian to Maastrichtian among the Hilal Shale (Albian to Coniacian) and the Atrun Limestone (Up. Coniacian to Maastrichtian) along the coastal area of Marsa Al Hilal.

In the Sirte Basin, both planktonic and benthonic zonation can be established in the Sirte Shale (mainly Campanian) and the Kalash Limestone (Maastrichtian). However, in the shallow-water Maastrichtian Waha Limestone or in the upper part of the Lower Satal Formation, stratigraphically important benthonic larger foraminiferal species *Orbitoides apiculatus, Omphalocyclus macroporus* and *Siderolites calcitropokies* are encountered. The Ghadames Basin comprises Maastrichtian Lower Tar Mari where both planktonic and benthonic biostratigraphy similar to that of the Sirte Basin can be recognised. The Cyrenaica Platform constitutes a single benthonic foraminiferal *Bolivina incressata gigantea* Zone in the Maastrichtian "Kalash Limestone" which continues into the neighbouring Sirte Basin.

INTRODUCTION

The Upper Cretaceous foraminiferal biostratigraphy of the Ghadames Basin, the Sirte Basin and the Cyrenaica Platform (fig. 1) falls within the Campanian to Maastrichtian interval. Although these regions have their individual stratigraphic and structural characters due to their depositional and paleogeographic setting, yet there exists a distinct relationship in their regional geological setting (fig. 2). This provides better perception in understanding the depositional style, biostratigraphic framework, facies variation, hydrocarbon habitat, and problems of stratigraphic nomenclature.

The pre-Upper Cretaceous discordance has great influence on the structural configuration and the stratigraphic framework in these regions. The marine Upper Cretaceous deposition marks the beginning of a new phase of structural adjustment in the entire region when greater subsidence is envisaged in the "rift-structure" Sirte Basin showing marked thickness and facies

This paper was presented at the international conference "West African Mesozoic and Cenozoic Stratigraphic Correlations" under the International Geological Correlation Programme, at Morocco in October, 1985.

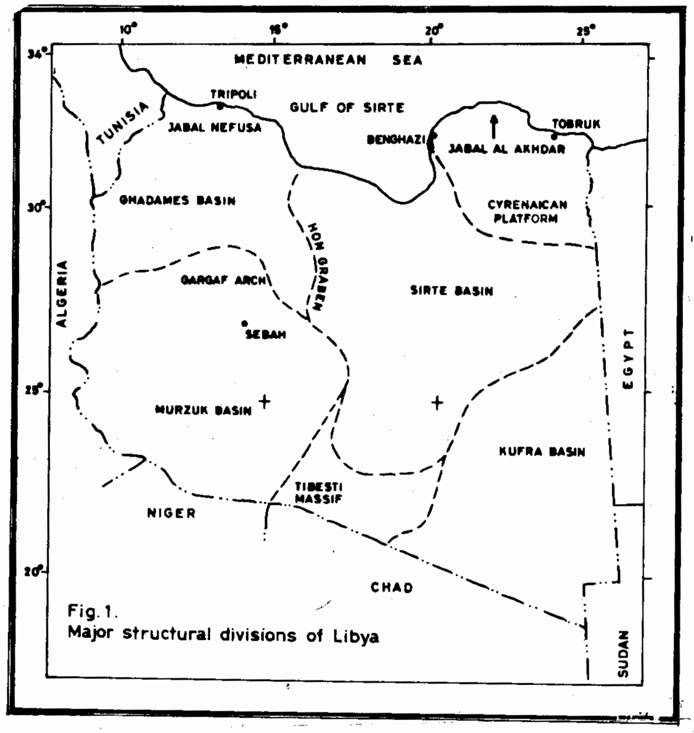

Fig. 1.
Major structural divisions of Libya

variations of sediments over the "horst-graben" blocks of the basin. The adjoining Ghadames Basin on the west and the Cyrenaica platform on the east, however, remained, as shallow shelf areas relative to the actively subsiding Sirte Basin.

North of the Cyrenaica Platform, is the Jabal Al Akhdar Trough, where Albian to Maastrichtian biostratigraphy can be established in the geographically limited extent of the Hilal Shale (Albian to Coniacian) and the Atrun Limestone (Up. Coniacian to Maastrichtian) along the coastal section of the Marsa Al Hilal area.

BIOSTRATIGRAPHY

Sirte Basin

Two benthonic foraminiferal zones, a lower ***Bulimina prolixa*** Zone and an upper ***Siphogenerinoides cretacea*** Zone, while a single planktonic ***Globotruncana plummerae*** Zone or alternatively, ***Globotruncana stuartiformis*** Zone can be recognised in the Campanian Sirte Shale (Butt, 1985).

Globotruncana gansseri Zone, among the standard planktonic zonation, is the most prominent in the Maastrichtian Kalash Limestone, whereas other recognisable planktonic zones include the highest ***Globotruncana conica*** Zone and the earliest ***Globotruncana havanensis (= Globotruncana citae)*** Zone. Only a single benthonic foraminiferal ***Bolivina incrassata gigantea*** Zone can be recognised.

In the shallow-water Maastrichtian Waha Limestone or in the upper part of the Lower Satal Formation, age-diagnostic benthonic larger foraminiferal species ***Orbitoides apiculatus***, ***Omphalocyclus macroprus*** and ***Siderolites calcitropoides*** are present.

Ghadames Basin

In the Ghadames Basin, the Maastrichtian Lower Tar Marl constitutes at first, the ***Golobotruncana gansseri*** Zone containing abundant planktonic foraminifera, while the uppermost part of the formation exclusively contains Maastrichtian benthonic larger foraminiferal species ***Omphalocyclus macroporus*** and ***Siderolites calcitropoides*** (Barr and Weegar, 1972), thus exhibiting both the biofacies similarities as well as the depositional environments with the Sirte Basin.

Cyrenaica Platform

A single benthonic smaller foraminiferal ***Bolivina incrassata gigantea*** Zone extending from the neighbouring Sirte Basin can be recognised in the Maastrichtian "Kalash Limestone" which contains small size globotruncanids of rare occurrence (Butt, 1985).

Jabal Al Akhdar

The most complete marine Upper Cretaceous sequence incorporating several standard planktonic zones from Albian to Maastrichtian is encountered in the coastal region of the Marsa Al Hilal area (Barr and Hammuda, 1971). It is, in fact, an extremely valuable section for the Upper Cretaceous planktonic biostratigraphy in northern Africa. Barr and Hammuda (1971) have divided the section into two formations, the Hilal Shale and the Atrun Limestone comprising the following planktonic zones:

ATRUN LIMESTONE
(Coniac-Maastrichtian)

Abathomphalus mayaroenisis zone
Globotruncana gansseri zone
Globotruncana tricarinata zone
Globotruncana elevata zone
Globotruncana concavata zone

HILAL SHALE
(Albian-Coniacian)

Globotruncana concavata concavata zone
Globotruncana concavata cyrenaica zone
Globotruncana sigali zone
Praeglobotruncana helvetica zone
Rotalipora cushinani zone
Rotalipora appenninica zone
Ticinella roberti zone

HYDROCARBON HABITAT

The factors which govern oil source capacity of a sedimentary rock are the quality of organic

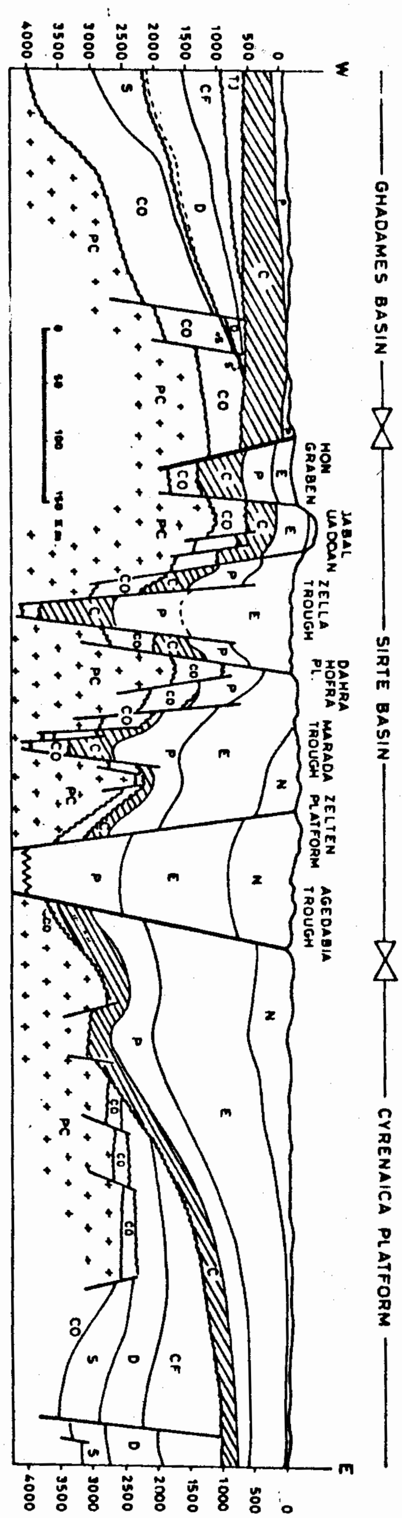

KEY_N=Neogene, E=Eocene, Oligocene, P=Paleocene, C=Cretaceous, TJ=Triassic_Jurassic, CF=Carboniferous, D=Devonian, S=Silurian, CO=Cambrian_Ordovician, PC=PreCambrian (Basement)

Fig. 2. EAST-WEST CROSS-SECTION THROUGH THE GHADAMES BASIN, THE SIRTE BASIN AND THE CYRENAICA PLATFORM (FROM MASSA AND DELORT, 1984). HATCHED AREA DEMONSTRATES THE PALEOGEOGRAPHIC SETTING OF THE STRUCTURAL UNITS DURING THE UPPER CRETACEOUS.

material in the rock, the oil-generative quality of that organic matter, its transformation into hydrocarbon in the deep subsurface under the influence of both subsurface temperature and geologic time and the oxygen-depleted environments of deposition with high sedimentation rate. Generally, the source rock potential quality is attributed to the shales or micrites, provided they have favourable stratigraphic and structural setting as well as the anoxic depositional environments.

In the Sirte Basin, the Upper Cretaceous Sirte Shale (mainly Campanian in age) is the source rock of prime importance because of its favourable geological conditions for the petroleum source bed deposition. This stratigraphic level in the adjacent Ghadames Basin to the west and the Cyrenaica Platform to the east, does not meet the favourable geological indices and, therefore, their source potential quality is precluded. This is primarily due to the structural setting of the entire region during the Upper Cretaceous period. On the other hand, the Silurian Shales in the Ghadames Basin are the prime candidate as a source rock because of favourable stratigraphic and structural setting, while in the Cyrenaican region, much older strata (Juraffic-Lower Cretaceous) meet the favourable geological requirements.

It is, therefore, believed that the structural configuration of these basins and the stratigraphic control is a key factor to evaluate the hydrocarbon habitat in these regions.

CONCLUSIONS

1. The coastal section of the Jabal Al Akhdar represents the most valuable section incorporating several standard planktonic zones. Moreover, the ***Bolivinoides*** lineage provides additional useful biostratigraphic framework.

2. ***Globotruncana gansseri*** Zone among the standard Maastrichtian planktonic biozonation, is widely recognised in the Libyan basins, while the highest ***Abathomphalus mayaroensis*** Zone has restricted application (i.e. Jabal Al Akhdar).

3. Among the benthonic foraminiferal biostratigraphy, a single Maastrichtian ***Bolivina incrassata gigantea*** Zone of global significance is recognised in the Sirte Basin and the Cyrenaica Shelf.

4. In shallow-water Maastrichtian strata, occurrence of benthic larger foraminiferal species ***Oribitoides apiculatus, Omphalocyclus macroporus*** and ***Siderolites calcitropoides*** is of great stratigraphic value.

5. Knowledge of the regional geological setting of the Ghadames Basin, the Sirte Basin and the Cyrenaica Platform is of great significance in evaluating the hydrocarbon potentials of the regions, especially the petroleum source bed deposition.

REFERENCES

BARR, F.T. (1968 a) Late Cretaceous planktonic foraminifera form the coastal area east of Susa (Appollonia), northeastern Libya. Jour. Paleont. **42** (2), pp. 308-21.

__________ (1968 b) Upper Cretaceous stratigraphy of Jabal Al Akhdar, northern Cyrenaica, Libya. ***In:*** Barr, F.T. (ed.) Geology and Archaeology of northern Cyrenaica, Libya. Petrol. Expl. Soc. Libya. Publ., Tripoli, pp. 131-47.

__________ (1972) Cretaceous biostratigraphy and planktonic foraminifera of Libya. Micropal. **18**, (1), pp. 1-46.

__________ **& HAMMUDA, O.Š. (1971)** Biostratigraphy and planktonic zonation of the Upper Cretaceous Atrun Limestone and Hilal Shale, northeastern Libya. Proc. 2nd Plankt. Conf., Rome, pp. 27-38.

__________ **& WEEGAR, A.A. (1972)** Stratigraphic nomenclature of the Sirte Basin, Libya. Petrol. Expl. Soc. Libya, Publ., Tripoli, pp. 1-179.

BUTT, A.A. (1985) Upper Cretaceous biostratigraphy of the Sirte Basin, northern Libya. (ABSTRACT) IX Micropal. Colloq. Paris (1983) "Geologie Mediterraneenne" (France).

MASSA, D. & DELORT, T. (1984) Evolution du bassin de Syrte (Libye) du Cambrien au Cretace basal. Bull. Soc. Geol. France, Ser. 7, **26**, (6), pp. 1087-96.

Manuscript received 30.11.1986
Accepted for publication 31.12.1986

ACTA MINERALOGICA PAKISTANICA
VOLUME 2 (1986) pp. 119-126.

SEDIMENTARY FACIES ASSOCIATIONS IN ORDOVICIAN AND SILURIAN ROCKS OF THE GALA AREA, SOUTHERN UPLANDS, SCOTLAND.

AKHTAR MOHAMMAD KASSI

Geology Department, University of Baluchistan, Quetta, Pakistan.

ABSTRACT:– The Gala area comprising turbidites of the Ordovician and Silurian age has been subdivided into six contrasting zones of facies associations based on sedimentary structures and Bouma sequences. These associations show sedimentary environments ranging from the inner to outer-fan and basin plain environments. It is suggested that the area as a whole represents at least three major progressions and regressions of the turbidite fans.

INTRODUCTION

The Gala area (fig. 1) is located in the southeast Scotland and the studied area covers the Northern Belt and part of the Central Belt of the Southern Uplands of Scotland (Peach & Horne, 1899). It is composed of greywackes interbedded with shales, silstones, conglomerates and black shales. The strata are mostly steeply dipping and the strike is NE–SW. It has been sugggested (McKerrow et al., 1977) that the lower Palaeozoic succession of the Southern uplands represent an accretionary prism in which contrasting turbidite sequences are separated by major strike faults. Fault bounded sequences become progressively younger to the south, whilst, individual fault blocks display an overall northward younging. The sequences range in age from upper Ordovician (mid-Caradoc) to lower Silurian (high Llandovery or perheps Wehlock).

The rocks are mainly turbidites (greywackes) of contrasting lithological characters and have been subdivided into verious litho-stratigraphic units (Walton 1955; Kelling 1962; Floyd 1975; Hepworth 1981; Kassi 1984) based on lithology, petrology and faunal evidence. In the studied area the Ordovician succession was subdivided (Kassi 1984) into 2 formations – the Falahill and Heriot Formations and the Silurian succession into four formations, namely the Hazelbank, Fountainhall, Buckolm and Selkirk Formations. It was observed that the rocks of the area although possessing comparable petrographic characters, show contrasting facies and facies associations related mainly to the processes of sedimentation and their responses rather than to the source of detritus. An attempt has been made to interpret the sedimentary facies and facies associations and some examples of depositional cycles within the area. As the area is very poorly exposed and the exposures very restricted and laterally discontinuous, interpretation is necessarily limited and tentative.

REGIONAL FACIES ANALYSIS

The area has been subdivided into zones of contrasting facies associations (fig. 1 & 2). Sedimentary structures and details of the Bouma sequences (Bouma, 1962) allowed recognition of A1, C1, C2 and D1 facies of Mutti & Ricci-Lucchi (1975). Brief details of each facies are given below :

Facies A1: Thick (up to several metres), massive, chaotic and disorganised conglomerates with profusion of rip-up clasts.

Facies C1: Thick (40 cm to 5 m), massive or poorly graded Tae or Ta (?bc) sequences.

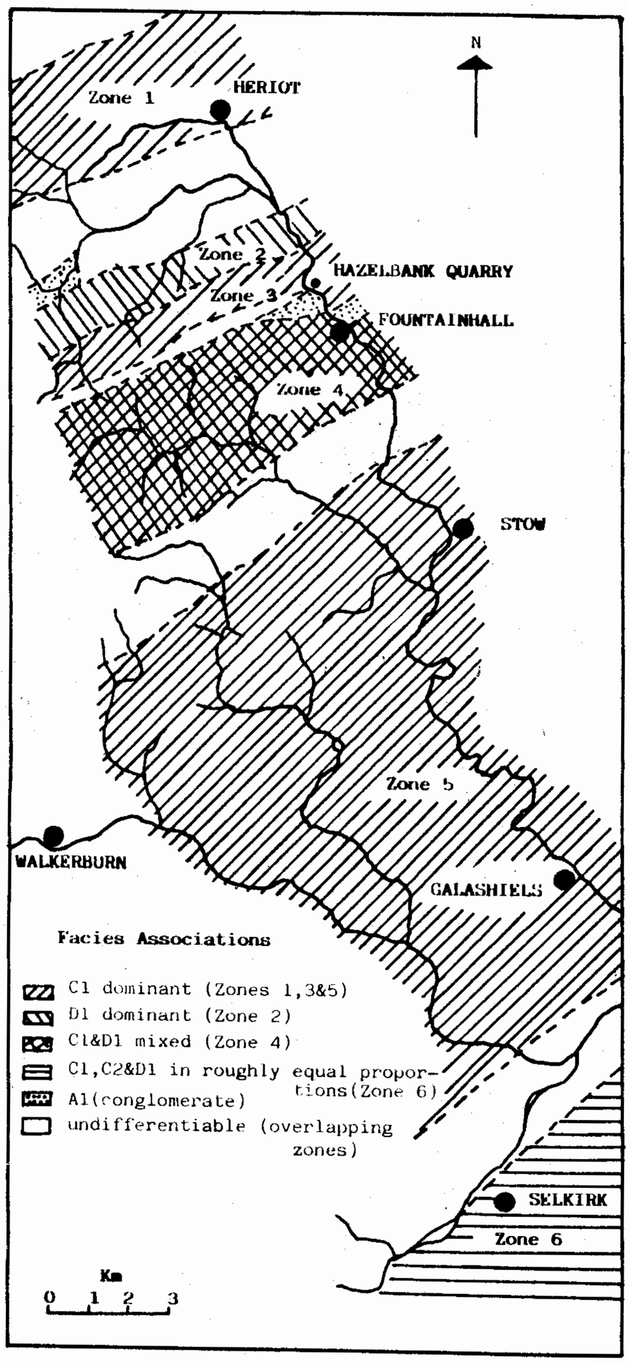

Fig.1:Map of the Gala area showing facies associations. C1,C2,D1&A1 are explained in text.

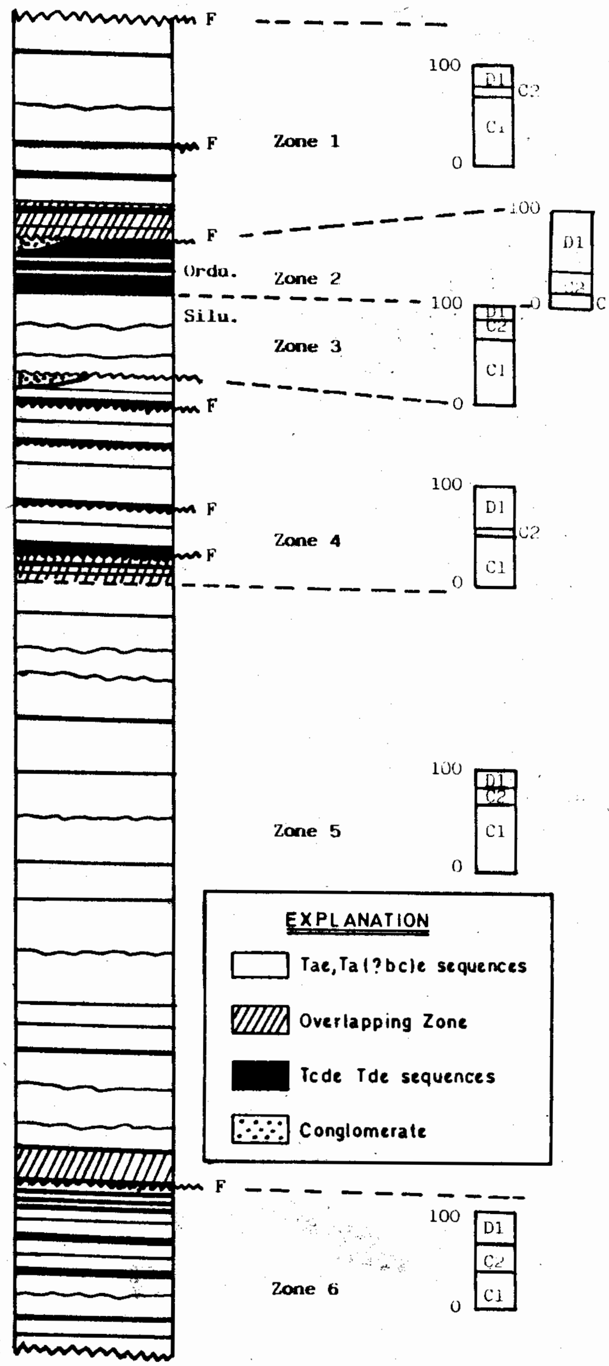

Fig. 2. Idealized columnar profile of the whole area with histograms of facies proportions. C1,C2, D1 and A1 are explained in text. Tae, Tabce, Tcde and Tde represent Bouma sequences (Bouma 1962).

Facies C2: Medium thick (10 to 40 cm), well graded Tabcde, Tbcde, Tcde and Tacde sequences.

Facies D1: Thin bedded (mostly over 10 cm), Tcde, Tde and T?bcde sequences.

The distribution of various facies was plotted on the map and boundaries between the most contrasting facies associations (fig. 1) assessed by visual discrimination. The zones are not sharply bounded and gradational zones of overlap are indicated. Histograms of the proportion of facies in each zone (fig. 2) show strongly contrasting facies associations. These contrasts reflect progressive changes in depositional environments through the succession. Dominant younging direction is northwards and minor folding and faulting within each block is considered not to be so intense as to influence the distribution of the second order cycles or "megasequences" (Ricci-Lucchi, 1975) and have accordingly been ignored. Detailed characteristics of the zones are as follows:

Zone 1

In this zone the rocks consist mainly of very thick (upto several metres) Tae and Ta(?bc)e sequences (Bouma, 1962) which are mostly poor graded but generally well graded towards the top of the sequences. The sequences are commonly amalgamated and localized horizons of very coarse texture can be observed. Tcde, Tde sequences are also present and may attain thicknesses of up to several metres. In some places fining-upwards cycles on a minor scale (7 m thick; Ricci-Lucchi, 1975) may be observed. The sole marks include logitudianl ridges and flute marks of parabolic narrow type. Thick bedding (40 cm to 5 m), occasional occurrence of lenticular bedding, very coarse grain size, common occurrence of amalgamated units and profusion of mud clasts in thick Tae sequences suggest channel fill deposits. The lateral discontinuity of exposures does not allow observation of the detailed geometry of the sequences. Facies C1 is most abundent (70%; fig. 2) suggesting a channelized mid-fan facies association. In this zone chaotic conglomerates (Facies A1) occurs attaining thickness of nearly 500 m. These conglomerates are thick, massive, obscurely bedded and have profusion of rip-up clasts which locally attain a length of several cm. Uneven sandy horizons reaching up to 1 m in thickness occur locally. No sedimentary structures were observed. These conglomerates are formed by mass deposition of extremely concentrated dispersions (Mutti & Ricci-Lucchi, 1975) and represent an inner-fan association.

Zone 2

In this zone thin "base-cut-out" Tcde, Tde sequences dominate with a subordinate proportion of medium thick (10 cm to 40 m) Tabcde sequences. Thick (40 cm to 5 m) and amalgamated Tae sequences are the least abundant in this zone. Sole marks are rare. Faning-upwards cycles of minor scale (a few metres thick) may be found. In this zone facies D1 is the most abundant and found in up to 60% of the exposures. Facies C2 is subordinate and C1 least abundant (fig. 2). This association suggests an outer-fan (fringe) environment. The columnar profile of a locality in this zone (fig. 7) gives an instance of the association of this kind.

Zone 3

The rocks of this zone consist of thick (upto several metres) Tae, and Ta(?bc)e sequences which are commonly amalgamated. The sequences are poorly graded, lenticular and very coarse grained with a profusion of rip-up clasts. Some of the sequences show reverse grading near the base and normal grading near the top (C1 of Mutti & Ricci-Lucchi, 1975). Some sequences are relatively thin and well graded Tabce, Tabcde and Tcde which represent 'classic' turbidites (C2 of Mutti & Ricci-Lucchi, 1975). These facies represent a channelized mid-fan facies association. Occasional pockets of thin Tcde, Tde sequences ranging between 40 cm and 2 m in thickness are present within the thick Tae sequences which probably represent overbank deposits. Sole marks include groove casts, longitudinal ridges and bounce, brush

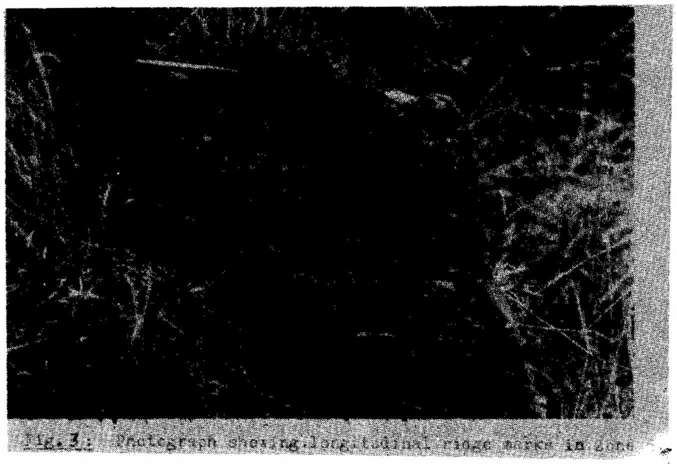

Fig. 3: Photograph showing longitudinal ridge marks in Zone

Fig. 4: Photograph showing irregular sole marks in Zone 5.

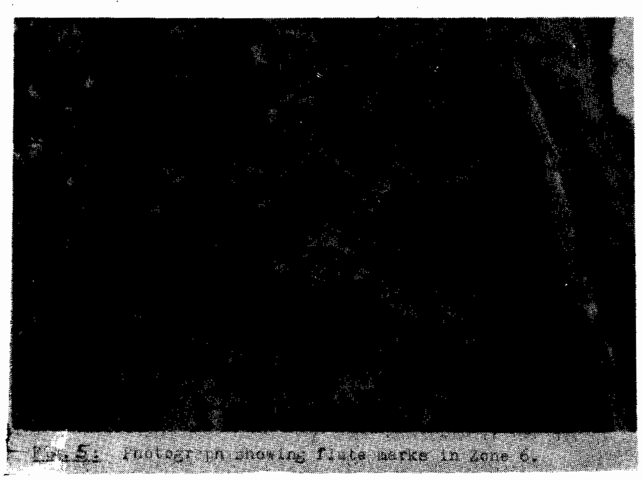

Fig. 5: Photograph showing flute marks in Zone 6.

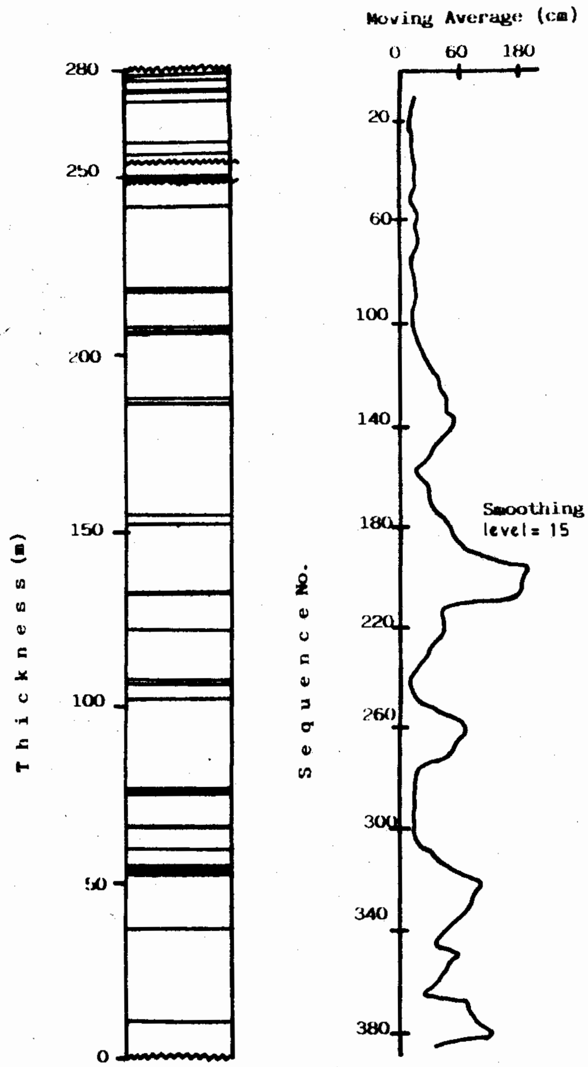

Fig. 6. Columnar profile and thickness diagram of the Hazelbank Quarry (Zone 3). White areas represent sandy (Tabc, Tbc) and black areas pelitic (Tcd, Tde) sequences of Bouma (1962).

and prod marks. Load structures along with the associated flame structures and convolute lamination are also developed locally.

Up to 68% of the exposures in this zone are C1 (channelized Tae sequences; fig. 2), whilst C2 ('Classic' Tabcde facies are subordinate, and D1 (thin Tcde and Tde) facies are the least abundant, suggesting a mid-fan facies association.

Zone 4

This zone represents a mixture of thick Tae (in up to 50% exposures) and thin Tcde and Tde (in upto 42% exposures) sequences. Thick Tae sequences are poorly graded and locally display amalgamation and are dispersed through the thin Tcde and Tde sequences which locally form successions up to several metres thick. Sequences of the intermediate thickness (5 cm to 40 cm) are rare. The zone is highly disturbed by faulting and tight folding and displays a mixture of both thick Tae and thin Tcde and Tde sequences, the relationship of which is largly obscured by the structural complexity.

Among the sole marks, logitudianl ridges ranging between a few cm and three cm wide are common. Occasionally very fine lineations can be seen on the upper surface of the pelitic units. Grooves and flute marks also occur.

In this zone a mixture of C1 and D2 facies are present (fig. 2), and although it can be deduced that these facies indicate environments varying between mid-fan and ocean floor, any depositional trend is obscured by the prevalence of faulting and tight folding. Massive conglomerate (facies A1) similar to the one described in Zone 3 is again exposed on the top of the zone.

Zone 5

This zone is characterised by very thick Tae sequences which may attain several metres of thickness with only a few millimetres of 'e' units. Bouma c and d units are generally very poorly developed, in some instances ripples of a few cm to 10 cm wavelength are well developed and visible on exposed top surfaces. Many are amalgamated "top-cut-out" units. Lenticles of very coarse grained texture and rip-up mud clasts are common. Apart from the thick sequences which are ubiquitus, pockets of dominantly thin pelitic Tcde and Tde sequences (up to 23%), locally reaching thicknesses of several metres are also present. Such pelitic sequences are typified by mottled lamination, trace fossils and occasional fine upper surface current lineation. The medium thick Tabcde and Tacde sequences are only locally present.

Among the sole marks longitudinal ridges (fig. 3) are commonly present, whilst, grooves and flute casts are subordinate. Other irregular sole marks (fig. 4) are also on record. Other sedimentary structures include lode casts and their associated flame structures, convolute lamination and occasional calcareous nodules. Intrabed groove marks are also present in certain beds which are revealed by internal parting of a thick Ta(?bc)e sequence a few cm above the sole of the bed showing comparable trend of current to that of the sole marks. It seems likely that such beds represent pulses of deposition from a single turbidity influx. The Tae sequences are very thick and locally lenticular and very coarse grained with abundant rip-up clasts.

This zone again displays the C1 facies in up to 75% of the observed localities suggesting a channelised mid-fan facies association. Successions of the D1 facies interspersed among the thick C1 successions suggest channel migration and the occasional introduction of the inter-channel deposits.

Zone 6

In this zone thin Tcde, Tde and thick Tae sequences are equally abundant. Medium thick Tabcde sequences are also present, though subordinate, attain their greatest frequency in this zone. Thick Tae sequences rarely show amalgamation and are mostly medium to fine grained. Channels are rarely observable and are shallow (less than 1.5 m deep). The southern and sequentially lower part of the zone tends

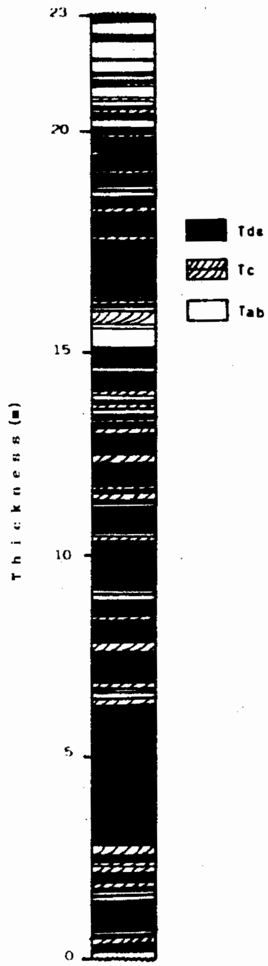

Fig. 7. Columnar profile of a locality (NS 419 543) in Zone 2. Tcd, Tc and Tae represent Bouma sequences (1962).

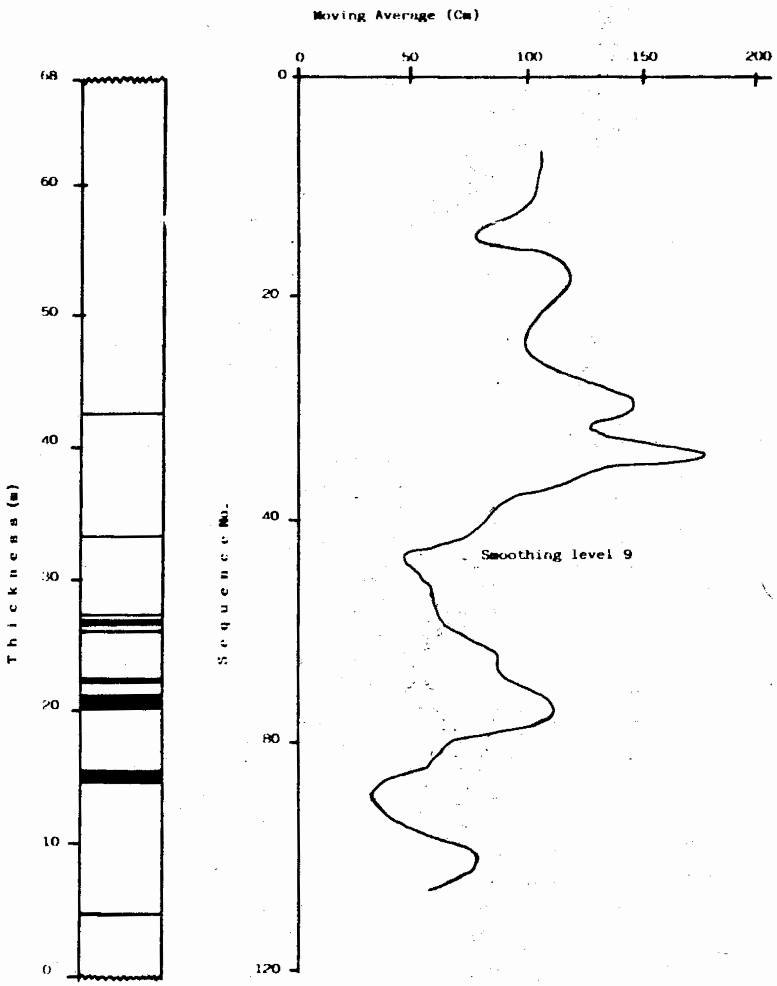

Fig. 8 Columnar profile and bed thickness digram of a locality (NS 429 501) in Zone 3. White areas represent sandy (Tabc, Tbc, Tc) and black area represent pelitic (Tde, Te) sequences of Bouma (1962).

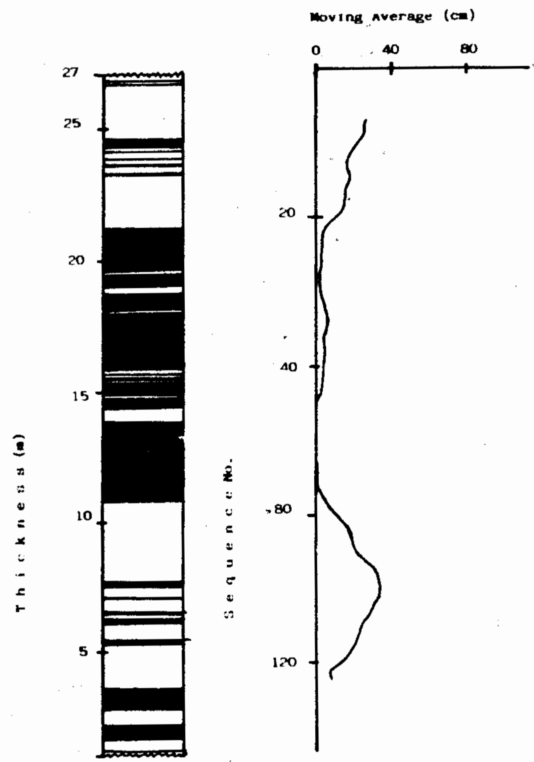

Fig. 9. Columnar profile and bed thickness diagram of a locality (NS 422 462) in an overlapping zone. White area represents sandy (Tabc, Tbc, Tc) and black area pelitic (Tcde, Tde) sequences of Bouma (1962).

to be richer in thick Tae sequences than the northern part.

Thick sequences commonly display longitudinal ridges and sporadic flute marks (fig. 5). The pelitic sequences sometimes show upper surface longitudinal ridge marks. In some localities fining-upwards cycles on a minor scale (a few metres thick) may be found.

In this zone C1 and D1 facies are almost equally abundant. C2 although subordinate, reaches its maximum development in this zone. The C1 facies is more typical of the southern and D1 of the northern part of the zone, suggesting an overall regression of the turbidite fan from a mid-fan to an outer-fan (fringe) position.

DEPOSITIONAL CYCLES

Individual Bouma sequences were measured in some of the best exposed localities of the area to evaluate the trend of the second order-cycles "megasequences" (Ricci-Lucchi 1975; figs. 6 to 9). A proximity index (Walker, 1967) was calculated for the succession at each locality. No definable trend could be discerned. The combined columnar profile and bed thickness variation diagram of the Hazelbank Quarry in Zone 3 (fig. 6) shows that thick and massive channelized sequences dominate with a proximity index of 91.5% (Walker, 1967). The diagram demonstrates that influxes of higher concentration mass deposition were followed by relatively lower density dispersions (Mutti & Ricci-Lucchi, 1975). Five major cycles are exposed and show neither positive (fining-upwards) nor negative (coarsening-upwards) trends. Likewise the thickness diagrams of other localities (fig. 7 — 9) also show comparable characters. The columnar profile of a locality (NS 419 543), taken as the representative of Zone 2 (fig. 7) shows traction current and fallout deposits, characteristic either of basin plane or outer fan (fringe) association (Ricci-Lucchi, 1975).

CONCLUSIONS

The area display facies associations ranging from inner-fan to outer-fan and basin plane environments.

In Zone 1 a channelised facies (C1) appears to persist throughout the zone. Zone 2 and 3 display a retrogression from a mid-fan facies dominated by C1 in Zone 3 to an outer-fan type in Zone 2, in which D1 facies prevails. Chaotic conglomerates of facies A1 at the top of Zone 2 suggests that the first retrogressive cycle was followed by a rapid progression of the turbidite fan. Zone 4 displays a mixture of C1 and D1 facies, suggesting a range of mid-fan to basin floor associations with no clearly discernible trend. Again the thick, chaotic and massive conglomerate terminate the Zone 4, suggesting another rapid progression.

In Zone 5 facies C1 is distributed almost uniformly with the intervening pockets of D1 representing the inter-channel deposits, the whole constituting a channelised mid-fan association. Again no depositional trend is evident.

In Zone 6 facies C1, D1 and C2 are almost equally abundant, the C1 facies tend to decrease northwards (upwards), being replaced by D1 facies. The high proportion of "classic" turbidites (C2) suggest relatively sluggish flows with traction and fallout deposits. It may be suggested that the zone represents a relatively slow retrogression from a lower mid-fan to an outer fan position.

REFERENCES

BOUMA, A.H. (1962) Sedimentology of some flysch deposits: A graphic approach to facies interpretation. Elsevier, Amsterdam.

FLOYD, J.D. (1975) The Ordovician rocks of West Nithsdale. Ph.D. thesis, Univ. St. Andrews Scotland (Unpublished).

HEPWORTH, B.C. (1981) Geology of the Ordovician rocks between Leadhills and Abington, Lanarkshire. Ph.D. thesis, Univ. St. Andrews Scotland (Unpublished).

KASSI, A.M. (1984) Lower Palaeozoic geology of the Gala area Borders Region, Scotland. Ph.D. thesis Univ. St. Andrews, (Unpublished).

KELLING, G. (1962) The petrology and sedimentation of Upper Ordovician rocks in the Rhinns of Galloway, Southwest Scotland. Trans. Roy Soc. Edinburgh 65, pp. 107-37.

McKERROW, W.S., LEGGETT, J.K. & EALES, M.H. (1977) An imbricate thrust model for the Southern Uplands of Scotland. Nature, London 267, pp. 237-9.

MUTTI, E. & RICCI—LUCCHI, F. (1975) Turbidite facies and facies associations. *In:* Mutti, E., Parea, G.C., Ricci-Lucchi, F., Sagri, M., Zanzucchi, G., Ghibaudo, G. & Jaccrino, S. Examples of turbidite facies associations from selected formations of the northern Apennines, IX Int. Congr. Sedim. (Nice), Field Trip, A–II, pp. 21-36.

PEACH, B. N. & HORNE, J. (1899) The Silurian rocks of Britain. Vol. I, Scotland. Mem. Geol. Surv. Scotland.

RICCI—LUCCHI, F. (1975) Depositional cycles in two turbidite formations of the northern Apennines, Italy. Jour. Sed. Pet. 45, pp. 3-43.

WALKER, R.G. (1967) Turbidite sedimentary structures and their relationship to proximal and distal depositional environments. Jour. Sed. Pet. 37, pp. 25-43.

WALTON, E.K. (1955) Silurian greywackes in Peeblesshire. Proc. Roy. Soc. Edinburgh B, 65, pp. 327-57.

Manuscript received 31.12.1986

ACTA MINERALOGICA PAKISTANICA
VOLUME 2 (1986) pp. 127 - 133.

SEDIMENTOLOGY OF PART OF THE ALOZAI GROUP, TANGAI AREA, ZIARAT DISTRICT, BALUCHISTAN AND ITS IMPLICATIONS ON THE PROPOSED STRUCTURE OF THE NEARBY GOGAI THRUST.

AKHTAR MOHAMMAD KASSI

Geology Department, University of Baluchistan, Quetta, Pakistan.

ABSTRACT:— Section exposed in Saro Nala east of Tangai village just below the unconformably overlying Siwaliks and mapped as the Parh Group by earlier workers does not resemble in any of its lithological and sedimentological characters to the Parh Group but may belong to the Alozai Group. The succession shows characters of turbidite sequences and is characterised by thin-bedded, very fine-grained and graded arenaceous limestones of brownish grey to dark grey colour interbedded with thin to thick pelagic or hemi-pelagic grey shales. The limestone horizons have very sharp and erosional lower bedding surfaces and show spectacular sole marks and parallel and cross-laminations. Bouma sequences recognised are mostly Tbce, Tce, Tc(?d)e and Tde and the limestone-shale ratio is over 2:3. The interbedded shales are characterised by dark colour and trace fossils. These characters suggest that the sequences are distal turbidites, most probably the outer-fan (fringe) deposits of deep sea origin and in Tangai area they suggest progradation of the turbidite fan. It is proposed that the fan has derived most of its detritus from the shallower part of the same basin where carbonates were depositing.

INTRODUCTION

Tangai area is about 100 kms northeast of Quetta. (fig. 1). The area was mapped by Hunting Survey Corporation (1960) and also studied by Kazmi (1955, 1979) and the studied rocks were mapped as the Cretaceous Parh Group. Tangai and surrounding area is attractive to geologists because of the nearby Gogai thrust and associated structures. It has been established (Kazmi, 1979) that in Gogai area the Parh Group has been thrusted over the Palaeocene Dungan Formation. The thickness and stratigraphic relationship of the succession is obscure due to intense faulting. It was observed by the author in the nearby Guaziz area about 5 kms southwest of Tangai village that slices of the Alozai Group (Triassic) and Loralai Limestone (Jurassic) are also exposed in addition to the Parh Group within thrust zones.

During a visit to the section exposed in Saro Nala east of Tangai Village just below the unconformably overlying Siwaliks, it was observed that the rocks do not resemble lithologically and sedimentologically to the rocks of the Parh Group. On the other hand, it seemed more convincing that the rocks resemble those of the Alozai Group of Triassic age (Hunting Survey Corporation, 1960; Fatmi, 1972). Therefore, the author decided to study the rocks in detail and compare them with those of the known sections of the Alozai Group nearby. It was confirmed that the characters of the studied section near Tangai Village closely correspond to those of the known sections of the Alozai Group in Rod Malazai area east of Khanozai. It was found in various sections of the Alozai Group in Rod Malazai as well as Tangai area that the sequences possess most of the characters of distal turbidites. Detailed study of the sequences was preferred in Tangai area where the succession is neither highly disturbed nor recrystallised (because of the nearby igneous intrusions), which on the other hand, is a common phenamena in sections of the Rod Malazai area, and tend to obliterate the sedimentary structures.

DESCRIPTION

As mentioned earlier, the succession of the Alozai Group studied possesses most of the characters of distal turbidites. It will therefore be appropriate to review very briefly the common characteristics of turbidites.

Turbidites are deposits of the turbidity currents which in general terms, are high-density currents flowing down a subaqueous slope. High-density and suspension-rich layers may flow down an available slope and spread out below the clear water of low density. Kuenen & Migliorini (1950) and Natland & Kuenen (1951) studied this concept experimentally and applied it to explain the origin of flysch sediments of deep sea origin. Bouma (1962) made a comprehensive study of ancient turbidites and developed a turbidite facies model, now called the Bouma sequence (fig. 2), illustrating that an ideal single turbidite sequence is made up of following five units with specific sedimentary structures:

1. *Graded Interval (Ta).* This is the lowermost part of the sequence which is commonly graded with no other sedimentary structures. It is sandy or gravelly in nature.
2. *Lower Interval of Parallel Lamination (Tb).* This interval shows predominantly thick parallel laminae of sand. Grading may be present. The contact with the lower graded interval is gradual.
3. *Interval of Current Ripple Lamination (Tc).* This interval is made up of fine sand and silty sediment showing small current ripple bedding. Sometimes convolute laminations are present. Indistinct grading is present from bottom to top. The contact with lower interval is rather sharp.
4. *Upper Interval of Parallel Lamination (Td).* This zone of very fine sandy to silty clay shows distinct parallel lamination. The contact with the lower unit may be distinct.
5. *Pelitic Interval (Te).* This interval of clayey sediment does not show any distinct sedimentary structures. Marine fossils may be found in this interval. The contact with the lower interval is gradational. Sometimes on top of the pelitic interval marl may be found representing pelagic sediments.

Bouma (1962) also pointed out that complete sequences with above 5 units are very rarely found only in thick layers of flysch deposits. Usually the sequence is incomplete. Incomplete sequences may include Tabc,sTbce, Tae, Tcde, Tde etc. The sequence is a deposit of decreasing current velocity (wanning current) and grain size in the direction of flow. Thus, near the source all intervals are represented (fig. 2-b) whereas in the downcurrent direction lower intervals are missing (Bouma, 1962; Walker, 1978). Walker (1967) determined the criteria on the basis of which proximal turbidites (deposited near the source) are recognised and differentiated from distal turbidites (deposited away from the source).

If one tries to put together various characteristics of turbidite deposits, following indices seems to be the most important:

1. Graded bedding.
2. Alternations of pelagic shales and sandstones.
3. Diversity of fauna in sandstones and adjacent pelagic shales.
4. Sole marks abundant on bottom of sandstone layers which develop as a result of scouring action of turbidity current on the muddy bottom over which the current flow.
5. Thick sequences, regular bedding, extensive lateral extention of individual units and rather uniform current direction shown by sole marks.
6. Absence of typical shallow water features e.g. wave ripples, beach features, bioherms, large-scale cross-stratification, well-sorted sand, etc.

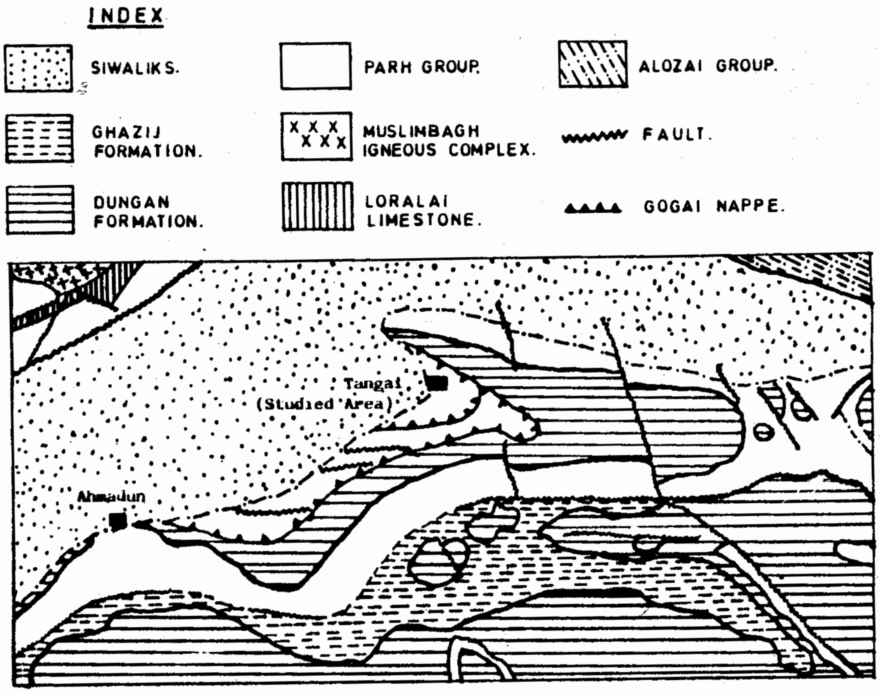

Fig.1. Geological map of the Tangai and surrounding area showing studied locality. (Taken from the Geological map of Pakistan, Hunting Survey Corporation (1960).

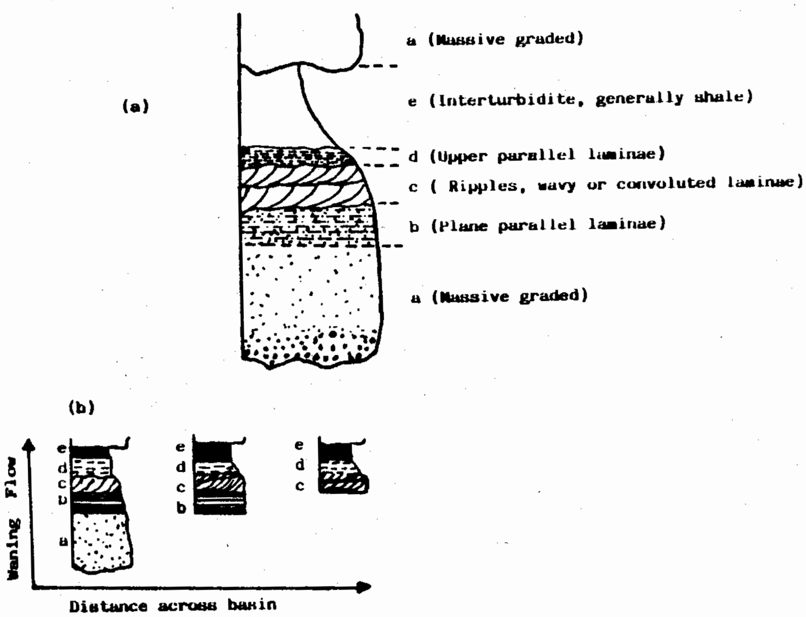

Fig.2.(a) Ideal sequence of sedimentary structures in a single turbidite deposite ("the Bouma sequence").

(b) Schematic diagram depicting interpretation of Bouma sequence (abcde) in terms of distance across basin, and waning flow conditions. This suggests that the turbidites beginning with divisions b and c represent deposition from progressively slower flows, which can be due to increasing distance across basin. However, the levees of the proximal turbidite environment may also show sequences beginning with divisions b or c (After Walker 1978).

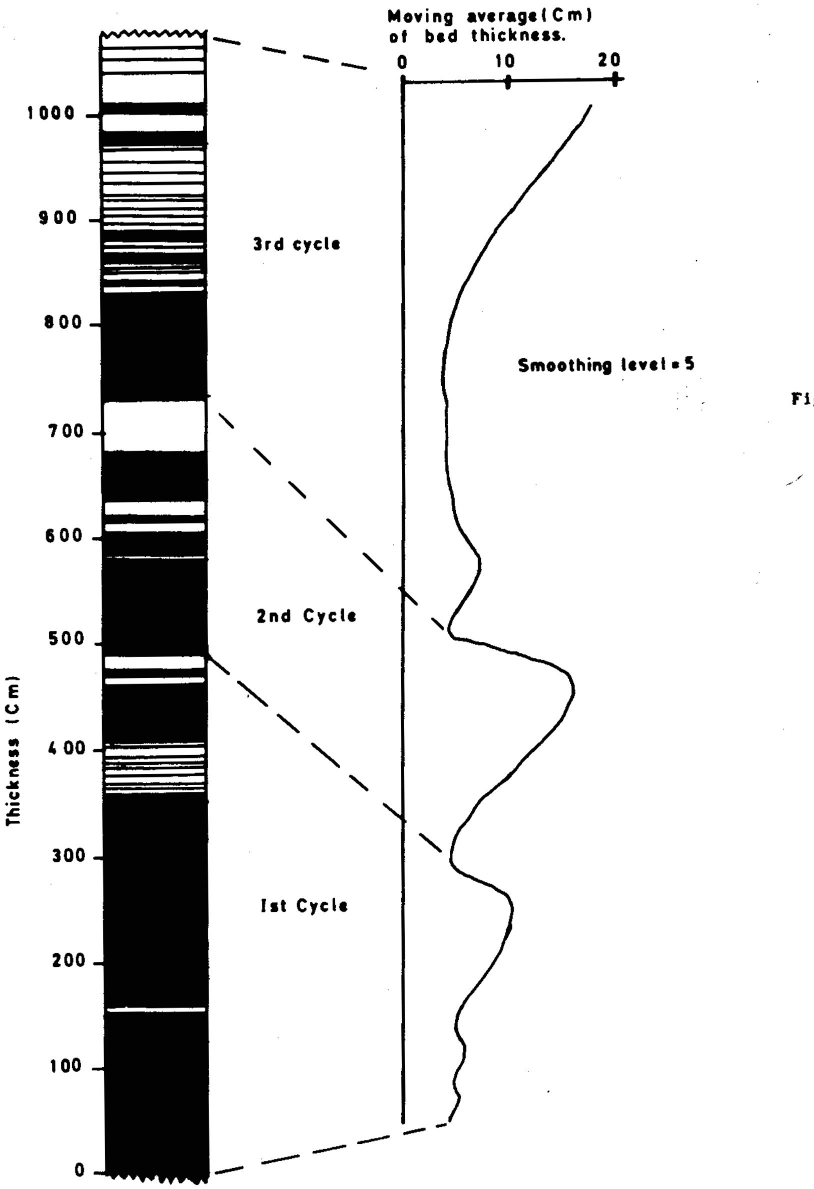

Fig.6: Columnar profile and bed thickness variation diagram of an exposure showing pronounced thickning-upward cycles. White areas represent Tbc and Tc units of Bouma sequence (Bouma 1962), whilst black areas represent massive hemipelagic/pelagic shales. The upper and lower ends of the exposure are obscured by scree deposits.

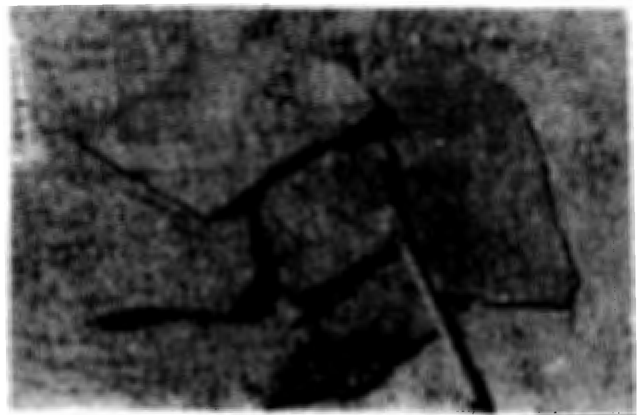

Fig.3: Photograph of Trace fossils found within the limestone and shale beds.

Fig.4: Photograph showing Flute casts found on the botton of limestone beds.

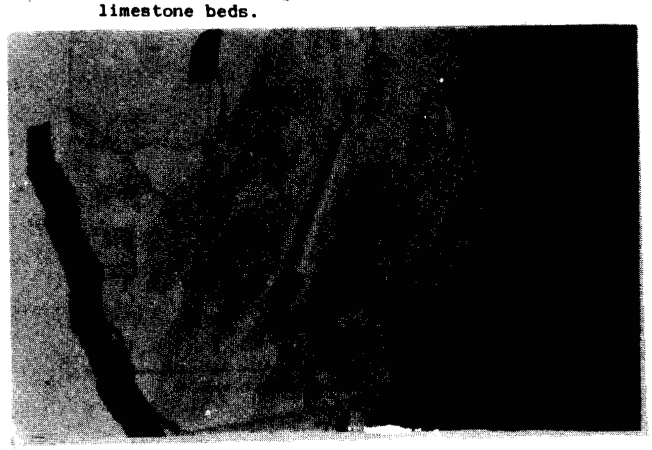

Fig.5 Photograph showing Congitudinal ridge casts found on the bottom of limestone beds.

7. Absence of features indicating subaerial exposure e.g. rain drop imprints.

In the light of above, the succession in exposed section near Tangai area shows alternate limestone and shale sequences. The limestones are brownish grey to dark grey, very fine grained, arenaceous, thin-bedded and range from a few cm to 30 cm in thickness with an average of about 9 cm. Thin sections of the limestone show that grains are detrital, ranging from very fine sand to silt cemented by sparry calcite and therefore may be called intra-sparite (Folk, 1959). No fossils were observed in the limestones. The interbedded shales are massive, dark brownish grey, dark grey or even black in colour and show spectacular trace fossils, mostly tracks, trails and burrows which are mostly inclined or nearly parallel to the bedding planes (fig. 3). ***No ther faunal evidence was found, however, trace fossils support the hemipelageic/pelagic origin of shales by indicating a calm period of fallout sedimentation offering opportunity for burrowing organisms to become active. Trace fossils have also been reported to occur in hemipelagic/pelagic shales elsewhere (Benton, 1982; Kassi, 1984).*** The limestone sequences show grading, parallel lamination, cross-lamination and sole marks which include flute casts (fig. 4), longitudinal ridge casts (fig. 5) prod casts, casts of trace fossils and other irregular marks. These characters indicate that the limestones are the deposits of turbidity currents and the shales formed by hemipelagic/pelagic deposition between turbidite sedimentation. ***The succession shows Tbce, Tc(?d)e and Tde units of the Bouma sequence (Bouma, 1962). The limestone-shale ratio is just over 2:3, indicating that shale is dominant over the limestone. These characters closely correspond to those of distal turbidites (Bouma, 1962; Walker, 1967) and suggest the predominance of sluggish tubidity flows giving rise to traction and fall-out deposits (Mutti & Ricci-Lucchi, 1975), and deposition in outer turbidite fan (fringe) position. Ricci-Lucchi (1975)*** studied cyclicity in the turbidite sequences in columnar profiles prepared by plotting individual bed thicknesses and their Bouma sequences. He proposed that thinning-upward and thickening-upward cycles

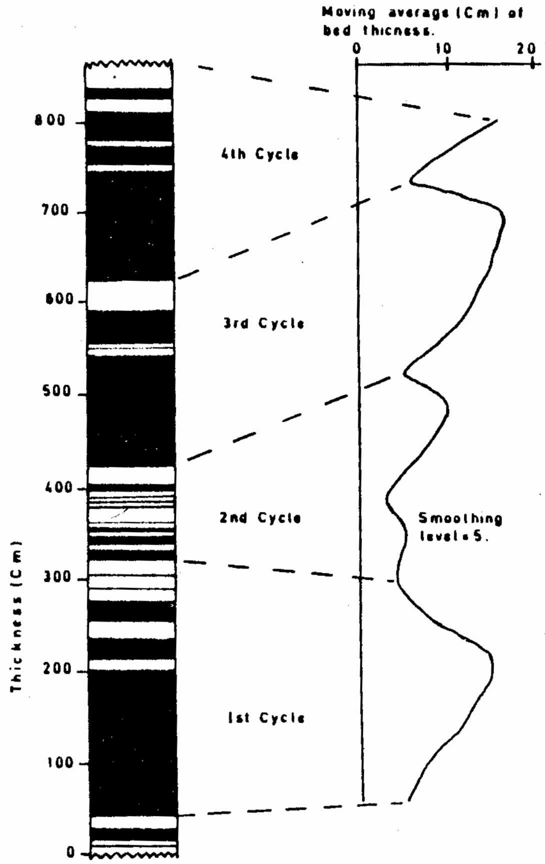

Fig.7. Columnar profile and bed thickness variation diagram of another exposure showing pronounced thickening upward cycles. White areas represent Tbc and Tc units of Bouma sequence (Bouma, 1962) whilst, black areas represent massive hemipelagic/pelagic shales. The upper and lower parts of the exposure are obscured by scree deposits.

may be found which correspond to the regressional and progradational trends of the turbidite fans, respectively. Similar studies were carried out to determine the trends of 2nd order cycles 'megasequences' (Ricci-Lucchi, 1975). The combined columnar profile and bed thickness variation diagrams (fig. 6–8) show very clear thickening-upward cycles, which suggest a progradational trend of the submarine turbidite fan. The calcareous detritus may be of intrabasinal derivation.

DISCUSSION

The sequences under discussion have been mapped as the Parh Group (Cretaceous) in the Geological Map of Pakistan (Hunting Survey Corporation, 1960; Kazmi, 1979), whereas the author observed characters closely comparable to those of the Alozai Group. It therefore becomes desirable to critically review the contrasts between the Parh Group and Alozai Group. The Samber Formation which is the lowermost unit of the Parh Group, consists of the belemnitic shales of pale green and greenish brown colour with only a few beds of dark grey limestone. The Goru Formation, representing the middle unit, consists of interbedded shales and limestones of greenish grey and maroon colour. The Parh Limestone is the uppermost unit of the Parh Group which consists exclusively of limestone of cream, white and reddish grey colour with or without chert bands and nodules. Neither any of the limestone bed of the Parh Group show any character of turbidites (grading, parallel or cross-lamination, sole marks etc.), nor any of the interbedded shales are trace fossils which are characteristic of the Alozai Group. In fact dark grey and arenaceous limestones are very rare in the Parh Group. Furthermore, the limestones of the Parh Group are mostly biomicrite (Folk, 1959) having a profusion of microfossils, whilst, the limestone of the Alozai Group is arenaceous (intra-sparite) and lacks fossils. The two groups, therefore, have contrasting characters and have been deposited in different depositional environments. It is suggested that the sequence exposed in Saro Nala east of Tangai village (fig. 1), which has been mapped as the Parh Group (Hunting Survey Corporation 1960; Kazmi 1979) in fact may be a portion of the Alozai Group of Triassic age. This suggestion is supported by the fact that its lithology and turbiditic origin is closely comparable to the known sections of the Alozai Group in Rod Malazai area east of Khanozai.

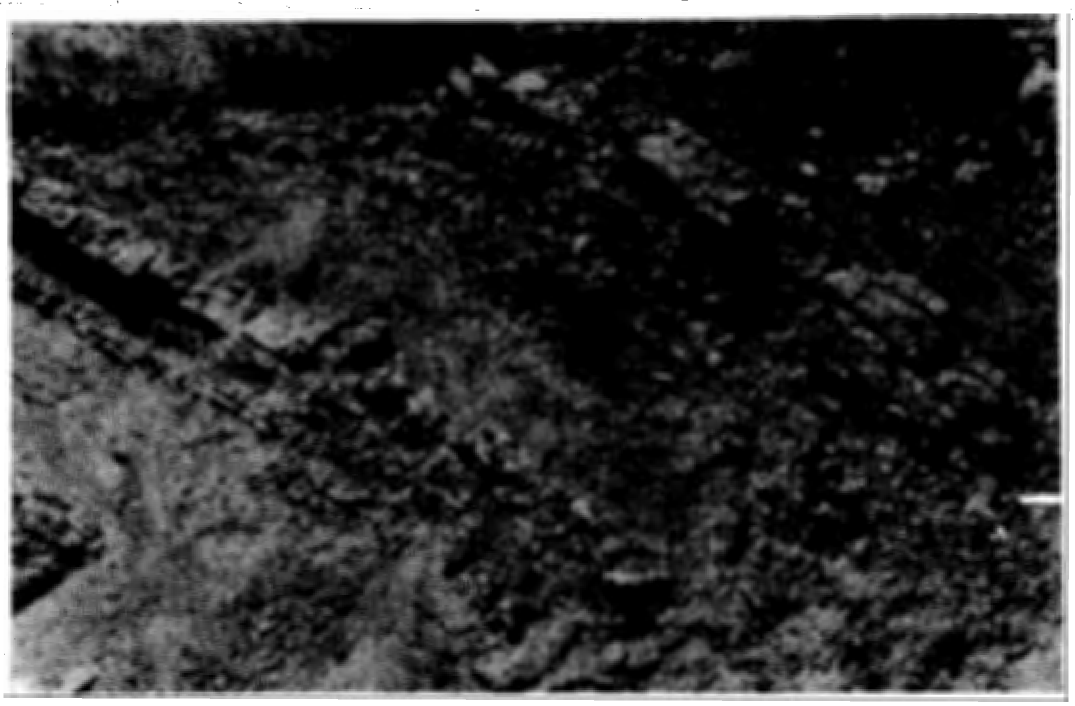

Fig. 8: Photograph showing pronounced thickening upward cycles in the succession.

Furthermore, it has been observed that in the nearby Guaziz area about 3 miles southwest of Tangai the Loralai Limestone is also exposed, underlying conformably the Samber Formation of the Parh Group. These new informations imply that the structure of Tangai, Gogai and surrounding area is not as simple as has been described by the Hunting Survey Corporation (1960) and Kazmi (1979). It is suggested that the Gogai Nappe, in addition to the Parh Group, consists of thrust blocks of even older rocks of the Alozai Group (Triassic) and Loralai Limestone (Jurassic).

CONCLUSIONS

(a) The limestone and shale sequences exposed in the Saro Nala, south of Tangai village just below the unconformably overlying Siwaliks, may not belong to the Parh Group (Cretaceous) but closely corresponds in lithological and sedimentological aspects to the Alozai Group (Triassic).

(b) The sequences are distal turbidites and hemipelagic/pelagic shales, deposited probably in the outer fan (fringe) environment and their second-order thickening-upward cycles suggest progradation of the turbidite fan.

ACKNOWLEDGEMENTS

Thanks to Abdul Salam, Bashir Ahmad, A.M. Farooqui, Dr. Abdul Haque and Dr. M. Niamatullah for their valuable criticisms and inspiring discussions.

REFERENCES

BENTON, M. J. (1982) Trace fossils from the lower Palaeozoic ocean floor sediments of the Southern Uplands of Scotland. Trans. Roy. Soc. Edinburgh: Earth Sci. 73, pp. 6787.

BOUMA, A.H. (1962) Sedimentology of some flysch deposits: A graphic approach to facies interpretation. Elsevier Amsterdam.

FATMI, A.N (1972) Stratigraphy of the Jurassic and lower Cretaceous rocks and Jurassic ammonites from northern areas of West Pakistan. British Mus. Nat. Hist Bull. (Geol.). 20(7), pp. 299-380.

FOLK, R.L. (1959) Practical petrographic classification of limestones. Bull. Amer. Assoc. Petrol. Geol. 43. pp. 1-38.

HUNTING SURVEY CORPORATION (1960) RECONNAISSANCE GEOLOGY OF PART OF WEST PAKISTAN. Colombo Plan Coorperative Project Toronto, Canada.

KASSI, A.M. (1984) Lower Palaeozoic geology of the Gala area, Borders Region, Scotland. Ph.D. thesis, Univ. St. Andrews, Scotland (unpublished).

KAZMI, A.H. (1955) Geology of Ziarat-Kach-Zardalu area of Baluchistan. D.I.C. thesis, Imperial College of Science and Technology, London (Unpublished).

———— (1979) The Bibai and Gogai Nappes in the Kach-Ziarat area of northern Baluchistan. *In:* Farah, A. & De Jong, K.A. (eds.). GEODYNAMICS OF PAKISTAN. Geol. Surv. Pakistan, Quetta.

KUENEN, Ph. H., & MIGLIORINI, C.I. (1950). Turbidity currents as a cause of graded bedding. Jour. Geol. 58, 91-127.

MUTTI, E. & RICCI-LUCCHI, F. (1975) Turbidite facies and facies associations. *In:* Mutti, F., Parea, G.C., Ricci-Lucchi, F., Sagri, M., Zanzucchi, G., Ghibaudo, G. & Jaccarino, S. Examples of turbidite facies associations from selected fromations of the northern Apennines. IX Int. Congr. Sedim. (Nice). Field Trip. A–II, pp. 21-36.

NATLAND, M.L. & KUENEN, PH. H. (1951) Sedimentary history of Ventura Basin, California, and the action of turbidity currents and the transportation of coarse sediments to deep water. Soc. Econ. Palaent. Mineral. Spec. Publ. 2, 76-107.

RICCI–LUCHI, F. (1975) Depositional cycles in two turbidite formations of the northern Apennines, Italy. Jour. Sediment. Petrol. 45, pp. 3-43.

WALKER, R.G. (1967) Turbidite sedimentary structures and their relationship to proximal and distal depositional environments. Jour Sediment. Petrol. 37, 25-43.

———— (1978) Deep-water sandstone facies and ancient submarine fans: Models for exploration for stratigraphic traps. Amer. Assoc. Petrol. Geol. Bull, 62, pp. 932-66.

Manuscript received 19.10.1986

ACTA MINERALOGICA PAKISTANICA
VOLUME 2 (1986) pp. 134 - 143.

COMPARISON OF THE UPPER DEVONIAN MIOSPORE ASSEMBLAGES OF NEW YORK STATE AND PENNSYLVANIA WITH THOSE FROM OTHER PARTS OF NORTH AMERICA

SARFRAZ AHMED

Institute of Geology, University of the Punjab, Lahore, Pakistan.

ABSTRACT:– A correlation of the palynological flora investigated from the Upper Devonian of New York State and Pennsylvania is attempted with areas from other parts of North America. Correlation is proposed with the USA and Canada including Southern Ontario, Maritime Provinces and Yukon Territory.

Upper Senecan to Chautauquan Series of New York State and Pennsylvania have been investigated which are equivalent to Upper Frasnian and Famennian stages in Europe.

Sixty four samples from four formations have been analysed, all of which contained palynomorphs. The material investigated is composed of shale, siltstone and silty sandstone.

INTRODUCTION

The western part of New York State is well known for its many geological features. House (1975) concludes "As an area in which relations between terrestrial and marine facies can be elucidated, the New York sequence must surely be the only complete succession in the world which can be regarded as forming an international standard".

Many previous workers have published papers on specific stratigraphic and palaeontologic topics within the area (Tesmer, 1975). The comprehensive, upto date information of Upper Devonian geology of the area investigated is given by Tesmer (1963, 1967, 1975) who conducted intensive field investigations in western New York State. Three groups are recognized, in ascending order, the Seneca, Arkwright and Conewango. The groups, in turn, are divided into formations and subdivided into members. Generalized stratigraphic succession showing the horizons sampled is shown on fig. 2. Tesmer (op. cit.) regards formations to be of regional extent, often traced through several counties, while members in the clastic sequence are often of more local occurrence. This scheme of stratigraphic subdivision has been adopted in the present work. The Upper Devonian strata outcropping in the area are together approximately 670m thick that are essentially clastic, for the most part interbedded shales and siltstone but with increasing precentage of sandstone and conglomerate towards the top. Marine invertebrates are quite abundant but plant and fish are also represented at various horizons. Conodonts are considerably more frequent than ammonoids. Frasnian goniatites of Europe are often represented by the same genera and sometimes identical species in North America.

Spores are particularly useful in that they may be deposited in large numbers, in both fresh water and marine sediments, thus providing a useful link between continental and marine stratotypes.

In general the preservation of palynomorphs; acritarchs, chitinozoans and scolecodonts is poor. Miospore assemblages especially in the

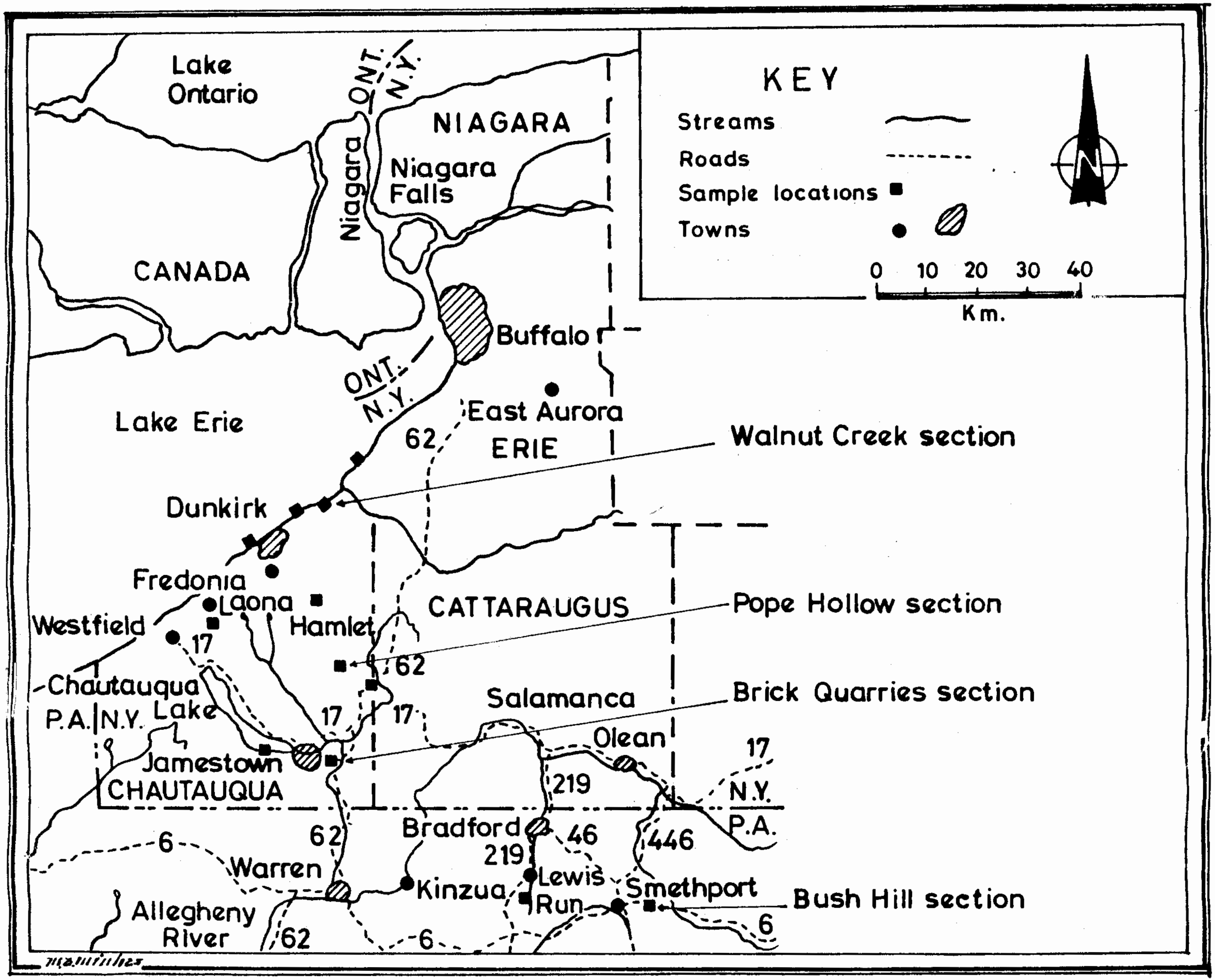

Fig. 1. Location map of sampling areas.

Java and lower part of Canadaway Formation are in an inferior state of preservation when compared with the nature of preservation in younger beds. Some of the specimens are difficult to identify, since they are squashed beyond recognition; others are brittle in nature. Occasionally well preserved specimens are found in upper part of the Canadaway Formation and more infrequently excellently preserved ones in the Chadakoin and Cattarangus Formations. Chitinozoans, and scolecodonts and acritarchs have also been counted, but they are not described systematically herein, since many of them can be attributed to existing species.

The palynological floras of marine and non-marine sediments of western New York State and northern Pennsylvania contain a diversity of trilete spores, together with an acritarch component that is relatively inconspicuous qualitatively and quantitatively.

In the samples from the Bush Hill Section (approximately 3 kms E of Smethport road cut on route 6, Pennsylvania, see fig. 1) no acritarchs or chitinozoa have been found and, since these microfossils are often abundant in brackish and marine sediments, their absence strongly supports the prevalent view that the sediments of the Bush Hill Section were laid down in continental regime.

Marine and non-marine facies may contain may species in common. In the Upper Devonian of New York State and Pennsylvania, this phenomenon has been observed in the marine Ellicott Member of the Chadakoin Formation and in the lower part of the non-marine Ellicott Member of the above mentioned formation, which have most species in common and concluded to be coeval.

In marine facies miospores range from 5 to 90 percent; whilst in continental strata they are hundred percent of the total assemblages. The occurrence of acritarchs is surprisingly erratic and ranges from 2 to 74 percent.

Aneurospora greggsii (McGregor) is the most numerous component in some of the samples of the present study. This is especially ture in sequences in the lower part of the Ellicott Member of the Chadakoin Formation where the population of *A.* ***greggsii*** (McGregor) ranges from 30 to 43.5 percent. In the assemblages of the overlying Cattaraugus Formation this taxon declines in abundance to only one percent or less of the total assemblages. This species is the most abundant in the continental strata, e.g., the Bush Hill Section, whilst in marine facies its numbers are reduced. The abundance of *A.* ***greggsii*** (McGregor) in sediments of siltstone and fine sandstone can be correlated with the presence of sporangia containing this spore species. In many of the samples, however, ***Streelispora catinata*** (Higgs) is by far the most abundant species ranging from 10 to 20 percent. The species ***Auroraspore torquata*** (Higgs) is also common and ranges from 5 to 10 percent in many samples. A miospore with multifurcate spines, ***Hystricosporites multifurcatus*** (Winslow) Mortimer & Chaloner is relatively abundant in certain samples namely the siltstone from the Bush Hill. Brick Quarries, Samples US9 – US4F (fig. 1, 2) (the Derterville Member) and Walnut Creek Sections, sample US 11A – US 10C (figs. 1 & 2). It is persistent component in both marine and non-marine facies, in other samples it is relatively rare (less than one percent) or absent.

COMPARISON

U.S.A.

Winslow's (1962) paper is still one of the major contributions on North American Upper Devonian palynology ever published. In her comprehensive and valuable work she dealt with megaspores, miospores and microplankton. The strata she investigated range in age from Middle Devonian to the Mississippian transition measures and come from Ohio, U.S.A. A number of miospores described and illustrated are comparable with the Upper Devonian-Lower Carboniferous assemblages reported from elsewhere. Worthy of special mention is the absence of diagnostic macrofossils in the succession, consequently the position of her systematic boundary is known to be tentative. The part of succession investigated by Winslow is summarised in table 1.

Winslow (op. cit.) placed Ohio Shale and Cleveland Member of Ohio Shale into the Upper Devonian and the overlying rock units, the Mississippian.

The evidence of the spore assemblages accrued from the Ohio Shale to Bedford Shale in above in agreement with an Upper Devonian age (Famennian). In general the miospores recorded from the Ohio Shale to Bedford Shale in above sequence in the Ohio, are in many respects similar to those described from the Java to Cattaraugus Formations of New York State and Pennsylvania, U.S.A. (table 2). The most striking similarity is in the existence of the taxon ***Hystricosporites multifurcatus*** (Winslow) Mortimer & Chaloner as ***Dicrospora multifurcata*** Winslow including both varieties ***multifurcata*** and ***impensa***. These distinctive forms occurred from upper part of the Olentangy Shale and persisted to top of the Bedford Shale in

Winslow's (1962) sequence. In the area investigated these species are infrequent throughout the sequence. Another miospore which is common to both areas is ***Hystricosporities porcatus*** ***(Dicrospora porcata*** of Winslow). Allen (1965) recorded indentical specimens from Givetian deposits in North and Central Vestspits bergen.s In the U.S.A. the taxon is vertically restricted to latest Devonian (Berea Sandstone), in the studied material the form is also found to be confined to the Uppermost Devonian.

Other species which are common and serve as stratigraphic markers are ***Vallatisporites vallatus*** var. ***hystricosus*** (Winslow) Clayton ***et al.***, and ***Retispora lepidophyta*** (kedo) Playford. The geographical distribution of these index fossils is remarkably widespread and they are used as inter-regional correlation tools. In Ohio, Winslow recorded some miospore forms referred to as ***Cirratriradites hystricosus*** and ***Lycospora?*** sp. *A.* which appear to be identical to ***Vallatisporites vallatus*** var. ***hystricosus*** (Winslow) Clayton ***et al.*** This form is restricted to the upper Cuyahoga Formation and to the mid Logan Formation. However, the species shows its stratigraphic debut at the base of Bedford Shale, within the range of ***R. lepidophyta*** (kedo) Playford as in other parts of the world.

Winslow investigated a distinctive miospore species known as ***Endosporites lacumosus*** Winslow which is usually accepted as equivalent to ***Retispora Lepidophyta*** (Kedo) Playford. It makes its debut high in the Cleveland Member of the Ohio Shale and occurs in abundance up to the top of Berea Sandstone. ***R. lepidophyta*** (Kedo) Playford again appears at the base of the Cuyahoga Formation after dying out at the top of the Berea Sandstone. Its isolated occurrence in the Cuyahoga Formation (only two specimens) may well indicate reworking since it is not present in the underlying Sunbury Shale. Winslow (op. cit.) recorded abundantly ***'Endosporites lacunosus'*** from the Cleveland Member of Ohio Shale at locality one but she also observed many specimens in the overlying Bedford Shale at localities 1, 2 and 3 and in the Berea Sandstone at localities 5 and 9.

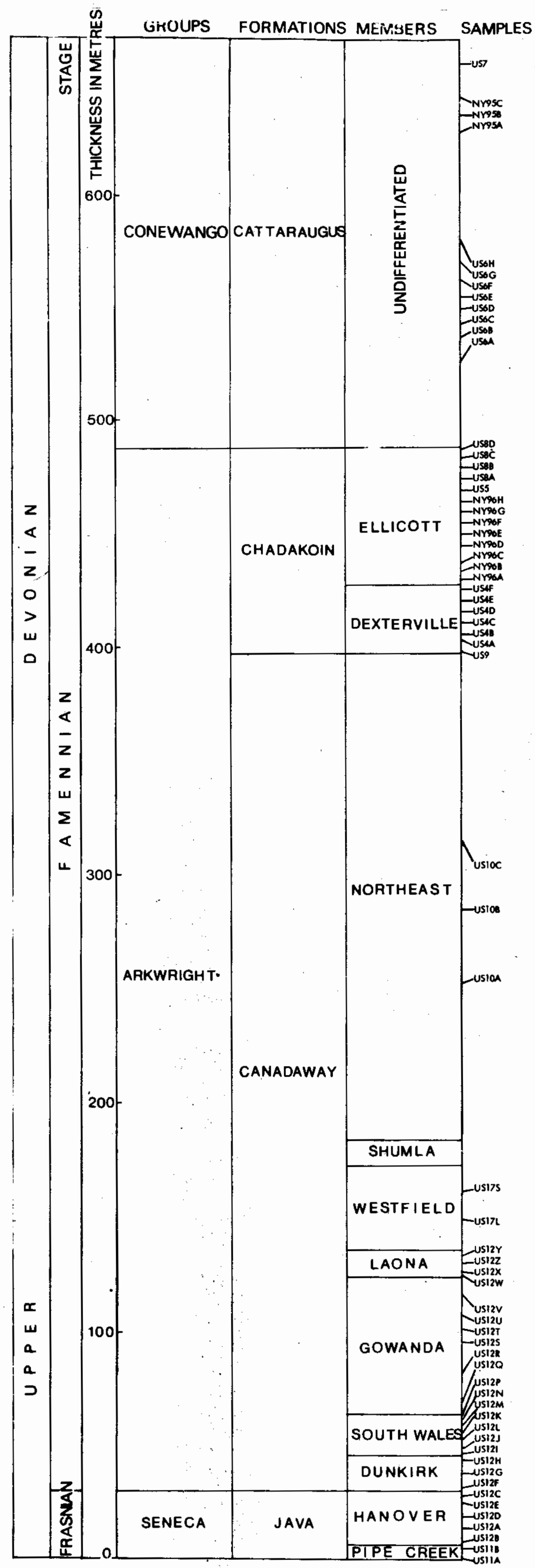

fig .2. Generalized stratigraphical succession showing the horizons sampled

The large pseudosaccate miospore ***Endosporites chagrenensis*** Winslow has an almost identical structural organization to ***Auroraspora torquata*** Higgs. Also the size is comparable in both forms from the two areas. ***E. chagrenesis*** Winslow is restricted to upper part of the Ohio Shale in Winslow's succession and ***A. torquata*** Higgs is similarly restricted in the area under study.

Smooth laevigate forms such as ***Punctatisporites***, cingulate elements e.g., ***Reticulatisporites*** (probably some form of the genus ***Knoxisporites)***, and the sculptured pseudosaccate genus ***Grandispora***, have all been observed in both areas. Spores of megaspore dimension are also present in both localities.

Radforthia radiate Winslow which is regarded as synonymous with ***Emphanisporites rotatus*** McGregor occurs consistently in the Ohio Shale, Bedford Shale and sporadically in the Sunbury Shale and Logan Formation. Its presence in the latter formation may be due to reworking since the species is not found in the underlying Cuyahoga Formation. In the area investigated the form is spasmodically represented throughout the sequence.

It can be concluded that the miospore sequence investigated from New York State and Pennsylvania is comparable to the section investigated by Winslow from the Ohio Shale to the Bedford Shale in Ohio, U.S.A. (table 1).

Streel & Traverse (1978) published on spores from the Devonian/Mississippian transition near the Horseshoe Curve Section. They recorded 33 spore forms from Altoona, of these eleven are regarded as common to the present material. The miospores which have been observed from the Horse-Shoe Curve Section and from New York State and Pennsylvania are as follows: ***Aneurospora greggrii*** (McGregor) Streel, ***Aneurospora incohata*** (Sullivan) Streel. ***Auroraspora poljessica*** (Kedo) Streel. ***Auroraspora torquata*** Higgs, ***Auroraspora solisorta.*** Hoffmeister ***et al.***, ***Emphanisporites*** rotatus McGregor, ***Grandispora corunata*** Higgs, ***Knoxisporites literatus*** (Waltz) Playford, ***Rugospora flexuosa*** (Jusch) Streel, ***Spelaeotriletes lepidophytus*** (Kedo) Streel ***Vallatisporites vallatus*** Hacquebard. Streel & Traverse (1978) also compared their assemblages with other part of the world including the Ardennes – Rhine basins, the British Isles basins, and the North American basins.

Molyneux, Manger & Owens (1984) obtained assemblages of well preserved miospores and microplankton of the Late Devonian age from the Bedford Shale and Berea Sandstone Formations of Central Ohio, U.S.A. They recorded 34 miospore species, of these 13 are common to the present material. The miospores which have been encountered from Ohio and from New York State and Pennsylvania are ***Punctatisporites solidus*** Hacquebard, ***Retusotriletes incohatus*** Sullivan, ***Emphanisporites rotatus*** McGregor, ***Hystricosporites multigurcatus*** (Winslow) Mortimer & Chaloner, ***Hystricosporites porcatus*** (Winslow) Allen, ***Dictyotriletes trivialis*** Naumona ***Knoxisporites literatus*** (Waltz) Playford, ***Knoxisporites pristinus*** Sullivan, ***Vallatisporites vallatus (V. Pussilites)*** Clayton ***et al.***, ***Spelaeotriletes lepidophytus*** (Kedo) Streel, ***Rugospore flexuosa*** (Jusch) Streel, ***Grandispora Corunata*** Higgs, and ***Grandispora echinata*** Hacquebard. They made a detailed comparison of the miospore assemblages obtained from the Central Ohio whith those recorded from other parts of North America.

Recently Wicander and Playford (1985) recorded twelve well preserved spore genera from the Upper Devonian (Upper Frasnian) Juniper Hill and Cerro Gordo members of the Lime Creek Formation, Floyd county, Iowa, U.S.A. It appears that apart from the long-ranging laevigate forms none of the spore taxa is comparable with the present material. This is probably the Lime Creek Formation which is older than the strata investigated from New York State and Pennsylvania, U.S.A.

Canada

McGregor (1960) investigated the palynology of the Devonian (Frasnian or probably Famennian) from Melville Island Canada Arctic Archipelago. He analysed bituminous coal

ROCK UNITS	SYSTEM
Logan Formation Cuyahoga Formation Sunbury Shale Berea Sandstone Bedford Shale	Mississippian
Cleveland Member of Ohio Shale Ohio Shale	Upper Devonian
Olentangy Shale	Middle Devonian

Table.1. Showing the sequences of Ohio, investigated by Winslow (1962).

samples which may represent restricted microfloras. However, his miospore sequence is perhaps equivalent to the Java and part of the Canadaway Formation in New York State, U.S.A. On the whole the miospores described by McGregor (1960, 1970) are very different from those observed during the present study. Some similarities are offered by ***Biharisporites***, ***Verrucosisporites***, ***Convolutispora*** and smooth laevigate forms such as ***Punctatisporites*** and ***Leiotriletes***.

McGregor (1970) recovered ***'Hymenozonotriletes lepidophytus'*** Kedo and associated miospores from the Devonian of Canada. He examined three widely spaced localities at the Devonian – Carboniferous boundary. It is unfortunate that the age of some of the sections investigated was not established on the basis of fauna. However, the miospore assemblages described by McGregor (op. cit.) are similar to the miospores observed during the present study.

1. Southern Ontario

Four formations namely Kettle Point, Bedford, Berea and Sunbury were analysed palynologically from two wells six kms apart and from surface material. To support the palynological results, palaeontological dating is available from conodonts (although not for the particular sections studied). It is of interest that the Kettle Point Formation (black shale) is the only stratigraphical unit of proved Devonian age and offers closest similarities with the Java, Canadaway and Chadakoin Formations investigated during the present work (table 2). ***Convolutispora*** sp. in McGregor & Owens (1966, pl. 28, fig. 19) appears to be similar to the present form referred as ***Convolutispora mellita*** Hoffmeister ***et al.*** Some of the specimens similar to Emphanisporites cf. ***E. rotatus*** in McGregor & Owens (op. cit. pl. 28, fig. 4) have been observed during this study. ***Verrucosisporites congestus*** Playford in McGregor &

Miospore Zones	NEW YORK STATE & PENNSYLVANIA PRESENT WORK		NORTH AMERICA		CANADA	
	FORMATION	MEMBER	WINSLOW 1962	PRESENT POSITION	SOUTH ONTARIO McGREGOR 1971	YUKON TERRITORY
HL	CATTARAUGUS	Undifferentiated	Ohio Shale	Bedford Shale and	Bedford Shale	Imperial Formation
	CHADAKOIN	Ellicott		Cleveland member of Ohio Shale		
FV		Dexterville		Ohio Shale	? Kettle Point Formation	
	CANADAWAY	Northeast				
CN		Shumla				
		Westfield				
		Laona				
		Gowanda				
		South Wales				
		Dunkirk				
	JAVA	Hannover				
?		Pipe creek				

Table. 2. A correlation of the Upper Devonian sequences of New York State and Pennsylvania with those from North America, based on miospore assemblages.

Owens (op. cit., pl. 28, fig. 15) is probably similar in construction to the form referred as *C.* sp. aff. V. ***congestus*** Playford in this work. ***?Perotriletes*** sp. McGregor & Owens (op. cit., pl. 28, fig. 25) is identical to the present form of ***Rugospora flexuose*** (Jusch) Streel, while the figures 17, 18 and 21 illustrated on the above mentioned plate appear similar to ***Synorisporites variegatus*** Ahmed & Richardson ***?Hymenozonotriletes varius*** Naumova var. minor Naumova in McGregor & Owens (op. cit., pl. 28, fig. 24) has also been recorded from the present material. The index forms are, of course, common having identical morphographic circumscription.s An equally striking difference is in the absence of multifurcate-spined moispores in the Kettle Point Formation.

The Bedford Formation (silty and sandy shales) also contains some miospore elements common to the underlying Kettle Point Formation. The miospores which are common to the present material are ***Knoxisporites literatus*** (Waltz) Playford, ***Aneurospora incohata*** (Sillivan) Streel, ***Hystricosporites multifurcatus*** (Winslow) Mortimer & Chaloner and ***Retuspotriletes*** sp. in McGregor (1970, pl. 21, fig. 8) which is regarded to be identical to ***Retusotriletes phillipsii*** Clendening ***et al.*** The overlying Berea Sandstone Formation is identical in miospore components to the underlying Bedford Formation. Berea Sandstone Formation is considered to be of Strunian age. Presence of ***Spathognathodus inornatus*** suggests an uppermost Famennian age for Bedford Formation.

In the Sunbury Formation spores similar to ***Hystricosporites multifurcatus*** (Winslow) Mortimer & Chaloner are probably not present (neither illustrated nor listed by McGregor, but a form similar to ***Spelaeotriletes microverrucosus*** (Kaiser) Ahmed & Richardson is illustrated as unidentified.

2. Maritime Provinces

The miospore assemblages have been recovered from the lower part of the Horton Group in Nova Scotia. No palaeontological evidence is available to support the palynological results. However, the following common species have been encountered in both areas: ***Aneurospora incohata*** (Sullivan) Streel, ***Regospora flexuosa*** (Jusch) Streel as ***Hymenozonotriletes famenensis*** in McGregor (1970 pl. 23, fig. 4), ***Hystricosporites multifurcatus*** (Winslow) Mortimer & Chaloner as ***?Dicorspora multifurcata*** (only one spine illustrated) and index forms ***V. vallatus*** var. ***hystricosus*** (Winslow) Clayton ***et al.*** – ***Retispora lepidophyta*** (Kedo) Playford.

3. Yukon Territory

McGregor (1970) analysed two samples from near the top of the Imperial Formation from the Trial River, three kms east of the Richardson Mountain front, in Yukon Territory. Here again there is no palaeontological evidence as to age of the section. In addition the well known index species ***Knoxisporites literatus*** (Waltz) Playford and ***Grandispora echinata*** Hacquebard may bear some resemblance to miospores recorded from New York State and Pennsylvania, U.S.A. On the basis of miospores recorded by McGregor the age of the section is considered to be Strunian.

McGregor (McGregor & Uyeno, 1972) established six spore assemblages of Siegnenian to lower Famennian from Melville and Bathurst Islands, in the Franklinian Miogeosyncline of the Canadian Archipelago. These assemblages are on the whole very different from the Upper Devonian miospores from New York State and Pennsylvania, U.S.A. However, spores probably belonging to the genera ***Retusotriletes, Apiculiretusispora, Geminospora, Dibolisporites, Convolutispora, Emphanisporites, Samarisporites, Spinozonotriletes, Rhabdosporites, Grandispora, Calyptosporites, Auroraspora, Ancyrospora*** and ***Hystricosporites*** occur in both.

About a decade ago, Chi, & Hills (1976) published a comprehensive paper which deals with megaspores and miospores from Arctic Canada. Seven assemblage zones of Givetian to Famennian age have been established on the basis of the relative abundance and the first or last occurrence of characteristic species. The majority of spores, however, are from the Givetian and Frasnian parts of the succession. The spore floras of Arctic Canada are very different from those from the New York State and Pennsylvania, U.S.A. However, ***Grandispora multiapicalis*** Chi & Hills which has been recorded from Frasnian deposits is similar in construction to ***Hystricosporites multifurcatus*** (Winslow) Martimer & Chaloner.sIt is interesting to note that Chi & Hills (op. cit.) recorded ***Rhabdosporites langi*** (Eisenack) Richardson from the Givetian to Frasnian sediments, while during the present study it has been found from Famennian deposits. In Europe ***R. Langi*** (Eisenack) Richardson appears to be limited to the Eifelian-Frasnian deposits.

CONCLUSION

A comparison is attempted on the palynomorphs of the present investigations with those from other parts of North America. Sediments from western New York State and Northern Pennsylvania (fig. 1) are correlated with those from other parts of the U.S.A.s and Canada including Southern Ontario, Maritime Provinces and Yukon Territory.

External Correlation is afforded by the strikingly close similarity between the microfloras describe from the present material and those reported previously from the Upper Devonian of North America. Detailed Comparison of these Famennian deposits with those from Canada and U.S.A. shows that ***Vallatisporites vallatus*** var. ***hystricosus*** (Winslow) Clayton ***et al.***, and ***Retispora lepidophyta*** (Kedo) Playford appear in the same horizon in Famennian (approximately at the base of Fa2d) in the area investigated as in other sequences of Canada and U.S.A.

Inter-regional correlation based on miospore assemblages has indicated that the Dexterville Member is equivalent to Evieus beds; whilst the Ellicott Member and overlying Cattaraugus Formation are probably coeval stratigraphically to the Comblain-An-Pont beds of Belgium (Ahmed, 1985). In terms of Belgium substages, the age of the strata investigated is shown to range from F3 to Fa2d (Upper Frasnian to Middle Famennian in terms of standard European stages). In term of North American nomenclature, the series range in age from Upper Senecan to Chautauquan.

The species ***Rugospora flexuosa*** (Jusch) Streel has frequently been observed in younger part of the sequences investigated. The species could be considered as an index fossil of the Middle Famennian (Fa2b – Fa2c), since it has been reported from almost equivalent stratigraphical levels in many parts of the world e.g., western Europe, North Africa and North America.

Apart from the index species of Famennian deposits such as ***Vallatisporites vallatus*** var. ***hystricosus*** (Winslow) Clayton ***et al.***, ***Retispora lepidophyta*** (Kedo) Playford, following important miospores have been regarded as common to sediments of New York State and Pennsylvania and to those from Canada and other parts of the U.S.A.; ***Rugospora flexuosa*** (Jusch) Streel, ***Punctatisporites solidus*** Hacquebard, ***Retusotriletes incohatus*** Sullivan, ***Retusotriletes phillipsii*** clendening ***et al.***, ***Aneurospora greggsii*** (McGregor) Streel, ***Aneurospora incohata*** (Sullivan) Streel, ***Dictyotriletes trivialis*** Naumova ***Emphanisporites rotatus*** McGregor, ***Knoxisporites literatus*** (Waltz) Playford, ***Knoxisporites pristinus*** Sullivan, ***Vallatisporites vallatus*** Hacquebard ***Auroraspora poljessica*** (Kedo) Streel,s ***Auroraspora torquata*** Higgs, ***Auroraspora pseudocrista*** Ahmed, ***Auroraspora solisorta*** Hoffmeister ***et al.***, ***Grandispora corunata*** Higgs, ***Grandispora echinata*** Hacquebard, ***Spelaeotriletes lepidophytus*** (Kedo) Streel, and miospores with multifurcate appendages such as ***Hystricosporites multifurcatus*** (Winslow) Mortimer & Chaloner.

Chi & Hills (1976) observed ***Rhabdosporites langi*** (Eisenach) Richardson from the Givetian to Frasnian deposits, while during the present study it has been recorded from Famennian deposits. In Europe ***Rhobdosporites langi*** (Eisenach) Richardson appears to be limited to the Eifelian-Frasnian deposits.

ACKNOWLEDGEMENTS

The author is indebted to Dr. John, B. Richardson of the Palaeontology Department, British Museum (Natural History), London, for providing the samples and for critically reading the manuscript. Grateful acknowledgements are also extended to Professor F.A. Shams, Director of the Institute of Geology, Punjab University, Lahore, and to Dr. Aftab A. Butt of the same Institute for constructive comments at different stages of this work. The author is thankful to Mr. Minhas for assistance in drafting the figures and to Mr. Akbar, Senior Stenographer for typing the final manuscript.

REFERENCES

AHMED, S. (1978) Palynology and biostratigraphy of some Upper Devonian deposits of western New York State and northern Pennsylvania, U.S.A. London University. Ph.D. Dissertation, (Unpublished) 355p.

———— (1980) Some forms of the genus Auroraspora from the Upper Devonian of New York State and Pennsylvania, U.S.A., Jour Univ. Kuwait (Sci.) s7, pp. 227-43.

———— (1984) Geographical variations in the Upper Devonian miospore assemblages. Kashmir Jour. Geol. 3, pp. 81-6.

———— (1984) Application of palynology in economic geology with special emphasis on palynological investigations of Upper Devonian rocks. First Pakistan Geol. Cong. Volume of Abstracts. pp. 77-9.

———— (1985) Comparison of the Upper Devonian miospore assemblages with different parts of the world. Geol. Bull. Punjab University, 20, pp. 60-70.

———— & RICHARDSON, J.B. Miospore forms from the Upper Devonian Sediments of New York State and Pennsylvania, U.S.A. (in preparation).

ALLEN, K.C. (1965) Lower and Middle Devonian spores of north and central Vestspitsbergen. – Palaeontology 8, pp. 687-748.

CHI, B.L. & HILLS, L.V. (1976) Biostratigraphy and taxonomy of Devonian megaspores, Arctic Canada. – Bull. Can. Pet. Geol. 24(4), pp. 640-818.

CLAYTON, G., HIGGS, K., GUEININ,s K.J. & VAN GEDER, A. (1974) Palynological Correlations in the Cork Beds (Upper Devonian –? Upper Carboniferous) of southern Ireland. Proc. R. Jr. Acad. 74B, pp. 145-55.

CLENDENING, J.A., EAMES, L.E. & WOOD, G.D. (1980) *Retusotriletes phillipsii* n.sp., a potential Upper Devonian guide palynomorph. – Palynology 4, pp. 15-22.

EAMES, L.E. (1974) Palynology of the Berea Sandstone and Cuyahoga Group of Northeastern Ohio. – Dissertation, Michigan State University, Lansing, Mich. (Unpublished).

———— (1978) A palynologic interpretation of the Devonian – Mississippian boundary from northeastern Ohio, U.S.A. (abst.) – Palynology 2, pp. 218-9.

HOUSE, M.R. (1975) Facies and time in Devonian tropical areas. – Proc. York. Geol. Soc. 40, 2(16), pp. 233-88.

McGREGOR, D.C. (1960) Devonian spores from Melville Island, Canadian Arctic Archipelago. – Paleontology 3, pp. 26-44.

———— (1970) *Hymenozonotriletes lepidophytus* KEDO and associated spores from the Devonian of Canada. – Congress et Colloques Univ. Liege. 55, pp. 315-26.

———— & OWENS, B. (1966) Illustrations of Canadian fossils: Devonian spores of eastern and northern Canada. – Geol. Surv. Canada, Paper 66-30, pp. 1-66.

———— & UYENO, T.T. (1972) Devonian spores and conodonts of Melville and Bathurst Islands, district of Franklin. – Geol. Surv. Canada. Pap. 71-13, pp. 1-37.

MOLYNEUX, S.G., MANGER, W.L. & OWENS, B. (1984) Preliminary account of Late Devonian Palynomorph assemblages from the Bedford shale and Berea Sandstones Formations of Central Ohio, U.S.A. – Jour. Micropalaeontology., 3(2), pp. 41-51.

RICHARDSON, J.B. (1960) Spores from the Middle Old Red Sandstone of Cromarty, Scotland. – Palaeonotology, 3(1), pp. 45-63.

———— & McGREGOR, D.C. (1986) Silurian and Devonian spore of the Old Red Sandstone Continent and adjacent regions. – Geol. Surv. Canada Bull. 364, pp. 1-79.

STREEL, M. & TRAVERSE, A. (1978) Spores from the Devonian/Mississippian transit ion near the Horseshoe section. Altoona, Pennsylavania, U.S.C. – Rev. Palaeobot. Palynol. 26, pp. 21-39.

TESMER, I.H. (1963) Geology of Chautauqua Country, New York, Part 1 – Stratigraphy and Palaeonotology. N.Y. State Mus. Bull. 391.

———— (1967) Upper Devonian stratigraphy and Palaeontology of southwestern New York State. – Int. Symposium on the Devonian system, Calgary, Alberta. 2, pp. 257-69.

———— (1975) Geology of Cattaraugus Country – Buffalo Soc. Nat. Sci. Bull. 27, pp. 1-105.

WICANDER,s R. & PLAYFORD, G. (1985) Acritarchs and spores from the Upper Devonian Lime Creep Formation, Iowa, U.S.A. – Micropalaeonotology, 31(2), pp. 97-138.

WINSLOW, M.R. (1962) Plant spores and other microfossils from Upper Devonian and Lower Mississippian rocks of Ohio. – U.S. Geol. Surv. Prof. Paper 364, 93p.

Manuscript received 10.12.1986
Accepted for publication 31.12.1986

ACTA MINERALOGICA PAKISTANICA
VOLUME 2 (1986) pp. 144 - 152.

A MINERALOGICAL STUDY OF THE INDUSTRIAL UTILIZATION OF BAUXITIC CLAYS OF NAWA AREA, KALA CHITTA RANGE, ATTOCK DISTRICT, PAKISTAN.

IFTIKHAR HUSSAIN BALOCH

Institute of Geology, University of the Punjab, New Campus, Lahore–20, Pakistan.

ABSTRACT:– This paper gives a detailed account of the mineralogy of the bauxitic clays of Nawa area from the Datta Formation of Early Jurassic age exposed in the Kala Chitta Range, Pakistan. The mineralogical studies show that kaolinite, diaspore and boehmite are the essential minerals, while chlorite, anatase, rutile, quartz and haematite are accessories. A brief account of the chemistry, phase transformation and detailed description of industrial utilization is also presented. Three grades of clays are found: one can be used as a high grade refractory, the second for ceramics and the third for common bricks.

INTRODUCTION

The Early Jurassic Datta Formation of the Kala Chitta Range contains well-known low iron bauxitic clays and laterites. The object of the present study is to investigate the mineralogical and chemical variation of the bauxitic clays from the Nawa area (figs 1, 2) of the Kala Chitta Range for the assessment of future utilization. For this purpose channel samples were collected from lithologically different zones of a profile (fig. 3) and studied by x-ray fluorescence spectrometer, x-ray diffractometer and scanning electron microscope. The stratigraphic relationship of the Datta Formation is given below.

In this work mineralogy was treated of prime importance because of its role in determining the validity of the deposit for future industrial utilization. The main method was the x-ray diffraction techniques in order to obtain a whole range of qualitative analyses of all the mineral phases present in the raw material. Chemical analyses were carried out with a Philips PW 1212 automatic x-ray fluorescent spectrometer. Twelve samples representing the whole range of variation were subjected to x-ray fluorescence analysis as described by Zussman (1979).

GEOLOGY

The area is tectonically disturbed and highly folded and faulted. The stratigraphic sequence is given in table 1. Other stratigraphic features are given by Hussain et al. (1967) Shah (1977) and Cheema (1974). The Samana Suk and Kingriali Formations are in contact with the Datta Formation in the project area.

Kingriali Formation consists of thin to thick bedded, massive, fine to coarse textured, light grey brown dolomite and dolomitic limestone with interbeds of greenish dolomitic shale and marl in the upper part. The thickness varies from 76 m to 106 m. The lower contact with the Tredian Formation is marked by interbedding of sandstone and dolomite. The upper contact with the Datta Formation is disconformable and shows the development of the ferruginous dolomite and uneven surface at the contact. Fossils are rare and poorly developed.

Datta Formation is mainly of continental origin and consists of variegated sandstone, shale, siltstone and mudstone with irregularly distributed calcareous, dolomitic, carbonaceous, ferruginous, and fireclay horizons. The fireclay is present in the lower part. The fireclay is creamy, brownish, greyish and fine grained.

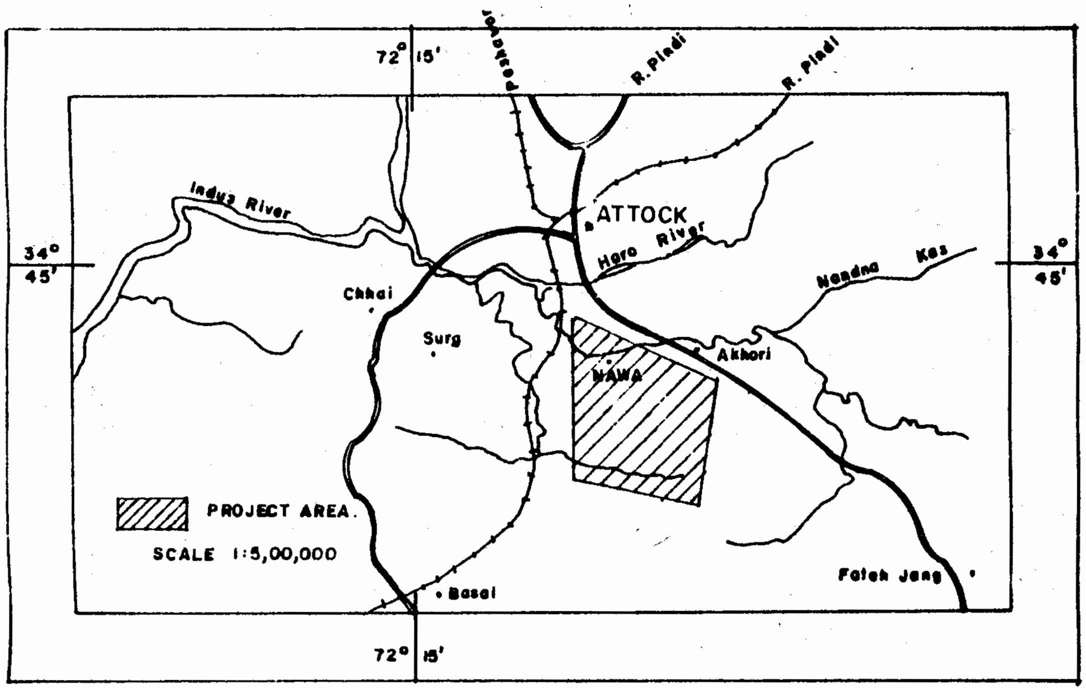

Fig. 1. LOCATION MAP OF NAWA AREA, ATTOCK DISTRICT, TOPOSHEET 43 C/6.

According to Ashraf et al. (1973), the composition varies from place to place in the area, and vertically too. It rests unconformably on Kingriali Formation, the upper contact with the Shinawari Formation is gradational. It is of Early Jurassic mainly pre-Toarcian age. The thickness in the type locality is from 212 m to 400 m.

The ***Samana Suk Formation*** is thin to thick bedded, shows folding and includes some dolomitic and ferruginous, sandy and oolitic beds in the Kala Chitta area. The oolites vary in size ranging from microscopic to megascopic. Some oolites have concentric or radial structures, while others are elliptical which shows the tectonic plasticity of the rock. The thickness varies from 170 m to 336 m. The lower contact is transitional with Shinawari Formation and the upper contact with the Chichali Formation is disconformable.

MINERALOGY

A qualitative mineralogical study of the raw fine grained bauxitic clay was carried out using x-ray diffraction (Brindley & Brown, 1980). The normal powder camera cannot be used because these clays show diagnostic reflections in the region 7.16Å, 6.11Å and 3.99Å and reflections at such d-spacing cannot be obtained with it.

The x-ray diffraction traces of six samples are reproduced in fig. 4 and 5 and are more or less the same for all samples except the sixth one.

Clay Minerals

(i) Kaolinite

The raw material is dominated by the presence of kaolinite as detected by XRD

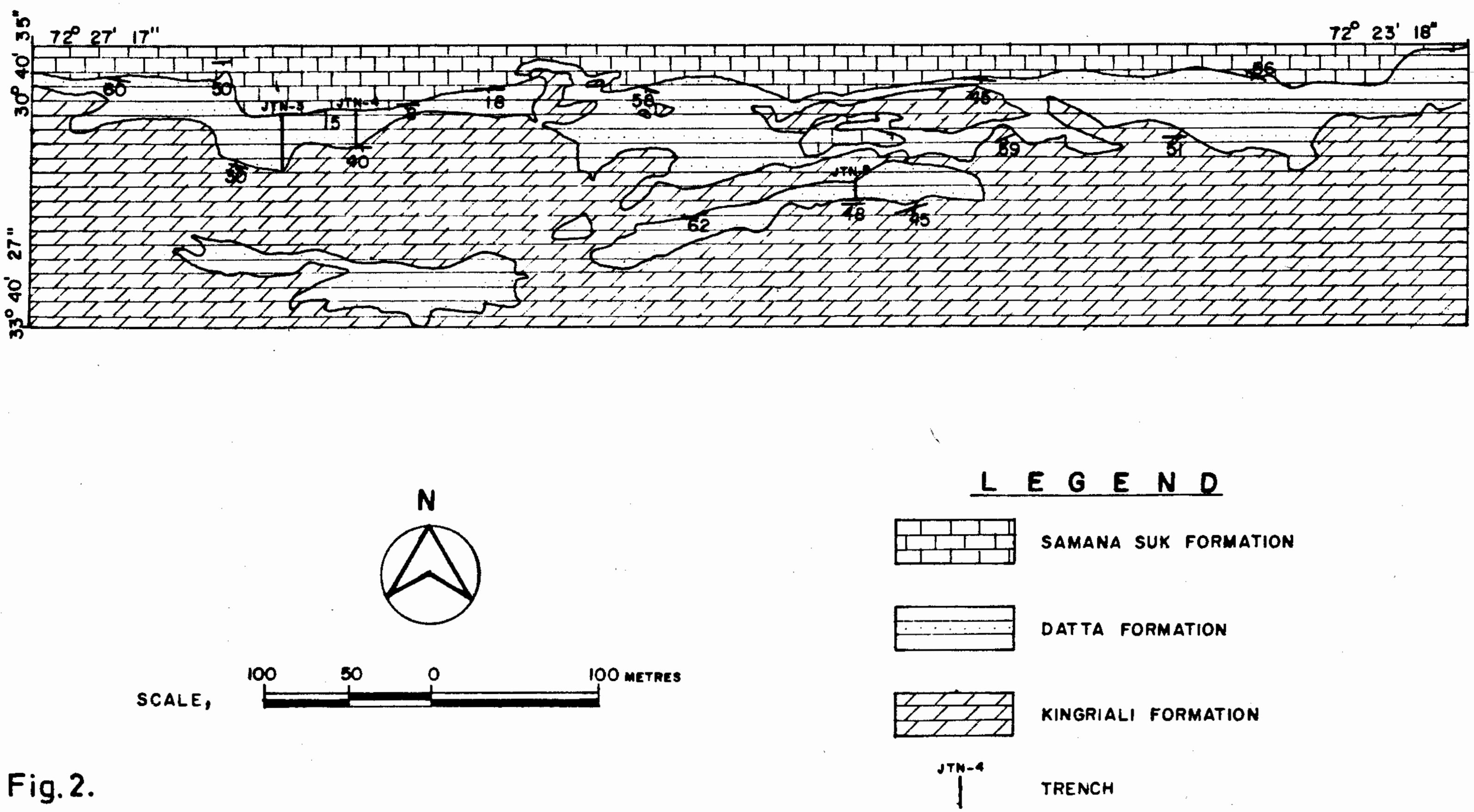

Fig. 2.

GEOLOGICAL SKETCH MAP OF NAWA AREA, KALACHITTA RANGE, DISTRICT ATTOCK, PAKISTAN

Table 1. Stratigraphic relationship of the Datta Formation.

EPOCH	FORMATIONS	THICKNESS IN METRES	LITHOLOGY (GENERALISED)
MIDDLE JURASSIC	SAMANA SUK	about 190	Light grey to greyish brown limestone and marl. Includes some dolomitic and ferruginous, sandy, oolitic beds. Thinbedded to thick-bedded or massive.
EARLY JURASSIC	DATTA	20 to 30	Variegated sandstone/shale in the upper part, calcareous, quartzose fireclay/bauxite in the middle/lower part and hematitic sandstone to ironstone near the base.
LATE TRIASSIC	KINGRIALI	91	Uneven surface of top beds, Grey to brown dolomitic limestone, dolomite, dolomitic shale, thick-bedded.

techniques in which all the peaks are found very sharp and smooth (fig. 4).

From the obtained data it might be concluded that the degree of crystallinity and the atomic order is moderate. The systematic sampling reveals that the amount of kaolinite decreases in the direction of dip. The possible reason for this process might be some sort of solution activity in which kaolinite is leached out.

This is present as a minor constituent only in one sample (NA–2). Its presence is indicated by a peak at 14.1 Å.

Non–Clay Minerals

(i) Diaspore

Diaspore is abundant in the sediments of this deposit. It is finegrained as well as crystalline.

The density of the pure diaspore is 3.4 but the sample in which the diaspore is maximum and kaolinite minimum has a density of 3.18. The sample, with maximum kaolinite and minimum diaspore has a density of 2.5.

(ii) Boehmite

It shows moderate to weak reflections on the XRD traces. However, there are some XRD traces which show strong reflections of boehmite (e.g., POT–1, P–1 and NA–2). Samples POT–1 and P–1 were collected from the adjoining area of the same stratigraphic horizon.

(iii) Antase/Rutile

The detrital grains of these minerals are present as essential accessory in the bauxitic clays.

The amount of anatase is significant enough to give low intensity peaks on the XRD traces of the raw material in most of the samples, whereas, rutile gave very low intensity peaks on the XRD traces as compared to the anatase except in one or two samples.

(iv) Haematite

The residual deposit under present investigation does not have any iron impurities except one sample whose iron is mainly in the form of haematite. In places,

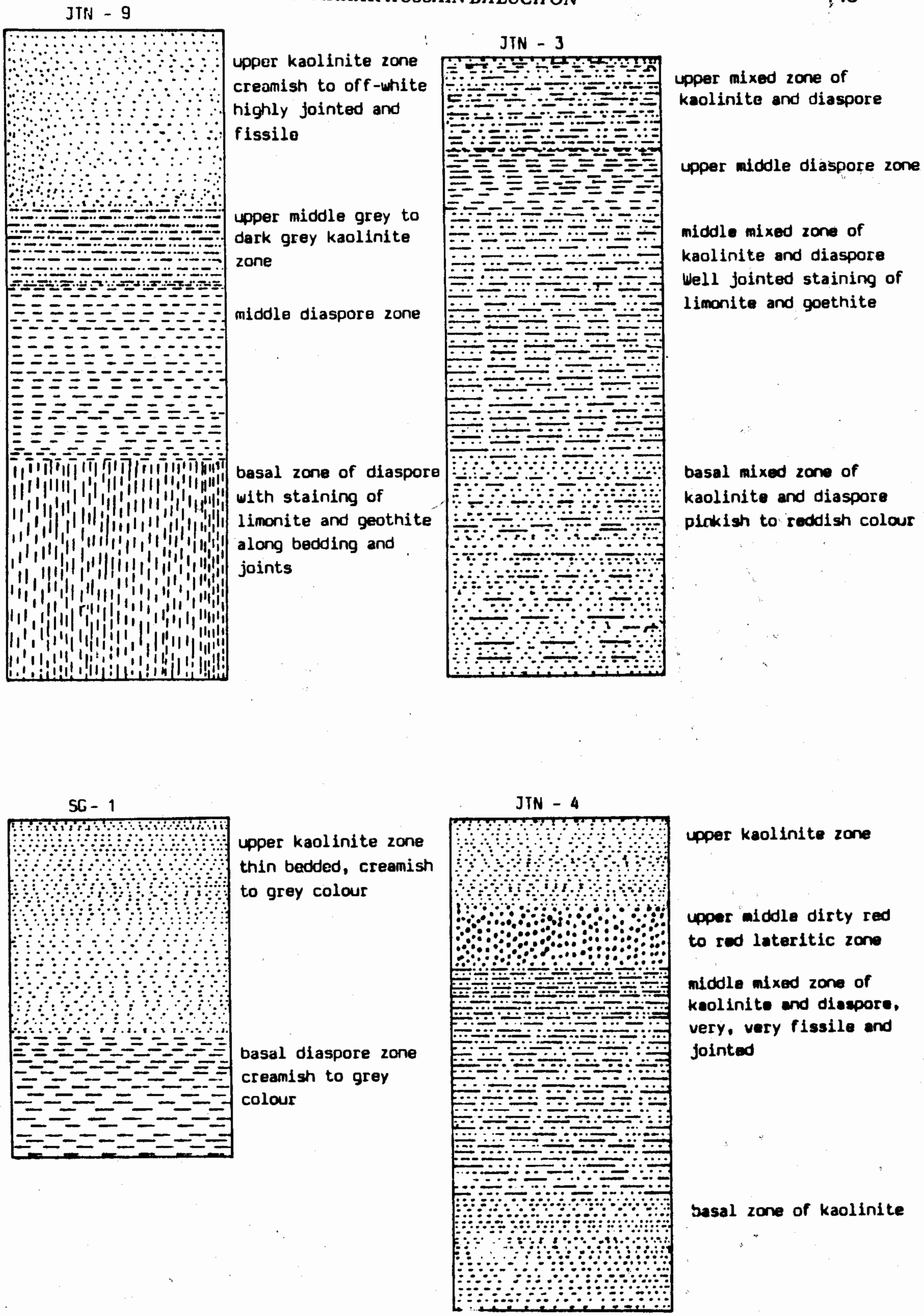

Fig. 3. Lithological variations through different profiles.

the leaching out of iron solution has deposited amorphous limonite and goethite, which mark all the structurally weak places like joints and fractures etc. with reddish brown to yellowish colours. Sample no. NA–10 shows the maximum amount of haematite on the XRD trace. This is due to the veinlets of iron-rich material at the sample spot.

Low quantities of iron-rich minerals make these bauxitic clays much more useful for the future utilization than any other such type of deposit in the adjoining area.

(v) **Quartz**

This gives moderate to weak peaks in some XRD traces of the raw material and suggests that free silica is not present in considerable amount.

DISCUSSION

The decrease in kaolinite and increase in diaspore content in the channel in the direction of dip (e.g. profile of JTN–9) suggests that the association of kaolinite has formed by some kind of leaching action associated with the development of the sink-holes. The genetic relation of the kaolinite to the diaspore is not clear.

Hydrolysis of silicate in a tropical climate produces an alumina silica gel; after subsidence and burial, diaspore crystallizes from the gel and is followed by kaolinite formation. (Deer et al., 1962).

Thus the diaspore and kaolinite-rich horizon may be expected in the tectonically disturbed areas like the one under present study.

The low percentage of iron in the deposit supports the idea of the necessity for a tropical climate, the temperature above 20°C helps chemical processes by which SiO_2 goes into solution and Fe_2O_3 and Al_2O_3 remain behind. In fact, the pH of the dissolving fluid is much more important because of the insolubility of alumina between pH 4 & 9, but soluble at a pH of < 4, with a moderate solubility of SiO_2 below a pH of 10.

Actually, low pH of about 3 and low Eh is necessary to achieve transport of iron with residual enrichment of alumina. Accumulation of free CO_2 on the surface is hindered during a wet season. The wet season of the tropics during which acid solutions are diluted, is one of the formation of Al_2O_3 and Fe_2O_3; the dry season, when acid residual solutions exist, is one of the leaching of silica from these oxides and, depending on local pH and Eh conditions, iron ions or colloids may be over long distances.

The presence of titanium minerals can be explained as several other elements dissolve the precipitate under similar conditions to aluminium, titanium is an example.

The chemical analyses by the XRF show the variations as follows:

The SiO_2 content varies from 5.12% to 43.05%; TiO_2 from 2.34% to 5.38%; Fe_2O_3 from 0.35% to 1.17%; CaO from 0.03% to 1.80%; K_2O from 0.01% to 0.66%; P_2O_5 from 0.05% to 0.34%; MnO from 0.00% to 0.87%; Na_2O from 0.00% to 0.05%; MgO from 0.00% to 0.16% and SO_3 from 0.00% to 0.14%.

Table 2. Bulk chemistry of bauxitic clay from Nawa (After Calibration for High Al)

Sample	N2A	NA–4	NA–1	NA–9	SG–2
SiO_2	5.12	12.01	37.57	43.05	42.91
Al_2O_3	75.17	68.27	43.27	39.42	36.99
TiO_2	4.95	4.95	2.87	2.92	2.67
Fe_2O_3	0.45	0.51	0.92	0.61	1.86
MnO	0.00	0.00	0.01	0.87	0.02
MgO	0.05	0.06	0.10	0.00	0.14
CaO	0.08	0.10	0.17	0.06	0.29
Na_2O	0.02	0.02	0.03	0.00	0.05
K_2O	0.07	0.02	0.05	0.66	0.34
P_2O_5	0.34	0.19	0.17	0.08	0.13
SO_3	0.14	0.07	0.11	0.08	0.08
LOI	14.58	14.37	14.45	14.99	14.34
Total	100.97	100.57	99.72	102.74	99.82

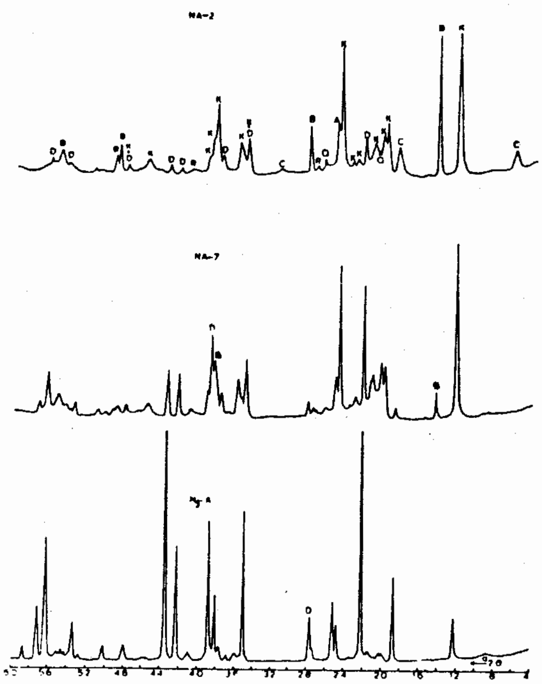

Fig. 4. X - RAY DIFFRACTION TRACES OF RAW MATERIAL USING Cu K_{α} RADIATION.

A = Anatase B = Boehmite C = Chlorite D = Diaspore
H = Haematite K = Kaolinite Q = Quartz R = Rutile

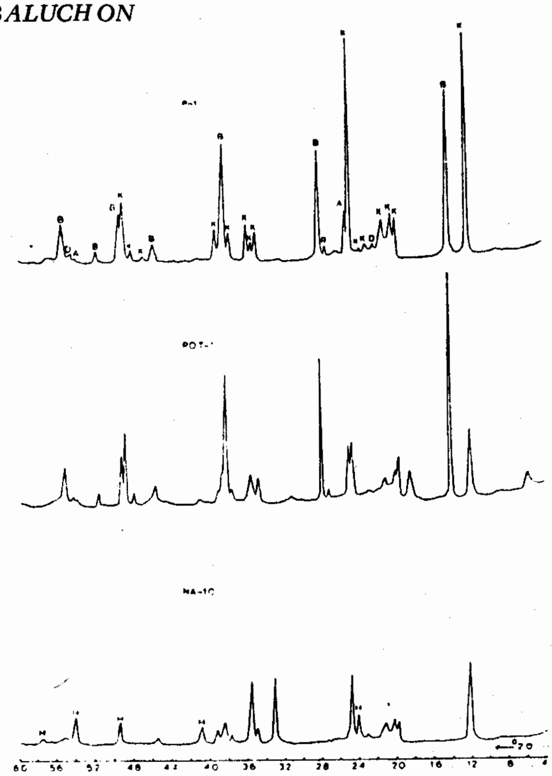

FIG. 5. X - RAY DIFFRACTION TRACES USING Cu K_{α} RADIATION

A = Anatase B = Boehmite C = Chlorite D = Diaspore
H = Haematite K = Kaolinite Q = Quartz R = Rutile

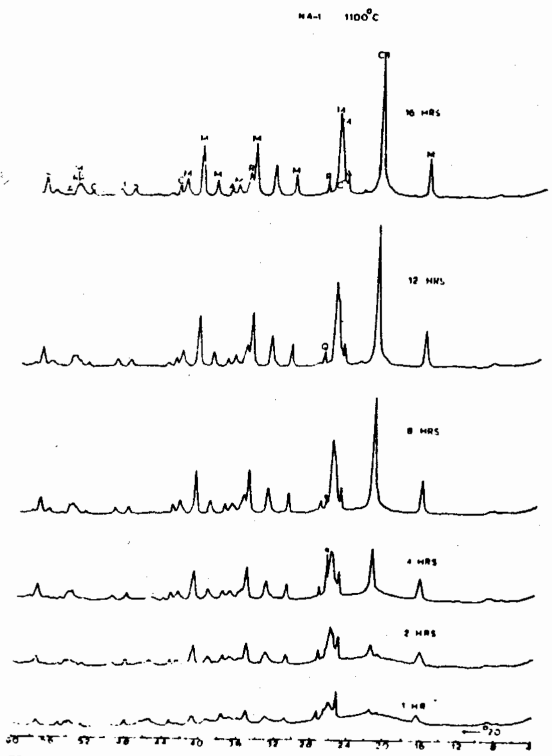

FIG. 6. X-RAY DIFFRACTION TRACES OF FIRED MATERIAL WITH Cu K_{α} RADIATION

A Anatase C Corundum CR Cristobelite
M Mullite Q Quartz R Rutile

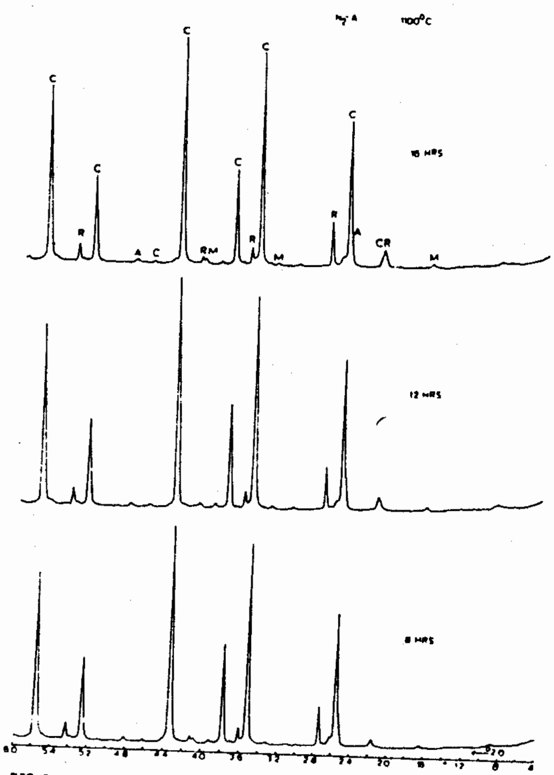

FIG. 7 X - RAY DIFFRACTION TRACES WITH Cu K_{α} RADIATION

A = Anatase C = Corundum CR = Cristobelite
M = Mullite Q = Quartz R = Rutile

Whereas the loss of ignition varies from 14.34% to 16.46%.

From this data it is quite possible to divide into the several small groups. In other words, selective mining is possible in view of definite end uses based on bulk chemistry. This can be elaborated, grouping the present data into three groups which came from the different sample locations.

CONCLUSIONS

The Early Jurassic bauxitic clay from the Nawa area, Kala Chitta Range of Pakistan were investigated. The area has latitudes 33°40′ to 33°40′ 35′ N and longitudes 72°22′ 17″ to 72° 23′ 8″ E.

The mineralogical studies revealed the presence of following phases in order of predominance: kaolinite, diaspore, boehmite, anatase/rutile, haematite, quartz and chlorite.

The effect of heat on the raw material was determined by firing them from 800°C to 1100°C in the time range of one to sixteen hours. A complete study of fired material with x-ray diffraction revealed the major phase transformation which took place with increasing temperature and time. The new phases obtained by firing tests include mullite, cristobalite and corundum. In fired material corundum is throughout consistent above 800°C while mullite and cristobalite appear at 1100°C. Some graphs are shown in fig. 6 & 7.

On the basis of detailed mineralogical studies, bulk chemistry and firing tests, it is possible to group the raw material in various grades and sub-grades meant for its final use in industry.

The groups are as follows :

Group 1: The investigations of this group revealed that these are highly pure bauxitic clays. Their high Al_2O_3 and low TiO_2 iron and alkali content makes them suitable for a high grade refractory material. This fact is further confirmed with the series of experiments which yield mullite and cristobalite from the original raw materials, hence, represents the high refractoriness. Therefore, it is strongly recommended to use this group material for high grade refractories.

Group 2: This group has a balanced proportion of Al_2O_3 and SiO_2 – with more alkalis than Group 1. All these facts collectively make this group a suitable material for ceramics and allied industries. The alkalis are particularly important constituent of this group because of their possible role as a flux in various ceramic products. Hence this group is strongly recommended for use in ceramics and allied industries.

Group 3 : In the last group silica contents are very high and range from 42.76% to 43.05%. However, the mineral constituents and their relative proportions do not prevent its use as a raw material for brick making industries. Therefore, this material is exclusively recommended for brick manufacturing industries with certain additives for desired brick colours.

ACKNOWLEDGEMENTS

The research was carried out at the Geology Department, Hull University, England, leading towards an M.Sc. thesis through a scholarship awarded by the British Council.

The author is indebted to Professor A.C. Dunham, Hull University, U.K. for his invaluable guidance and help for comprehensive and successful completion of this work.

The author expresses his gratiude to Dr. Aftab Ahmed Butt, Punjab University, for his suggestions and critical review of the script.

Special thanks are due to Messrs Abdul Jalil Abrar, Muhammad Kamil Sheikh and Abdul Quddos Khan, Directorate General of Hydrogeology, WAPDA, Lahore, for their help.

REFERENCES

ASHRAF, M., AHMAD M. & FARUQI, F.A. (1973) Jurassic bauxite and kaolinite deposits of Chhoi area, Kala Chitta Range, Punjab, Pakistan. *The Geological Bulletion* 12, pp. 41-46, 52, 53.16, 52, 53.

BRINDLEY, G.W. & BROWN, G. (1980) CYSTAL STRUCTURES OF CLAY MINERALS AND THEIR X-RAY IDENTIFICATION Min. Soc. Monograph 5, London.

CHEEMA, M.R. (1974) Geology of chhoi-Jabbi-wala kas area with emphasis on early Jurassic high alumina clay and bauxite deposits, northern Kala chitta, Compbellpur district, Punjab Province, Pakistan. Geol. Surv. Pakistan Technical Report 129, pp. 19-34.

DEER, W.A., HOWIE, R.A. & ZUSSMAN, J. (1962) AN INTRODUCTION TO THE ROCK FORMING MINERALS. Longman, London, 439p.

HUSSAIN, T. AND KHAN, A.L. (1967) FIRECLAY DEPOSITS OF KALA CHITTA RANGE, DISTRICT CAMPBELLPUR, WEST PAKISTAN. Geol. Survey Pakistan, pp. 1-89.

LEFOND, S.L. (1983) INDUSTRIAL MINERALS AND ROCKS. 5th Edition Soc. Min Engg. New York.

SHAH, S.M.I. (1977) Stratigraphy of Pakistan. Mem. Geol. Surv. Pakistan 12, pp. 34-43.

ZUSSMAN, J. (1979) PHYSICAL METHODS IN DETERMINATIVE MINERALOGY. Academic press, London, pp. 217-251.

Manuscript received 20.12.1986
Accepted for publication 31.12.1986

ACTA MINERALOGICA PAKISTANICA
VOLUME 2 (1986) pp. 153-157.

MICROSTRUCTURES OF VALLETA–MOLIERE FAULT OF FRANCE & ITALY

ABDUL HAQUE

Department of Geology, University of Baluchistan, Quetta, Pakistan.

ABSTRACT:– The mylonite of Valleta-Moliere is a crushed zone, defined lithologically by various geologists. Structurally it has always been described as major dextral strike-slip fault which divides the massif of Argentera-Mercantour into two different petrographical domains: the western and the eastern (Faure-Muret, 1955). The microstructures within this zone and their interpretation confirm the dextral sense of this major strike-slip fault.

INTRODUCTION

The mylonite of Valleta-Moliere, a crushed zone, is the product of major strike-slip fault which divides the massif of Argentera-Mercantour into two petrographic domains: the western and the eastern. Each of the two domains is further subdivided into different petrological series (Faure-Muret, 1955).

This major strike-slip fault is situated in France and Italy. In France it outcrops near Saint-Martin Vésubie, while in Italy it is located near Saddle Ferriere. The length of this crushed zone is 45 to 50 kms, whilst its width varies from few cms near the saddle of Passo Sattano, to 100-150 m (Faure-Muret, 1955; Bogdanoff, 1980). In the mapped area, the mylonite of Valleta-Moliere has been lithologically and structurally studied in the NW of Moliere (fig. 1b), where its orientation is NW–SE, further towards south it orients NS. Romain (1978) further extends it to Saint-Martin Vésubie in the eastern direction. The width of this fault measures to few hundred metres in the NW of Moliere, while it pinches near the Tete of the Marges (Abdul Haque, 1984).

LITHOLOGY

The mylonite of Valleta-Molière has been lithologically defined by various geologists. Franchi considered it as the product of the deformation of gneisses and migmatites, whereas Sacco defines it as the ancient crystalline schists. Faure-Muret interprets it as crushed Paleozoic synclines. Malaroda (1966), distinguished paleomylonite from that of mylonite in this zone. Recently, Bogdanoff (1980), defined it as a schistose formation of sedimentary origin, which is prior to all ductile deformation of the massif of Argentera-Mercantour, and is subsequently tectonized by Alpine and former orogenies. Near Valleta, he demonstrated a lithological succession from the western contact to the eastern limit and named it as Valleta-Formation.

In the mapped area, near the migmatites of Rabuons the original rock is black to grey migmatite which grades to dark yellow to grey schist towards east and at the eastern contact the zone is marked by massive green and beige migmatite of Adus.

Bogdanoff proposed Early Paleozoic to this mylonite whereas Vernet (1950) had given it an Alpine age. In the studied area, Permian red shales have been wedged out in this mylonite which suggests the Post-Permian age.

STRUCTURES

Within the mapped area the outcrop of the mylonite of Valleta-Moliere, situated in the NW of the Moliere is very small with respect to its

Table 1. Succession of the Valleta Formation.

	Formation Nomenclature	**Lithology**	Thickness
	Migmatites of Adus		in the east.
	Valleta Formation		
5		Miliary gneiss with biotite	270 m
		White gneiss with biotite	50 m
		Black schists	20 m
		Marble band	2 m
		Black schists	60 m
		Alternation of black schists and marble	60 m
		Layered marble	2 m
4		Feldsphatic quartzites	5 m
3		Black and greenish schists and micaschists	250 m
2		Layered amphibolites	30 m
1		Black schists and micaschists	200 m
	Migmatites of Rabuons		in the west.

length and width as given above. However, the structures within this crushed zone and the structural relationship with its western and eastern limits are interpreted below.

Western limit

This limit of Valleta-Molière with the migmatites of Rabuons is curved contact. On both sides of this limit the orientation of lineations within the foliation and the axes of the folds are of the same directions. The folds within the mylonite and in the migmatites of Rabuons have the same style but the number of folds (frequency) become less within the former (Bogdanoff, 1980).

Over the terrain, this western contact outcrops for a few hundred metres, and is oriented *N140-N150*, showing also the general direction of the foliation within the basement of Argentera-Mercantour. This western contact is intercepted by parallel faults trending *N30* due to which rotation of foliation has taken place. Thus, the dip of foliation *70E* (before rotation) becomes *35 W* (after rotation).

Mylonitic Zone

From the western to the eastern contact the crushed zone has the following structures. According to Bogdanoff (op. cit.) migmatites are not present in Valleta-Formation, but it contains minerals like muscovite, chlorite, epidote, calcite, late tourmaline; and Malaroda identifies that garnet grains are fractured sub-grains.

Romain (1978) has given a microscopic description of the lithology of this mylonite. She mentioned three stages of mylonitization. In the first stage, the percentage of phenocrysts is highly abundant with less developed losangic fractures. Thus, rock as a whole gives cataclastic aspect where mica flakes are recrystallized both in the cracks of quartz and in the crushed feldspar. These mica grains also give torsion figures, a phenomenon posterior to the recrystallization. In the second stage, losangic fragments are more abundant than phenocrysts. Quartz grains are rounded showing mortar structures and in their voids recrystallization of secondary mica has taken place. Finally, the

Explanations of Figures 1a and 1b

1. Saint Etienne de Tinée; 2. Isola; 3. Molière; 4.Saint Souveur sur Tinée; 5. Saint Dalmas; and 6. Saint Martin Vésubie.

a

see fig. 1c and 1d.

Mapped area

b

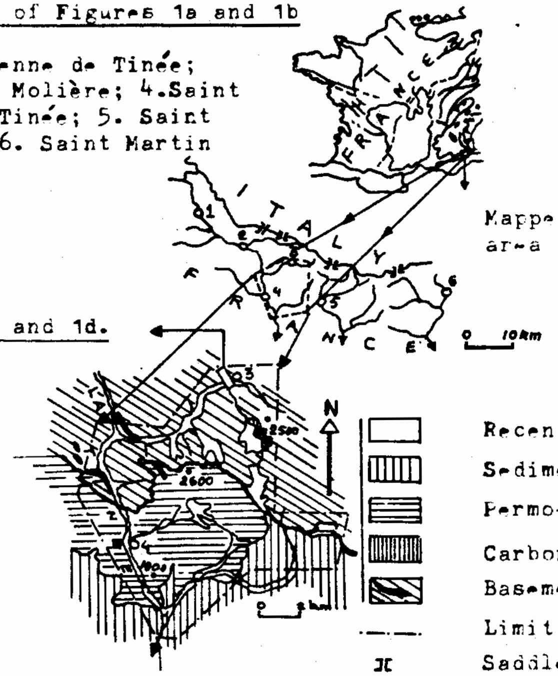

Recent.

Sedimentary Cover.

Permo-Triassic.

Carboniferous.

Basement rocks with amphibolites.

Limit of the mapped area.

Saddle

c

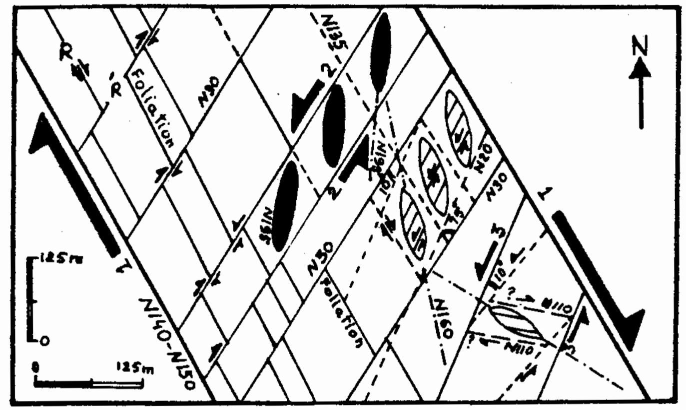

d

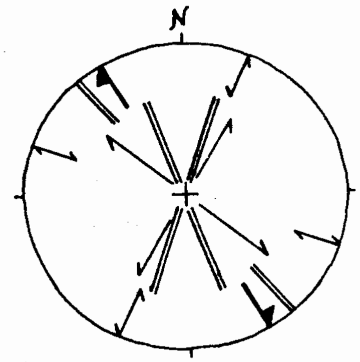

Figure 1a Schematic geological map of France and geographical limits of mapped area.

1b Geological map of the studied domain between Saint Sauveur sur Tinée, Molière and Saint Dalmas.

1c Analysis of the microstructures within the mylonitic zone of Valleta-Molière.

1d Strike-frequency diagramme representing faults and tension joints within the zone of Valleta-Molière.

third and the last stage is represented by an ultramylonite where all the aforesaid textural elements are not present and the rock becomes sericitized schist.

The general direction of foliation *N140-N150* is displaced transversely by sinistral, sometimes dextral faults *N30* which make an angle of 60 to 70 degrees with the general orientation of Valleta-Molière. In the eastern part of this crushed zone, anastomized tension fractures *N160* and *N195* have been observed which control the sinistral sense of the faults *N30.* Thus, faults *N30* are antithetic of Reidel of second order with respect to the main dextral strike-slip fault of Valleta-Molière which is synthetic in nature and parallel to the foliation *N140-N150.*

These anastomized tension fractures filled syntectonically with quartz and are subsequently cut by micro-sinistral fractures *N20.* Thus, these *N20* faults are of third order of Reidel and synthetic with respect to the faults *N30.* The faults antithetic of third show the same direction as the dextral strike-slip fault.

Eastern Limit

The eastern limit of Valleta-Molière with migmatites of Adus has been structurally divided into two sectors: the northern and the southern.

Northern Sector. In this sector the contact of Valleta-Moliere is very sharp with the migmatites of Adus. In these migmatites we can measure two sets of ***diaclases NS to N20*** and *N160-N165.* These ***diaclases*** situated in the leucocratic bands of migmatites are filled by recrystallized chlorite. They are also cut posteriorly by daxtral faults of direction *N135* and sinistral faults *N60* and *N80.*

An Alpine phase of folding *N140* to *N150* is represented by metamorphosed carbonate rocks of Triassic age being wedged out in the basement of Argentera-Mercantour.

Southern Sector. This limit of Valleta-Molière with the migmatites of Adus has been defined by Faure-Muret as faulted contact. In this sector the detretic Carboniferous rocks are folded in EW direction by Hercynian orogenesis and subsequently retaken by Alpine tectonics being represented by strike-slip faults *N120* and *N160* (Abdul Haque, 1986).

CONCLUSION

The mylonite of Valleta-Moliere is tectonically an ancient crushed zone, which divides the massif of Argentera-Mercantour into two different petrological domains (Faure-Muret, 1955). It has been defined lithologically by various geologists and structurally always been described as major dextral strike-slip fault. Presently the author takes into consideration for the first time, the microstructures within this zone and their interpretation confirms the dextral sense of this major strike-slip fault.

According to Bogdanoff (1980), the oldest age of this mylonite is Early Paleozoic. The presence of Triassic rocks forming tight synclines as well as the presence of small outcrops of Permian red shales, parallel to this zone suggests an Alpine age for this mylonite.

Hercynian compression directed *NS* has produced first order EW foldings of the Carboniferous rocks of the mapped area with respect to dextral strike-slip fault of Valleta-Moliere oriented NW-SE. Second order folding of Triassic rocks into NW-SE within the studied area, with respect to Valleta-Moliere give an Alpine compression of direction NE-SW.

ACKNOWLEDGEMENTS

I am grateful to Messieurs M. Lanteaume and M. Rioult Professors in the University of Caen, France, for their assistance during the field and laboratory investigations. I also express my thanks to Mr. Sher Bahadur, geologist in Baluchistan Development Authority, Quetta, Pakistan, for his valuable discussion in the course of preparation of this paper.

REFERENCES

ABDUL HAQUE (1984) Analyse des structures Alpines du socle-tegument de l'Argentera-Mercantour et de la couverture sur la transversale de la Tinée (Alpes-Maritimes, France) These 3 cycle, Univ. Caen, pp. 1-153. (Unpublished).

———— (1986) Some structural and petrographical aspects of the massif of Argentera-Mercantour situated in the French maritime Alps. Presented 15 Dec. 1986, in the 4th Miami Internat. Symp. Miami Beach, Florida, USA.

BOGDANOFF, S. (1980) Analyse structurale dans la partie occidentale de l'Argentera-Mercantour (A.M). These Doct. es-sciences Univ. Paris-sud, pp. 1-317. (Unpublished).

FAURE–MURET, A. (1955) Etudes geologiques sur la massif de l'Argentera-Mercantour et ses enveloppoes sédimentaires. Mem. Expl. Carte Geol. France, 336p.

MALARODA, R. (1966) Mylonites et Paleomylonites dans le massif de l'Argentera-Mercantour. Rend. Acc. Naz. Lincei. fasc. 3-4, VII, Vol. XLI

ROMAIN, J. (1978) Etude pétrographique et structurale de la bordure sudoccidentale du massif de l'Argentera, de Saint-Martin Vésubie á la cime du Diable (A.M.). Thèse 3 cycle, Univ. de Nice, 365p. (Unpublished).

VERNET, J. (1950) Les synclinaux de Trias Inférieurs et les structures majeures du soulevement de l'Argentera (A.M). C.R. Acad. Sci. Paris, 249(D), pp. 1696-1698.

Manuscript received 20.12.1986
Accepted for publication 31.12.1986

ACTA MINERALOGICA PAKISTANICA
VOLUME 2 (1986) pp. 158 - 160.

PETROGRAPHY OF METASEDIMENTARY ROCKS OF BARIAN–KUNDUL SHAHI AREA, NEELUM VALLEY, AZAD KASHMIR, PAKISTAN.

M. KHURSHID KHAN RAJA

Institute of Geology, University of Azad Jammu & Kashmir, Muzaffarabad, Pakistan.

ABSTRACT:– A detailed petrography of pelitic-psammitic rocks of 20 km^2 area with modal analyses of 16 thin sections is presented. These metasediments include schists of the Salkhala formation, metamorphosed under greenschist facies to epidote-almandine subfacies conditions. The details of index minerals are given.

INTRODUCTION

The studied area lies on the right bank of river Neelum and both sides of Jagra Nala, at 73° 5' 30"E and lat. 34° 3'30"N on toposheet no. 43F/14 and 43F/15 of the Survey of Pakistan.

The pelitic-psammitic rocks outcrop in the Barian and Kundulshahi areas as metasediments into which Jura granite has intruded. They belong to the Precambrian Salkhala Formation (Wadia 1931).

The previous geological contributions on the area are rather restricted. Wadia's (1931) work was basically of regional level. Ghazan far et al., (1983) have done mapping, but made few changes in Wadia's (1931) work.

GENERAL GEOLOGY

The studied area lies on the NE of Hazara-Kashmir syntaxis (fig. 1). It is found in middle Neelum Valley of middle Himalayas. It is dominantly composed of metasediments. The metasediments studied have southern contact with intrusive rocks near Barian. Northern contact near Dhanbella is also intrusive. Barian Kundulshahi metasedimentary rocks appear similar throughout except with minor petrographic variations. The metasediments are moderately to strongly schistose. They are well jointed and laminated. Their weathering colour varies from greenish to purplish brown. The quartz veins and dykes of basic rocks are commonly found. Microstructures like microfolding, cleavage, crenulation is also found. In Barian area garnet is microscopic while near northern contact with intrusive rocks and further northwards garnet grains are visible by naked eye. Near Kundulshahi garnet specks can be observed in hand specimens.

PETROGRAPHY

The rocks display a moderate to strongly schistose texture. Quartz is abundantly present as fine to medium sized, subhedral to anhedral grains. It frequently forms segregation bands. Garnet is present as light brown, irregularly subhedral shaped porphyroblasts, generally fractured. Biotite is present as brown to reddish brown flakes. It occurs in association with chlorite. Muscovite is present as scaly colourless flakes in aggregates and segregated layers, parallel to schistosity. It occurs in association with biotite as well. Brown limonite is found as secondary product of oxidation of hematite. Epidote is present in colourless aggregates associated with biotite. Minor amount of sphene and apatite is present. Opaque magnetite is present as anhedral to subhedral grains.

BASIC ROCKS

In the metasediments, diabasic discrete intru-

Table 1. Modal compositions of pelitic to psammitic rock samples of the Neelum Valley area. Sp. no. = Storage numbers of Laboratory of Mineralogy, Institute of Geology, Punjab University, Lahore.

Sp. No.	Quartz	Muscovite	Chlorite	Biotite	Garnet	Magnetite	Epidote	Apatite	Sphene	Limonite	Hematite
20547	56.3	11.7	–	8.4	–	–	–	–	2.8	–	0.8
20548	12.6	28.6	00.2	45.6	06.0	3.0	–	–	–	1.0	–
20549	74.8	7.5	2.4	12.4	3.7	1.8	–	–	1.4	–	–
20550	51.5	39.4	3.5	1.3	–	3.4	–	–	1.4	–	–
20552	61.2	2.9	–	30.6	2.3	1.0	2.0	–	–	–	–
20558	84.1	–	–	10.6	1.4	–	0.6	–	–	–	0.3
20559	50.0	15.0	8.0	13.0	6.0	5.0	–	–	1.0	2.0	–
20566	63.9	–	10.4	17.9	–	3.7	–	–	1.0	–	–
20567	59.8	3.6	19.0	12.7	2.0	1.7	–	–	0.2	–	–
20577	34.0	20.9	02.0	25.0	4.9	8.1	4.1	–	1.0	–	–
20578	59.0	4.6	15.6	15.8	–	2.7	0.8	0.6	0.9	–	–
20579	75.2	1.8	5.4	4.9	7.6	1.8	1.8	–	1.6	–	–
20583	42.3	–	30.0	21.6	–	3.6	–	–	1.5	–	–
20593	45.0	16.0	3.0	18.0	8.0	5.0	4.0	–	1.0	–	–
20596	55.6	4.3	15.3	14.1	6.6	1.1	–	–	3.0	–	–
20598	69.0	1.8	–	30.2	–	–	–	–	–	–	–

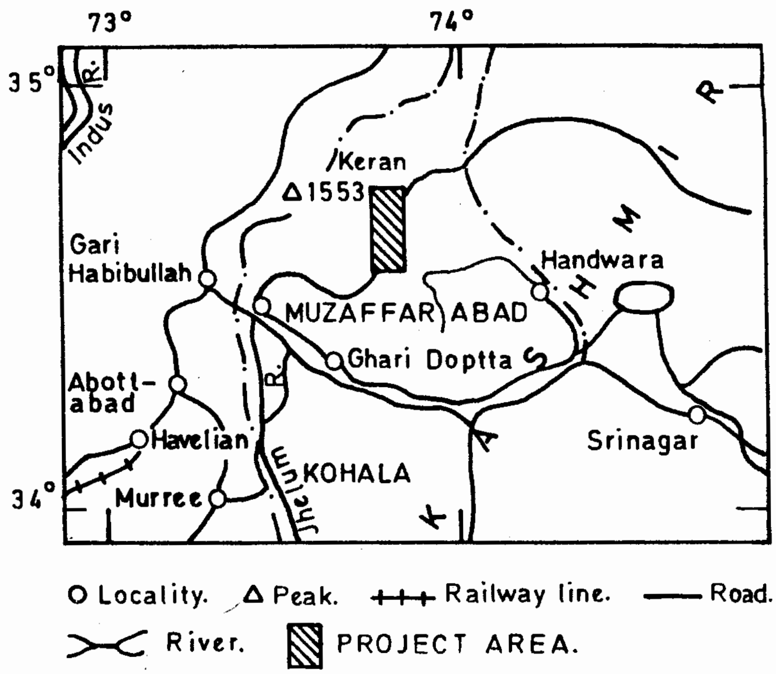

Fig.1. LOCALITY MAP.

sions of basic alkaline magma are intruded in the form of dykes. They show ophitic texture. They form olivine-bearing dolerites. Plagioclase is usually labradorite. Variable mineralogical and textural peculiarities suggest that they may be product of assimilation.

CONCLUSIONS

The rocks of Salkhala Formation exposed in Barian-Kundulshahi area have been regionally metamorphosed from chlorite to garnet grade of regional metamorphsm. The grade of metamorphism generally increases from south (Barian) to north (Kundulshahi). Garnet (almandine) size increases in Kundulshahi shile in Barian it forms grains of microscopic size. The mineral assemblage indicates that the rocks vary from greenschist facies to epidote almandine subfacies.

REFERENCES

GHAZANFAR. M., BAIG, M.S. & CHAUDHARY, M.N. (1983) Geology of Titwal Kel Neelum Valley, AJ & K. Kashmir Jour. Geol. 1, pp. 1-10.

HARKER, A. (1939) METAMORPHISM. Methuen and Co. Ltd., London.

RAJA,M.K.K. (1986) Geology and petrology of a part of Jura granites, Neelum Valley, Azad Kashmir. Kashmir Jour. Geol. 4, pp. 103-10.

SHAH, S.M.I. (1973) STRATIGRAPHY OF PAKISTAN. Mem. Geol. Surv. Pakistan 12, pp. 4-5.

SPRY, A. (1969) METAMORPHIC TEXTURES. Pergamon Press, Oxford.

SHAKOOR, A. (1976) The geology of Muzaffarabad-Nauseri area, Azad Kashmir, with comment on the engineering behaviour of rocks exposed. Geol. Bull. Punjab Univ. 12, pp. 79-90.

TUNER, F.J. & VERHOOGEN, J. (1960) IGNEOUS AND METAMORPHIC PETROLOGY. McGraw-Hill,

TURNER, F.J. & VERHOOGEN, J. (1960) IGNEOUS AND METAMORPHIC PETROLOGY. McGraw-Hill, New Yok.

WADIA, D. N. (1931) The syntaxis of the northwest Himalayas: Its rocks, tectonics and orogeny. Rec. Geol. Surv. India, 65, pp. 189-220.

WADIA, D.N. (1957) GEOLOGY OF INDIA. Macmillan and Co. London, 3rd Ed., 536p.

WILLIAM, H., TURNER, F.J. & GUILBERT. M. (1954) PETROGRAPHY. W.H. Freeman and Co., San Francisco.

WINKLER, H.G.F. (1965) PETROGENESIS OF METAMORPHIC ROCKS. Springer-Varlag, Berlin.

Manuscript received 10.12.1986
Accepted for publication 31.12.1986

ACTA MINERALOGICA PAKISTANICA
VOLUME 1(1985) pp. 161 - 162.

SHORT COMMUNICATIONS

APPRAISAL OF TWO MARBLE DEPOSITS FROM NORTHERN AREAS, PAKISTAN

TARIQ MAHMOOD

Regional Development Finance Corporation, 20 Blue Area, Islamabad, Pakistan.

The field and laboratory studies on the mineability of two deposits of marble are reported below, one after the other.

A. Marble Deposit of Shahnoz Khaiber Area, Gilgit District, Pakistan

The marble is capping the Shahnoz Hill near famous Batura Glacier on roadside of the Karakorum Highway (KKH) at a distance of 160 km from Gilgit in Hunza Valley. Its coordinates are 36° 35'N, 74° 50' E. Its approximate height from ground level is 4500 feet. The deposit has been mentioned previously by Shah & Khan (1980). The regional geology has been described by Stauffer (1982) and Desio & Martina (1972).

The marble directly overlies 90 m thick grey coloured limestone beds. The limestone, in turn, overlies intensely sheared dark coloured slates whose height from ground level exceeds 4,000 feet. The average dip angle of marble is 50° SW. The marble deposit is without any overburden.

The colour of marble is bright green disseminated with white. It is compact, takes good polish and bears no fracture, suitable for decorative purpose and novelties. The marble is composed of the fine grains completely embedded in each other. Apart from said green marble, there is thick bed of reddish coloured, fine grained compact marble which takes good polish and beautiful appearance on cutting.

The chemical analyses are given in table 1.

Table 1. Chemical analyses, in weight percents, of marble samples from (A) the Shahnoz Khaiber deposit, and (B) the Chutran deposits. (Analysts: Geochemical Laboratory. Pakistan Mineral Development Corporation, Rawalpindi).

(Constituents)	(A)	(B)
Fe_2O_3	1.9	0.1
SiO_2	6.7	0.06
Al_2O_3	6.0	0.1
CaO	42.9	31.4
MgO	5.4	22.4
Loss on ignition	37.1	45.9

The area is unexplored, mining has not been done; the leeward side of marble peak could not be studied due to inaccessibility to cross the cliff of mountainous peak and probably a large part of marble deposit is under glacier.

The exposed dimensions were measured as approximate length 500 metres, thickness 150 m and height 30 m. It has been planned to excavate the marble blocks by blasting and their transportation to ground level by sliding over the outcrop of sheared slates, which has an overall hill slope of 50°. The sliding down of marble blocks has been practically demonstrated. This method may result in 25% breaking/ wastage of blocks. It is proposed to set a small marble cutting plant at Gilgit and to market it within Northern Areas particularly Gilgit town.

B. Marble deposits of Chutran Area, Baltistan District, Pakistan.

The marble deposit is located near village Chutran 48 km northeast of Skardu town. Its coordinates are 35° 46′ N, 75° 23′ E. The marble deposit is linked with Skardu by an unmetalled jeepable road along Shighar Valley. The marble beds show dips between 45-50° SE and are exposed by stream erosion, road cutting and land sliding. The marble is dolomitic with more than 20% MgO; produces smell on hammering, shows vitreous lustre. It is grey to blackish on weathered surfaces and white to light grey on fresh surfaces. There is hillock of marble having a height of 200 metres above ground level. The marble is without any overburden, in the central part of hillock. A 60-75 metres thick bed of alluvium is deposited at foothill.

Based on texture and colour, the marble of Chutran area is divided into three categories.

Fine grained milky white marble

The milky white fine grained marble with uniform texture is on the northern part of hill cut by stream. The dip angles are comparatively gentle. These beds were traced for a distance of 1.5 km towards south. The beds extend towards northwest along a valley for probably long distance which could not be traversed due to difficult approach.

Light grey fine grained marble

The marble beds of light grey colour with alternate white and black bands are located in the central part of hill. The marble is fine grained with uniform texture. The length of deposit is 2 km.

Shining white marble

The shining white coloured marble beds are located in the southern part of hill having a length of more than 2 km. The grain size is coarse and texture is sugary. These beds are well exposed along roadside and show major fractures and block joints. This part is a southern end of hill merging in river-bed plane, on this side percentage of MgO is comparatively low.

The fine grained milky white marble is of superior quality which resembles in physical appearance to the white marbles of Italy & Greece. It takes good polish and can easily be cut. The marble samples were cut and polished which showed beautiful appearance of white colour with shining dots. The marble is suitable for decorative purposes. It is proposed to set a marble cutting and polishing plant at site near Skardu.

The market survey shows that this quality of marble will easily find market within country, and there is potential of its export subject to standard of mining, cutting and finishing.

Fig.1. Outcropping marble beds of the Chutran deposit.

REFERENCES

DESIO, A. & MARTINA, E. (1972) Geology of the upper Hunza Valley, Karakorum, West Pakistan. Boll Soc. Geol. Ital. 91, pp. 283-314.

SHAH, S.H. & KHAN, S. (1980) Geology and geochemistry of part of Hunza Area, Gilgit Agency. Geol. Surv. Pakistan Information Release 115, 39p.

STAUFFER, K.W. (1968) Geology of Gilgit–Hispar area, Gilgit Agency, West Pakistan. U.S. Geol. Surv. Project Rep. (IR) PK–19, 38p.

Manuscript received 10.10.1986
Accepted for publication 12.12.1986

ANNUAL REPORT OF THE CENTRE OF EXCELLENCE IN MINERALOGY, QUETTA (1986)

STAFF AND STUDENTS

ACADEMIC STAFF

Professor & Director — **Date of joining C.E.M.**

ZULFIQAR AHMED
Ph.D. (London), P.D.M.P. (Min. Univ., Austria)
M.Sc. & B.Sc. Hons. (Punjab). 25.8.1984

Assistant Professor

MOHAMMAD MUMTAZUDDIN
M.Sc. (McGill), B.Sc. (Aligarh). 1.4.1974

Lecturer

MOHAMMAD MUNIR
M.Sc. (Baluchistan) 1.10.1976

JAWED AHMED
M.Sc. (Karachi). 1.4.1980

Visiting Lecturer

CHRISTOPHE MIOULLET
D.E.A. (Bordeaux, France) 15.12.1986

Part-time Lecturers

AFTAB AHMAD BUTT
Ph.D. (Utrecht, Holland),
M.Sc. (Punjab).

ABDUL HAQUE
Dr. 3ème Cycle (France),
M.Sc. (Baluchistan)

GENERAL STAFF

Administrative Officer
S. SHAHABUDDIN
M.Sc. (Baluchistan) 21.5.1977

Accounts Officer
MIRZA MANZOOR AHMED
B.Com. (Karachi) 7.5.1980

Technician
KHUSHNOOD AHMED SIDDIQUI
Dipl. Assoc. Engr. (Hyderabad) 13.7.1976

Photographer
HUSSAINUDDIN 16.6.1981

Assistant Librarian
ABDUL GHAFOOR
M.L.S. (Baluchistan) 2.5.1985

Draftsman
AHMED KHAN MANGI
B.A. (sind), Cert. Drawing. 1.7.1981

Steno-typist
GHALIB SHAHEEN 17.7.1985

Assistant (Office)
LAL MOHAMMAD DURRANI 12.5.1973

Store Keeper
MUSA KHAN 20.8.1977

Senior Clerk
MOHAMMAD ANWAR 18.9.1973

Junior Clerk
GHULAM QASIM 3.10.1983

Cashier-cum-clerk
JUMA KHAN 11.6.1985

Laboratory Assistant
SHER HASSAN 22.8.1977

Rock Cutter
FARID KHAN 8.4.1985

Junior Mechanic
ABDUL QADIR 21.8.1977

Driver
ALI MOHAMMAD 17.7.1984

Loader
RAWAT KHAN 2.7.1977

Laboratory Attendants
GHULAM RASOOL 20.8.1977
MEHRAB KHAN 21.8.1977

Peons (Naib Qasid)
SIKANDAR KHAN 30.4.1976
MOHAMMAD RAFIQ 12.10.1978
ATTA MOHAMMAD 25.3.1986

Cleaner
NAZIR MASIH 1.4.1977

POSTGRADUATE STUDENTS

(SESSION 1984–86)

ABDUL TAWAB, M.Sc. (Baluchistan)
HASSAN KHAN KHAROTI, M.Sc. (Baluchistan)
SHAMIM AHMED SIDDIQUI, M.Sc. (Punjab)
JAWED AHMED, M.Sc. (Karachi)

(SESSION 1985–87)

ABDUL WAHEED TAREEN, M.Sc. (Baluchistan)
QAISER MAHMOOD, M.Sc. (Punjab)
MEHRAB KHAN, M.Sc. (Baluchistan)
KHALID MAHMOOD, M.Sc. (Baluchistan)
MORTAZA BOSTANI, M.Sc. (Baluchistan)

M.PHIL. DISSERTATIONS COMPLETED IN 1986.

1. ABDUL SALAM KHAN
   Petrology of layered ultramafic and mafic rocks, west of Bagh area, Saplaitorgarh.

2. MOHAMMAD MUNIR
   Petrology of metamorphic rocks of the north end of Jang Tor Ghar in the Muslimbagh area.

3. WAZIR KHAN
   Geology and petrochemistry of a part of the Parh Group volanics near Chinjan.

ACADEMIC ACTIVITIES

Jawed Ahmed has continued the work already began in 1985, on the clay minerals associated with the coal-bearing, lower Eocene, Ghazij Formation. X-ray powder patterns have now been obtained by him on the forty samples collected from three, relatively undisturbed, stratigraphic sections of the Ghazij Formation. The cooperation in carrying out this work extended by the Pakistan Atomic Energy Minerals Centre, Lahore, is gratefully acknowledged. The dissertation including the results obtained is under preparation.

The work on the Pakistan Science Foundation sponsored research project "Geology and mineralogy of selected Pakistani ophiolites" has been carried further by detailed field mapping and sampling of the Bela ophiolite by Zulfiqar Ahmed. Due to its vast territorial spread, the Bela ophiolite is being studied in parts. This year, the areas to the west and north of Nal in Khuzdar District, and near Kararo, also in the Khuzdar District, were studied and sampled. Basalts with well-developed pillow structures occur widespread and are not uncommonly associated with bedded basalts. In basalts, interbeds of shale, marl and limestone are observed and a few locations showing subaerial pahoehoe lavas. The following article has been published:

Ahmed, Zulfiqar (1986) Ophiolites and chromite deposits of Pakistan. *In:* Petraschek, W.E., Karamata, S., Kavchenko, G.G., Johan, Z., Economou, M. & Engin, T. (eds.) CHROMITES, Theophrastus Publications S.A., Athens, Greece, pp. 241–262.

The work on the genesis and controls of mineralization of the Mississippi Valley–type zinc-lead-iron sulphides and barite deposits of Gunga, Surmai and Shekran areas near Khuzdar, is being continued by Shamim Ahmed Siddiqui. Detailed studies on these deposits have also been started by the Geological Survey of Pakistan and Japanese consultants on the same deposits.

Mohammad Munir is starting studies on the south-western part of the Zhob Valley ophiolitic belt and its sedimentary envelope rocks.

The M.Phil. students Abdul Tawab, Hassan Khan Kharoti, Qaiser Mahmood, Khalid Mahmood and Mehrab Khan are continuing petrographic studies related to their dissertation work. Mortaza Bostani has completed partly his field studies in the Kala Chitta hills with emphasis on petroleum geology.

Mohammad Munir participated in a training programme in laboratory techniques held at Maden Tetkik Arama (MTA), Ankara, Turkey, during July and August, 1986. The programme was organized by ECO. He has received training in coal thin section and polished section preparation, ore microscopy, X-ray diffraction and electron probe microanalysis. The instructors were Drs. Selami Toprak and Gul Takin of MTA.

The staff and students of the Centre participated actively in the symposium "Science and Industry" organized by the Pakistan Science Foundation at the University of Baluchistan, Quetta, in December, 1986. Zulfiqar Ahmed read an article entitled "Academic institutions and industry in the minerals sector".

The symposium-cum-workshop "Plate tectonics and crust of Pakistan" was held at the Himalayan Research Centre, Khanuspur, Ayubia, from 27th July to 31st July, 1986. The Centre participated with the following three research papers :—

1. Ophiolite related mineral resources of Pakistan. By Zulfiqar Ahmed.

2. Geochemical characterization of the upper crust from southern Malkand Agency, Pakistan. By Zulfiqar Ahmed.

3. Whole-rock chemistry of rocks from near northwest contact of the Jangtor Ghar segment of the Zhob Valley ophiolite, Pakistan. By Mohammad Munir.

The paper by Mohammad Munir was read on his behalf by Zulfiqar Ahmed, as the former was in Turkey for training in laboratory techniques. The first volume of Acta Mineralogica Pakistanica was the subject of active discussion in the symposium and the exhibition of publications held simultaneously at Khanuspur.

Dr. A.A. Butt of the University of the Punjab, Lahore, delivered a series of 15 lectures covering various aspects of sedimentary petrology, during September and October, 1986. These lectures were held at the Centre under the Extension Lectures Scheme of the University Grants Commission, Islamabad. Dr. Butt also conducted a field excursion with the Centre's staff to collect sedimentary rock samples from the Bolan Valley.

1986 PAPERS OF REGIONAL INTEREST FROM OTHER JOURNALS

1. AHMED, Zulfiqar. Ophiolites and chromite deposits of Pakistan. ***In:*** Petraschek, W., Karamata, S., Kravchenko, G.G., Johan, Z., Economou, M. & Engin, T. (editors) CHROMITES: UNESCO's IGCP–197 Project "Metallogeny of Ophiolites". Theophrastus Publications S.A., Athens, Greece, pp. 241-262.

2. Unpublished dissertation in German language.
ARSHADI–KHAMSEH, Sirous. Geological and petrographical investigations of the Fanuji region (Beluchestan, Makran, SE-Iran) with special attention to the ophiolite complex. [Geologishe und Petrographische Untersuchungen des Fanuj–Gebietes (Beluchestan, Makran, SE-Iran) unter besonderer Berucksichtigung des Ophiolith–Komplexes] Aachen: Technische Hochschule, Dissertation, 203 p.

3. CHERVEN, Victor B. Tethys–marginal sedimentary basins in western Iran. GEOLOGICAL SOCIETY OF AMERICA BULLETIN, Vol. 97, No. 5, pp. 516-522.

4. KHAN, M.A., AHMED, Riaz, RAZA, Hilal A. & KEMAL, Arif. Geology of petroleum in Kohat-Potwar depression, Pakistan. THE AMERICAN ASSOCIATION OF PETROLEUM GEOLOGISTS BULLETIN, Vol. 70, No. 4, pp. 396-414.

5. KHAN, M.A. & RAZA, Hilal A. The role of geothermal gradients in hydrocarbon exploration in Pakistan. JOURNAL OF PETROLEUM GEOLOGY, Vol. 9, pp. 245-258.

6. MIAN, Ihsanullah & LE BAS, M.J. Sodic amphiboles in fenites from the Loe Shilman carbonatite complex, NW Pakistan. THE MINERALOGICAL MAGAZINE, Vol. 50, No. 356, pp. 187-197.

7. SARWAR, Ghulam & DE JONG, Kees A. Composition and origin of the Kanar Mélange, southern Pakistan ***In:*** Raymond, L.A. (editor) MELANGES: THEIR NATURE, ORIGIN AND SIGNIFICANCE. The Geological Soiety of America Special Paper No. 198, pp. 127-138.

8. SEARLE, M.P. & WINDLEY, B.F. ***(Comment)*** BUTLER, R. & COWARD, M.P. ***(Reply)*** Thrust tectonics and the deep structure of the Pakistan Himalaya. GEOLOGY, Vol. 14, No. 5, pp. 441-442 & 443-444.

9. USMANI, Parveen & AHMED, M. Rais. Paleoecology of Paleocene benthonic smaller foraminifera from the Lakhra area, Sind. NEUES JAHRBUCH GEOLOGISCHE PALAONTOLOGISCHES MH., Hefte 8, pp. 479-488.

10. USMANI, Parveen & AHMED, M. Rais. Some probably new species of smaller benthonic foraminifera from the Lakhra area, Sind, Pakistan. NEUES JAHRABUCH GEOLOGISCHE PALÄONTOLOGISCHES MH., Hefte 9, pp. 570-576.

RESEARCH PAPERS LIST

GEOLOGICAL SOCIETY OF AMERICA SYMPOSIUM :

"TECTONICS AND GEOPHYSICS OF THE WESTERN HIMALAYA"

A symposium on the above topic was organized by the Geological Society of America during its 1986 annual meeting held at San Antonio, Texas, U.S.A. on Tuesday, November 11, 1986. The programme included the research papers listed below. Their publication is expected shortly.

1. Valdiya, K.S.: Trans – Himalayan intracrustal thrust fault and basement upwarps south of Indus – Tsangpo suture zone.
2. Rowely, D.B., Lottes, A.L., Nie, S.Y. & Ziegler, A.M., Tectonic evolution of the Himalayas within the context of Gondwanan – Eurasian relative motions.
3. Yeats, R.S. & Nakata, T.: Active fault map of the Himalaya.
4. Burchfiel, B.C., Hodges, K.V., Rovden, L.H. & Liu, B.: East-west striking Miocene (?) normal faults within the High Himalaya, South Central Tibet.
5. Lawrence, R., Carter, S., Lafortune, J., Madin, I., Snee, L., Verplanck, P., Palmer-Rosenberg, P., Kazmi, A., Ahmad, I., Ghauri, A., Rehman, S. and Tahirkheli, R.: Deformation of crustal rocks beneath suture in western Himalaya, Pakistan.
6. Coward, M.P.: Folding and imbrication of the Indian crust beneath Kohistan during Himalayan collision.
7. Lillie, R., Yeats, R., Leathers, M., McDougall, J., Jaume, S., Duroy, Y. & Baker, D.: Active foreland thrusting in the sub-Himalaya of Pakistan.
8. Farah, A. & Duroy, Y.: Reinterpretation of the gravity field of the Himalayan foreland in Pakistan.
9. Malinconico Jr., L.L. & Adams, K.: Lithospheric underthrusting in the western Himalaya, inferred form gravity data.
10. Ni, J., Snyder, N.D. & Barazangi, M.: Deep crustal structure and seismotectonics of the Zagros collision zone and a comprison with the Himalayas.
11. Khan, M.J., Jan, M.Q. & Humayun, M.: A new Netoethyan closure model in western and central Himalayas.
12. Tahirkheli, R.A.K.: An overview of the major tectonic and geologic elements of the Himalaya and Karakorum in northern Pakistan.

13. Creveny, P.F., Tahirkheli, R.A.K., Johnson, N.M. & Bonis, N.R.: Position and source area of the ancestral Indus river during the past 18 million years.

14. Zeitler, P.K., Sutter, J.F., Williams, I.S., Zartman, R.Z. & Tahirkheli, R.A.K.: The Nanga Parbat – Haramosh massif, Pakistan : geochronology and cooling history.

15. Chamberlain, C.P., Zeitler, P. & Jan, M.Q.: Pressure-temperature – time paths in the Nanga Parbat massif : constraints on the tectonic development of the northwest Himalaya.

16. Jan, M.Q.: Composition of the plutonic core of the Kohistan island arc, NW Himalaya.

17. Searle, M.P., Rex, A.J., Windley, B.R. Tirrul, R., Onge, M.S. & Hoffman, P.: Metamorphism, magmatism and structure of the Baltoro-Muztagh Karakorum, N. Pakistan.

18. Hanson, C.R. & Lyons, J.B.: Bedrock geology of the Shighar Valley area, Skardu, northeast Pakistan.

19. Srimal, N., Basu, A.R., Sutter, J.F., Sinha, A.K. & Kyser, T.K.: Geochemistry and tectonics of eastern Karakorum.

20. Johnson, W.P. Cronin, V., Johnson, G.D. & Johnson, N.M.: The physical and magnetic polarity stratigraphy of a basin – fill remnant in the Skardu Basin, Pakistan : Implication for Recent tectonics of the Karakorum Himalaya.

21. Cronin, V.S.: Notes on the structural evolution of Skardu intermontane basin, Karakorum Himalaya Mountains, Pakistan.

22. Shroder Jr., J.F., Khan, M.S., Lawrence, R.D. & Maiden, I.: Chronology and deformation of Quaternary sediments, middle and upper Indus, Pakistan.

23. Barry, J.C.: Implications of Siwalik faunal changes.

GLOBAL SEDIMENTARY GEOLOGY PROGRAMME

At no time in the long history of sedimentary geology have there been so many advances in approaches and concept and the application of new tools, as during the past four decades. During this period, there have been major developments in chronostratigraphy (biostratigraphy, magnetostratigraphy, and radiometric dating). The facies model approach to ancient sediments has come of age and now provides predictive models of facies geometry that are widely used in exploration and development of natural resources (hydrocarbons, water, metallic ores). Seismic profiling and wireline logging of subsurface deposits have led to new levels of delineating anatomy and mass properties of facies. Isotope geochemistry has become routine for estimating paleotemperatures and charting the course of diagenesis of mineral and organic components. Geophysical models of oceans and atmosphere circulation and cycling, and of crustal movements are guiding observations and analysis of sedimentary rocks. Plate tectonics provides a new framework for considering the global distribution of facies, faunas, floras, and links between sediments and tectonics. This arsenal of new tools, new approaches and new concepts is the foundation for a major expansion of sedimentary geology to global-scale questions.

As a first step in developing the Global Sedimentary Geology Program (GSGP), an International Workshop was held in Miami, Florida in June, 1986. The Workshop was sponsored by the Society of Economic Paleontologists, the International Association of Sedimentologists, and IUGS Committee on Sedimentology. Financial support was provided by the National Science Foundation and the United States Geological Survey. Twenty-five participants from nine countries spent three and a half days preparing a report outlining an initial plan for the GSGP.

The Report of the Workshop proposed three main research themses; I) Global Rhythms and Events, 2) The Sedimentary Record of Global Evolution, and 3) Global Analysis of Sedimentary Lithofacies. For each of these themes, the Report outlines fundamental questions and provides examples of global-scale research initiatives. Examples of these research projects are 1) testing the idea of globally synchronous fluctuations of sea level (Sequence Stratigraphy); 2) coordinated study of the global occurrence of black shales (Oceanic Anoxic Events) in the Cretaceous; 3) assembling and analyzing the global distribution of time specific facies such as Carboniferous coals or Early Paleozoic platform carbonates; 4) making a global inventory of the mass of sediments through time; and 5) extending paleoceanography back to Mesozoic examples such as the sedimentary record of Tethys.

Each of these research projects is global in scope and will therefore require participation by earth scientists from many countries. This collaboration offers a special opportunity for exchanges and the training of scientists especially those from developing countries. In addition to this kind of internship, the Report recommends that GSGP develop continuing education courses and seminars, and organize visits from senior scientists to the developing nations.

Some 2000 copies of the Report of the Workshop have been distributed worldwide and the response has been enthusiastic.Ten societies and committees in North America and abroad have already formally endorsed the concept of GSGP. With this kind of support it is expected that the Program will be approved as an international effort early in 1987 and the implementation of the Report can begin. In the meanwhile, the current Steering Committee (Robert N. Ginsburg, Chairman; Edward Clifton and Robert Weimer) welcomes comments and suggestions as well as requests for the Report of the Workshop for which there is no charge. Write to GSGP, University of Miami, Fisher Island, Miami Beach, FL 33139, USA.

INFORMATION FOR AUTHORS

ACTA MINERALOGICA PAKISTANICA publishes in English annually the results of original scientific research in the multi-faceted field of mineral sciences, covering mineralogy, petrology, crystallography, geochemistry, economic geology, isotope mineralogy, petrography, petrogenesis, mineral chemistry and related disciplines. Review articles and short notes are also considered for publication.

Authors of the articles submitted for publication in ACTA MINERALOGICA PAKISTANICA should send two complete copies of the manuscript, typed double-spaced on one side of the paper only. Copies of tables should be in final format. As far as possible, tables and figures should be prepared for reduction to the single column size or to the page size (204mmX278mm). Use of mineral symbols by Kretz (The American Mineralogist, 1983, Volume 68, pp. 277–279) is recommended for superscripts, subscripts, equations, figures and tables. The Concise Oxford Dictionary is adopted for spelling.

Only articles not previously published and not about to be published, wholly or in part, in either Pakistani or foreign journals, are considered for publication. Publication is subject to the discretion of the Editor. Accepted papers become copyright of the Centre of Excellence in Mineralogy, Quetta. Authors alone are responsible for the accuracy of the contents and views expressed in their respective papers. Fifty off-prints of each published paper will be sent to authors free of charge. Additional copies may be ordered just after receiving the acceptance letter from the Editor. Manuscripts should be sent to: Acta Mineralogica Pakistanica C/O Centre of Excellence in Mineralogy, University of Baluchistan, Sariab Road, Quetta, Pakistan.

ACTA MINERALOGICA PAKISTANICA VOLUME 2 ,1986.

CONTENTS